THERMODYNAMIC STUDIES USING (~~GALVANIC~~) CELLS WITH SOLID ELECTROLYTES

A THESIS

submitted for the

DEGREE OF DOCTOR OF PHILOSOPHY

in the

UNIVERSITY OF LONDON

by

Brian Charles Hilton Steele

Department of Metallurgy,
Royal School of Mines,
Imperial College.

June 1965.

C7 - 7 JUL 1965

ABSTRACT

The measurement of a wide range of oxygen chemical potentials [$0 > \Delta\mu_{O_2}$ (1000°C) > -145 Kcal.] is described using an emf technique with galvanic cells incorporating solid oxide electrolytes. Oxygen chemical potentials associated with the two phase equilibria, Cu-Cu_2O, Pb-PbO, Ni-NiO, Fe-FeO, NbO_2-Nb_2O_5, NbO-NbO_2, Nb-NbO, are reported, together with data obtained in a preliminary investigation of the non-stoichiometric Nb_2O_{5-x} system.

Solid oxide electrolytes based on zirconia exhibited significant electronic conductivity at low oxygen chemical potentials [μ_{O_2} (1000°C) < -90 Kcal.] , and under these conditions it was essential to use thoria-based electrolytes. The electrolytic transport properties of the thoria solid solutions, ThO_2-$YO_{1.5}$, ThO_2-$LaO_{1.5}$ and ThO_2-CaO as a function of composition and oxygen partial pressure were therefore examined, and it was established that the p-type conductivity possessed by these oxide electrolyte systems becomes negligible below oxygen partial pressure of approximately 10^{-6} atm. At very low oxygen chemical potentials [$\Delta\mu_{O_2}$ (1000°C), -145 Kcal.] it appears that the thoria-based electrolytes may also be reduced and exhibit n-type conduction. Evaluation of the derived thermochemical data indicated that

this emf method is capable of great accuracy and precision provided certain precautions were observed, and special features of the cell arrangement included provision for separate electrode compartments, operation in purified argon or high vacuum atmospheres, the inclusion of 'getters', and protective electrode collars to promote local equilibrium at the electrode/electrolyte interface. Under conditions where the transport properties of the oxide electrolytes were not well defined, it was also very desirable to supplement the usual procedures for demonstrating electrode reversibility by considerably increasing the resistance of the electrolyte component and noting whether any change occurs in the observed voltages.

CONTENTS

CHAPTER ONE

INTRODUCTION

1.A. Prologue 1

1.B. Measurement of Oxygen Chemical Potentials . 3

1.B.1. Definition 3

1.B.2. General Techniques 4

1.B.3. Electrochemical Methods . . . 5

1.C. Electrochemistry of Galvanic Cells with Solid Electrolytes 10

1.C.1. EMF: Theoretical Considerations . 10

1.C.2. Ionic Conductivity 17

1.C.3. Ionic Transference Numbers . . . 23

1.C.4. Electrode Kinetics and Polarisation 26

1.D. Electrolytic Conductivity in Solid Oxide Systems 28

1.E. Research Programme 33

CHAPTER TWO

EXPERIMENTAL DETAILS

2.A. General 35

2.B. Preparation of Electrolytes and Electrodes . 35

2.B.1. Electrolytes 35

2.B.2. Electrodes 41

2.C. Examination of Electrolytes and Electrodes . 43
2.C.1. X-ray Investigation 43
2.C.2. Metallographic Examinations . . . 43
2.C.3. Density Measurements 44
2.D. EMF and Conductivity Apparatus 44
2.E. Influence of Gaseous Environment 47
2.E.1. Preliminary Observations . . . 47
2.E.2. Modifications to Cell Design . . 51
2.E.3. Vacuum Operation 54
2.E.4. Gaseous Electrodes 57
2.F. EMF Measurements 58
2.G. Conductivity Measurements 61
2.H. Standard Procedures and Precautions . . . 63
2.H.1. Apparatus 64
2.H.2. Experimental Procedure 65

CHAPTER THREE

PROPERTIES OF THORIA-BASED ELECTROLYTES

3.A. X-ray, Density and Ceramographic Examinations 67
3.A.1. General Structural Considerations . 67
3.A.2. $ThO_2.YO_{1.5}$ Solid Solutions . . . 68
3.A.3. $ThO_2.LaO_{1.5}$ Solid Solutions . . . 70
3.A.4. $ThO_2.CaO$ Solid Solutions . . . 71
3.B. Conductivity Measurements 72
3.B.1. Preliminary Comments 72

3.B.2. $ZrO_2.YO_{1.5}$ System 74
3.B.3. $ThO_2.YO_{1.5}$ System 75
3.B.4. $ThO_2.LaO_{1.5}$ System 77
3.B.5. $ThO_2.CaO$ System 78
3.C. Discussion of Electrical Conductivity Data . 78
3.C.1. General Comments 78
3.C.2. Positive Hole Conduction 79
3.C.3. Ionic Conduction 84
3.D. Determination of Ionic Transference Numbers . 94
3.D.1. Relevant Theoretical Equations . . 94
3.D.2. Zirconia s.s. at High Oxygen Potentials 96
3.D.3. Thoria s.s. at High Oxygen Potentials . 98
3.D.4. Thoria s.s. at Low Oxygen Potentials . 101
3.D.5. Zirconia s.s. at Low Oxygen Potentials 102
3.D.6. Commercial Solid Oxide Electrolyte Material 107
3.E. Summary of Transport Data 109
3.E.1. Conductivity Behaviour 109
3.E.2. Ionic Transference Numbers . . . 110

CHAPTER FOUR

EMF MEASUREMENTS AT HIGH OXYGEN CHEMICAL POTENTIALS

4.A. General 113
4.B. Reference Electrode 114
4.B.1. Preliminary Considerations . . . 114

4.B.2. Iron-Wustite Equilibria 118
4.C. Nickel-Nickel Oxide Equilibria 122
4.C.1. EMF Measurements 122
4.C.2. Evaluation of Thermochemical Data . 125
4.D. Copper-Cuprous Oxide Equilibria 131
4.D.1. EMF Measurements 131
4.D.2. Evaluation of Thermochemical Data . 135
4.E. Lead-Lead Oxide Equilibria 141
4.E.1. EMF Measurements 141
4.E.2. Evaluation of Thermochemical Data . 143
4.F. Conclusions 149

CHAPTER FIVE

OXYGEN CHEMICAL POTENTIALS IN THE NIOBIUM-OXYGEN SYSTEM

5.A. General 153
5.B. Nb-NbO Equilibria 155
5.B.1. EMF Measurements 155
5.B.2. Discussion of EMF Data 162
5.B.3. Thermochemical Data 168
5.C. $NbO-NbO_2$ Equilibria 171
5.C.1. EMF Measurements 171
5.C.2. Thermochemical Data 176
5.D. $NbO_2-Nb_2O_{5-x}$ Equilibria 178
5.D.1. EMF Measurements 178
5.D.2. Comparison of Thermochemical Data . 180

5.E. Non-Stoichiometric Nb_2O_{5-x} 181

5.E.1. EMF Measurements 181

5.E.2. Discussion of Thermochemical Data . 185

5.F. Thermochemical Data for Nb_2O_5 192

5.G. Conclusions 196

ACKNOWLEDGEMENTS 198

REFERENCES 199

APPENDICES

Appendix I i

Appendix II v

Appendix III xiv

Appendix IV xvii

Appendix V xix

Appendix VI xxi

CHAPTER ONE

I N T R O D U C T I O N

1.A PROLOGUE

In principle, the measurement of the electromative force (emf) of a reversible galvanic cell is one of the most accurate methods of obtaining thermodynamic data associated with chemical reactions. To acquire accurate data, however, it is necessary to observe certain precautions, many of which arise from the fundamental reason that a galvanic cell possessing a finite electrical potential, considered as a system, is not in a state of complete equilibrium. If it was, the potential would be zero. Whenever a galvanic cell is on open circuit the electrons in the one electrode do not have the same electrochemical potential as those in the other electrode, and this difference of electrochemical potential can only exist because the electrolyte phase of the cell is a very poor electronic conductor. The existence of the emf thus depends on the cell being in a state of metastable equilibrium with

regard to the internal flow of electrons.

The precautions to be observed are pertinent to the research reported in this thesis which is concerned with the measurement of oxygen chemical potentials using galvanic cells incorporating solid oxide electrolytes. The object of the research was to establish and use this electrochemical technique to determine the oxygen chemical potentials associated with such reactive metals as niobium, vanadium, titanium, and their respective oxides. These systems possess a high affinity for oxygen and the measurment of their correspondingly low oxygen chemical potentials is of considerable interest. For example, any discussion of the gross departures from ideal stoichiometry exhibited by these systems requires a knowledge of their thermodynamic properties, which are also relevant to the technical problems associated with the production of the pure metals and their mechanism of oxidation.

A major problem in this investigation was to satisfy the requirement that the electronic contribution to the total conductivity of these solid oxide electrolytes remained a negligible factor, under the highly reducing conditions associated with very low oxygen chemical

potentials. It follows that a considerable portion of the present investigation was devoted to a critical examination of the properties of solid oxide electrolytes, with special emphasis on those electrolytes based on thoria solid solutions. These preliminary experiments also provided useful thermodynamic data for the systems $Cu - Cu_2O$, $Pb - PbO$, $Ni - NiO$, and $Fe - FeO$. The subsequent application of this electrochemical technique to systems of low oxygen chemical potential, was confined to the niobium-oxygen system.

1.B MEASUREMENT OF OXYGEN CHEMICAL POTENTIALS

1.B.1. Definition

The chemical potential of oxygen (μ_{O_2}), or alternatively the partial molar free energy of oxygen($\overline{G}_{O_2}$), in a system is defined by the relation,

$$\mu_{O_2} = \mu^{\circ}_{O_2} + RT \ln p_{O_2},$$

where $\mu^{\circ}_{O_2}$ is the standard chemical potential (i.e. the standard Gibbs free energy) per mole. No absolute value can be assigned to $\mu^{\circ}_{O_2}$, and it follows that only differences in chemical potential ($\Delta\mu_{O_2}$) can be determined. Implicit in any reference to the measurement of a chemical potential in a system is the recognition that such measurements must in fact be relative to the chemical potential of a standard state, which for oxygen is usually

defined as the gas at 1 atm. and at the temperature under consideration.

1.B.2 General techniques

The general techniques and problems encountered in the measurement of chemical potentials in the heterogeneous equilibria associated with metal-metal oxide systems, are discussed in the reviews of Kubachewski and Evans [1], Richardson and Alcock [2], and Chipman, Elliott and Averbach [3]. In many investigations, for example, the Fe - FeO equilibria, it is convenient to allow a mixture of gases such as H_2/H_2O or CO/CO_2 to come to equilibrium with the condensed phases, and then the corresponding oxygen chemical potential can be measured by analysis of the relevant gas mixture. However, for very low oxygen potentials this technique cannot be applied owing to the magnitude of the equilibrium gas ratios.

A useful method for determining extremely low oxygen potentials was first demonstrated by Kubachewski et al [4,5,6] in work on the thermodynamics of oxygen dissolved in vanadium, titanium and zirconium. The metal under study, for example, titanium, was treated with mixture of Mg/MgO, Ca/CaO or Ba/BaO. After equilibration, the surplus reducing metal and its oxide were removed, and the oxygen content of the titanium determined by vacuum fusion.

Obviously this technique was limited at any one temperature to the three oxygen potentials associated with the Mg/MgO, Ca/CaO and Ba/BaO equilibria. However, Komarek and co-workers[7,8] recently extended the application of this method by combining it with an isopiestic technique. The metal specimens were held in a temperature gradient in intimate contact with, for example, magnesium oxide, and equilibrated with magnesium vapour. The oxygen chemical potentials could thus be varied along the temperature gradient by imposing an appropriate magnesium vapour pressure which was kept constant during an experiment by placing the source of magnesium at the lowest temperature in the system. The partial molar free energies of oxygen in the metal alloys (Ti - O, Zr - O, Hf - O) have been studied in this way.

The ranges over which oxygen chemical potentials have been determined by existing experimental techniques are conveniently summarised on a free energy temperature diagram (Fig. 1.B.1) similar to that compiled by Richardson and Jeffes[9], and it is immediately apparent that new methods must be developed to measure partial molar free energies of oxygen in the region -100 to -200 kilocalories. A method of possible application to these systems possessing low oxygen chemical potentials is an electro-chemical technique. The galvanic cells used by

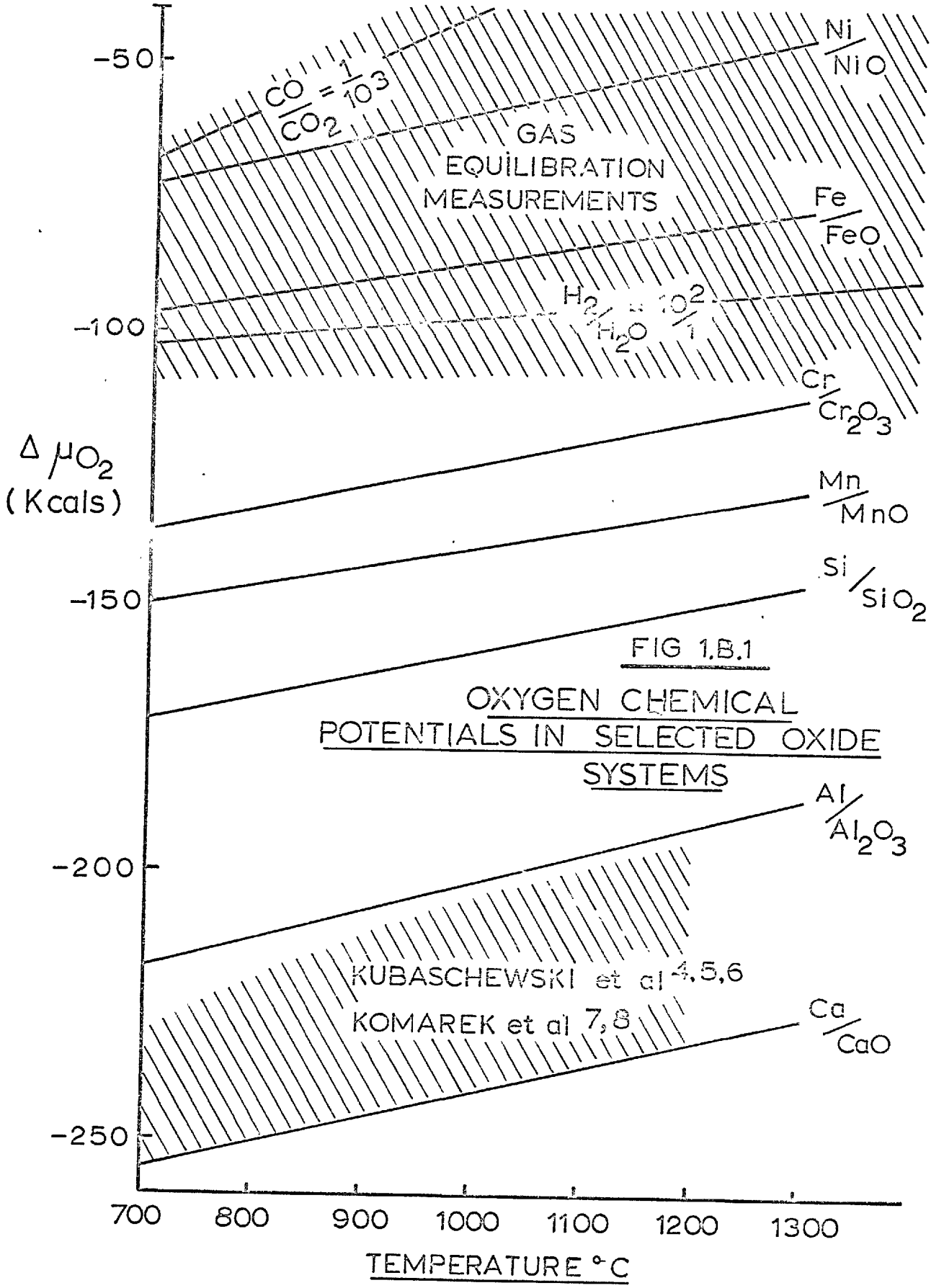


FIG 1.B.1

OXYGEN CHEMICAL POTENTIALS IN SELECTED OXIDE SYSTEMS

Treadwell[10,11] and his associates to determine the standard free energies of formation of Al_2O_3 and MgO illustrate the potentiality of this method, which is discussed in the following sections.

1.B.3. Electrochemical methods

Commercial galvanic oxygen recorders using aqueous electrolytes are available, as for example, the Hersch oxygen meter[12], which consists basically of the following cell*:

$$Pb/KOH\ (aq)/O_2,\ Ag$$

These instruments suffer from the disadvantage that they must be calibrated empirically owing to the lack of thermodynamic reversibility exhibited by the oxygen electrode. The difficulties in achieving fully reversible oxygen electrodes in aqueous systems have been reviewed by Ives[14].

It has been demonstrated, however, that the oxygen electrode can behave reversibly when incorporated in certain high temperature cells and the following selection illustrates the wide variety of molten and

---

* The cell notation adopted in this thesis follows the recommendations of the I.U.P.A.C. Stockholm Convention[13], (1953)

solid electrolytes that have been used.

Although the cells used in the early experiments (1905) of Haber and Moser[15],

Pt, CO + CO_2 / Thüringer glass /O_2, Pt.

exhibited asymmetrical voltages; Treadwell[16] in 1916 successfully employed an auxiliary intermediate porcelain electrolyte to determine the oxygen chemical potentials in equilibrium with a number of metal-metal oxide systems, e.g.

Cu (s) / Cu_2O(s), borate melt / porcelain /O_2, Ag(l)

Reference has already been made to other cells used by Treadwell[10,11] and his associates to determine the free energies of formation of Al_2O_3 and MgO, namely:

$$\text{Al(l)} \left| \begin{matrix} Na_3AlF_6\text{(l)} \\ Al_2O_3\text{(s)} \end{matrix} \right| \text{porcelain} \left| \begin{matrix} Na_3AlF_6\text{(l)} \\ Al_2O_3\text{(s)} \end{matrix} \right| O_2, \text{ Pt.}$$

$$\text{and Mg(l)} \left| \begin{matrix} MgF_2\text{(s)} \\ MgO\text{ (s)} \end{matrix} \right| \begin{matrix} MgF_2\text{(s)} \\ MgO\text{(s)} \end{matrix} \left| \begin{matrix} \\ \end{matrix} \right| O_2, \text{ Pt.}$$

More recently, Rose, Davis and Ellingham[17] reported in 1948 that reproducible, reversible e mf s could be obtained for the following cells using molten electrolytes,

Sn / SnO_2 in NaOH / O_2, Pt or Ag

Pb / PbO in NaOH / O_2, Ag.

Similarly, the results of Flood, Forland, and Motzfeldt[18] indicated that the concentration cell, Pt,(O_2, CO_2, N_2)/ Na_2SO_4 - Na_2CO_3 // Na_2SO_4 - Na_2CO_3 /(O_2, CO_2, N_2) Pt
C_1 C_2
was reversible, and by using fixed partial pressures of O_2, CO_2 and N_2, it was shown that the e.m.f's obeyed the Nernst relation over the composition range from pure Na_2SO_4 to Na_2CO_3.

All the cells mentioned above, and many others, were critically assessed in 1957 by Kiukkola and Wagner[19] in a survey of the types of cells, involving both molten and solid electrolytes, which could be used at elevated temperatures for the determination of the free energies of formation of oxides, sulphides, halides, and other compounds. This survey emphasised the advantages to be gained by the use of solid electrolytes. By providing an effective barrier to the transport of material from one electrode compartment to another, solid electrolytes can eliminate the occurrence of 'mixed potentials', and do not require a non-reactive container to hold the electrolyte.

Another advantage, that of simple cell design,

was clearly demonstrated by Kiukkola and Wagner[20] in their experiments with several cells incorporating solid electrolytes. The excellent results obtained with such cells as,

$Fe,FeO \;/\; ZrO_2 + CaO$ (solid solution) $/\; Ni,NiO,$

stimulated the electrochemical measurement of oxygen activities. Nearly all the investigations subsequently reported have involved measurements of fairly high oxygen chemical potentials which could have been obtained by gas equilibration techniques as illustrated by the following typical examples,

$Fe,FeO \;/\; ThO_2 + La_2O_3 \;/\; FeO_x + CO + CO_2$ [21]

$Fe,FeO \;/\; ZrO_2 + CaO \;/\; UO_{2+x}$ [22,23,24]

$Fe,FeO \;/\; ZrO_2 + CaO \;/\; Mo,MgO,MgMoO_3$ [25]

$Ni,NiO \;/\; ZrO_2 + CaO \;/\; Ni - Cu,NiO$ [26]

In principle, similar types of cell, for example, Nb, NbO / solid oxide electrolyte / Fe, FeO could also be used to determine the low oxygen chemical potentials associated with the reactive metals, Nb, V, Ti, Zr. There was, however, no information available

about the behaviour of the electrodes and solid oxide electrolytes under these highly reducing conditions when the present study was commenced.

1.C ELECTROCHEMISTRY OF GALVANIC CELLS WITH SOLID ELECTROLYTES

1.C.1 E m f : theoretical considerations

No new fundamental principles are involved in the theoretical treatment of galvanic cells incorporating solid electrolytes, although it is necessary to recognise that the term electrolyte has a different meaning than in the more conventional aqueous systems. In the latter case the electrolyte is merely an ionized solute, and in the former the whole of the system.

The theoretical requirements associated with the simple relationship,

$$\Delta G = - nEF,$$

are difficult to realise experimentally in even the simplest possible type of electrochemical cell, as for example,

$$Ag \;/\; AgCl \text{ (solid)} \;/\; Cl_2,\ Ag,$$

which is classified as a "formation cell without transference". The problems which may arise have been

discussed by Kiukkola and Wagner[19], and may be summarised as follows:-

(i) electrodes not thermodynamically reversible,

(ii) the presence of electronic conduction in the electrolyte,

(iii) mutual solubility of electrode and electrolyte and secondary electrode reactions,

(iv) diffusion of a component from one electrode compartment to the other, resulting in a "mixed potential",

(v) very low electrolyte conductivity.

To overcome the various limitations imposed by these experimental difficulties, cells are often designed which incorporate auxiliary electrolytes. For example in the cell used by Treadwell[16],

$$Cu(s) \;/\; Cu_2O(s),\ \text{borate melt} \;/\; \text{porcelain} \;/\; O_2, Ag(l)$$

the auxiliary porcelain electrolyte, in the form of a gas tight tube, successfully prevented both the oxidation of copper and the cuprous oxide by gaseous oxygen. Similarly, in the type of cell used in the present

investigation,

Pt, / Fe,FeO /(ZrO_2 + CaO) solid solution/ Ni,NiO / Pt.

the auxiliary solid oxide electrolyte (ZrO_2 + CaO) suppresses the electronic conduction exhibited by the iron and nickel oxides, and also functions as a barrier to the diffusion of iron and nickel which will occur at elevated temperatures. The role of this auxiliary electrolyte is more evident when the cell is written,

$$\text{Pt,Fe} \left| \begin{matrix} \text{FeO} \\ (ZrO_2 + \text{CaO}) \end{matrix} \right| (ZrO_2 + \text{CaO}) \left| \begin{matrix} \text{NiO} \\ (ZrO_2 + \text{CaO}) \end{matrix} \right| \text{Ni,Pt.}$$

All cells incorporating auxiliary electrolytes, together with obvious concentration cells such as,

$$\text{Pt},O_2(p_1) \left| \begin{matrix} \text{solid oxide} \\ \text{electrolyte} \end{matrix} \right| O_2(p_2),\text{Pt},$$

suffer from the disadvantage that any attempt to derive an expression for their emf must consider the transfer of the electrolyte constituents between different activity levels. The irreversible diffusion processes in these "cells with transference" tend to produce a separation of charge due to the different mobilities of the various ions. The separation, however, is only incipient since the formation of a space charge immediately affects the flow of charged particles in such a way as to restore electrical neutrality, and a steady-state condition

is established which is characterised by the existence of an electric field known as the diffusion (or junction) potential. The diffusion potential is discussed in Appendix I, in which the following expression is derived,

$$E_{\text{diffusion}} = -\frac{1}{F}\int_{I}^{II} \sum_{i} \frac{t_i}{z_i}\, d\mu_i \quad \ldots . \text{ Eq. I.C.1}$$

The transference number ti of each ion is defined by the arbitrary choice of a particular reference frame for all the ions. The relationships between such theoretically defined transference numbers and those obtained experimentally are discussed in Appendix III.

Unfortunately, diffusion potentials as defined above are as indeterminate as single electrode potentials and the activities of individual ions, and appear as an integral part of the measured emf of a galvanic cell with transference. It is often possible, however, to determine the conditions under which the error introduced by the diffusion potential is negligible. These determinations require data on the transference numbers of the various ions, and are illustrated by reference to the cell,

$$\text{Pt,Fe} \;\Big|\; \underset{\phi^{\alpha}}{\text{FeO}} \;\Big|\; (ZrO_2 + CaO) \;\Big|\; (ZrO_2 + CaO) \;\Big|\; \underset{\phi^{\beta}}{\text{NiO}} \;\Big|\; \text{Ni,Pt.}$$

It is assumed that the solid oxide solutions adjoining each electrode in the above cell, meet in an intermediate boundary zone in which the composition varies continuously from one extreme to the other. This zone may be considered as being located between the two broken lines. In Appendix II, it is shown that the emf of any cell may be expressed as:

$$E = \frac{1}{F}\left(\mu_e^{\alpha} - \mu_e^{\beta}\right) + \left(\phi^{\beta} - \phi^{\alpha}\right) \quad \text{.....Eq.1.C.2}$$

where μ_e^{α} , μ_e^{β} are the chemical potentials of the electrons in the electrolyte adjoining the respective electrodes (α and β), and ϕ^{α}, ϕ^{β} are the associated electrical potentials within the electrolyte. The term $(\phi^{\beta} - \phi^{\alpha})$ represents the diffusion potential which is given by Eq. 1.C.1. for the above cell, i.e.

$$\Delta\phi = -\frac{1}{F}\left[\int_{\alpha}^{\beta}\frac{t_{Zr^{4+}}}{4}\,d\mu_{Zr^{4+}} + \int_{\alpha}^{\beta}\frac{t_{Ca^{2+}}}{2}\,d\mu_{Ca^{2+}} + \int_{\alpha}^{\beta}\frac{t_{Fe^{2+}}}{2}\,d\mu_{Fe^{2+}} + \int_{\alpha}^{\beta}\frac{t_{Ni^{2+}}}{2}\,d\mu_{Ni^{2+}} - \int_{\alpha}^{\beta}\frac{t_{O^{2-}}}{2}\,d\mu_{O^{2-}} - \int_{\alpha}^{\beta} t_e\,.\,d\mu_e\right]$$

As will be discussed later, it is known for the solid oxide electrolyte (ZrO_2 + CaO)

$$t_{O^{2-}} >> t_{Zr^{4+}},\ t_{Ca^{2+}},\ t_{Fe^{2+}},\ t_{Ni^{2+}},$$

and therefore the expression for the diffusion potential reduces to

$$\Delta\phi = -\frac{1}{F}\left[-\int_{\alpha}^{\beta}\frac{t_{O^{2-}}}{2}\cdot d\mu_{O^{2-}} - \int_{\alpha}^{\beta} t_e \cdot d\mu_e\right]$$

If this equation is combined with the term $\frac{1}{F}\left(\mu_e^{\alpha} - \mu_e^{\beta}\right)$, then the following expression for the electromotive force of the cell may be derived (see Appendix II),

$$E = \frac{1}{4F}\int_{\mu_{O_2}^{\alpha}\,(Fe/FeO)}^{\mu_{O_2}^{\beta}\,(Ni/NiO)} t_{\text{ion}} \cdot d\mu_{O_2} \qquad \text{Eq. 1.C.3.}$$

Also if the electronic transference number is negligible, then

$$E = \frac{1}{4F}\Delta\mu_{O_2} = \frac{1}{4F}\left[\mu_{O_2}^{\beta}(Ni,NiO) - \mu_{O_2}^{\alpha}(Fe,FeO)\right] = \frac{RT}{4F}\ln\frac{P_{O_2}(Ni,NiO)}{P_{O_2}(Fe,FeO)}$$

It is now possible to summarise the conditions which permit the diffusion potential to be neglected, and which allow the simple expression,

$$\Delta G = -nEF\ ,$$

to be applied to the cells used in the present study.

(1) The general expression (Eq.1.C.2.) derived in Appendix II for the emf of a galvanic cell assumed local thermodynamic equilibrium at the electrodes. The cell must therefore be shown to be reversible, and it is also necessary to confirm the absence of secondary reactions at the electrodes.

(2) The transference number of the principle conducting ion in the solid oxide electrolyte must greatly exceed the transference numbers of the other charged species present in the electrolyte, including the dissolved electrode constituents. This ensures that the diffusion potential can be neglected irrespective of the magnitude of the electrode solubility in the solid electrolyte.

(3) It is essential to demonstrate that the electronic contribution to the electrolyte is negligible under the prevailing experimental conditions. This is particularly important as interference due to electronic conduction is usually more serious with solid electrolytes than with molten or aqueous electrolytes..

It follows that the properties of the selected solid oxide electrolyte must satisfy the most exacting requirements, and it is therefore appropriate to consider the main factors which influence ionic conductivity in these materials.

1.C.2. Ionic conductivity

The migration of ions through an ionic crystal under the influence of an electric field is impossible if the crystal is perfect, and it follows that the concept of lattice disorder, or defects, originally developed by Frenkel[27], Shottky,[28] and Wagner,[29] is fundamental to the study of electrolytic conductivity in ionic solids. The theoretical models proposed for the mechanism of ionic conduction are extensively discussed in the review of Lidiard[30](1957), and the following conclusions are relevant to the present study.

The intrinsic concentration (Ci moles,cm^{-3}) of a lattice defect (vacancy or interstitial), i, is governed by an equilibrium constant of the form, $Ki = \exp \frac{-\Delta G_f}{RT}$

The quantity ΔG_f represents the molar free energy of formation of a complementary pair of defects, i.e.

$$Ci = A \exp \frac{-\Delta G_f}{2RT} ,$$

where A is an appropriate constant.

The defects also move in response to thermal fluctuations with a jump frequency (w), given by,

$$w = \nu \exp \frac{-\Delta G_m}{RT} \quad ^{*},$$

where ΔG_m is the increase in the free energy associated with the transfer of a species from its normal into an activated position, midway between the two sites, and ν is a characteristic vibration frequency.**

In the presence of an electric field $\frac{\partial \phi}{\partial x}$, the activation energy for motion (ΔG_m) will be modified in the x-direction by an amount $\pm \frac{1}{2} z_i F a_i \cdot \left(\frac{\partial \phi}{\partial x}\right)$, where z_i is the valence, F represents Faraday's constant, and a_i*** is the elementary jump distance between the two equilibrium positions. Under these conditions the following expression may be obtained for the absolute mobility (Bi) of the i^{th} species,

---

* This expression was originally derived by Eyert[31], using statistical mechanics.

** The precise definition of ν is one of the more difficult aspects of the theoretical model, and it is often taken as equal to the Debye frequency.

*** The elementary jump distance a is related to the lattice parameter a_o, by a factor γ which is determined by the geometry of the appropriate sub-lattice upon which the particular species moves,

i.e. $a = \gamma a_o$

$$B_i = a^2 w / kT \quad ,$$

$$i.e. \qquad B_i = \frac{a^2 \nu}{kT} \exp\left(-\frac{\Delta G_m}{RT}\right)$$

In addition, the partial conductivity (σ_i), absolute mobility (B_i) and concentration of defects (C_i), are related by the following equation which is derived in Appendix I,

$$\sigma_i = C_i z_i^2 e F B_i \quad , \qquad \text{Eq. 1.C.4.}$$

Introduction of the exponential terms for C_i and B_i gives,

$$\sigma_i = (A a^2 z_i^2 e F) \frac{\nu}{kT} \cdot \exp\left(-\frac{\Delta G_f}{2RT}\right) \cdot \exp\left(-\frac{\Delta G_m}{RT}\right)$$

The Gibbs free energies, ΔG_f and ΔG_m, may also be replaced by the appropriate enthalpy and entropy terms, i.e.

$$\sigma_{i.T} = \left[\frac{(A a^2 z_i^2 e F)\nu}{k} \exp\left(\frac{\frac{\Delta S_f}{2} + \Delta S_m}{R}\right)\right] \exp\left[-\frac{\frac{\Delta H_f}{2} + \Delta H_m}{RT}\right]$$

$$\text{Eq. 1.C.5.}$$

This expression may be identified with the simple empirical equation,

$$\sigma . T = \sigma_c \exp.\left(-Q/RT\right) \quad ,$$

by making the following assumptions,

(i) the total conductivity is entirely due to one type of charged species,

(ii) the vibration frequency, ν, is independent of temperature,

(iii) the enthalpy and entropy terms are also independent of temperature.

If these conditions are fulfilled then a plot of log (σT) as a function of the reciprocal temperature should be a straight line. In practice a straight line is also obtained when logσ is plotted against T^{-1}. The log T term is not usually important enough to cause measurable departures from linearity, although its omission may lead to a slightly different gradient which does not possess the significance of

$$-\left(\frac{\frac{\Delta H_f}{2} + \Delta H_m}{R}\right)$$

The required linear relationship has often been demonstrated for a variety of ionic solids including the alkali halides, silver halides, and many oxides. It should be noted, however, that $\log\sigma$ versus T^{-1} plots may appear accurately linear when more than one mechanism is contributing to the conductivity. For example, the $\log\sigma$ versus T^{-1} plot for KCl [32] crystals appears to be nearly linear even though the fraction of current carried by the anions increases rapidly with increasing temperature. From the linearity of such curves, it is therefore not possible to infer the presence of only one conductivity mechanism or type of carrier.

Whilst the above theoretical model provides a basis for the interpretation of experimental results, it is not, in general, able to make quantitative or specific predictions about particular solids. Attempts have been made to calculate the heat of formation of defects in alkali halides* which require assumptions about the coulombic (Madelung) and non-coulombic (repulsive

---

* Experimental values (2.0 - 2.2 e V)[33] for the heat of formation of Schottky defects in NaCl, derived from conductivity and diffusion measurements on samples of pure and doped crystals, are in good agreement with the theoretical values (1.9 - 2.1 eV)[34].

and polarization) energy terms. It is difficult, however, to estimate the relative importance of these energy terms in other systems which may also possess an appreciable Van der Waals energy*. Even more uncertainty is associated with theoretical calculations of the activation energy for migration according to the comments of Fumi and Tosi[34].

It is evident that conductivity measurements can only provide information about the net behaviour of all the charged species including electrons and positive holes. They give no indication of the concentration of the various charge carriers or the magnitude of the associated mobilities. Although conductivity values may be combined with the results of supplementary investigations, such as transference number and diffusion measurements, interpretation of all the relevant data is often further complicated due to interaction between the various defects, which is briefly discussed in Chapter 3.

---

* The large Van der Waals energy in AgCl and AgBr, for example, is probably responsible for the occurrence of Frenkel rather than Schottky disorder, and the relatively high mobility of the silver ion in these structures.

1.C.3. Ionic transference numbers

The various experimental methods available for the determination of transference numbers in solid materials have been reviewed by Wagner[35], and the relationships between theoretically defined transference numbers, t_i , where

$$t_i = \frac{\sigma_i}{\sigma_{TOTAL}} ,$$

and those obtained experimentally are discussed in Appendix III.

If data are available about the transference number of a particular ionic species, then the appropriate partial conductivity can be calculated ($\sigma_i = \sigma_T \times t_i$) , and related to diffusion measurements by means of the Nernst - Einstein equation,

$$D_i = B_i k T ,$$

$$\text{i.e.} \quad \frac{\sigma_i}{D_i} = \frac{C_i z_i^2 e F}{k T} \qquad \ldots\ldots\ldots \quad 1.C.6.$$

In practice, this equation has to be modified by the introduction of a correlation factor, f_i. Theoretical correlation factors for a variety of structures and mechanisms have been calculated by Compaan and Haven[36], and

experimental values have been discussed by Lideard[37], Friauf[38] and Le Claire[39]. Application of the Nernst - Einstein equation tacitly assumes that the same charged species contributes to both ionic conduction and diffusion. It is obvious, however, that if mobile complexes with no net charge exist in the crystal, then the motion of these associated defects can make a contribution to diffusion whilst they make no contribution to conduction. Hence failure to satisfy the Nernst - Einstein equation may indicate the presence of interaction between defects and the formation of complexes.

It is not always essential or indeed convenient to obtain precise measurements of ionic transference numbers, and it may be sufficient to merely demonstrate the presence of significant electronic conduction by measuring the total conductivity as a function of the partial pressure of the anion constituent. For example, oxide systems of potential use as solid electrolytes possess a large energy gap between the valence and conduction bands. Although little is known about the defects present in these wide-gap metal oxides as a function of impurity content and deviation from stoichiometry, or the mechanisms by which electronic charges migrate, it is convenient to represent the measured conductivity

as the sum of three terms,

$$\sigma_T = \sigma_{ionic} + \sigma_{\oplus} + \sigma_{\ominus}$$

where $\sigma_{\oplus}$ is the conductivity due to positive hole conduction (p-type) and $\sigma_{\ominus}$ is the conductivity due to electrons (n-type). If the concentration of lattice defects is relatively insensitive to changes in the ambient oxygen partial pressure (as in the very stable electrovalent compounds MgO, Al_2O_3, ThO_2, etc), or is fixed by composition as in certain solid solutions (e.g. ZrO_2 + CaO), then the ionic contribution to the total conductivity will not be a function of oxygen partial pressure. Although the possibility of a pressure-independent electronic component cannot be ignored, it is likely that such a term would only become significant at very high temperatures, and in general, the positive hole conduction will increase with increasing oxygen pressure, and the electron conduction will increase with decreasing oxygen partial pressure.

It follows that the total conductivity is related to oxygen partial pressure as follows,

$$\sigma_T = \sigma_{ionic} + k_1 p{O_2}^{\frac{1}{m}} + k_2 p{O_2}^{-\frac{1}{n}} \quad \ldots\ldots \text{I.C.7}$$

The values of n and m will be determined by the type of defects predominating over a given range of oxygen

partial pressures. Thus if the total conductivity is a function of oxygen partial pressure, an electronic contribution is implied, and the ionic transference number, t_{ion}, will not be unity.

1.C.4. Electrode kinetics and polarisation

The measurement of emf requires a finite current to be drawn from the galvanic cell, and when current is taken from such a cell the observed voltage may be lower than the open-circuit value due to the resistance of the cell and polarisation phenomena at irreversible electrodes. The voltage drop due to both of these factors is a function of the current density and is obviously minimised by using a high impedance measuring instrument.

The logical definition of a reversible electrode is one which occurs with zero overpotential(η). This definition, however, implies an infinite exchange current (i_o) according to the relationship,*

$$i \propto i_o \eta \frac{F}{RT} ,$$

---

* This relationship has been derived for aqueous electrolyte systems by applying the concepts of chemical kinetics to electrode processes 40.

where i is the resultant cathodic or anodic current, and it follows that all real electrodes must possess a finite overpotential. It is more appropriate, therefore, to consider an electrode as functioning reversibly so long as the polarisation voltage cannot be detected at the current densities encountered in the relevant experiment.

Activation polarisation depends on the particular rate-determining chemical and electrochemical reactions at the electrode, and the concentration polarisation involves mass transfer of reactants and products. There is very little information about these processes for cells incorporating solid oxide electrolytes, although Karpachev and Pal'guev[41,42] have reported anodic polarisation in the cell,

$$Pt,(CO + CO_2) \,/Zr_{0.85}\, Ca_{0.15}\, O_{1.85} \,/\, Pt,(O_2)$$

at 1020°C, with currents as low as 300μA, and interpret their results in terms of both concentration and activation polarisation. The pure oxygen platinum electrode, $Pt(O_2)$, however, appears to be negligibly polarised even at current densities as high as $10mA.cm^{-2}$ when incorporated into high temperature(~1000°C)solid

fuel cells,[41,43,44] and it therefore provides a convenient reference electrode for the examination of other high temperature electrode materials.

1.D. ELECTROLYTIC CONDUCTIVITY IN SOLID OXIDE SYSTEMS

It is significant that the extensive review on ionic conduction by Lidiard[30] in 1957 did not discuss electrolytic conductivity in solid oxide systems, an omission justified by the meagre and conflicting data then available. However, in the intervening years many oxides have been shown to possess either mixed conduction (electronic and ionic) or predominately ionic conduction. Mixed conduction, for example, is exhibited by the simple binary oxides*, MgO[46,47,48], CaO,[48,49] SrO,[48] Al_2O_3,[45,50] ZrO_2,[51] HfO_2[52]. An additional feature of the conductivity behaviour of all these oxides is the existence of a minimum in the conductivity curve when this property is measured as a function of oxygen partial pressure, although it has not been established whether the p-type conductivity at high oxygen partial pressures, and the n-type conductivity at low oxygen partial pressures is an intrinsic

---

* Schmalzried [45] has reported that the binary oxides, SiO_2, Nd_2O_3, Sc_2O_3, Sm_2O_3, Yb_2O_3 behave as PURE ionic conductors when incorporated into certain galvanic cells.

property of these materials[x], or is due to the presence of very small concentrations of impurities. A maximum value for the ionic transference number (t_{ion}) is associated with this minimum in the total conductivity curve, and typical data reported[48] for the mean ionic transference numbers of the alkaline earth oxides at 1200°C are given in the following Table 1.D.1.

TABLE 1.D.1.

Cell	$Pt(O_2, 10^{-12}atm)$/solid oxide/$Pt(O_2, 1\ atm)$			
Solid Oxide	BeO	MgO	CaO	SrO
Mean Ionic Transference Number	0.98	0.95	0.76	0.67

Galvanic cells incorporating MgO as a solid oxide electrolyte have been[53], and are still being used[54], to determine oxygen chemical potentials. The electronic component known to be present in MgO, however, must inevitably make such measurements difficult to interpret.

Although significant in simple binary oxides, this electronic contribution has been shown to be negligible in certain oxide solid solutions based on

---

x Materials displaying both p- and n-type conductivity are sometimes classed as 'amphoteric' conductors.

zirconia. The electrolytic properties of oxide solutions of this type were first observed by Nernst[55](1900) who detected the electrolytic evolution of oxygen from a specimen of composition $Zr_{0.85}Y_{0.15}O_{1.925}$. In 1943, Wagner[56] postulated that oxide solid solutions of the type, $(ZrO_2)_{1-x}(CaO)_x$ and $(ZrO_2)_{1-x}(Y_2O_3)_x$ are defect solid solutions, the defects being anion vacancies created to preserve lattice neutrality when either Ca^{2+} or Y^{3+} ions are substituted for Zr^{4+} ions in the fluorite-type structure. He further suggested that these oxygen vacancies should give rise to high oxygen mobilities. Hund[57] confirmed this oxygen vacancy model by correlating x-ray and density measurements, and after demonstrating that the conductivity of the solid oxide solution $Zr_{0.85}Ca_{0.15}O_{1.85}$ remained constant when exposed to a wide range of oxygen partial pressures, Kiukkola and Wagner [20] successfully used this material as an electrolyte in galvanic cells designed to measure free energy of formation of various metal oxides. Kingery[58] et al. have determined the oxygen ion diffusion coefficients in $Zr_{0.85}Ca_{0.15}O_{1.85}$, and relating these data to the total electrical conductivity by means of the Nernst - Einstein equation, they concluded that the anionic transference

number is virtually unity. The cation (Zr^{4+},Ca^{2+}) diffusion experiments of Rhodes and Carter[59], and Mobius et al[60], confirm that the cationic transference number must be very small[x] and for most practical purposes may be neglected. Attempts have also been made by Weissbart and Ruka[43], and Bray and Merten[61], to determine the electronic transference number in zirconia solid solutions, and these experiments indicate that the electronic contribution is less than 0.5% (i.e. $t_{eletronic} < 0.005$). It may be concluded, therefore, that these fluorite solid solutions of zirconia satisfy the requirements specified earlier in section 1.C.1., and application of the simple expression, $\Delta G = - nEF$, to galvanic cells incorporating zirconia-based electrolytes is fully justified.

These excellent properties of zirconia based electrolytes, however, were all determined at relatively high oxygen partial pressures. In 1958, Peters and

---

x At 1000°C, $D_{O^{2-}} = 1.5 \times 10^{-7}$ cm.^{2} sec.$^{-1}$ (Kingery et al[58])

$D_{Zr^{4+}} = 3.7 \times 10^{-19}$ cm.^{2} sec.$^{-1}$

$D_{Ca^{2+}} = 7.0 \times 10^{-19}$ cm.^{2} sec.$^{-1}$ (Rhodes and Carter[59]) extrapolated

Möbius[62] mentioned that electronic conductivity in zirconia based electrolytes does, in fact, become significant at low oxygen partial pressures, and this observation was subsequently confirmed in more detail by Schmalzried,[63] and by results obtained in the present work.

It was necessary then to consider alternative solid oxide solutions which might be more suitable for the proposed measurments at low oxygen chemical potentials. The extensive solid solutions formed by ZrO_2, HfO_2, CeO_2, and ThO_2 with many of the Group IIA, Group IIIA, and rare earth oxides are well known, and the review of Möbius[64] contains a useful summary of the available information. In view of the greater thermodynamic stability* of thoria compared to that of zirconia, it was reasonable to expect that solid solutions based on thoria would be less susceptible to reduction than the corresponding zirconia solid solutions, and thus more appropriate for measurements at low oxygen chemical potentials. The available data,

---

* At 1000°C, $\Delta\mu_{O_2}$ (Zr/ZrO_2) = - 203.9 Kcal.mole^{-1}; $\Delta\mu_{O_2}$ (Th/ThO_2) = - 234.1 Kcal.mole^{-1} } Coughlin[64]

however, on the electrolytic properties of thoria solid solutions were conflicting. Kiukkola and Wagner[20] had noted that the conductivities of certain thoria based solid solutions were dependent upon the ambient oxygen partial pressure, indicating a substantial electronic component, whereas Peters and Möbius[62] reported that the electronic conductivity in similar thoria based electrolytes only became significant at high oxygen partial pressures, but gave no further details. Kiukkola and Wagner[20], and Peters and Mann[66,67] had also determined the oxygen chemical potentials associated with the Fe/FeO, Co/CoO, Ni/NiO, Cu/Cu_2O equilibria, but it was not known whether discrepancies in their results could be attributed to the different cell design, or to the thoria-based electrolytes employed by Peters and Mann. No other relevant information about the electrolytic properties of alternative solid oxide materials was available in 1958 when the present investigation was commenced.

1.F. RESEARCH PROGRAMME

The programme of research was obviously dictated by the need to examine the transport properties

of thoria-based or alternative electrolyte materials which might be suitable for the electrochemical measurement of low oxygen chemical potentials. Conductivity measurements as a function of oxygen partial pressure, and comparison of emf values obtained for similar galvanic cells incorporating either zirconia or thoria-based electrolytes, were the methods selected to obtain the relevant transport data. In addition, it was envisaged that special techniques might have to be developed to overcome problems associated with electrodes possessing very low oxygen chemical potentials, and such features as electrode reversibility and influence of the gaseous environment, would also have to be investigated.

CHAPTER TWO

EXPERIMENTAL DETAILS

2.A. GENERAL

A considerable number of preliminary experiments were associated with the development of such features as fabrication of the electrolytes, design of the emf apparatus, and arrangement of the galvanic cell. The principal conclusions of these experiments are reviewed in the appropriate experimental section, and the chapter concludes with a summary of the procedures and precautions eventually adopted for the emf and conductivity measurements.

2.B. PREPARATION OF ELECTROLYTES AND ELECTRODES

2.B.1. Electrolytes

An initial series of experiments were conducted with electrolytes prepared according to the procedure described by Kiukkola and Wagner[20]. The oxide solid solutions were produced by careful evaporation of a mixed nitrate solution containing the appropriate 'Analar' or 'G.P.' reagents, followed by heat treatments at 1000°C (~ 24 hours) and 1200°C(~ 24 hours). The oxide powders were lightly ground in an agate

mortar between the two heat treatments and at the completion of the 1200°C firing. Fabrication of the electrolyte pellets in the form of discs, 0.5 in diameter, and 0.1 - 0.2 in thick, was completed by pressing the moistened powders in hardened steel discs at 20 tons/sq. in, removing the surface impurities introduced from the metal die, and sintering in air at 1400°C for 24 hours.

The zirconia- and thoria-based electrolytes prepared by this procedure were incorporated in the cell,

Fe,FeO / electrolyte / Ni,NiO ,

and provided suitable precautions were observed (section 2.E.1), it was possible to record voltages which were in good agreement ($\pm$2mV) with the data reported by Kiukkola and Wagner. It was noted, however, that the electrolyte surface which was in contact with the Fe-FeO electrode rapidly became contaminated, and the extent of this penetration of iron could be attributed, at least in part, to the porosity of the sintered pellets, the density of which varied from 86 - 95% of the theoretical value. Other undesirable features associated with the porosity of the electrolytes such as permeability to gaseous molecules (O_2, H_2, H_2O, CO, CO_2 etc), and the presence of adsorbed gases, had to be eliminated in later experiments involving electrodes of lower oxygen chemical potentials, and it became essential, therefore, to improve the quality of the electrolyte pellets. The decision to use materials of greater purity (Johnson Matthey 'Specpure' chemicals), and to examine electrolyte compositions containing small quantities (1 mole %) of added cation (Y^{3+} , La^{3+} , C^{2+}), also made it very

important to develop an alternative method of fabrication which would reduce to a minimum possible sources of contamination. In this connection, the technique of producing ceramic components by hydrostatic pressing[68,69] had obvious advantages in that components with a more uniform and higher density could be prepared, and possible contamination of the ceramic powders by metallic impurities would be avoided. Moreover, a modification of this technique had been developed by Penrice[70] which appeared to be very suitable for small-scale laboratory production of ceramic articles. In this method, pressure is applied isostatically to the ceramic powder by means of a reversible polyvinyl chloride(P.V.C.) gel which behaved as a liquid at high pressures. A few trial experiments were sufficient to confirm the advantages of this particular fabrication process and the ancillary equipment* was designed and constructed. A proprietary reversible gel, designated Vinamold 1028**, was employed throughout the present investigation, and the process involved preparing moulds from this material such that ceramic components of the required size and shape could be produced, after making due allowances

---

* This principally consisted of a suitable metal die. Two of these were constructed, with internal diameters of 1" and 2" respectively, from EN24 steel(nickel-chromium-molybdenum steel) suitably heat-treated to withstand pressures of 50 tons/sq.in.

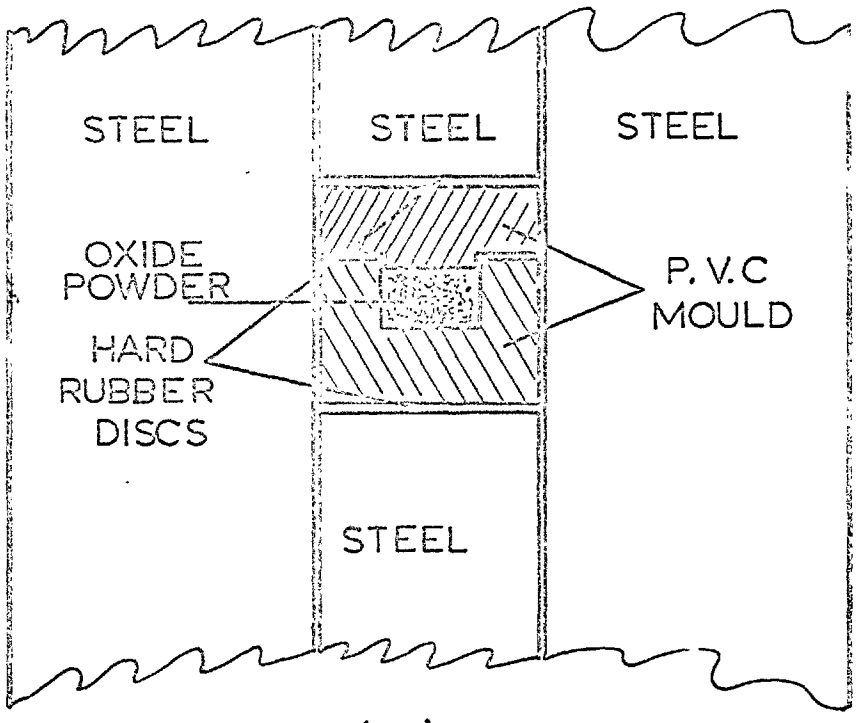
* Supplied by Vinatex Ltd., Surrey, U.K.

for the dimensional changes* associated with the pressing and sintering operations. The moulds were prepared by carefully heating the P.V.C. gel to 160°C and pouring the molten material into brass containers of appropriate shape and size. When the P.V.C. moulds had solidified they could be placed in the metal die as shown in fig. 2.B.1.a. and the oxide powder introduced into the bottom half of a mould. The top half of the mould was next placed in a position, and the whole assembly subjected to a pressure of 30 tons/sq.in. The hard rubber discs on either side of the P.V.C. mould were necessary to prevent any plastic material from being extruded down the sides of the steel tool pieces. It should be emphasised that a different mould was used for each electrolyte composition, and it was also noticed that the quality of the pressed components deteriorated when a given mould was employed in more than three pressing operations. The quality of the pressed component was also adversely affected if its diameter was large compared to the wall thickness of the P.V.C. mould, and for this reason the electrolyte pellets were always fabricated in a 2" diameter die. In addition to eliminating any possibility of metal contamination, this process had the important advantage of enabling more complex ceramic shapes to be easily fabricated. The production of crucibles by this technique, for example, is illustrated in fig. 2.B.1.b.

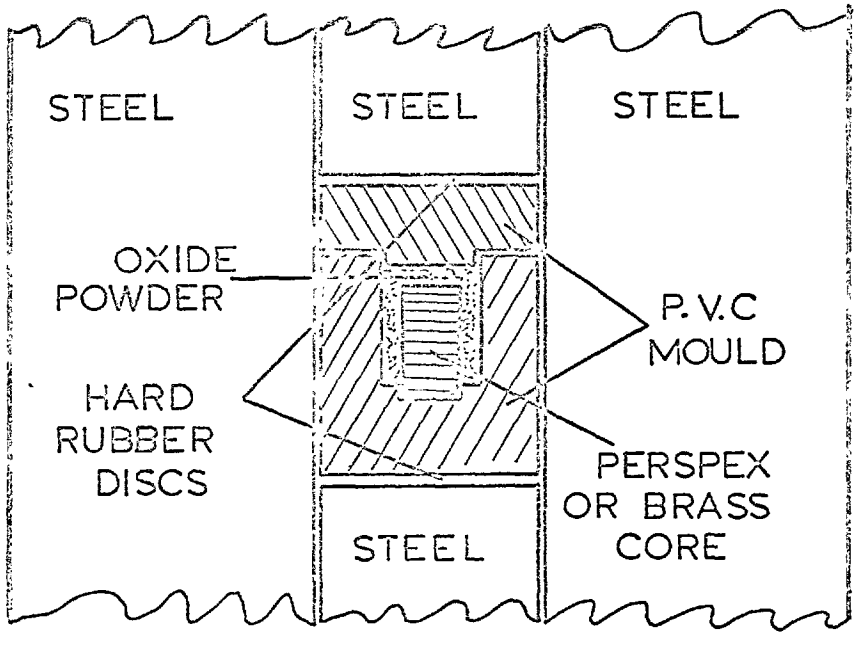
The only difficulty encountered with this method of fabrication was the tendency of certain of the oxide powders to become embedded in the walls of the P.V.C.

---

* Typical mould dimensions required to produce a dense sintered (2000°C) electrolyte pellet, 12 mm diameter and 2.5 mm thick were: diameter: 18 mm; depth: 4 mm.



(a)



(b)

FIG 2. B. 1 P.V.C MOULDS FOR PREFABRICATING OXIDE ELECTROLYTE COMPONENTS

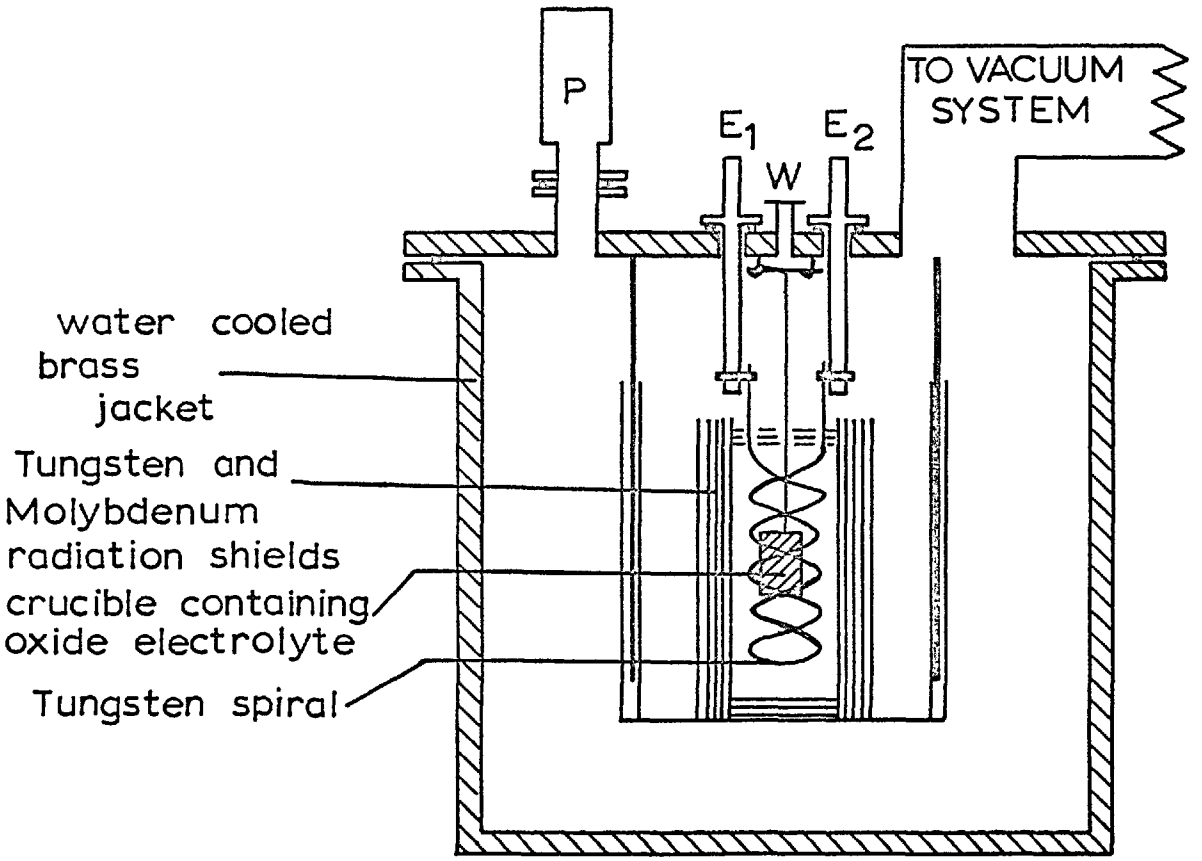
mould which caused the pellets to be pulled apart when the pressure was released. This problem was successfully overcome by using a poly-methyl methacrylate [x] temporary binder (2-3 wgt %) for the oxide powders. Although the methyl methacrylate binder could be removed in vacuum, it was considered more satisfactory to eliminate all organic material, which could also include traces of the P.V.C. gel, by firing the pressed electrolyte components in air at 1200°C.

Preliminary experiments had indicated that the quality of the pellets was also improved by increasing the temperature of the final sintering process and a tungsten element vacuum furnace was therefore constructed. This apparatus is shown in fig. 2.B.2. and consisted basically of a water-cooled metal jacket with tungsten and molybdenum radiation shields. A technique was devised for fabricating the tungsten spiral element from 1/8" diameter rod, and the power input to the furnace at 2000°C was approximately 4.5 kilowatts (250 amp. x 18 volts). Temperatures were recorded through a glass window with an optical pyrometer which was focussed on the crucible suspended from the top of the furnace chamber, and the pressure ($\sim 1 \times 10^{-5}$ torr. at 2000°C) was registered by a Penning ionisation guage (Edwards Model 5M5). The electrolyte materials were placed in either pure thoria[xx] or stabilized zirconia[xx] crucibles with close-fitting lids,

---

x This material, dissolved in toluene, was supplied by Imperial Chemical Industries Ltd., under the proprietary names, 'Cranko' or Bedacryl 144 TL. The ash content was > 0.01%.

xx The crucibles were supplied by either Morgan Refractories Ltd. or Thermal Syndicate Ltd., and were pre-treated in vacuum at 2000°C for 6 hours prior to their use as containers for the electrolyte material.



KEY

E_1, E_2 water cooled copper electrodes

P...Penning vacuum gauge

W...window for optical measurement

FIG. 2.B.2 VACUUM SINTERING FURNACE

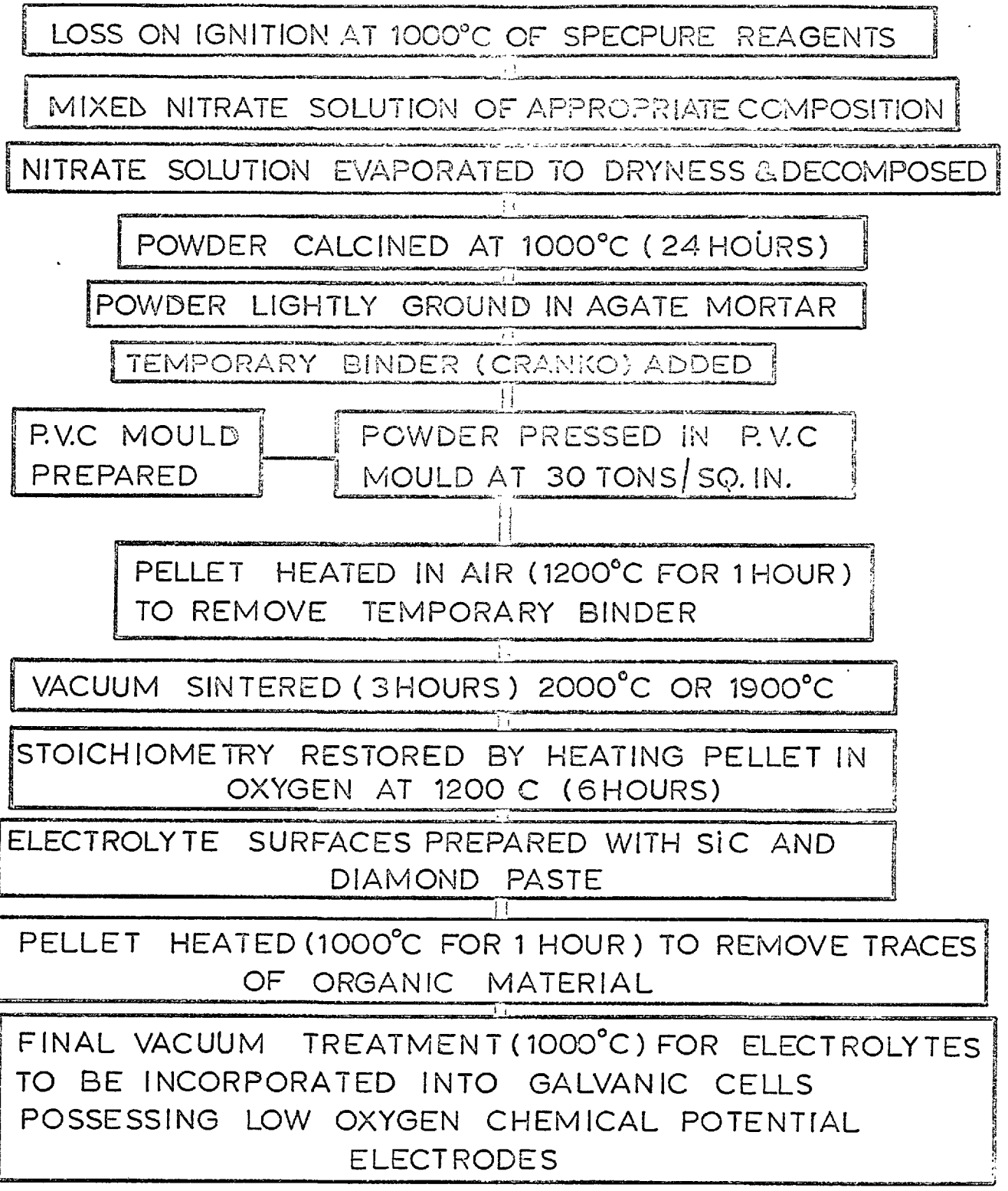


FIG. 2. B.3 SEQUENCE OF OPERATIONS INVOLVED IN THE PREPARATION OF OXIDE ELECTROLYTE COMPONENTS

and sintered for 3 hours at the selected temperature, which was 2000°C for the thoria-based electrolytes and 1900°C for the zirconia-based electrolytes. This high temperature vacuum sintering process produced very dense grey, or black, oxygen-deficient electrolytes which were converted to the stoichiometric composition by a further heat treatment in oxygen at 1200°C for 6 hours.

The next step was to prepare the electrolyte surfaces using the appropriate grades of SiC paper, followed by a final polishing operation with 10 micron diamond paste. Traces of organic material were removed by washing the electrolyte in acetone or alcohol and heating to 1000°C in air (1 hour). The electrolyte was also subjected to an additional vacuum treatment at 1000°C prior to being incorporated in a cell if it was to be in contact with an electrode possessing a low oxygen chemical potential.

Developments in the techniques used to fabricate the electrolyte components were accompanied by investigations into the best procedure to prepare the oxide solid solutions. It was concluded from these experiments, which are detailed in Appendix IV, that a method based on the straight forward evaporation of the mixed nitrate solution was preferable to procedures involving co-precipitation of hydroxides or oxalates, even though the evaporation method was more laborious and required continuous stirring to avoid fractional crystallisation. The standard procedure eventually adopted for the preparation of the solid oxide electrolytes is summarised in the adjoining

fig. 2.B.3., and spectrographic analyses of the Johnson Matthey 'Specpure' chemicals employed, are included in Appendix V.

2.B.2. Electrodes

The electrodes usually consisted* of an intimate, equimolar, mixture of two phases (e.g. metal and metal oxide) in the form of pellets 0.1 in. thick and possessing diameters of either 0.5 in. or 0.25 in. The smaller pellets were used in the lower electrode compartment and as auxiliary electrodes in certain polarisation experiments.

The various procedures developed for the different electrode constituents are outlined below.

Cu - Cu_2O : 300 mesh electrolytic copper (Hopkin and Williams) and cuprous oxide powder (Hopkin and Williams) were thoroughly mixed and pressed at 10 tons/sq.in. in a hardened steel die. The pellets were sintered at 800°C for 5 hours in purified argon.

Pb - PbO : Appropriate quantities of 'Analar' lead and yellow lead oxide (Hopkin and Williams) were mixed and placed in the electrolyte crucibles.

---

* Exceptions included the single non-stoichiometric phase Nb_2O_{5-x}, and certain Nb-NbO electrodes composed of various proportions of the metal and metal oxide phases.

Ni - NiO : Carbonyl nickel powder (Johnson Matthey) was mixed with nickel oxide prepared by decomposition of 'Analar' nickel nitrate. The mixed powders were pressed at 10 tons/sq.in. and sintered in purified argon or vacuum at 900°C for 6 hours.

Fe - FeO : Carbonyl iron powder (Johnson Matthey) was mixed with ferric oxide prepared by decomposition of 'Analar' ferric ammonium sulphate. Compacts of the mixture were fired in vacuum at 1000°C for 24 hours and then crushed and ground to a powder (<100 mesh). Pellets pressed from this powder were annealed for a further 24 hours in vacuum at 1000°C.

Nb - NbO ($NbO-NbO_2$) ($NbO_2-Nb_2O_5$) (Nb_2O_{5-x}) : Appropriate quantities of Johnson Matthey 'Specpure' niobium metal powder and niobium pentoxide were thoroughly mixed and pressed into pellets, which were placed in pure thoria crucibles and fired in vacuum at 1400°C (Nb-NbO, $NbO-NbO_2$) or 1200°C ($NbO_2-Nb_2O_5$, Nb_2O_{5-x}) for 24 hours, followed by another heat treatment at 1000°C for 48 hours. The pellets were subsequently ground, repressed, and annealed in vacuum at 1000°C for a further 24 hours.

Whatever the method of preparation, all the electrodes possessed smooth surfaces and did not require any further treatment before being incorporated into a cell . Once an electrode had been used in a cell however, the original surface was ground away with successive grades of SiC paper to expose a fresh polished surface for the next experiment.

2.C. EXAMINATION OF ELECTROLYTES AND ELECTRODES

2.C.1. X-ray investigations

The Debye-Scherrer powder technique was used to check the phases present in certain of the electrode compositions and to determine unit cell parameters of the thoria solid solutions. Samples taken from the sintered electrode or electrolyte pellets[x] were crushed, and the powder put into thin-walled glass capillaries.

The x-ray photographs were taken with a Phillips 11.45 cm. camera using copper Kα radiation and a thin nickel filter. Lattice parameter values were obtained by measuring diffraction lines with $2\theta > 100°$ and extrapolating by the method of Nelson and Riley[71].

2.C.2. Metallographic examination

No special treatment was given to the surfaces of the metal-metal oxide electrode pellets as the two phases were clearly visible by eye, or with a low power

---

x Samples for lattice parameter measurements were taken from electrolyte pellets after the final vacuum treatment (see fig. 2.B.3). The pellets were annealed at 1000°C for one hour, and then cooled fairly rapidly by switching off the power to the vacuum furnace.

microscope, provided the standard procedure described in section 2.B.2. were followed.

The thoria-based electrolytes, however, were given a final polish with 1/4 micron diamond paste and then etched with hot sulphuric acid, or thermally etched[72] in air at 1400°C.

2.C.3. Density measurements

The electrolyte pellet was weighed in air, and then placed in a beaker inside a vacuum desiccator which was subsequently evacuated ($\sim 10^{-2}$ torr.) Di-butyl ppthalate was next admitted into the beaker, and the pellet re-weighed whilst suspended in this liquid. By this technique the apparent solid volume (true solid volume and volume of closed pores) was determined, and thus the apparent solid density could be calculated.

2.D. E.M.F. AND CONDUCTIVITY APPARATUS

The exploratory emf experiments were carried out in a silica apparatus similar to that used by Kiukkola and Wagner,[20] in which the cell arrangement simply consisted of two electrode pellets and an electrolyte disc pressed together between spring-loaded platinum contacts, with a stream of purified argon maintaining an inert atmosphere around the cell. However, preliminary measurements on cells containing electrodes with low oxygen chemical potentials, (section 2.E.1) soon showed the importance of being able to provide separate

electrode compartments, and this and other desirable features, such as rapid assembly of the cell, operation in vacuum or purified argon at temperatures up to 1400°C, were incorporated in the final design of the apparatus which is now described.

The cell and conductivity sample holder, illustrated in Fig. 2.D.1, could be completely removed from the main apparatus, and consisted principally of two fixed components, an impermeable ceramic tube A (O.D. 0.5", I.D. 0.4") and a hollow brass cylinder B. The ceramic component A was either an open-ended pure alumina tube[x] or a closed-ended stabilized zirconia tube[xx], and was located on top of the brass cylinder by an 'O' ring seal. The spring loaded alumina tube, T, situated inside the fixed tube, enclosed the platinum connecting wire from the lower electrode E, and was attached to the brass tube C with another 'O' ring seal. The metal bellows D ensured that the spring-loaded alumina tube could still move when the lower part of the metal tube C was connected via a further 'O' ring seal to the hollow brass cylinder B. Purified argon entered the lower electrode compartment through the tube C and left through the opening at F; both inlet and outlet could also be connected to a vacuum system. The upper electrode (E_2) was firmly pressed against the electrolyte or conductivity specimen S by means of a horizontal alumina rod R which passed through two holes drilled in the wall of a small piece

---

x Supplied by Morgan Refractories Ltd.,

xx Supplied by Zirconium Corporation of America, Ohio, U.S.A.

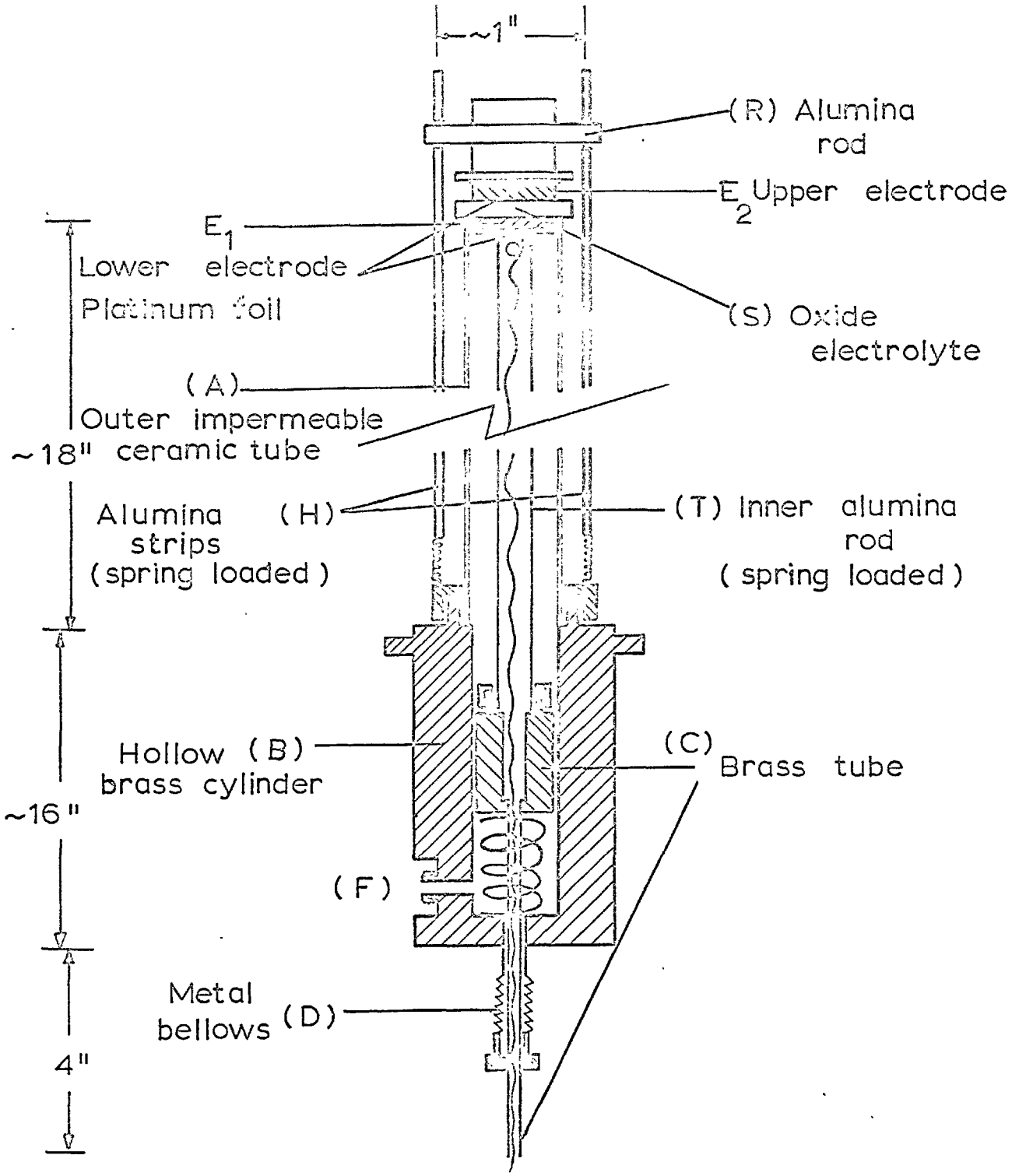


FIG 2.D.1. CELL AND CONDUCTIVITY SAMPLE HOLDER

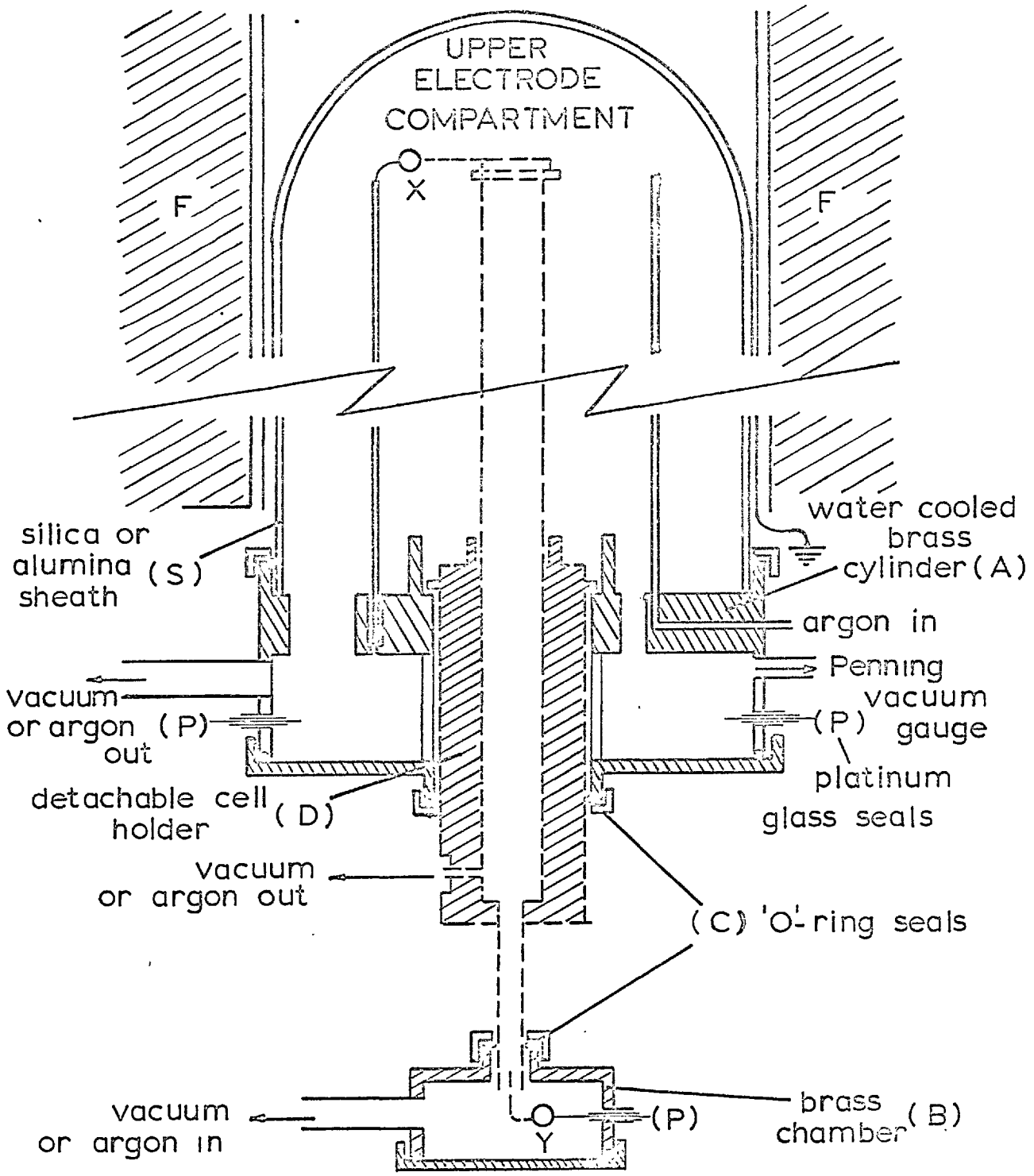


FIG. 2.D.2 CELL AND CONDUCTIVITY APPARATUS

of alumina tube G placed on an alumina disc. The arrangement was completed by attaching two alumina strips H which were joined to springs, to the opposite ends of the horizontal alumina rod.

The assembled cell and holder were located in the main part of the apparatus as shown in Fig. 2.D.2. A metal framework supported the water-cooled brass cylinder A and the brass chamber B, and both these components could be connected to the same vacuum system* or to two separate supplies of purified argon. 'O' ring seals C also enabled the detachable cell holder unit D to be incorporated in the vacuum or argon system. A sheath S, internal diameter 65 mm, of silica or alumina enclosed the upper electrode compartment which also contained alumina supporting tubes for the thermocouple (Pt/Pt-13% Rh.) and upper electrode leads (platinum). Connections to these wires and also to the lower electrode were made via platinum-glass seals P incorporated in the brass components A and B. A non-inductively wound platinum furnace** F could be lowered over the refractory sheath which was surrounded by an earthed metal screen (nichrome tape, or nickel sheet). Attempts to prevent oxidation of this screen using nitrogen or forming gas were only partly successful and it had to be replaced at frequent intervals.

---

* The vacuum system incorporated a 2" diameter silicon vapour diffusion pump backed by a single stage rotary pump; the pressure was registered with standard Pirani and Penning guages.

**The platinum furnace was controlled($\pm$1°C) by a Mark IV Kelvin and Hughes proportional instrument using a Pt/Pt-13% Rt thermocouple adjacent to the furnace winding.

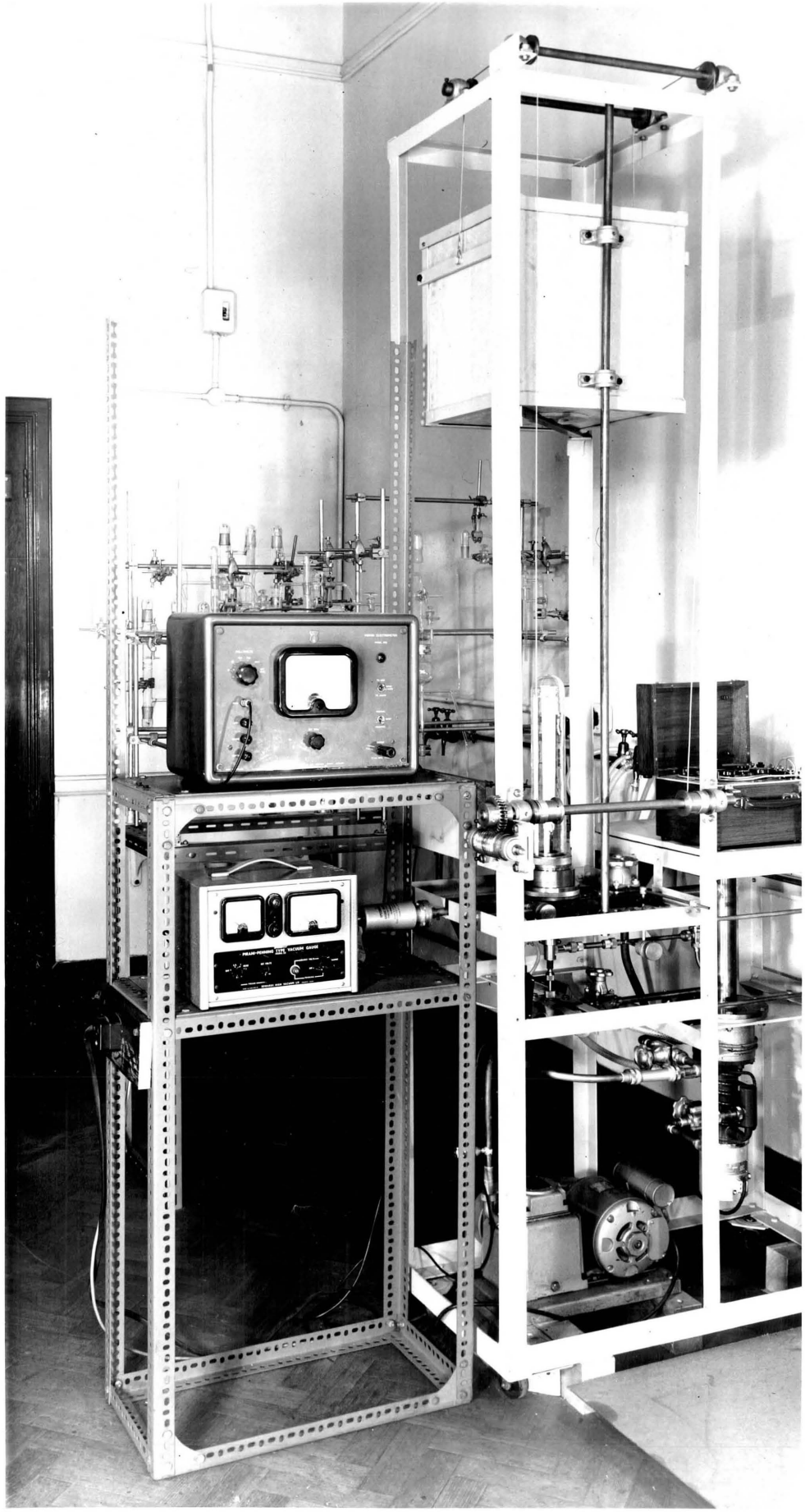


FIG.
2.D.3

Once the cell had been assembled and located in the main apparatus only two electrical connections had to be made. The upper electrode was connected to the measuring circuit by welding together two lengths of platinum wire at X, with an oxy-gas torch, and the platinum lead from the lower electrode was attached to the platinum-glass seal at Y.

An impression of the complete apparatus and ancillary equipment may be obtained from the photograph reproduced in Fig. 2.D.3.

2.E. INFLUENCE OF GASEOUS ENVIRONMENT

2.E.1 Preliminary observations

As mentioned earlier, the initial version of the cell used in the present investigation consisted of three pellets (two electrodes and the electrolyte) of approximately equal diameter and thickness pressed together between platinum contacts as illustrated in Fig. 2.E.2(a). An inert atmosphere around the cell was provided by a stream of argon purified by passing the gas through vertical columns containing Sofnalite (CO_2 absorbent), silica gel, magnesium perchlorate, and titanium granules maintained at 900°C. The gas train was constructed entirely of glass except for the pure Al_2O_3 tube holding the titanium granules. At the beginning of each experiment the silica apparatus enclosing the cell assembly was also evacuated ($\sim 10^{-3}$ torr.) and refilled with the purified argon at least twice.

With this simple apparatus and cell arrangement, excellent reproducible voltages over the temperature range 600-900°C were recorded for the cell,

$$\text{Ni-NiO}/\underset{\text{(POROUS)}}{\text{ZrO}_2.\ \text{CaO(85.15 mole \%)}}/\text{Cu-Cu}_2\text{O}$$

These voltages also remained constant ($\pm$ 2mV) when the argon flow-rate was varied from 5-100 mls/min. provided the temperature of the cell did not exceed 900°C. At higher temperatures the cuprous oxide was progressively reduced by the purified argon and the emf values gradually decreased.

It was much more difficult, however, to obtain reliable consistent results for the cell,

$$\text{Fe-FeO} \;\Big|\; \underset{\text{POROUS}}{\begin{matrix}\text{ZrO}_2.\text{CaO(85.15 mole \%)} \\ \text{OR} \\ \text{ThO}_2.\text{YO}_{1.5}\text{(85.15 mole \%)}\end{matrix}} \;\Big|\; \text{Ni-NiO}$$

The recorded voltages were invariably too low, and were also dependent upon the argon flow-rate as can be seen from the typical results reproduced in Fig. 2.E.1(a) for two separate cells at 900°C. The presence of carbon monoxide and hydrocarbons in the argon was indicated by traces of carbon deposited in the cooler parts of the emf apparatus and so cupric oxide (maintained at 550°C) was incorporated in the gas train prior to the CO_2 absorbent. The introduction of cupric oxide, which significantly reduced, but did not entirely eliminate, the deposition of carbon in the apparatus, was accompanied by a marked

improvement in the emf data. The voltage was less affected by changes in the argon flow-rate and the reproducibility of the emf values was usually ± 3 mV, although occasional experiments still produced larger variations. The inclusion of a liquid oxygen trap and calcium turnings (contained in a stainless steel tube at 600°C) in the gas purification train was attended by no significant change in the reproducibility of the results, and these items were later omitted from the apparatus.

Attention was now directed towards the electrolyte, and it was found that more consistent results (± 1 mV) could be obtained if the porous electrolyte was heated in vacuum (1×10^{-5} torr)[x] for several hours at approximately 1000°C. When the vacuum furnace had cooled, purified argon was admitted, the electrolyte removed, and kept in an inert atmosphere until ready to be incorporated in a cell. This treatment also reduced the proportion of runs that had to be rejected, and presumably eliminated adsorbed gases in the electrolyte[xx] such as CO_2 and H_2O which could affect the equilibria at the electrode/electrolyte interfaces by "ferrying" oxygen from the Ni-NiO to the Fe-FeO electrode. A similar improvement was noted when the porous electrolytes were replaced by the dense, inpervious, pellets prepared as described in section 2.E.1. With these developments, and procedures designed to keep

---

x The preparation of the electrodes, Fe-FeO and Ni-NiO already included a vacuum heat treatment (Section 2.B.2)

xx Brown and Chitty[73] have reported that thoria adsorbs up to 20µl. of CO_2 per gram when fired in air at 1400°C and allowed to cool to room temperature.

the interior surfaces of the apparatus scrupulously clean (free from grease, fingerprints, etc), then the simple apparatus could be relied upon to give satisfactory reproducible emf values for cells incorporating Ni-NiO and Fe-FeO electrodes.

However, experiments with the cell,

$$\text{Fe-FeO} \;\Big|\; \begin{matrix} ZrO_2 \,.\, CaO(85.15 \text{ mole } \%) \\ \text{(DENSE, IMPERMEABLE)} \end{matrix} \;\Big|\; \text{Cu-Cu2O}$$

revealed further inadequacies of the simple cell design. Although voltages (~540 mV) close to the expected values could be obtained if the cell was rapidly cycled through the temperature range, it was observed that any attempt to maintain the cell at a constant temperature was accompanied by a steady decrease in the recorded emf. The voltages were also influenced by variations in the argon flow-rate. The performance of cells incorporating electrodes with low oxygen chemical potential (e.g. Nb-NbO) was even worse. The cell,

$$\text{Nb-NbO} \;\Big|\; \begin{matrix} ThO_2.YO_{1.5}(90.10 \text{ mole } \%) \\ \text{(DENSE, IMPERMEABLE)} \end{matrix} \;\Big|\; \text{Fe-FeO}$$

for example, should have developed a voltage greater than 600 mV at 1000°C yet the maximum voltage ever recorded for this cell in the simple apparatus was 500 mV. These voltages, moreover, were very erratic and showed a marked dependence upon the argon flow-rate which is illustrated for a typical cell in Fig. 2.E.1(b). The

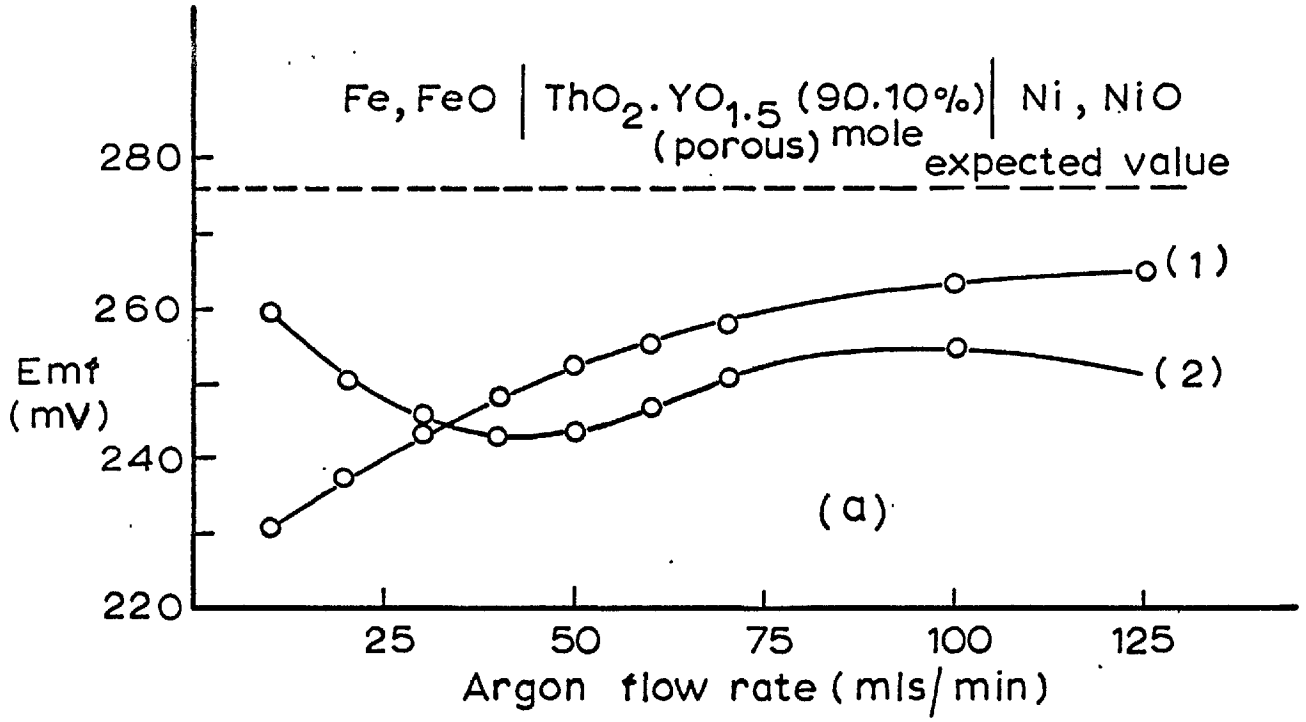
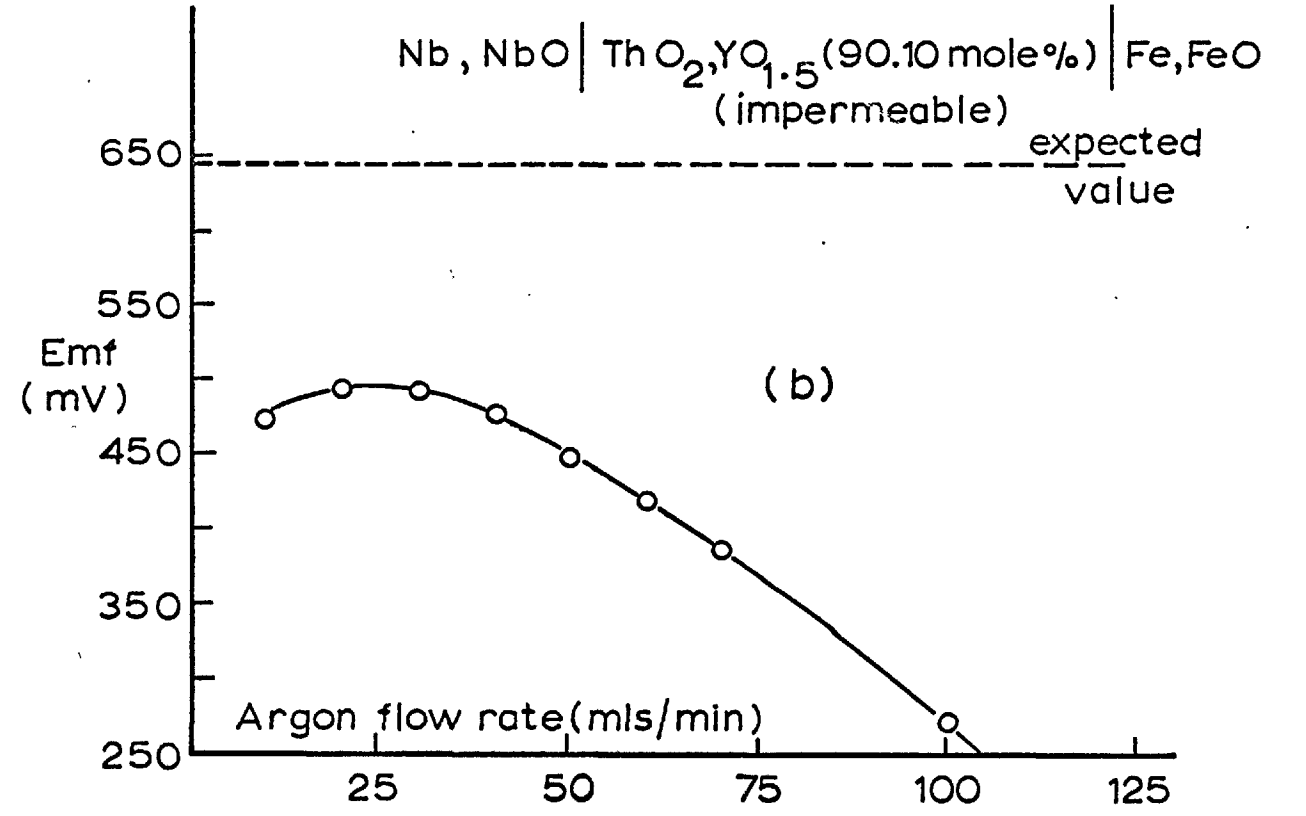


FIG 2.E.1

Emf as a function of argon flow rate



presence of zirconium getters in the apparatus did not improve the performance of the cell and it was concluded that the original simple cell arrangement was inadequate to obtain reliable meaningful data for electrodes possessing low oxygen chemical potentials.

2.E.2. Modifications to cell design

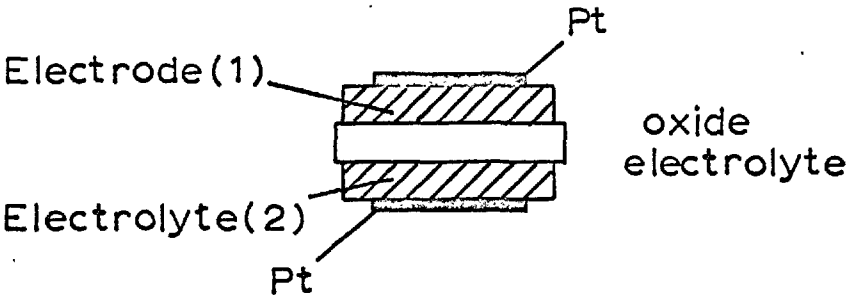
Anomalous behaviour arising from interaction between glavanic cells incorporating solid oxide electrolytes and their gaseous environment has been noted by other investigators[26,74,75,76] Attempts to reduce these spurious voltages lead Benz and Schmalzried[74], for example, to fit their electrodes into recesses provided in the opposite ends of the zirconia-based electrolyte (Fig.2.E.2(b)), whilst Schmalzried[75] used a more complicated electrolyte design, illustrated in Fig. 2.E.2(c), for measurements involving the free energy of formation of various spinels.

In the present investigation the problem was overcome by constructing the emf apparatus described earlier (section 2.D), which enabled cells with separate electrode compartments to be assembled. The initial cell design of this type is shown in Fig. 2.E.3(a) and simply consisted of two electrode pellets pressed against the opposite faces of a closed and commercial lime stabilized zirconia tube*. Two separate streams of purified argon were provided and excellent results($\pm$1 mV), which were independent of argon flow-rate, were immediately recorded for the cells,

---

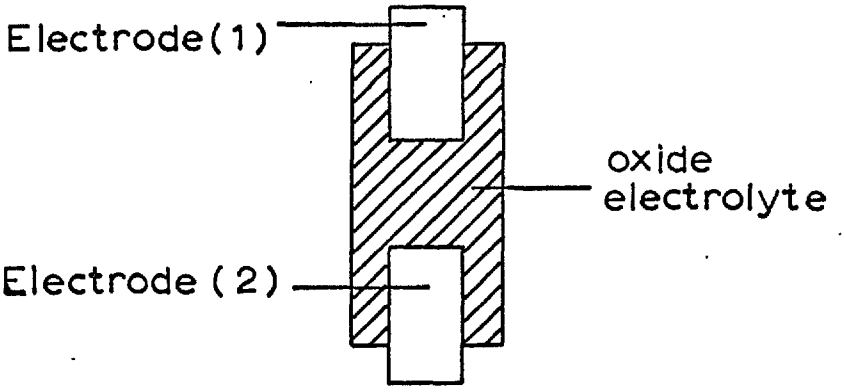
* Supplied by Zirconium Corporation of America, Ohio, U.S.A.

(a)

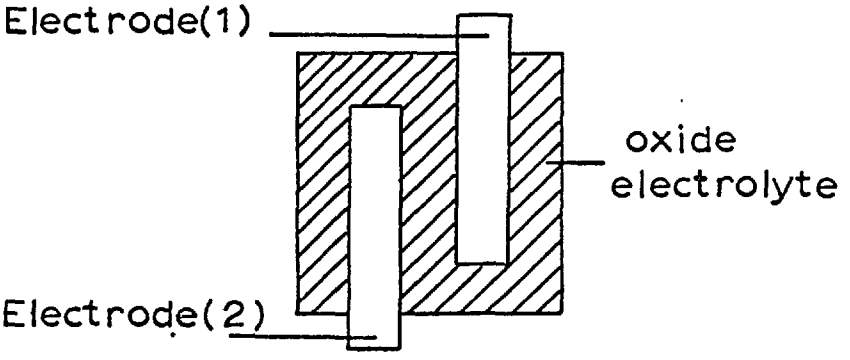


INITIAL CELL ARRANGEMENT
(cf. Kiukkola and Wagner[20])

(b)



BENZ AND SCHMALZRIED[72]



Schmalzried[73]

FIG. 2.E.2 CELLS WITHOUT SEPARATE ELECTRODE COMPARTMENTS

Fe-FeO	COMMERCIAL STABILIZED ZIRCONIA	Ni-NiO
Fe-FeO	COMMERCIAL STABILIZED ZIRCONIA	Cu-Cu_2O

Low results, however, were still obtained for similar cells incorporating the Nb-NbO electrode, and it was eventually established (see Chapter 3) that the zirconia-based electrolyte was reduced under these conditions and possessed a significant electronic conductivity. Thoria-based electrolytes were therefore placed next to the stabilized zirconia tube as illustrated in Fig. 2.E.3(b). This arrangement not only prevented reduction of the zirconia electrolyte by the Nb-NbO electrode, but also eliminated contamination of the zirconia electrolyte tube by such electrode constituents as iron. Although emf values obtained with the cell,

Nb-NbO	$ThO_2.YO_{1.5}(90.10)$	COMMERCIAL STABILIZED ZIRCONIA	$ThO_2.YO_{1.5}(90.10)$	Fe-FeO

were now much more satisfactory than voltages hitherto recorded for cells incorporating the Nb-NbO electrode, the values were still 30-100 mV lower than expected and not very reproducible. Some improvement in the cell performance was achieved by passing a small current (10μA for 3 hours) through the cell at 900°C in such a direction as to transfer

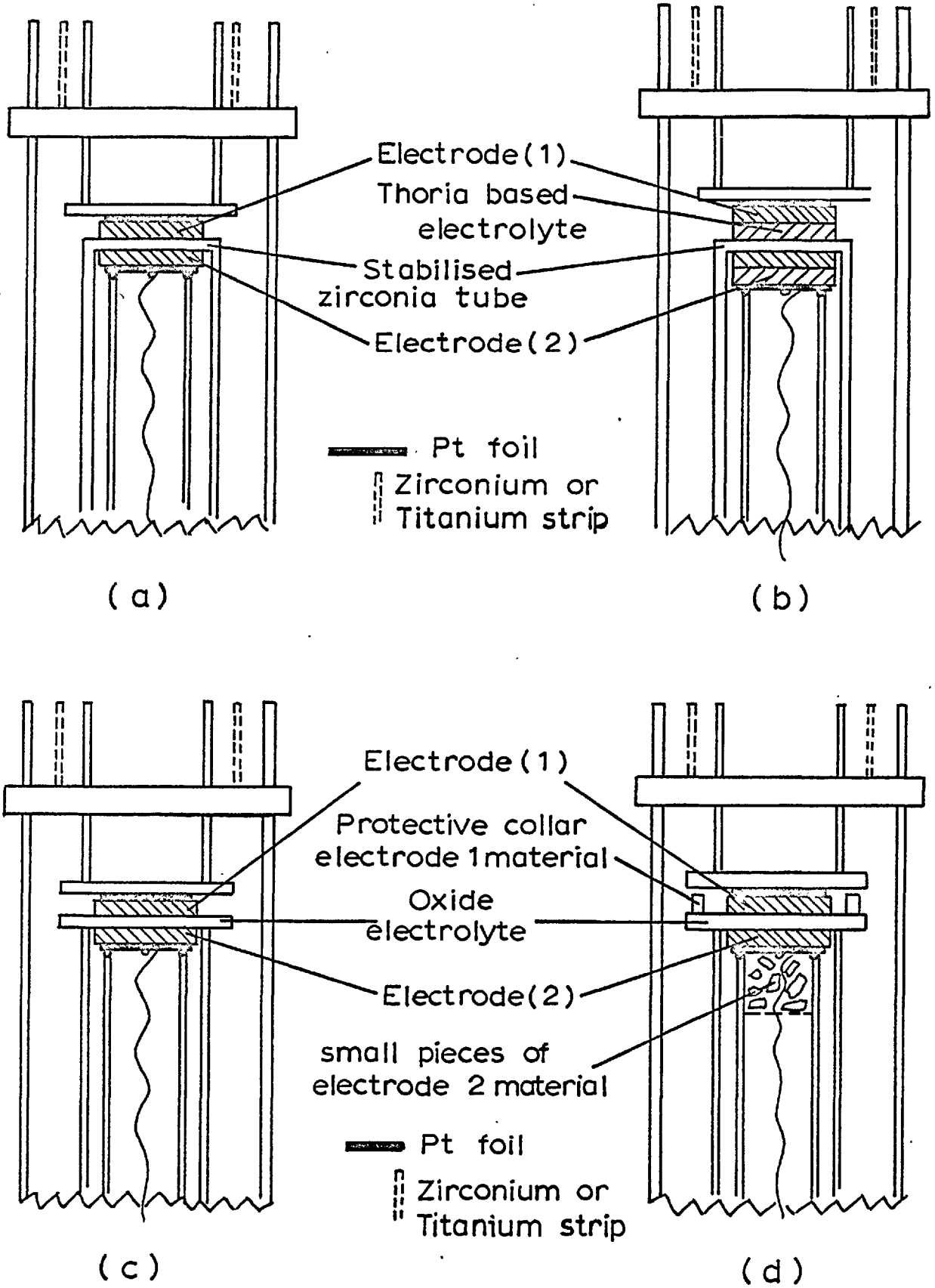


FIG. 2.E.3 DESIGN OF CELLS WITH SEPARATE ELECTRODE COMPARTMENTS

oxygen from the Nb-NbO electrode to the Fe-FeO electrode. The cell was allowed to come to equilibrium overnight, and the voltages subsequently recorded as the cell was cycled through a range of temperatures (700 - 1000°C) were fairly reproducible ($\pm$25 mV).

Much more significant was the improvement associated with the pressure of 'getters' in the upper electrode compartment. Provided the 'getter' had a greater affinity for oxygen than the metal constituent of the electrode (i.e. Nb), then the cell behaved very well indeed, and the reproducibility of the recorded voltages attained $\pm$10 mV. Small strips of titanium or zirconium, as well as titanium granules, were successfully used, whereas the inclusion of strips of iron or nickel did not improve the cell performance. The consistency of the data was further improved ($\pm$2 mV) in subsequent experiments, reported in Chapter 5, with different electrolyte compositions.

The cell design now appeared adequate to determine low oxygen chemical potentials and was subsequently adopted by Markin and his associates at A.E.R.E., Harwell, to measure the partial molar free energies of oxygen associated with the non-stoichiometric UO_{2+x} [77] and PuO_{2-x} [78] phases. It was further modified, however, in the present investigation to avoid the necessity of using expensive commercial stabilized zirconia tubes. This arrangement is illustrated in Fig. 2.E.3(c), and consisted of an impermeable pure alumina tube surmounted by a dense impermeable thoria-based electrolyte pellet prepared by

the method discussed in section 2.B.1. The top surface of the alumina tube and the electrolyte disc were highly polished (1/4 micron diamond paste), and when pressed together provided an effective seal between the two electrode compartments. This was confirmed by successful experiments with cells incorporating electrodes with low oxygen chemical potentials such as Nb-NbO.

2.E.3. Vacuum operation

The improvements associated with the introduction of 'getters' in the upper electrode compartment suggested that the stream of purified argon was not very effective in removing the adsorbed gases released as the apparatus was heated. Experiments were therefore conducted in vacuum (1×10^{-5} torr. at 1000°C) using the final cell arrangement described in the previous section, with an Nb-NbO electrode in the upper electrode compartment. Provided the apparatus had been thoroughly degassed at the highest temperature used in the investigation, then voltages identical ($< \pm 1$ mV) to the values recorded in the purified argon were obtained in the presence of Ti or Zr getters. If these latter components were absent the cell performance was poor, and low irreproducible voltages were recorded.

It was possible, moreover, to change from vacuum to a purified argon atmosphere whilst the cell was maintained at high temperature. The introduction of the purified argon was always accompanied by a decrease in the emf value which was only regained after 30-60 mins.

Very little change in the cell voltage, however, was observed when the vacuum was re-applied. Typical results for this sequence of events are reproduced in Fig. 2.E.4. for the cell,

$$\text{Fe-FeO} \;\Big|\; \underset{\text{(DENSE, IMPERMEABLE)}}{\text{ThO}_2.\text{YO}_{1.5}\ (90.10\ \text{mole}\ \%)} \;\Big|\; \text{Ni-NiO}$$

During a series of experiments in vacuum (without getters) it was observed that the voltages of the symmetrical cell,

$$\text{Ni-NiO} \;\Big|\; \underset{\text{(DENSE, IMPERMEABLE)}}{\text{ThO}_2.\text{YO}_{1.5}\ (90.10\ \text{mole}\ \%)} \;\Big|\; \text{Ni-NiO}$$

never exceeded ± 1 mV over a period of 24 hours at 1000°C, although when the experiment was continued for a further 24 hours the asymmetrical voltages gradually increased to 20 mV. Subsequent examination of the pellets revealed that the electrode in the upper compartment had undergone slight surface reduction. Similar symmetrical cells with Fe-FeO electrodes could be maintained at 1000°C for 48 hours without any obvious deleterious effects, and the associated voltages were never greater than ± 1 mV. However, the incorporation of a small piece of titanium strip in the upper electrode compartment produced asymmetrical voltages of 20-30 mV. after about 6 hours. The spurious voltages recorded for both these electrodes could be reduced to acceptable values (± 1 mV) by surrounding the electrode in the upper compartment with a protective collar composed

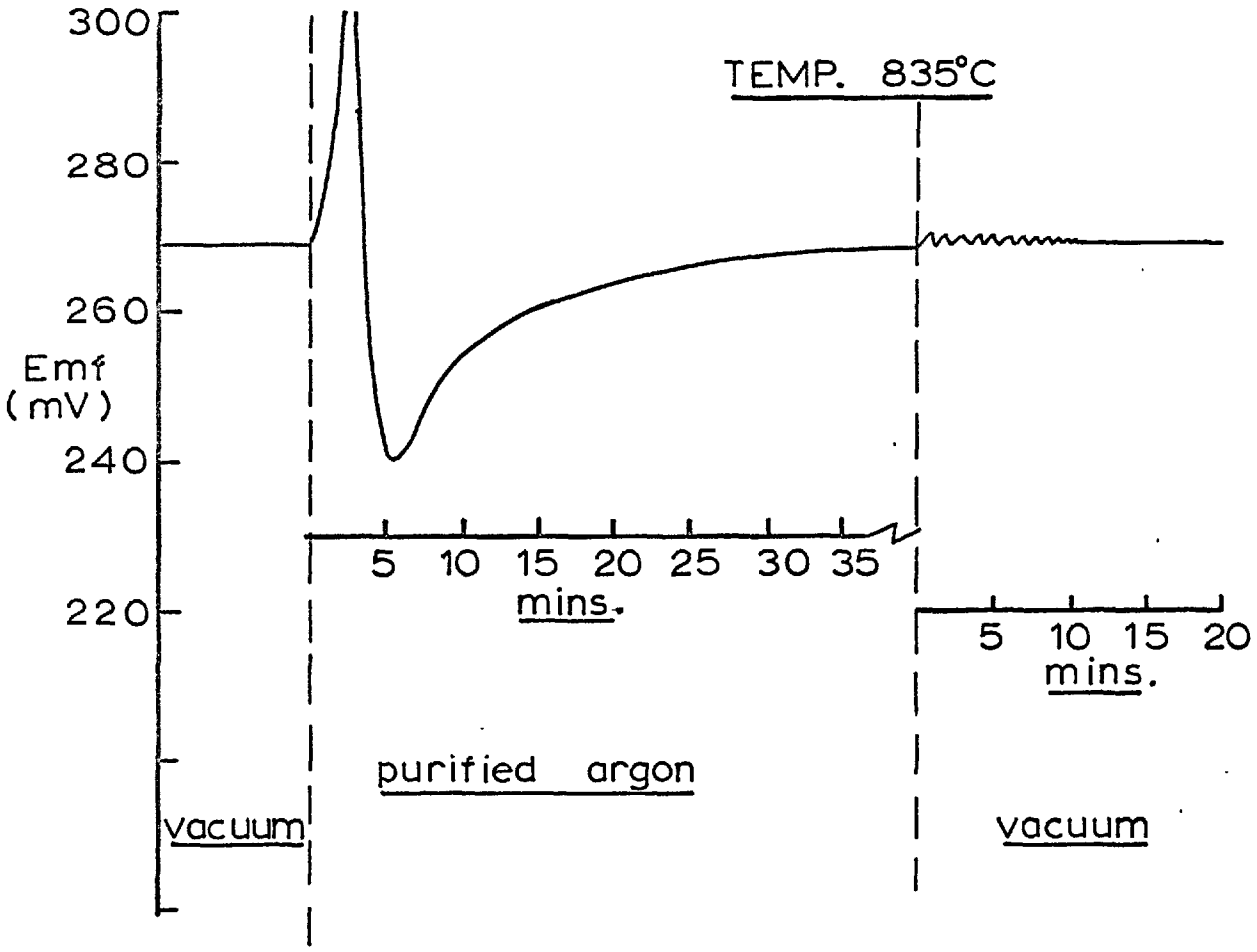


FIG. 2.E.4 VOLTAGE RESPONSE OF CELL

$Fe, FeO \mid ThO_2.YO_{1.5}$ (90.10 mole %) $\mid Ni, NiO$

TO CHANGES IN GASEOUS ENVIRONMENT

of the same material as the electrode. It was obviously desirable, therefore, to include any feature in the cell assembly which could promote local equilibrium between an electrode and its immediate gaseous environment, and it became standard procedure to include a protective collar around the upper electrode, and material of appropriate composition was also placed adjacent to the lower electrode. Fig. 2.E.3(d) therefore represents the final cell design eventually adopted for experiments in either vacuum or purified argon.

During the present investigation, other workers also reported experiments with galvanic cells incorporating solid oxide electrolytes using high vacuum atmospheres. Although Rapp[79] concluded that the use of a high vacuum atmosphere may prove generally unsuitable for cell measurements involving low oxygen chemical potentials, many apparently successful experiments in vacuum have been described by Rezukhina et al.[25,80,81] In particular these Russian workers demonstrated the possible advantages of high vacuum operation by measuring the free energy of formation of iron aluminate by means of the cell,[81]

$$Fe, Al_2O_3, Fe\ Al_2O_4 \;\Big|\; \text{solid oxide electrolyte} \;\Big|\; FeO, Fe.$$

Earlier measurements on a similar cell,

$$Fe, Al_2O_3, Fe\ Al_2O_4 \;\Big|\; \text{solid oxide electrolyte} \;\Big|\; Ni, NiO,$$

by Schmalzried[75] had apparently failed due to interaction

of the left-hand electrode (anode) with impurities in the inert gas surrounding the cell assembly.

2.E.4. Gaseous electrodes

The provision, in the final design of the apparatus, for separate electrode compartments enabled cells to be constructed with gaseous electrodes. The arrangement of these cells was similar to that shown in Fig. 2.E.3(a) with a closed end stabilized zirconia tube as the electrolyte. The upper electrode simply consisted of platinum gauze pressed against the top of the zirconia tube, and the lower electrode was either another platinum gaseous electrode or an appropriate metal-metal oxide such as Ni-NiO or Fe-FeO.

Employed as an oxygen meter this cell design was used to check the oxygen content of the purified argon, and oxygen partial pressures in the range 10^{-14} - 10^{-16} atm. were usually recorded. A similar galvanic oxygen meter with a stabilized zirconia electrolyte has been described by Weissbart and Ruka.[82]

The same cell arrangement, incorporating a pure oxygen electrode, was also used to obtain data on the thermodynamics and electrode kinetics of Fe-FeO and Ni-NiO mixtures which were extensively employed in the present investigation as reference electrodes. These experiments are described in Chapter 4.

2.F. EMF MEASUREMENTS

Cell voltages were measured with a high impedance (10^{13} ohms), low capacity (20pF), vibrating condenser electrometer*, the principles of which have been described by Palevsky et al.[83] One electrode of the cell was connected to the appropriate insulated "high" terminal on the instrument with screened non-microphonic co-axial cable. The other side of the cell, together with the metal screens used to prevent electrical pick-up, the metal components of the apparatus, and the metal outercasing of the electrometer, were all joined to a common earth point by thick copper wire. As mentioned earlier in section 1.C.4. it was essential to use a very high impedance instrument for emf measurements on cells possessing a high internal resistance or electrodes which were easily polarised (e.g. Nb-NbO), and it was equally important to ensure that the remainder of the measuring circuit was also adequately insulated to prevent any small currents leaking to earth. The insulation when the apparatus was heated to 1000°C, was therefore regularly tested with a Megger to ensure that the resistance to earth always exceeded 10^8 ohms.

A series of millivolt ranges were available on the electrometer, and the precision of the recorded voltages varied from ± 5 mV on the 0-1000 mV range to 0.1 mV on the lowest range 0-10 mV. As many of the cells developed large voltage (e.g. $\sim$ 650 mV for cells incorporating

---

* Model 33B Vibron, Electronic Industries Ltd., U.K.

Fe-FeO and Nb-NbO electrodes), it was therefore desirable to bias* the instrument so that emf values could be registered with greater precision on one of the lower ranges, and the 0-30 mV ($\pm$0.3 mV) range was usually selected. The accuracy of the measured voltages at the higher temperatures was also checked by a Tinsley potentiometer model 3184D (precision $\pm$0.1 mV), and it was soon established that this particular potentiometer was also suitable for measuring voltages as low as 600°C for cells incorporating zirconia-based electrolytes, and 800°C for cells incorporating thoria electrolytes and low oxygen chemical potential electrodes. Below these temperatures the response of the potentiometer was very poor; the accuracy of the measurements progressively decreased and it became essential to use the electrometer. The precision of the emf measurements thus varied from $\pm$0.1 mV at the higher temperatures to $\pm$0.3 mV at the lower temperatures.

It was also necessary to establish that the recorded cell voltage was reversible. This was usually done by passing a small current (1-10μA) through the cell for one minute and noting whether the original emf value was regained. The procedure was then repeated with the current flowing in the reverse direction. More extensive polarisation experiments were conducted with certain electrodes in which the voltage was continually recorded, with the aid of an auxiliary reference electrode, whilst the polarisation current was flowing through the cell.

---

* This was accomplished by using a potentiometer to impose a known voltage on the electrometer and adjusting the millivoltmeter to register zero.

The circuit and cell assembly for these experiments are illustrated in Fig. 2.F.1, and the associated polarisation data are discussed in the appropriate section devoted to the relevant electrode equilibria.

Asymmetrical voltages were another possible source of erroneous data and cells composed of identical electrodes were therefore examined to provide information about these spurious voltages. This type of cell has already been mentioned in connection with vacuum operation of the apparatus (section 2.E.3). When electrodes possessing high oxygen chemical potentials (Fe-FeO, Ni-NiO, $Cu-Cu_2O$) were incorporated in the final cell design and shielded by additional electrode material (fig. 2.E.3(d)), then the asymmetrical voltages were found to be negligible (< 0.5 mV) provided the cell had first been heated above a certain minimum temperature, which was approximately 600°C for the $Cu-Cu_2O$ electrode and 700°C for the Fe-FeO electrode. Below these temperatures, large asymmetrical voltages, which varied from 10-100 mV, could be observed as the cell was heated. Asymmetrical voltages as high as 2 mV were often recorded with electrodes possessing very low oxygen potentials (e.g. Nb-NbO) even when the cell had been maintained at 1000°C for several hours, and much larger voltages (10-20 mV) often persisted until the cell temperature had exceeded 900°C. A related feature which was occasionally observed with such cells as,

Nb-NbO/thoria-based electrolyte/Fe-FeO

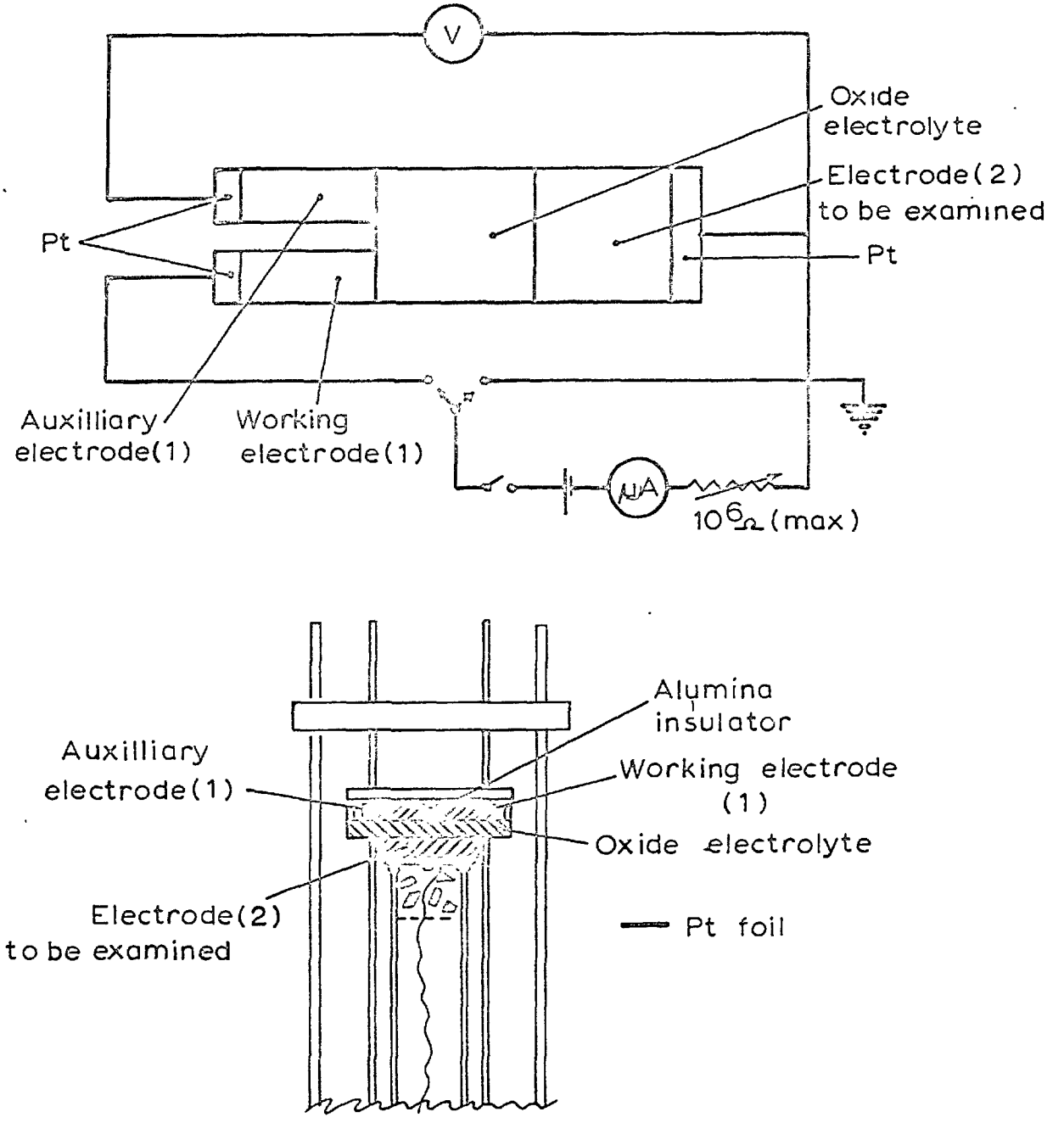


FIG.2.F.1 CIRCUIT AND CELL ARRANGEMENT FOR POLARISATION EXPERIMENTS

concerned the different emf values that could be obtained by initially earthing the anode (Nb-NbO electrode), and then switching the connections so that the cathode (Fe-FeO electrode) was earthed. Normally the voltage agreed better than ± 1 mV, but occasionally discrepancies of up to 5 mV could be recorded and the experiment was terminated. A satisfactory explanation of these spurious voltages, and the inability of the electrode to function reversibly until the cell temperature had exceeded some empirical value, is impossible at present due to lack of information about the relevant electrode kinetics.

2.G. CONDUCTIVITY MEASUREMENTS

Two-terminal A.C. conductivity measurements were made on the dense impermeable electrolyte pellets in the apparatus described in section 2D. The shape of the available samples made two-terminal measurements inevitable, and consequently an A.C. technique was more appropriate in view of the electrolytic nature of the zirconia and thoria solid solutions. In the initial experiments a layer of platinum[x] was applied to the opposite faces of the electrolyte pellets which were then fired in air at 1000°C, before being pressed between platinum foil contacts. However, later experiments indicated that similar results could be obtained without a preliminary application of platinum and this treatment was subsequently omitted.

---

x Platinum paste supplied by Engelhard Industries Ltd., (Hanovia Ceramics Division), London, U.K.

Adequate contact was ensured by giving the electrolyte surfaces a final polish with 1/4 micron diamond paste, and annealing the assembled electrolyte sample and platinum foil contacts for 24 hours at 1000°C prior to making any measurements.

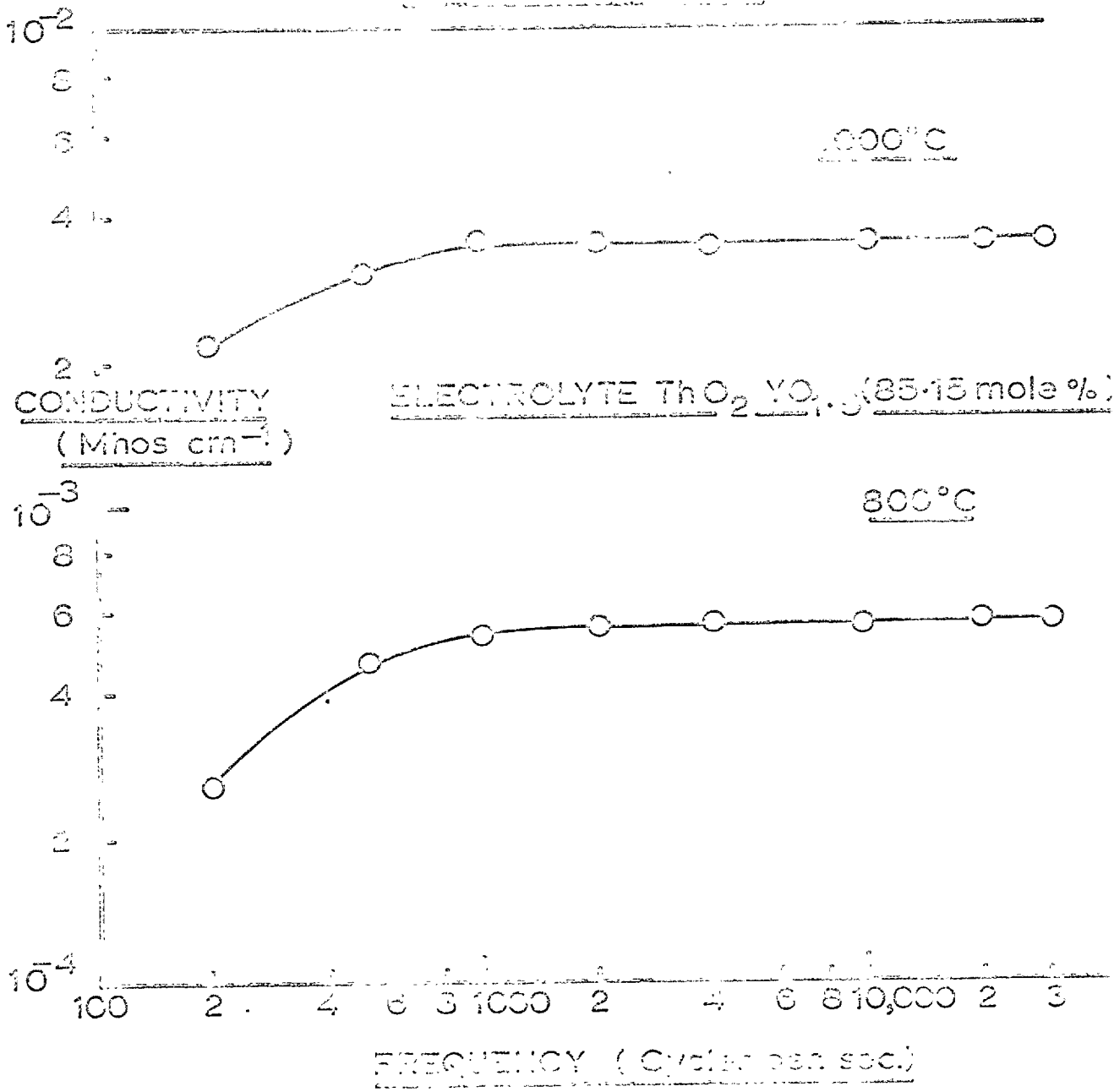
Conductivity data were recorded in the range 700-1050°C and the samples were maintained at the selected temperatures until consistent values were obtained, a procedure which usually required 1-3 hours. Every sample was exposed to three different oxygen partial pressures and on each occasion was cycled through the temperature range at least twice. The appropriate oxygen partial pressures were provided by pure oxygen (p_{O_2} = 1 atm.), argon dried with magnesium perchlorate (p_{O_2} = 10^{-6} atm.), and forming gas (H_2 content: 10%) saturated with water-vapour at 20°C (p_{O_2} =~ 10^{-15} atm. at 1000°C). Whenever the oxygen partial pressure inside the apparatus was changed the specimen was equilibrated for 24 hours at 1000°C before continuing the conductivity measurements. In addition the two lower oxygen partial pressures (10^{-6} and 10^{-15} atm.) were periodically checked with the oxygen gas meter already described (section 2.E.4).

A series of measurements with a variable frequency (200-30,000 c.p.s.) A.C. resistance bridge* established that the A.C. frequency used in the measurements was not a

---

* This instrument was assembled in the laboratory and incorporated variable capacitors and resistors which could be adjusted until a cathode ray oscilloscope indicated the balance point by displaying a horizontal linear trace.

FIG. 2.6.1 [illegible] AS A FUNCTION OF FREQUENCY



significant variable provided the frequency exceeded 1000 c.p.s. Below 1000 c.p.s., the conductivity values decreased as the A.C. frequency was reduced. Typical conductivity values for a $ThO_2.YO_{1.5}$ (85.15 mole %) electrolyte as a function of the applied frequency are shown in Fig. 2.G.1.

A fixed frequency (1592 c.p.s.) A.C. resistance bridge,[xx] however, was more readily available and the conductivity data reported in Chapter 3 was obtained with this instrument.

2.H. STANDARD PROCEDURES AND PRECAUTIONS

Nearly all the emf data reported in subsequent chapters were obtained using the apparatus described in section 2.D, and the final cell design illustrated in Fig. 2.E.3(d). The principal procedures and precautions involved in these emf measurements are summarised below, and details of typical experiments incorporating a variety of electrodes and electrolytes are reproduced in Appendix VI. A few results associated with different cell designs are also discussed in later chapters, and details of the experimental arrangements and procedures are included in the relevant sections.

---

[x] Cintel capicitance-resistance bridge Type 1862 supplied by Cinema-Television Ltd., London, U.K.

2.H.1. Apparatus

(i) The argon purification system was periodically checked using the oxygen gas meter (section 2.E.4). If the oxygen partial pressure in the argon exceeded 10^{-12} atm. then the reagents (titanium granules, magnesium perchlorate, etc) in the gas train were replaced, and the apparatus examined for leaks.

(ii) The apparatus was thoroughly degassed at the highest operating temperature (1100°C), and purified argon was always admitted prior to exposing the interior of the apparatus to the laboratory atmosphere.

(iii) The apparatus was only exposed to the laboratory atmosphere when a cell was being dismantled and a new cell assembled. This operation required approximately 30 minutes, and great care was taken to avoid leaving grease or fingerprints on the interior surfaces of the apparatus.

(iv) Correct operation of the apparatus and measuring circuits was regularly tested by incorporating a 'standard' cell in the apparatus, i.e.,

Ni,NiO | ZrO_2. CaO (85.15 mole %) | Cu,Cu_2O
or Fe,FeO | ThO_2. $YO_{1.5}$(85.15 mole %) | Ni,NiO,

and occasionally a symmetrical cell,
Fe,FeO | ThO_2. $YO_{1.5}$(85.15 mole %) | Fe,FeO

was also used to check that no spurious voltages were being developed in the apparatus.

(v) The electrical insulation was periodically checked with a Meggar.

(vi) The cell thermocouple and platinum electrode leads were replaced at frequent intervals.

(vii) If 'getters' were to be incorporated in the apparatus then a new piece of titanium or zirconium foil was used for each experiment.

2.H.B. Experimental procedure

(i) If appropriate, the cell components were treated in vacuum before being incorporated in the cell assembly.

(ii) For argon operation, the apparatus was evacuated and refilled with purified argon (twice), and then both the argon flow-rates were adjusted to 50 mls/min. The normal heating schedule consisted of raising the temperature of the cell to 200°C in 2 hours, and then allowing the temperature to slowly increase to 650°C overnight. The following day the temperature was further increased to 900°C over a period of two hours.

(iii) The above heating schedule was also usually followed for vacuum operation, although an additional condition was imposed in that the pressure registered by the Penning guage should not exceed 7×10^{-5} torr., and so

occasionally the heating-rate was slower.

(iv) It was normal practice to wait until the cell had reached 900°C before any measurements were taken. Thereafter emf values were recorded at approximately 15 minute intervals until the cell had attained equilibrium. The cell was then checked for reversible behaviour, and for argon operation it was also necessary to demonstrate that the voltage was independent of the gas flow-rates which were varied between 10-100 mls/min.

(v) Emf values were subsequently obtained at approximately 50°C intervals, with the cells being maintained at the selected temperatures from 2-24 hours until reproducible values were recorded. A cell was usually cycled through the temperature range at least twice, and again checked for reversible behaviour at the lowest temperature involved in the emf measurements.

CHAPTER THREE

PROPERTIES OF THORIA - BASED ELECTROLYTES

3.A X-RAY, DENSITY, AND CERAMOGRAPHIC EXAMINATIONS

3.A.1 General structural considerations

Pure thoria and the thoria solid solutions employed as electrolytes in the present investigation, possess the fluorite structure. In this structure (fig. 3.A.1) the anions are arranged in simple cubic packing with half the interstices filled by cations. This gives rise to a unit cell (M_4X_8) in which the cations are characterised by face-centred cubic packing with a space at the centre (½, ½, ½) corresponding to the unfilled interstice in the simple oxygen lattice. The resulting 8:4 co-ordination is only found in the fluorite structure.

It is interesting to note that neutron diffraction studies on UO_2 and ThO_2 carried out by Willis[84] have lead to the suggestion that as the temperature increases, the oxygen ions tend to be displaced from the fluorite-type sites at $\frac{1}{4}, \frac{1}{4}, \frac{1}{4}$

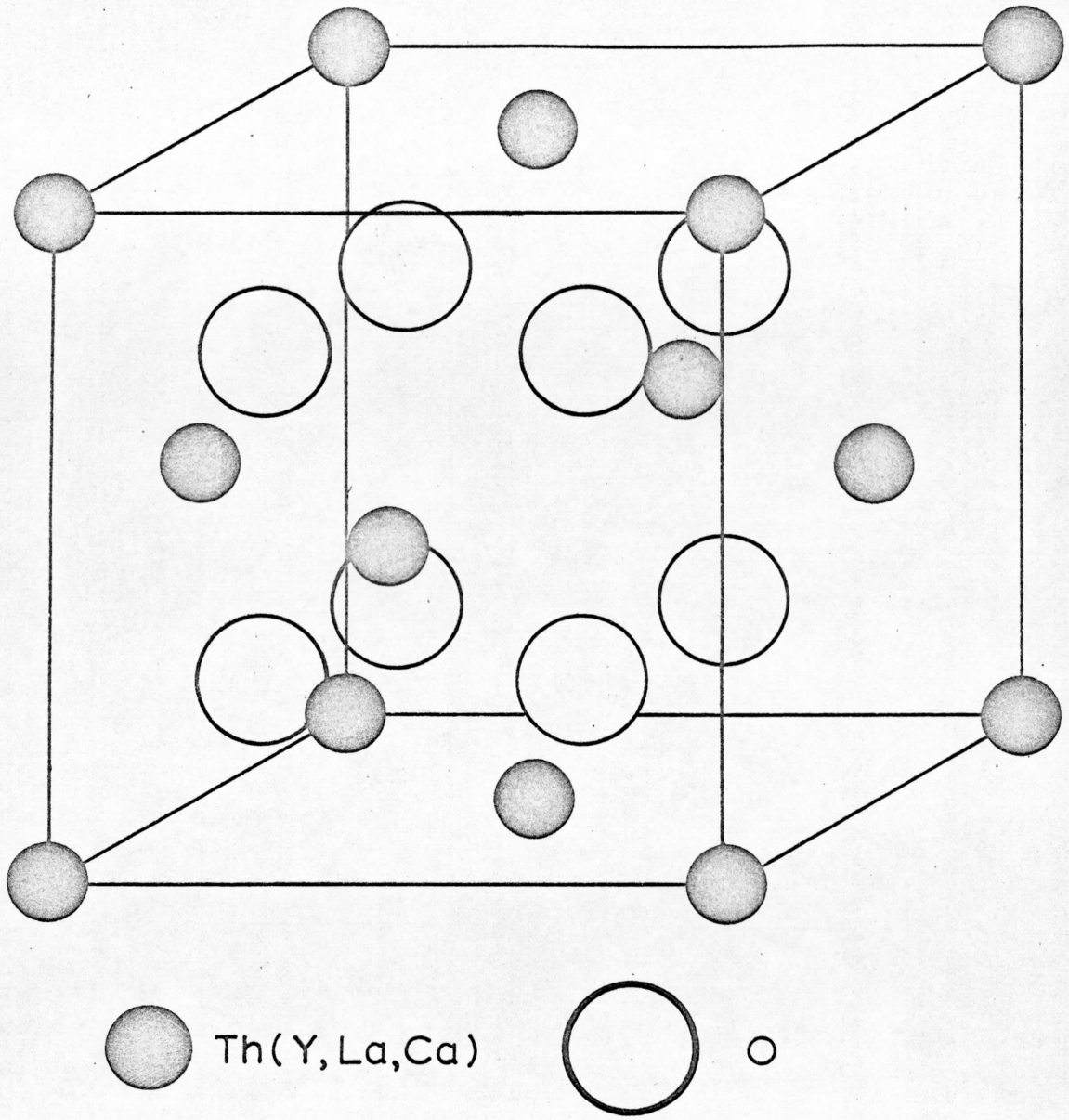


FIG. 3. A. 1 THE FLUORITE STRUCTURE

towards the large interstial holes at ½, ½, ½.

When the Th^{4+} ion in ThO_2 is replaced by an aliovalent cation (Y^{3+}, La^{3+}, Ca^{2+}) charge neutrality may be restored by one of two structural schemes;

(i) the cation sub-lattice is completely filled and the appropriate number of anion vacancies are created,

(ii) the anion sub-lattice is complete, and the excess cations occupy interstial sites.

To distinguish between the two models, the appropriate theoretical densities were calculated using lattice parameters derived from x-ray measurements. These theoretical densities were then compared to the experimentally determined densities of the relevant sintered pellets.

3.A.2 ThO_2 - $YO_{1.5}$ solid solutions

Yttrium oxide crystallises with the C-type rare earth oxide structure (M_4X_6). This structure is closely related to that of the fluorite structure (M_4X_8), from which it may be derived by an ordered omission of one-quarter of the anions, followed by a slight re-arrangement of the remaining ions. This

structural similarity results in extensive solid solution in the system, $ThO_2 \cdot YO_{1.5}$, and Hund and Mezger[85] have reported that approximately 30 mole % $YO_{1.5}$ is soluble in ThO_2 at 1200°C.

Four of the five compositions (4, 10, 15, 25 mole % $YO_{1.5}$) examined in this series sintered extremely well to produce very dense impermeable pellets, which were always very translucent and often contained completely transparent regions. Pellets prepared from the fifth composition ($ThO_2 \cdot YO_{1.5}$ 99.1 mole %) and from pure ThO_2, however, were usually opaque due to the presence of a small amount of closed pore porosity, which was responsible for the slightly low density values reported in Fig. 3.A.3.

The lattice parameter measurements* for the solid solutions are summarised in Fig. 3.A.2. as a function of composition and can be seen

---

* X-ray measurements on the two compositions 4 and 25 mole% $YO_{1.5}$ were made by P. K. R. Moody, Metallurgy Department, Imperial College.

FIG. 3. A. 2 LATTICE PARAMETERS IN THE SYSTEM $ThO_2 \cdot YO_{1.5}$

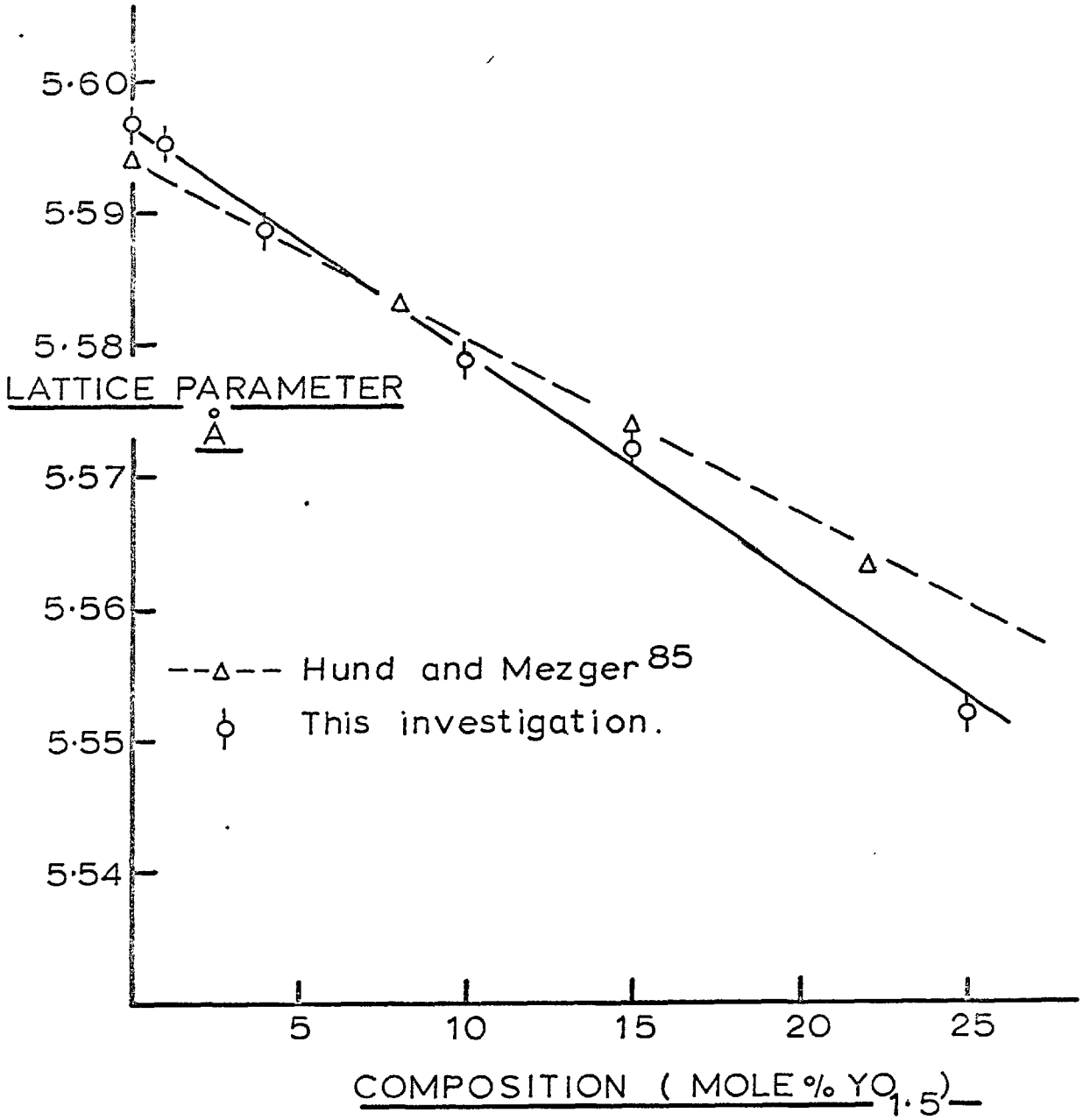
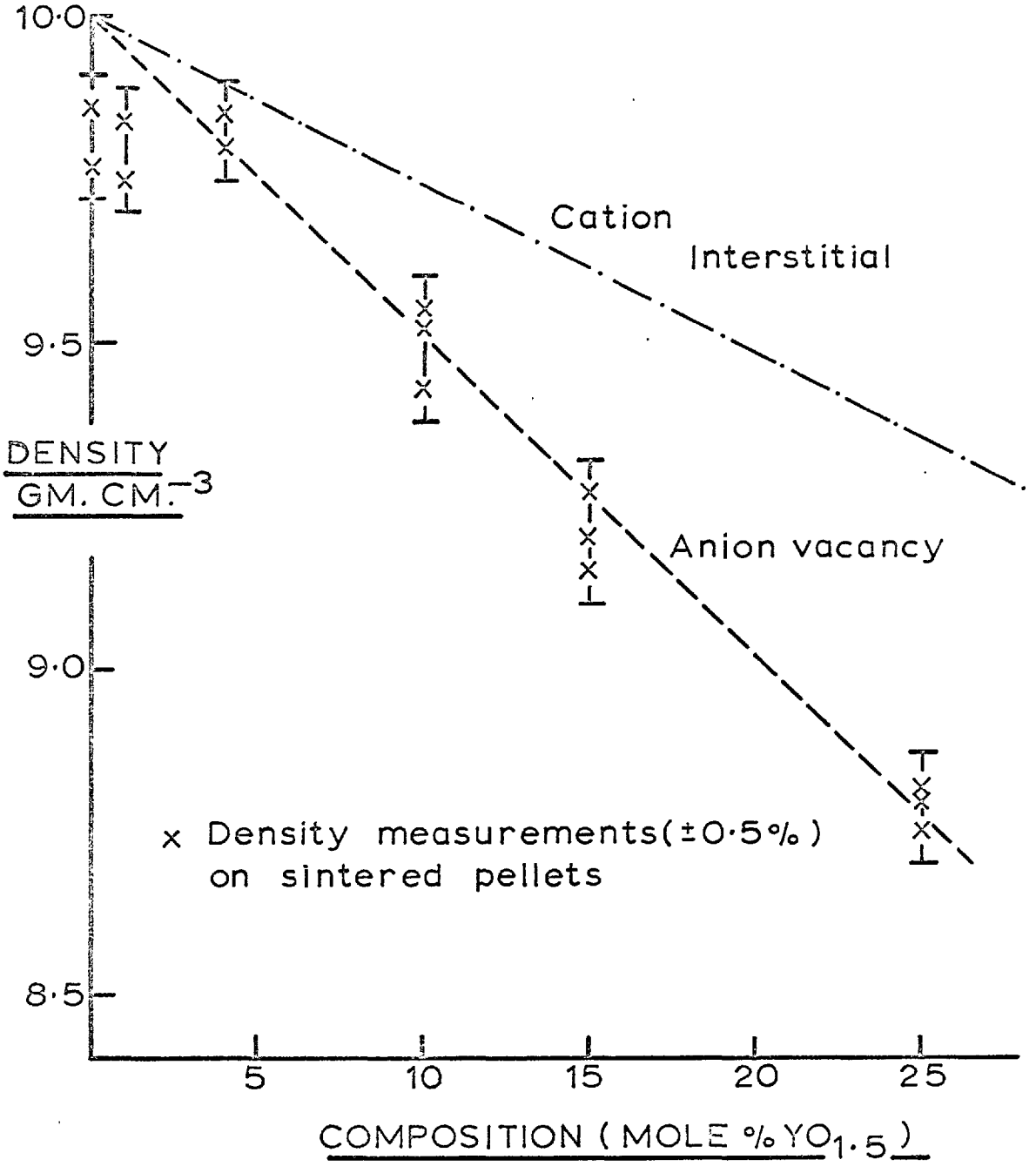


FIG. 3.A.3 DENSITIES OF ThO_2–$YO_{1.5}$ SOLID SOLUTIONS



to be in reasonable agreement with the results reported by Hund and Mezger[85]. The associated theoretical densities for the two structural models mentioned in the preceding section (3.A.1) are reproduced in fig. 3.A.3, as a function of composition, together with the measured densities of the sintered pellets. On the basis of this data it is reasonable to conclude that $ThO_2 . YO_{1.5}$ solid solutions have fluorite-type structure with a filled cation sub-lattice and anion vacancies. These solid solutions can be represented by the formula $Th_{1-x} Y_x O_{2-\frac{x}{2}}$ and if the simple defect model is valid, then the percentage of vacant anion sites, fixed by composition, equals $\frac{x}{4}$ x 100 %.

3.A.3 ThO_2 - $LaO_{1.5}$ solid solutions

In the temperature range, 1300-1400°C, it appears that ThO_2 can accommodate about 50 mole % $LaO_{1.5}$ in solid solution,[86,87] with the formation of a corresponding number of anion vacancies. Two electrolyte compositions were prepared in this system, 10 and 15 mole % $YO_{1.5}$, and although samples were not subjected to x-ray and density measurements, the sintered pellets were almost transparent which indicated that the residual porosity was very small.

3.A.4. ThO_2 - CaO solid solutions

The ionic radii of Th^{4+} and Ca^{2+} are very similar. For six-fold co-ordination both Pauling[88] and Ahrens[89] suggest the following values:

Th^{4+} : 1.02 A^{o}
Ca^{2+} : 0.99 A^{o}

It follows that the unit cell dimensions of the ThO_2 lattice will only be slightly modified when the Th^{4+} ion is replaced by Ca^{2+}, and consequently it is difficult to establish the extent of the solid solution. Curtis and Johnson[90] suggested that the maximum solubility of calcium oxide was at least 12.5 mole %, whereas Mobius et al[91] have reported that the solid solution is limited to approximately 8 mole % CaO at 1600°C.

The sintered electrolyte pellets of the three compositions, 1.5, 5, and 15 mole % CaO, studied in the present investigation, were very dense, translucent, and contained only a few very small closed pores. All the x-ray diffraction lines could be indexed on the basis of a fluorite structure, and the lattice parameter (5.598 ± 0.001 Å) derived for the 15 mole %CaO composition was almost identical to that obtained for pure ThO_2 crystals

(5.597 ± 0.001 Å) . There was also no evidence for a second phase when polished specimens were examined under the microscope using reflected light. These observations support Curtis and Johnson's[90] suggestion that the maximum solubility of calcium oxide is at least 12.5 mole %.

If the solid solution is represented by the formula $Th_{1-x}Ca_xO_{2-x}$, then the percentage of anion vacancies determined solely by the composition equals $\frac{x}{2} \times 100$ %.

3.B. CONDUCTIVITY MEASUREMENTS

3.B.1. Preliminary comments

Conductivity measurements were made on two samples of each electrolyte composition involved in the present investigation. The results usually agreed with 10%, which was considered sufficiently accurate for these preliminary experiments and a best straight line, determined visually, was drawn through the plotted data. If the discrepancy for a given pair of samples was greater than 10%, measurements were made on additional specimens, and all the results were used in the final assessment.

The data were analysed by plotting the logarithm of the specific conductivity against the reciprocal of the absolute temperature as required by the empirical Arrhenius type equation:

$$\sigma = \sigma_0 \exp -\left(\frac{Q}{RT}\right).$$

Typical results at three oxygen partial pressures, are shown in fig. 3.B.1 for two samples of $ThO_2.YO_{1.5}$ (85.15 mole %), and in fig. 3.B.2 for one specimen of $ThO_2.YO_{1.5}$ (99.1 mole %). All the conductivity data is summarised in Tables 3.C.2. and 3.C.3. (p.86-7) which list the relevant activation energies, pre-exponential factors, and associated errors, as a function of composition.

In the introductory discussion on ionic conductivity (section 1.C.2), it was suggested that it was more meaningful to plot $\log(\sigma T)$, instead of just $\log\sigma$ as a function of the reciprocal of the absolute temperature. This has been done for the conductivity results obtained in oxygen for the two specimens of composition, $ThO_2.YO_{1.5}$ (85.15 mole %). The values are plotted in fig. 3.B.3., and the data can be represented by a linear equation possessing an activation energy of 26.3 ± 2.5 k cals., which is not significantly different

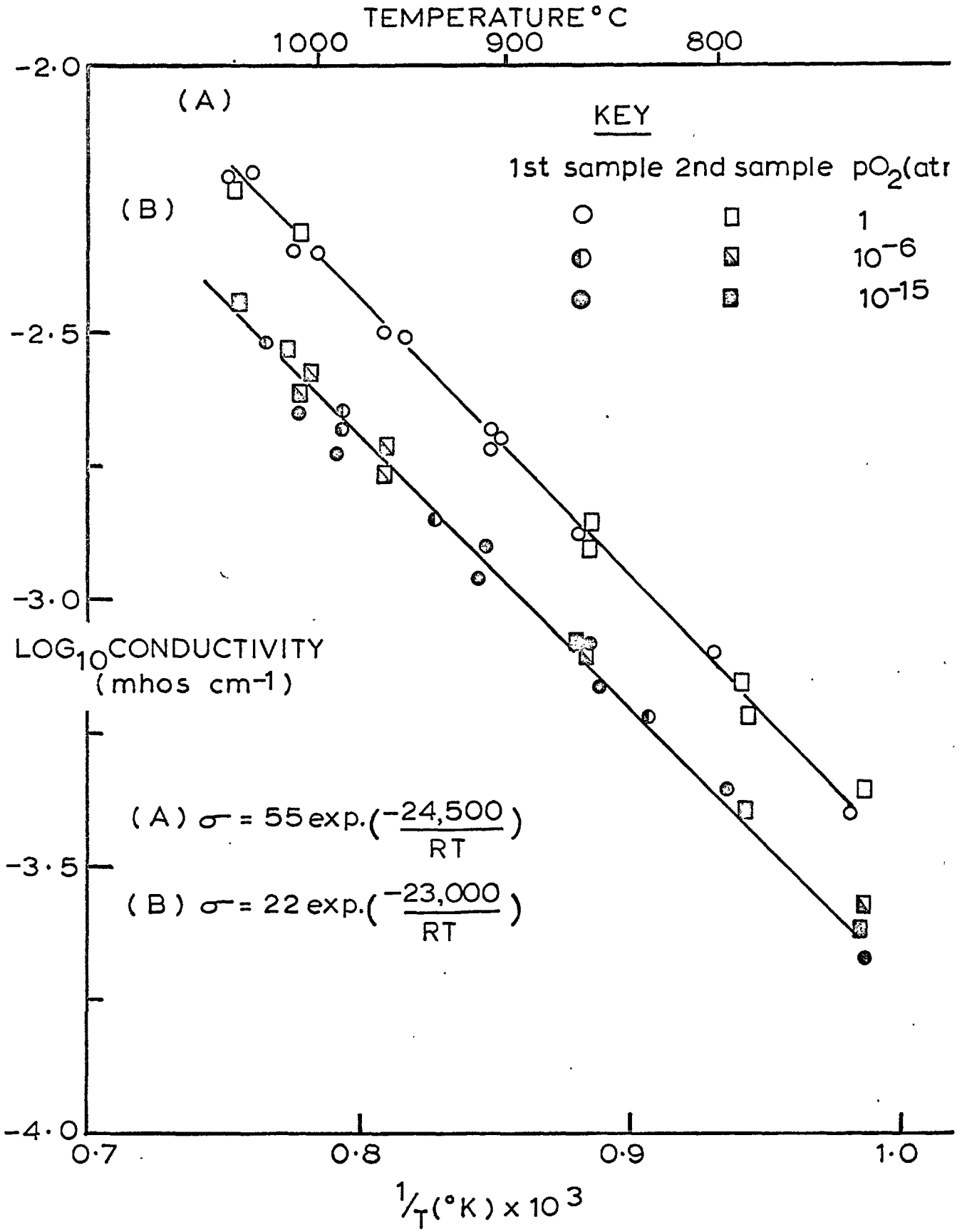
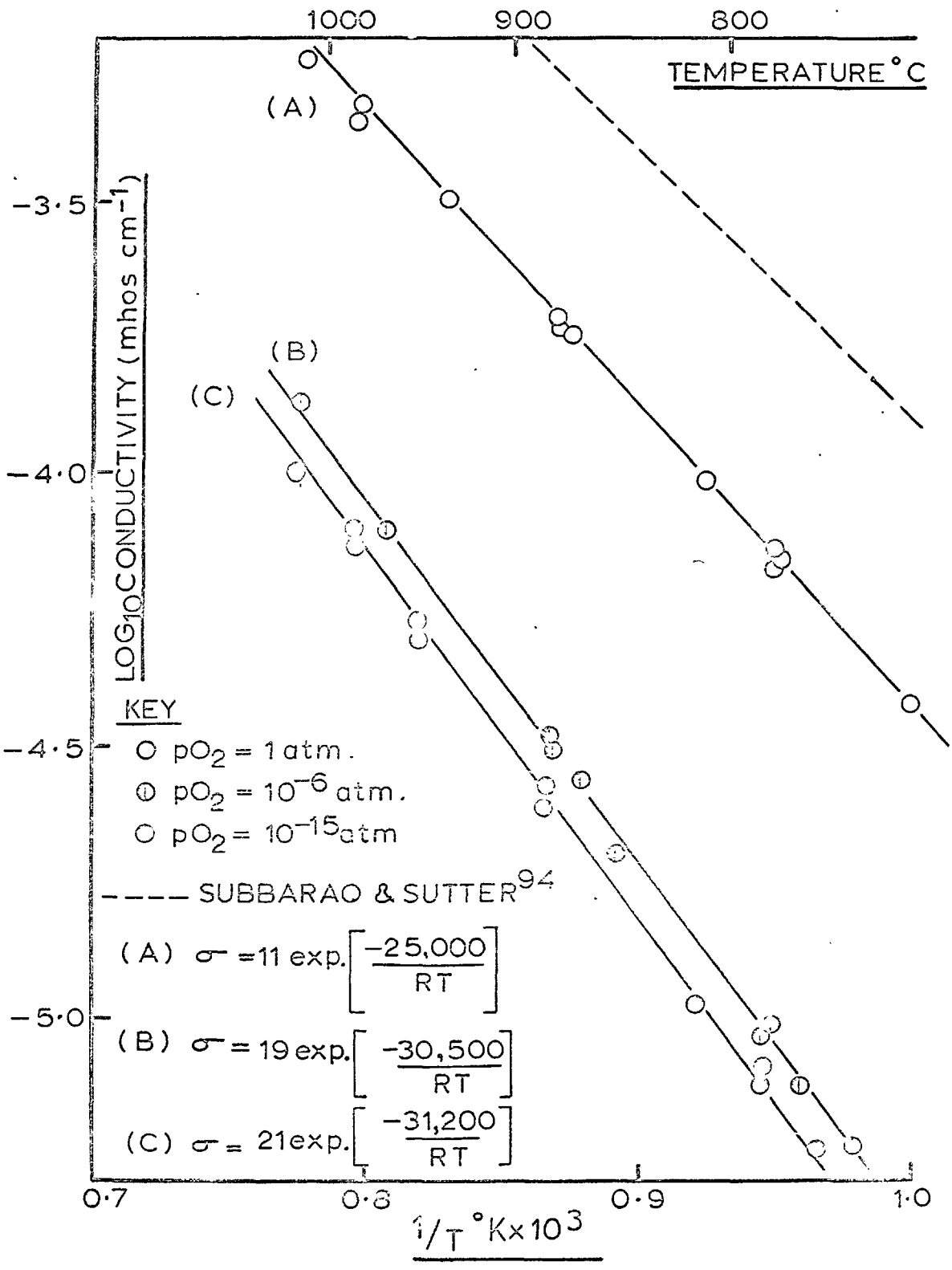


FIG. 3.B.1 LOG σ v. $^1/_T$ FOR ELECTROLYTE $ThO_2 \cdot YO_{1.5}$ (85.15 mole %)

FIG. 3.B.2 · LOG σ v $^{1}/_{T}$ FOR $ThO_2.YO_{1.5}$ (99·1 mole %)



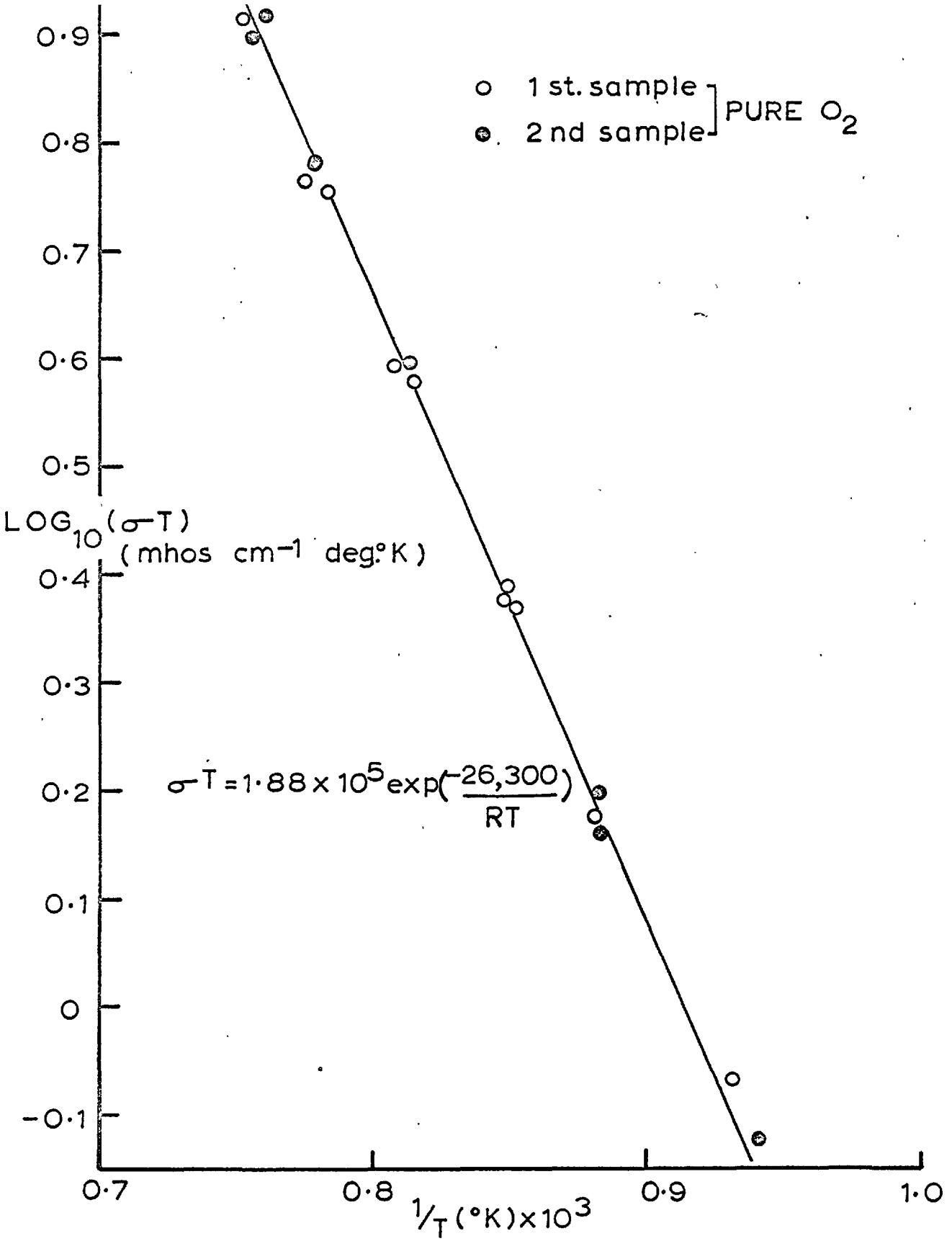


FIG. 3.B.3 LOG (σT) v. $^1/_T$ FOR ELECTROLYTE $ThO_2 . YO_{1.5}$ (85.15 mole%)

from the activation energy 24.5 ±2.5 kcal. obtained by simply plotting log σ against $^1/T$ (fig. 3.B.1). It appeared then, that no special advantage was to be gained in using the function log(σ.T), and as nearly all the relevant activation energies reported in the literature had been determined from simple log σ v $^1/T$ plots, the same procedure was adopted in this investigation.

The results obtained for each electrolyte system are next considered separately.

3.B.2 ZrO_2 $YO_{1.5}$ system

Only one composition, 20 mole % $YO_{1.5}$, was examined in this series, and the relevant data, together with values* obtained in two other investigations,[92,93] can be represented by the straight line reproduced in fig. 3.B.4. Taking into consideration the slightly different compositions and the known variation of

---

* Strickler and Carlson[92] employed a two-point A.C.(1000 c.p.s) technique.
Dixon et al[93] used a four-point A.C.(1000 c.p.s) method.

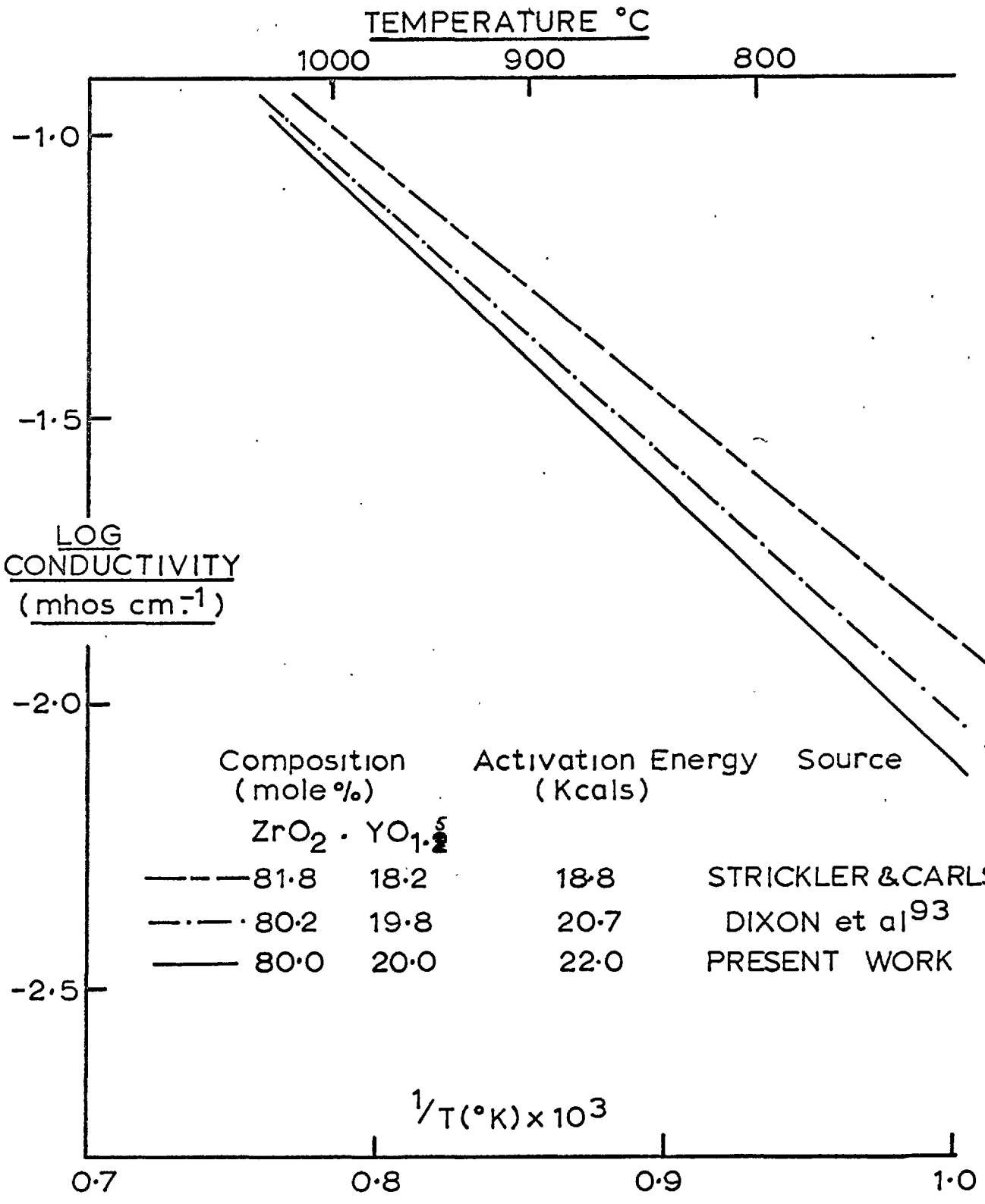


FIG.3.B.4 LOG CONDUCTIVITY AS A FUNCTION OF TEMPERATURE FOR SELECTED ZIRCONIA-YTTRIA COMPOSITIONS

conductivity with composition (section 3.C.3), then both the magnitude of the conductivity values and the associated activation energies are in good agreement, and provide evidence of the reliability of the conductivity values measured in the present investigation.

3.B.3. ThO_2 - $YO_{1.5}$ system

The present investigation appears to be the only systematic study of the electrical conductivity of this oxide solution as a function of both composition and oxygen partial pressure. Conductivity measurements[85,94,95] carried out in air, however, have been reported for a number of selected compositions, and these data are compared in Fig. 3.B.5, at the two temperatures, 800 and 1000°C, with values obtained in the present work in an atmosphere of pure oxygen. Differences in specimen density and purity undoubtedly account for the considerable spread of results recorded in fig. 3.B.5. For example, the pellets used by Hund and Mezger[85] were only sintered at 1400°C, and although Subbarao and Sutter[94] achieved densities 96-98% of the theoretical values by sintering at 2200°C, they employed materials which were less pure than those used in the present research.

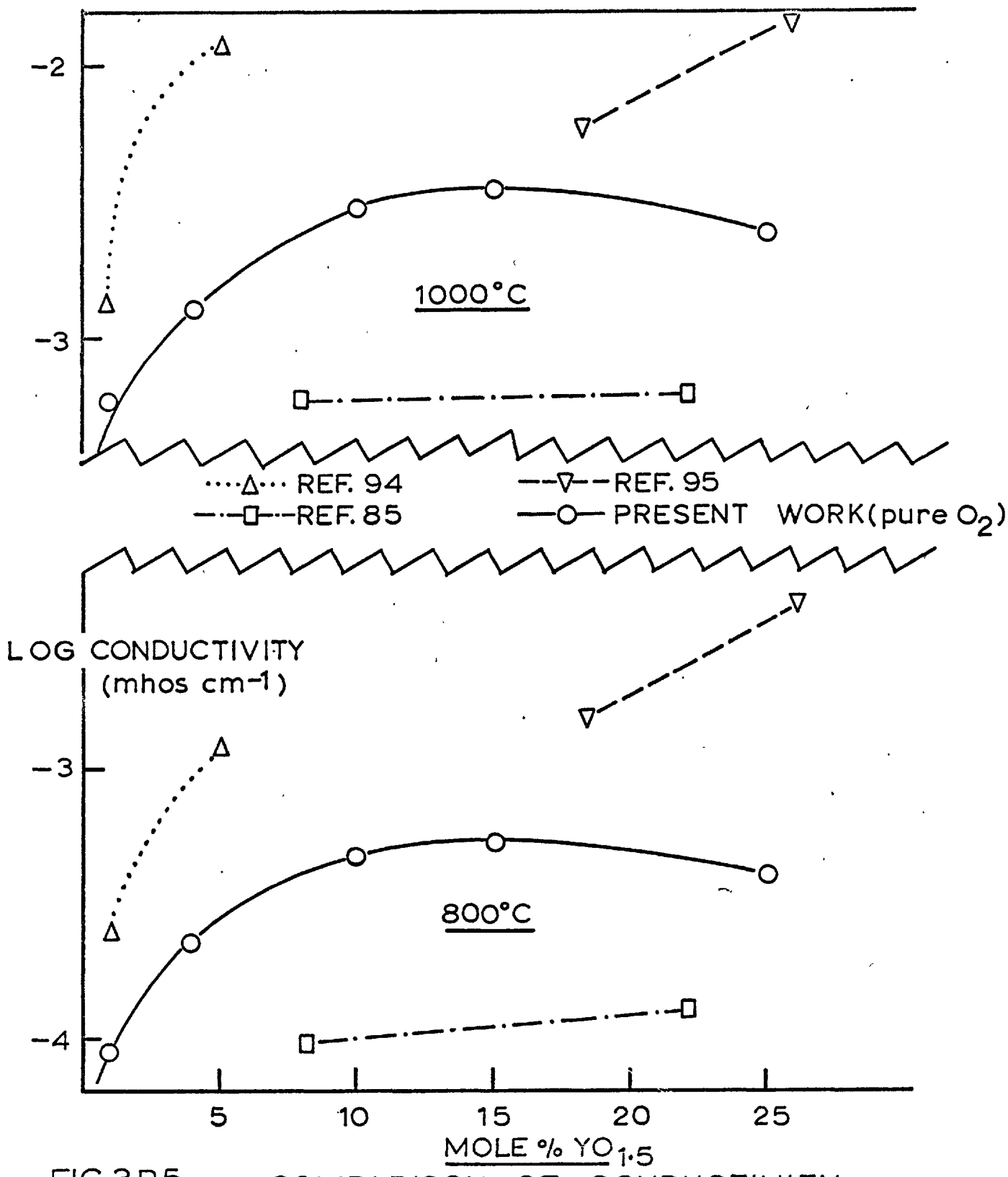


FIG. 3.B.5 COMPARISON OF CONDUCTIVITY ISOTHERMS (1000°, 800°C) AS A FUNCTION OF COMPOSITION IN THE ThO_2–$YO_{1.5}$ SYSTEM

All the investigators noted that the specimens were coloured. The intensity of the colour deepened with increasing yttria content, and varied from yellowish-cream ($\sim$10 mole % $YO_{1.5}$) to reddish or chocolate-brown ($\sim$30 mole % $YO_{1.5}$). In the present study, pellets containing 10 mole % $YO_{1.5}$ and above also exhibited a slight yellowish colouration when they were heated in air or pure oxygen; this colour, however, disappeared upon heating in argon or vacuum at 1000°C, resulting in white transluscent pellets. It is possible that rare-earth impurities (e.g. Tb_4O_7) known to be present in the "Specpure" yttria, were responsible for this colouration.

The electrical conductivities of all the $ThO_2 \cdot YO_{1.5}$ compositions examined were a function of oxygen partial pressure, and this dependence at 1000°C is illustrated in figs. 3.B.6 and 3.B.8. These results conflict with the observations of Markin et al[96] who have reported that the conductivity of the electrolyte $ThO_2 \cdot YO_{1.5}$(85.2/14.8 mole %) was independent of oxygen partial pressure when the latter was varied between 1 atm. and 10^{-34} atm. at 1000°C. These workers employed materials of similar purity (Johnson Matthey

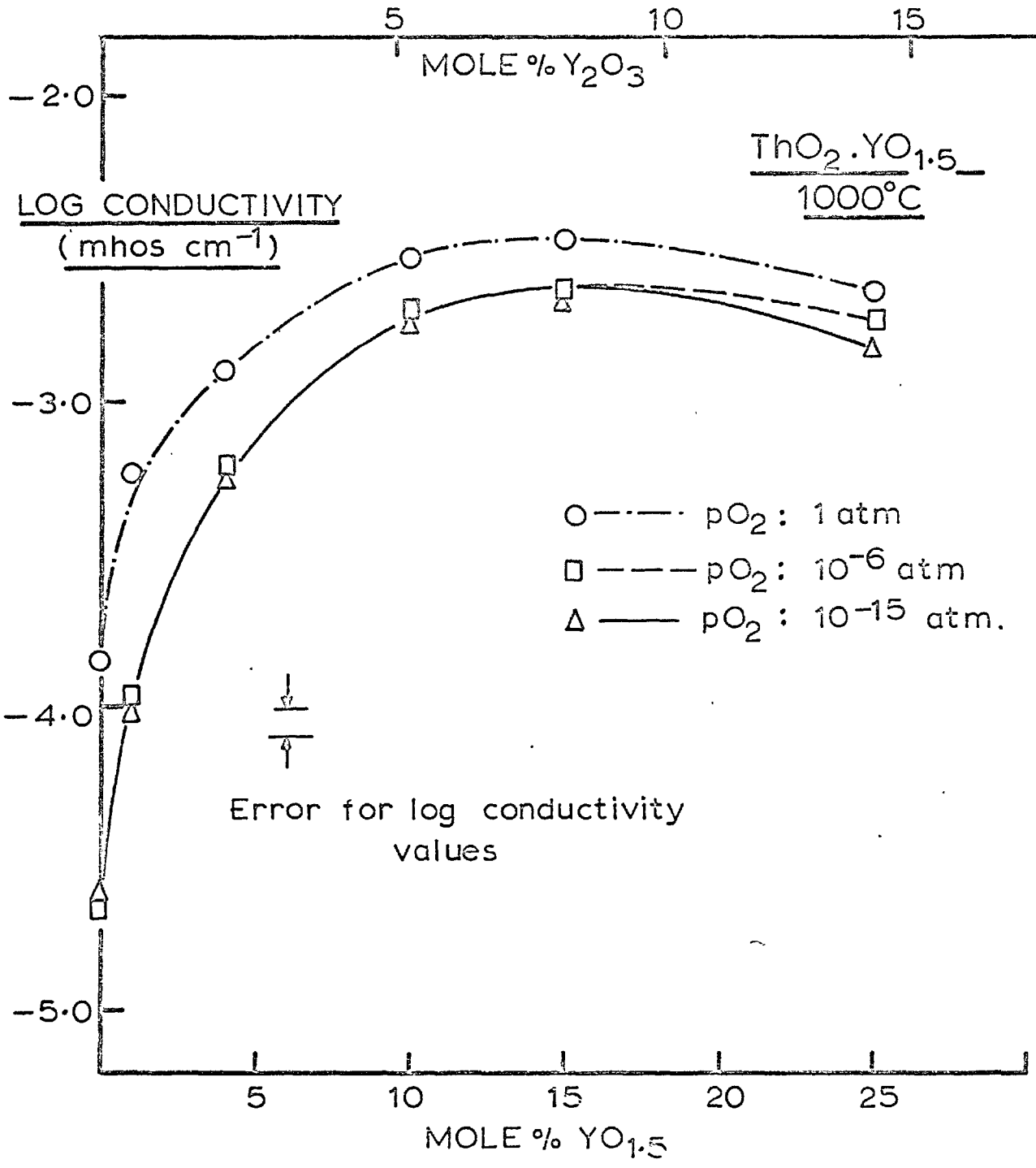


FIG. 3.B.6 LOGARITHM OF CONDUCTIVITY AS A FUNCTION OF COMPOSITION FOR THE ThO_2-$YO_{1.5}$ SOLID SOLUTIONS

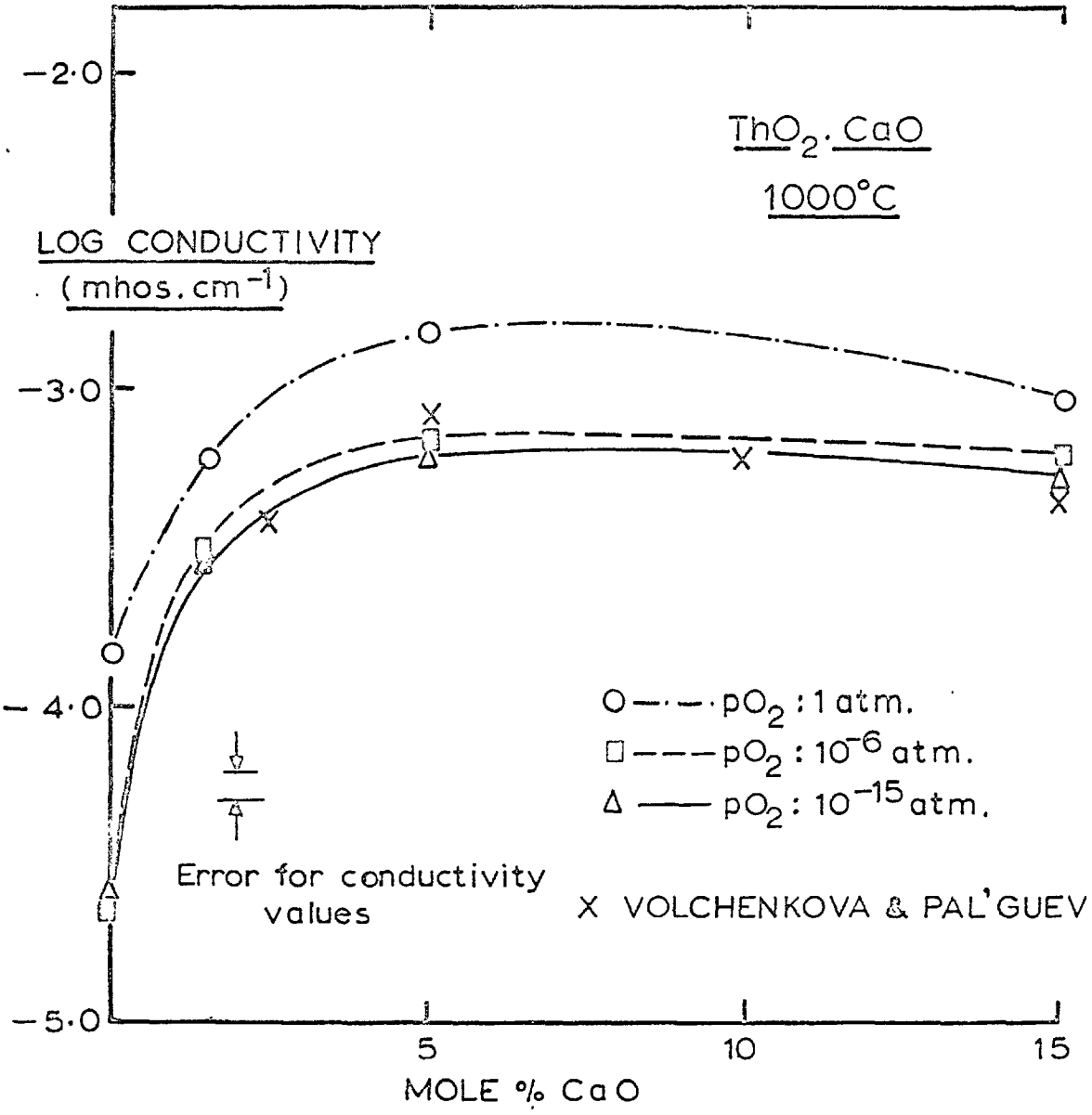


FIG. 3.B.7 LOGARITHM OF CONDUCTIVITY AS A FUNCTION OF COMPOSITION FOR THE ThO_2·CaO SOLID SOLUTIONS

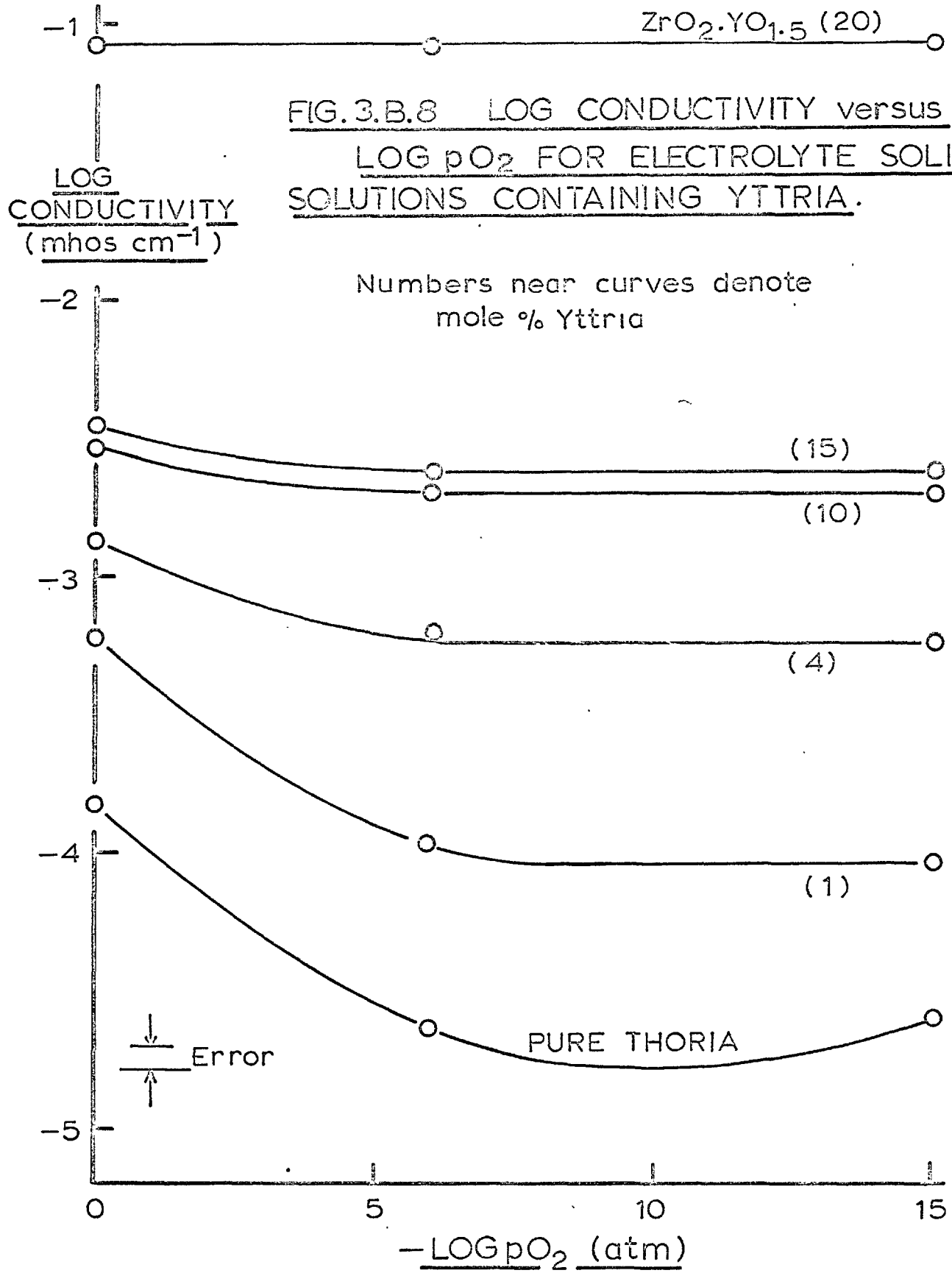


FIG. 3.B.8 LOG CONDUCTIVITY versus LOG pO_2 FOR ELECTROLYTE SOLID SOLUTIONS CONTAINING YTTRIA.

'Specpure' reagents), but employed a different technique to fabricate their conductivity samples in that powdered platinum was mixed with portions of the electrolyte powder, prior to pressing and vacuum sintering at 1650°C, to provide low-resistance contacts which were an integral part of the electrolyte pellet. It is possible, however, that this procedure could introduce metallic impurities into the electrolyte sample and so produce erroneous conductivity values.

3.B.4 ThO_2-$LaO_{1.5}$ system

Two compositions were examined in this series, 10 and 15 mole % $LaO_{1.5}$. The conductivity values for these electrolytes were about 10% (0.08 on the $\log_{10}$ scale) higher than the corresponding ThO_2-$YO_{1.5}$ compositions, otherwise their properties were almost identical to the ThO_2-$YO_{1.5}$ solid solutions. The same pattern of oxygen partial pressure dependence was followed, and a slight yellowish colouration was again evident when the specimens were heated in pure oxygen or air. Heat treatment at 1000°C in argon or vacuum (i.e. at low oxygen partial pressure) removed this colour.

3.B.5 ThO_2 - CaO system

Activation energies and pre-exponential factors of the relevant Arrhenius equations for the three compositions, 1.5, 5 and 15 mole % CuO are given in Table 3.C.3. Examination of the conductivity data as a function of oxygen partial pressure (figs. 3.B.7 and 3.B.8) indicates that these compositions also exhibit p-type conductivity at the higher oxygen partial pressure. However, in contrast to the ThO_2 - $YO_{1.5}$ and ThO_2 - $LaO_{1.5}$ solid solutions, the ThO_2-CaO specimens retained a white translucent appearance although subjected to a wide range of oxygen partial pressures ($1-10^{-15}$atm) at various temperatures. Volchenkova and Pal'guev[97] also measured the electrical conductivity in air of various ThO_2-CaO compositions, and their results are included in fig. 3.B.7. It is difficult, however, to compare the two sets of data owing to the lower sintering temperature (1600°C) employed by the Russian workers, and to lack of information about the purity of their preparitive materials.

3.C. DISCUSSION OF ELECTRICAL CONDUCTIVITY DATA

3.C.1 General comments

There must be reservations about any electrical

conductivity measurements based on the small number of samples and limited temperature range ($\sim$300°C) employed in the present work. It is believed, however, that the principal features involved in the electrical conductivity behaviour, as a function of composition and oxygen partial pressure, have been established for the relevant thoria solid solutions. The self-consistent results, and satisfactory agreement with the data of other investigators for the electrolyte $ZrO_2.YO_{1.5}$ (80.20 mole %) has already been mentioned in section 3.B.2. It is possible, of course, that erroneously high conductivities were recorded due to the presence of surface and grain boundary conduction. However, the agreement noted by Carter and Roth[98] between the conductivity values for both single crystal and polycrystalline zirconia-based electrolytes, and the relatively little effect caused by variations in the A.C. frequency employed in the present measurements (section 2.G), suggest that grain boundary conduction, at least, is not important in these materials.

3.C.2 Positive-hole conduction

It is instructive to compare the properties of the thoria-based electrolytes with the similar

fluorite solid solutions based on zirconia. The large oxygen diffusion coefficient[58] in calcia-stabilized zirconia is qualitatively understandable in terms of the large anion vacancy concentration, and it was concluded earlier (section 3.A.2) that the thoria solid solutions have a similar structure. As expected, then, the IONIC conductivity of the thoria-based electrolytes, increases, at least initially, with increasing anion vacancy concentration (fig. 3.C.1). The thoria-based electrolytes, however, appear to be unique in exhibiting p-type conduction at high oxygen partial pressures (figs. 3.B.6, 3.B.7, 3.B.8). This positive-hole conduction becomes negligible below oxygen partial pressures of approximately 10^{-6} atm., according to the emf experiments reported later in section 3.D.3. which provide information about the relevant ionic transference numbers. This conclusion is also supported by the observation that the total conductivity is independent of the ambient oxygen pressure (fig. 3.B.8), provided the latter does not exceed about 10^{-6} atm.

Examination of the relevant data (figs. 3.B.6, 3.B.7, and 3.B.8) indicates that the p-type conductivity appears to be greatest in the ThO_2-CaO compositions, and

it is interesting to note that in the ThO_2-$YO_{1.5}$ solid solutions, the positive-hole conduction is a minimum at the compositions which exhibit maximum total conductivity. Reference has already been made (section 1.D) to the p-type conductivity exhibited by such binary oxides as MgO, CaO, Al_2O_3. It is not yet known whether this property involves any measure of non-stoichiometry or whether it is wholly attributable to residual impurities, and the same uncertainty is associated with the p-type conductivity shown by the thoria-based electrolytes. The large number of anion vacancies, possessed by these electrolytes, and the correspondingly high oxygen mobilities, however, might be expected to reduce the importance of impurity charge carriers, and it is perhaps significant that higher positive-hole conductivities were observed in the ThO_2-CaO system in spite of the smaller concentrations of impurities present in the 'Specpure' calcium carbonate (Appendix V) compared to the yttrium and lanthanum oxides, although it is also true (figs. 3.B.8 and 3.C.1) that the oxygen mobilities appear to be slightly lower in this system.

The vacuum-sintering treatment could also introduce additional impurities such as tungsten[x] and molybdenum. There was, however, no significant change in the electrical behaviour of a sample having the composition, $ThO_2 \cdot YO_{1.5}$ (75.25 mole %), when it was subjected to two high temperature (2000°C) vacuum anneals lasting 1 hour and 6 hours respectively. Pellets of a similar composition also exhibited p-type conduction even though the sintering process was carried out in a gas-fired furnace at 1800°C. It may be concluded, therefore, that the possible introduction of tungsten or molybdenum into the thoria solid solutions is not responsible for the departures from purely ionic conduction at the higher oxygen pressures.

If the p-type conductivity is indeed an intrinsic property it must be associated with the incorporation of excess oxygen into the lattice, and Anderson[99] suggests that the positive holes produced by such a process are more likely to be localised on the oxygen ions ($O^{2-} + e^+ \rightarrow O^-$) rather than trapped by inert gas-like cations such as

---

x It has been reported[51] that the tungsten content of ZrO_2 specimens fabricated by hot-pressing in tungsten dies, could be reduced from 1000 ppm to less than 10 ppm by heating the samples in pure oxygen at 1000°C (cf. the heat treatment used in the present investigation after the vacuum sintering process).

Ca^{2+}, Y^{3+}, and Th^{4+}.

Further comments on the p-type conductivity exhibited by the thoria-based electrolytes are confined to the following observations.

(i) Additions of yttria in the range 0-15 mole % increase both the ionic and p-type conductivity (fig. 3.B.8), although the relative increases of the positive-hole conduction are smaller than those associated with the ionic conduction.

(ii) Activation energies for the p-type conduction appear to be relatively insensitive to changes in composition. This is illustrated in the adjoining Table 3.C.1 for the two compositions containing 1 and 15 mole % $YO_{1.5}$ respectively.

TABLE 3.C.1.

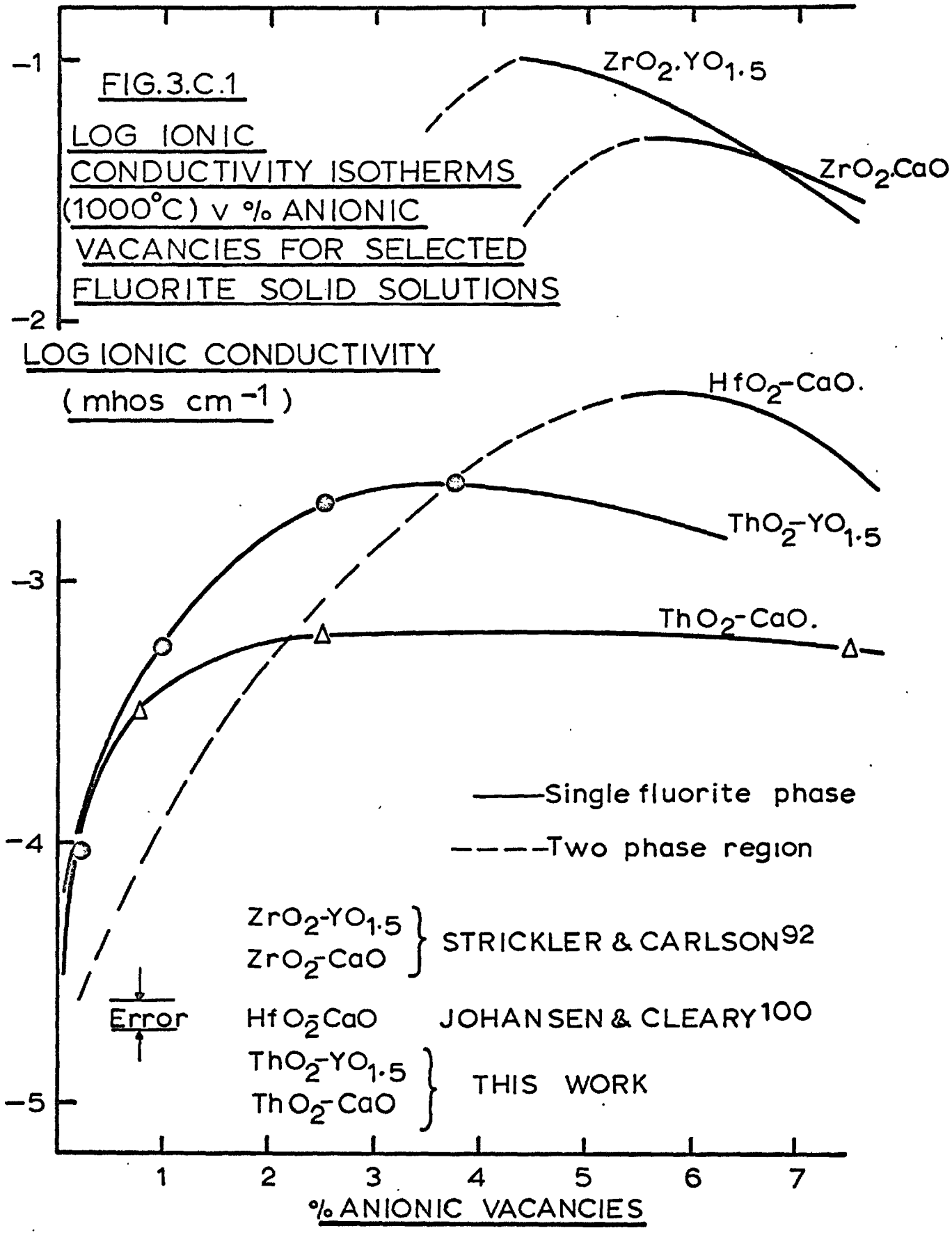
POSITIVE-HOLE AND IONIC ACTIVATION ENERGIES

Composition $YO_{1.5}$ mole %	Activation energy(Kcal) (p_{O_2} = 1 atm.)		
	p-type	Ionic	Resultant
1	24.0	31.7	25.0
15	25.0	23.1	24.5

3.C.3 Ionic conduction

It is possible to compare the IONIC conductivities of several solid oxide electrolytes based on the Group IV A oxides, ZrO_2, HfO_2, and ThO_2. The ionic transference number, t_{ion}, for the zirconia solid solutions is virtually unity (>0.995[43]) over a wide range of compositions, and therefore the conductivity measurements carried out in air, reported by Strickler and Carlson[92], represent the ionic conductivities for the appropriate zirconia electrolytes. Ionic conductivities for the thoria solid solutions may be evaluated from the present work because at low oxygen partial pressures ($<10^{-6}$atm.), the transference number may also be taken as unity. Finally, it may be assumed that the conductivities (in argon) measured by Johansen and Cleary[100] for hafnia solid solutions are also ionic conductivities, at least for the single phase fluorite compositions. These ionic conductivity values at 1000°C are summarised in fig. 3.C.1.

The initial increase in ionic conductivity shown by the thoria solid solutions with increasing vacancy concentration is not sustained beyond a vacancy concentration of about 3%, and in fact, these preliminary measurements suggest that the conductivity may subsequently decrease


FIG.3.C.1
LOG IONIC CONDUCTIVITY ISOTHERMS (1000°C) v % ANIONIC VACANCIES FOR SELECTED FLUORITE SOLID SOLUTIONS
LOG IONIC CONDUCTIVITY
(mhos cm⁻¹)
-1
-2
-3
-4
-5
ZrO2.YO1.5
ZrO2.CaO
HfO2-CaO.
ThO2-YO1.5
ThO2-CaO.
——Single fluorite phase
----Two phase region
ZrO2-YO1.5
ZrO2-CaO
STRICKLER & CARLSON92
Error
HfO2CaO
JOHANSEN & CLEARY100
ThO2-YO1.5
ThO2-CaO
THIS WORK
1
2
3
4
5
6
7
% ANIONIC VACANCIES

with increasing vacancy concentration. A decrease in ionic conductivity with increasing vacancy concentration has often been demonstrated for zirconia-based electrolytes,[92,93,98,101] and it is generally believed that maximum conductivity in these zirconia-systems is exhibited by compositions located near the phase boundary* separating the two phase region from the fluorite solid solution.

According to equation 1.C.4. derived in Appendix I a decrease of conductivity with an apparent increase in the defect concentration can arise from either, or both, of the following:

(i) a decrease in the charge carrier concentration,

(ii) a decrease in carrier mobility.

In the solid solutions under discussion, the defect concentration (aliovalent cations + anion vacancies) is very high and the formation of impurity -vacancy

---

* This phase boundary at 1000°C is situated at the following compositions:

ZrO_2.CaO system . . . 11-12 mole % CaO

ZrO_2.$YO_{1.5}$ system . . . ~17.5 mole $YO_{1.5}$ (~9.5 mole % Y_2O_3)

TABLE 3.C.2.

ACTIVATION ENERGIES AND PRE-EXPONENTIAL FACTORS FOR ELECTROLYTE SOLID SOLUTIONS CONTAINING YTTRIA

Solid Solution	Source of Data	Oxygen Partial Pressure(atm)	MOLE % $YO_{1.5}$						
			1	4	10	15	20	25	40
			% ANIONIC VACANCIES						
			0.25	1	2.5	3.75	5.00	6.25	10
			ACTIVATION ENERGY (kcal)*						
$ZrO_2.YO_{1.5}$	Dixon et al[93]	Air	T.P.	T.P.	T.P.	T.P.	20.7	24.3	28.5
$ZrO_2.YO_{1.5}$	Strickler and Carlson[92]	Air	T.P.	T.P.	T.P.	T.P.	20.2	27.0	29.3
$ThO_2.YO_{1.5}$	Present Work	1	25.0	24.7	23.7	24.5	-	24.7	-
		10^{-6}	30.5	28.7	24.9	23.1	-	25.2	-
		10^{-15}	31.2	28.8	24.9	23.1	-	25.9	-
			PRE-EXPONENTIAL FACTOR(MHOS.CM^{-1})						
$ZrO_2.YO_{1.5}$	Strickler and Carlson[92]	Air	-	-	-	-	-	1700	-
$ThO_2.YO_{1.5}$	Present Work	1	11	23	35	55	-	42	-
		10^{-6}	19	53	38	22	-	39	-
		10^{-15}	21	51	38	22	--	42	-

T.P. : Two phase region. * Estimated accuracy for activation energies derived from results of present work is ± 2.5 kcal.

TABLE 3.C.3

ACTIVATION ENERGIES AND PRE-EXPONENTIAL FACTORS FOR ELECTROLYTIC SOLID SOLUTIONS CONTAINING CALCIA

Solid Solution	Source of Data	Oxygen Partial Pressure(atm)	MOLE % CaO						
			⁎⁎1.5	5	10	13	15	18	20
			% ANIONIC VACANCIES						
			0.75	2.5	5	6.5	7.5	9	10
			ACTIVATION ENERGY ⁎(kcal).						
ZrO_2.CaO	Tien and Subbarao[101]	Air	T.P.	T.P.	T.P.	25.6	28.0	30.0	31.1
ZrO_2.CaO	Carter and Roth[98]	Air	T.P.	T.P.	(21.8)	26.0	29.2	34.0	360
ThO_2.CaO	Present Work	1	23.7	24.2	-	-	25.5	-	-
		10^{-6}	26.9	25.1	-	-	25.8	-	-
		10^{-15}	27	25.2	-	-	26.0	-	-
			PRE-EXPONENTIAL FACTORS(MHOS.CM^{-1})						
ZrO_2.CaO	Tien and Subbarao[101]	Air	T.P.	T.P.	T.P.	1300	1500	1700	1400
ZrO_2.CaO	Carter and Roth[98]		T.P.	T.P.	200	1400	4000	10000	12,000
ThO_2.CaO	Present Work	1	7.2	22	-	-	22	-	-
		10^{-6}	14	13	-	-	17	-	-
		10^{-15}	14	13	-	-	16	-	-

T.P. . . . . Two-phase region.

⁎ Estimated accuracy for activation energies derived from results of present work is ±2.5 kcal.

⁎⁎ Measurements on this composition were made by P.K.R. Moody, Metallurgy Department, Imperial College.

complexes[x], for example, is very probable. However, the number of free carriers will still continue to increase with increasing defect concentration, although at a lower than linear rate. Thus the simple association theory alone cannot account for decreasing conductivity due to reduced carrier concentration.

As the defect concentration is fixed by composition, then the activation energies for conduction listed in Tables 3.C.2 and 3.C.3. represent the energies associated with the MOVEMENT of ions, and do not include an energy term $\frac{\Delta Hf}{2}$ for the formation of the oxygen vacancies. The increasing energy for ion movement with increased

---

x Evidence for the existence of such associated complexes may be revealed by departures from linearity in the log (σ.T) versus 1/T plots, or by examining the conductivity isotherms as a function of impurity ion concentration. These analyses, however, require data of greater accuracy than is at present available for the oxide solid solutions. Dielectric loss measurements can also provide information about the existence of associated defects, and the internal friction and dielectric relaxation experiments conducted by Wachtman[102] on the thoria solid solution, ThO2.CaO (1.5 mole % CaO), support the proposal, that at low temperatures (~500°K) at least, an oxygen vacancy is tightly bound to a substituted calcium ion. An activation energy for motion of an oxygen vacancy adjacent to a substituted calcium ion was also deduced from these measurements,

cont/

vacancy concentration exhibited by the calcia- and yttria-zirconia solid solutions (see also Fig. 3.C.2,, which depicts the relevant activation data for the yttria solutions), is not necessarily accompanied by a decrease in the oxygen ion mobility which could thus explain the lower conductivity values as suggested by Tien and Subbarao[101]. An increasing energy for ion movement with increasing vacancy concentration has also been observed for the diffusion of iron in the non-stoichiometric compounds FeO (Himmel, Mehl, and Birchenall[103]) and FeS (Condit and Birchenall[104]). Accompanying decreases in the iron diffusion coefficients, however, were only noted in

---

* (Cont. from previous page) and for the relevant composition, a value of 20.5 Kcal. was calculated. Oxygen vacancies bound to the calcium ions do not contribute to anionic conduction, and the number of free oxygen vacancies will be a function of the energy of association of the impurity-vacancy pairs and the temperature. The activation energy for IONIC conduction (27 Kcal.) derived from the results of the present work, should therefore represent the sum of an energy for motion and half the energy of association. If the present data is extrapolated to 500°K, a value for the energy of association, 13 Kcal., is thus obtained. For NaCl and KCl crystals, the energy of association between a CATION vacancy and a substituted Ca^{2+} ion is generally believed to be of the order 7-9 Kcal.[30,33]. The cations in the fluorite structure, however, are relatively immobile, and so the possible existence of impurity-vacancy complexes cannot explain the apparent failure of the conductivity and diffusion data to satisfy the Nernst-Einstein equation as indicated by the recent oxygen diffusion measurements of Hagel[106].

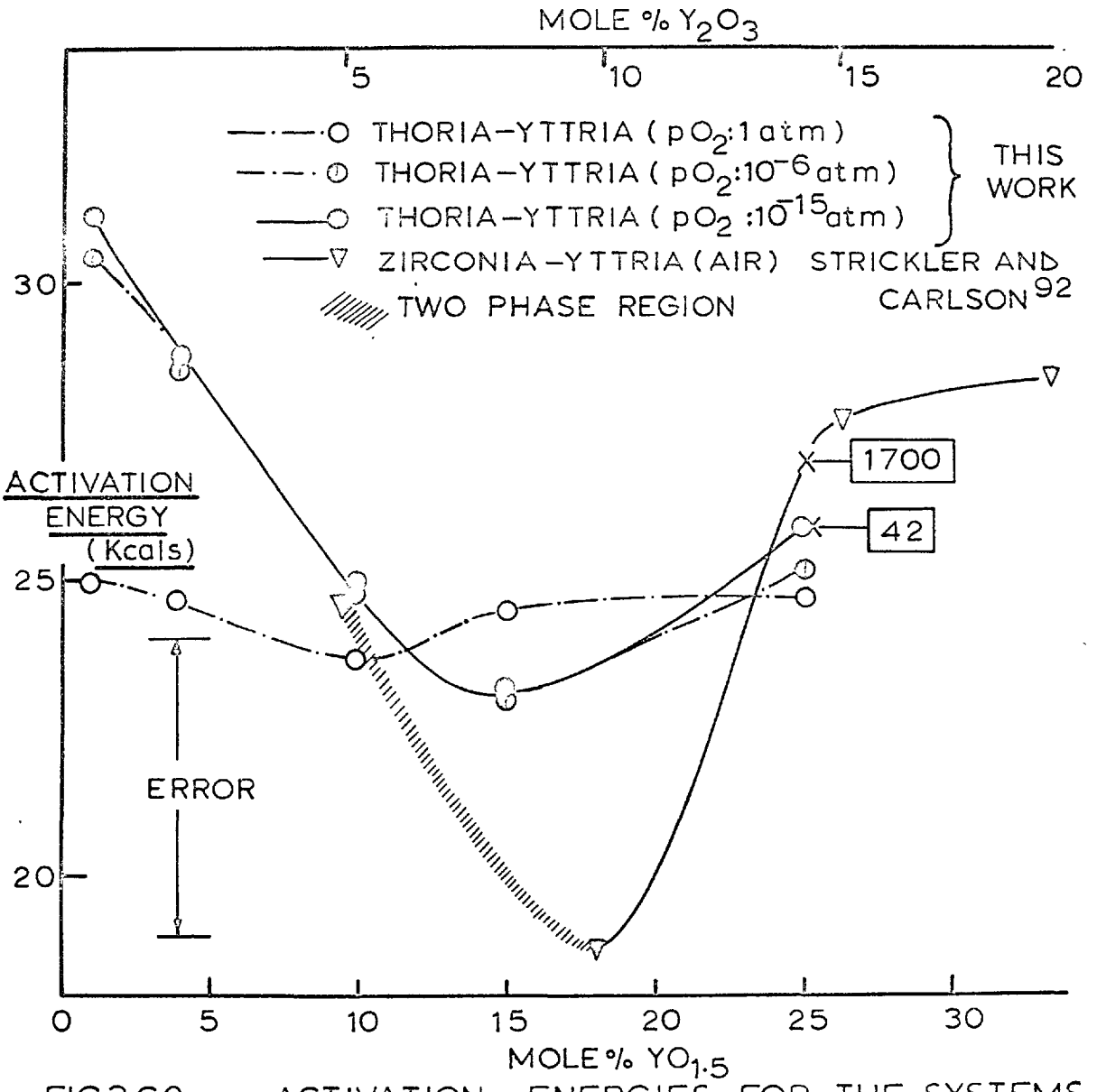


FIG.3.C.2 ACTIVATION ENERGIES FOR THE SYSTEMS ThO_2.$YO_{1.5}$ and ZrO_2 $YO_{1.5}$ NUMBERS IN BOXES DENOTE PRE-EXPONENTIAL FACTORS FOR SELECTED COMPONENTS

experiments with the FeS at temperatures below 330°C, and these observations could be explained on the basis of previous evidence[105] for the ordering of vacancies on the iron sites. In addition, the recent experiments of Hagel[106] indicate that the oxygen diffusion rate, unlike the electrical conductivity, in calcia stabilized zirconia, increases with increasing calcium oxide content.

The situation is further complicated, at least for the zirconia solid solutions, in that there is evidence[92,98,101,107], that the cations become ordered at temperatures around 1000°C. Although the relevant x-ray superlattice lines displayed by annealed (~ 1000°C) zirconia-based electrolytes must be primarily associated with re-arrangement of the cations, the fact that the ordered state exhibits lower conductivity (one-third to one-half that of the disordered state) implies that the anion vacancies also assume ordered sites instead of being randomly distributed. Presumably, the ordered Ca^{2+} or Y^{3+} cations, which possess very low diffusion rates[59,60], attract the more mobile anion vacancies to nearest-neighbour positions. The neutron-diffraction studies of Carter and Roth[98] provide additional evidence that the anion vacancies can become ordered, and it

appears that these order-disorder transformations, involving both cations and anion vacancies, are somewhat analogous to the transitions from an ordered pyrochlore to a disordered fluorite structure reported[108] in certain of the zirconia-rare earth oxide systems.

How much of the preceding discussion is applicable to the thoria solid solutions examined in the present investigation is not clear at present. The results suggest a maximum value for the conductivity as a function of composition (fig. 3.C.1), but the ranges of composition were not sufficiently extensive to demonstrate convincingly that the conductivity subsequently decreased with increasing defect concentration in a similar manner to the zirconia solid solutions. It is also doubtful whether the slightly larger activation energies for conduction (Tables 3.C.2 and 3.C.3) observed at the higher defect concentrations are significant in view of the large errors (2.5-3 kcal) associated with these quantities. Moreover, x-ray examinations of samples having the composition $ThO_2 \cdot YO_{1.5}$ (75.25 mole %), which were annealed at 1000°C for 12 days ($\sim$300 hours) and quenched, did not reveal any superlattice lines, and in this

respect the thoria solid solutions may resemble the defect fluorite structures possessed by non-stoichiometric oxides CeO_{2-x}[109] and PrO_{2-x}[110] which also appear to be disordered at the temperatures involved in the present conductivity measurements. Direct comparison, however, of these two types of defect structure is not strictly justified, as electron exchange can take place readily in the mixed valence binary systems whereas the cations in the ternary system are relatively immobile.

Another interesting feature is the relative magnitude of the ionic conductivities exhibited by the zirconia, hafnia, and thoria solid solutions possessing equal defect concentrations. These conductivity values (Fig. 3.C.1.) appear to be principally determined by the relevant host lattice (ZrO_2, HfO_2, ThO_2) and are influenced much less by changes in the aliovalent cations substituted into the host lattice. For example, the zirconia solid solution containing 25 mole% $YO_{1.5}$ (6.25% anion vacancies) has an ionic conduction approximately 50 times that of the corresponding thoria solution. Table 3.C.2. and Fig. 3.C.2. indicate that the activation energies for conduction are comparable (27 and 26 Kcal., respectively) but that the pre-exponential terms differ considerable for these two solid solutions. It is impossible, however, to attribute this difference of

about two orders of magnitude to changes in the vibrational frequency and entropy values associated with the pre-exponential term contained in the following equation derived in chapter one (equation 1.C.5.), i.e.,

$$\sigma_i.T = \left[\frac{(Aa^2 z_i^2 eF)\nu}{k}\exp\left(\frac{\Delta S_m}{R}\right)\right] \exp\left[-\frac{\Delta H_m}{RT}\right]^{*}$$

Differences in the size[**] and polarizability of the thorium and zirconium ions, which are reflected in the different structures[***] possessed by the two pure oxides, will undoubtedly influence the electrical

---

* The quantity $\frac{\Delta Hf}{2}$ associated with the energy of formation of the relevant defects is omitted from the above equation.

** There is no obvious correlation between relevant lattice parameters and the observed electrical conductivities, although it is of interest to note that the highest values of conductivity so far reported were obtained with ZrO_2-Sc_2O_3 solid solutions [111]. This system is the only fluorite solid solution investigated in the ZrO_2-M_2O_3 series which exhibits a decrease in lattice parameter with increasing M_2O_3 content.

*** The monoclinic structure possessed by pure ZrO_2 transforms to a tetragonal phase around 1200°C. There is also some evidence for the existence of a cubic structure at very high temperatures (~2000°C).

behaviour of the associated solid solutions. It is apparent, however, that a satisfactory interpretation of the electrical properties of both the zirconia and thoria fluorite solid solutions requires considerably more information about the behaviour of oxygen vacancies, and anion defects in general, than is at present available. Further speculation at present, then, is of little value except to mention the possibility that the transport of oxygen in these defect solid solutions may also involve abnormal charged species such as the anion complexes, or "molecule ions"[112], $(O_2)^{2-}$, $(O_2)^{-}$.

3.D. DETERMINATION OF IONIC TRANSFERENCE NUMBERS

3.D.1. Relevant theoretical equations

As already mentioned in chapter one (section 1.C.1) when an oxide electrolyte exhibiting both ionic and electronic conductivity is incorporated into an oxygen concentration cell, e.g.

$$Pt, O_2(\mu'_{O_2}) \;\Big|\; \text{electrolyte} \;\Big|\; O_2(\mu''_{O_2}), Pt,$$

then the resulting emf may be related to the ionic transference numbers as follows:

$$E = \frac{1}{4F} \int_{\mu'_{O_2}}^{\mu''_{O_2}} t_{ion}\, d\mu_{O_2} \quad \ldots\ldots\ldots \text{Eq.3.D.1.}$$

where μ'_{O_2}, μ''_{O_2} denote the equilibrium oxygen chemical potentials at the two electrodes. Evaluation of this expression requires either the assumption of a constant mean ionic transference number, or relevant information about the oxygen pressure dependence of t_{ion}. A useful approach to this problem has been suggested by Schmalzried[45,63]. Using the following expressions introduced in section 1.C.3,

$$\sigma_T = \sigma_{IONIC} + \sigma_{\oplus} + \sigma_{\ominus} \quad \ldots\ldots\ldots \text{Eq.3.D.2.}$$

and

$$\sigma_T = \sigma_{IONIC} + k_1 p_{O_2}^{1/m} + k_2 p_{O_2}^{-1/n} \quad \ldots\ldots\ldots \text{Eq.3.D.3.}$$

and by defining two parameters $p_{\oplus}$ and $p_{\ominus}$ as the oxygen partial pressures at which σ_{IONIC} equals $\sigma_{\oplus}$ and $\sigma_{\ominus}$ respectively, then it is possible to derive expressions for the ionic transference number as a function of oxygen partial pressure. These expressions and the corresponding emf equations are given in the adjoining Table 3.D.1. The appropriate values of m and n either have to be assumed, or determined empirically from the available conductivity and emf data. Application of these equations derived by Schmalzried will be demonstrated in subsequent sections,

which include the relevant data for transference number determinations at both high* and low oxygen partial pressures.

3.D.2. Zirconia solid solutions at high oxygen chemical potentials

Coulometric titrations[43], and emf measurements[61] on cells incorporating zirconia-based electrolytes and gaseous electrodes, have indicated that the anionic transference numbers of these materials are at least 0.995 in the range 800-1100°C, provided the oxygen partial pressures imposed at the electrodes do not become too reducing ($>10^{-15}$atm at 1000°C). Additional information was also available from experiments conducted in the present investigation on the cells,

Ni,NiO	Commercial Stabilized Zirconia Tube	O_2(1 atm),Pt,
Fe,FeO	Commercial Stabilized Zirconia Tube	O_2(1 atm),Pt.

Voltages** were only recorded at one temperature (890°C), and the following results in Table 3.D.2, which are also discussed in chapter four, were obtained.

* Oxygen chemical potentials possessing values more POSITIVE than those associated with the Fe-FeO equilibria were regarded as HIGH in the present investigation.

** Theoretical voltages and errors were calculated from the thermodynamic data recommended in chapter four.

TABLE 3.D.1

Expressions derived by Schmalzried

Electrolyte System	t_{ion}	E.m.f.
Type a*	$\left[1+\left(\frac{p''_{O_2}}{p_\oplus}\right)^{1/n}+\left(\frac{p'_{O_2}}{p_\ominus}\right)^{-1/n}\right]^{-1}$	$\frac{nRT}{4F}\left[\ln\frac{p_\oplus^{1/n}+p'^{1/n}_{O_2}}{p_\oplus^{1/n}+p''^{1/n}_{O_2}}+\ln\frac{p_\ominus^{1/n}+p''^{1/n}_{O_2}}{p_\ominus^{1/n}+p'^{1/n}_{O_2}}\right]$
Type b	$\left[1+\left(\frac{p'_{O_2}}{p_\ominus}\right)^{-1/n}\right]^{-1}$	$\frac{nRT}{4F}\left[\ln\frac{p_\ominus^{1/n}+p''^{1/n}_{O_2}}{p_\ominus^{1/n}+p'^{1/n}_{O_2}}\right]$
Type c	$\left[1+\left(\frac{p''_{O_2}}{p_\oplus}\right)^{1/m}\right]^{-1}$	$\frac{mRT}{4F}\left[\ln\frac{p''^{1/m}_{O_2}}{p'^{1/m}_{O_2}}+\ln\frac{p_\oplus^{1/m}+p'^{1/m}_{O_2}}{p_\oplus^{1/m}+p''^{1/m}_{O_2}}\right]$

* Derivation requies the pressure exponents n and m to be equal.

TABLE 3.D.2.

TEMPERATURE : 890°C		
Cell	Measured emf mV	Theoretical emf mV
Ni,NiO/electrolyte/O_2(1atm),Pt	$699^{+}_{-}2$	$701^{+}_{-}3.5$
Fe,FeO/electrolyte/O_2(1atm),Pt	971 $\pm$2	976 $\pm$3

These data confirm that the MEAN electronic transference number of the zirconia-based electrolytes does not exceed 0.5% under the relevant experimental conditions, and this conclusion is supported by the available information on the conducting behaviour as a function of oxygen partial pressure (fig. 3.B.8). It was convenient, therefore, to examine the electrolytic properties of the thoria solid solutions with reference to the two zirconia based electrolytes, ZrO_2.CaO (85.15 mole %) and ZrO_2.$YO_{1.5}$ (80.20 mole %).

3.D.3. Thoria solid solutions at high oxygen chemical potentials

All the thoria solid solution compositions prepared in the present investigation were incorporated in the following cells,

Ni,NiO | electrolyte | Cu,Cu_2O

and,

Fe,FeO | electrolyte | Ni,NiO

At least two samples of each selected composition were examined, and the appropriate precautions and procedures detailed in chapter two were followed. All the experiments with the cell containing the $Cu-Cu_2O$ electrode were conducted in purified argon in contrast to the experiments with the other cell, which were carried out in either vacuum or purified argon.

Results for both the cells at the two temperatures 800 and 1000°C are summarised* in Table 3.D.3. and the relevant electrode oxygen chemical potentials and oxygen partial pressures are also listed in the adjoining Table 3.D.4. It is immediately apparent that all the thoria solid solutions possess the same ionic transference number as the zirconia-based electrolytes when incorporated in the second cell containing Fe,FeO and Ni,NiO electrodes, but that there are small differences for certain of the thoria-based electrolytes when included in the first cell which contains electrodes with a higher mean oxygen

---

* Detailed results for certain of the electrolytes are reproduced in Appendix VI.

TABLE 3.D.3.

E.m.f. measurements at 1000°C and 800°C

Comparison of data for various electrolytes

ELECTROLYTE COMPOSITION (MOLE %)	CELL			
	$Ni, NiO \mid$ ELECTROLYTE $\mid Cu, Cu_2O$		$Fe, FeO \mid$ ELECTROLYTE $\mid Ni, NiO$	
	800°C ± 1 mV	1000°C ± 1 mV	800°C ± 1 mV	1000°C ± 1 mV
$ZrO_2.CaO$ (85/15) $ZrO_2.YO_{1.5}$ (80/20) $ThO_2.YO_{1.5}$ (96/4) $ThO_2.YO_{1.5}$ (90/10) $ThO_2.YO_{1.5}$ (85/15) $ThO_2.LaO_{1.5}$ (90/10) $ThO_2.LaO_{1.5}$ (85/15)	273	259	266	286
$ThO_2.YO_{1.5}$ (99/1)	265	247	266	286
$ThO_2.YO_{1.5}$ (75/25)	270	254	266	286
$ThO_2.CaO$ (95/5)	273	257	266	286
ThO_2 (pure)	148	140	-	-
HfO_2 (pure)	153	152	-	-

TABLE 3.D.4.

Equilibrium oxygen chemical potentials

at 800°C and 1000°C

Metal-Metaloxide	Cu - Cu2O		Ni - NiO		Fe - FeO	
Temperature (°C)	800	1000	800	1000	800	1000
Oxygen Potential (kcal)	-47.1	-36.9	-68.4	-60.5	-92.9	-86.7
$\log_{10} pO_2$ (atm)	-9.6	-6.3	-13.9	-10.4	-18.9	-14.9

chemical potential. The presence of a significant electronic transference number is in accordance with the p-type conductivity displayed by the thoria solid solutions at high oxygen partial pressures. However, provided the oxygen partial pressures are sufficiently low, it can be concluded from the emf data that the MEAN ionic transference numbers of the thoria based electrolytes are virtually unity(>0.995). The emf data, moreover, can be combined with the conductivity results to provide estimates of the oxygen partial pressure above which the electronic transference number exceeds 1%. It follows that below this oxygen partial pressure value, the ionic transference number t_{ion} exceeds 0.99.

The estimates were based on the equations derived by Schmalzried which were applied as follows:

(i) A value of t_{ion} when the oxygen partial pressure equals 1 atm can be derived from the relevant conductivity data. This value can be substituted in the appropriate equation (Table 3.D.1) which contains two unknown quantities $p_{\oplus}$ and m .

(ii) Another equation (Table 3.D.1) incorporating $p_{\oplus}$ and m is available by using the emf results

recorded for the cell,

$$Ni,NiO \;\big|\; \text{electrolyte} \;\big|\; Cu,Cu_2O \;.$$

(iii) Having determined the values of $p_{\oplus}$ and m^{*} which satisfy both the above equations, then the appropriate oxygen partial pressure limit for which t_{ion} equals 0.99 can thus be calculated, and values for the various thoria based electrolytes at 1000°C are summarised in fig. 3.E.2.

3.D.4. Thoria solid solutions at low oxygen chemical potentials

The behaviour of the thoria solid solutions at very low oxygen chemical potentials, and the relevant data, are fully discussed in chapter five which describes the electrochemical measurements associated with the Nb-O system. Reference is made (section 5.B.2) to the emf experiments carried out by Zador[**] on the cell,

$$Mn,MnO \;\big|\; ThO_2.YO_{1.5}(90.10 \text{ mole } \%) \;\big|\; Fe,FeO(\text{or } Ni,NiO),$$

using the same apparatus employed in the present investigation. The equilibrium Mn-MnO[***] oxygen chemical potentials

---

* Preliminary calculations indicated values of m in the range 2-3, and a mean value of 2.5 was eventually adopted in subsequent calculations.

** S. Zador, Metallurgy Department, Imperial College.

*** For the Mn-MnO equilibrium at 1000°C,

$$\Delta\mu_{O_2} = +\,139.5 \text{ kcal., and } p_{O_2} = 10^{-23.9}\text{atm}$$

derived from these measurements were in good agreement with those calculated from the latest calorimetric data, and it was concluded that the MEAN electronic contribution to the total conductivity was less than 1% over the relevant range of oxygen partial pressures. There was some evidence (section 5.B.1), however, that the electronic component became more significant at the slightly lower oxygen chemical potentials associated with the Nb-NbO equilibria[x]. It was considered reasonable, therefore, to assume that the electronic transference number became greater than 0.01 at some oxygen partial pressure intermediate between the values associated with the Mn-MnO and Nb-NbO, and an appropriate estimate is included in figs. 3.E.2 and 3.E.3.

3.D.5. Zirconia solid solutions at low oxygen chemical potentials

It was mentioned in chapter two (section 2.E.2) that cells incorporating zirconia-based electrolytes in contact with electrodes possessing low oxygen chemical potentials, e.g.

Nb, NbO	ZrO_2.CaO(85.15 mole %) DENSE, IMPERMEABLE	Fe, FeO

x For the Nb-NbO equilibrium at 1000°C

$\Delta\mu_{O_2} = -145$ kcal., and $p_{O_2} = 10^{-24.8}$ atm

still produced erroneous emf values even when assembled in the modified apparatus and provided with separate electrode compartments. Voltages recorded under dynamic conditions as the cell temperature was steadily increased are reproduced in fig. 3.D.1, and illustrate the behaviour of this type of cell containing a zirconia based electrolyte. Evidence that the electrolyte was becoming non-stoichiometric and exhibiting electronic conduction in contact with the Nb-NbO, was provided by the observation that if the electrolyte was removed from the cell, heated in air at 1000°C, and then incorporated in another cell having electrodes with relatively high oxygen partial pressure ($Cu-Cu_2O$, Ni-NiO, Fe-FeO), then reproducible voltage in excellent agreement ($\pm$ 1 mV) with the expected values were recorded.

It was also noted in chapter two that the cell functioned satisfactorily when thoria-based electrolytes were placed between the Nb-NbO electrode and the zirconia electrolyte, viz.

$$\text{Nb-NbO} \;\Big|\; \underset{(90.10\ \text{mole\%})}{ThO_2 \cdot YO_{1.5}} \;\Big|\; \underset{(85.15\ \text{mole\%})}{ZrO_2 \cdot CaO} \;\Big|\; \text{Fe-FeO}$$

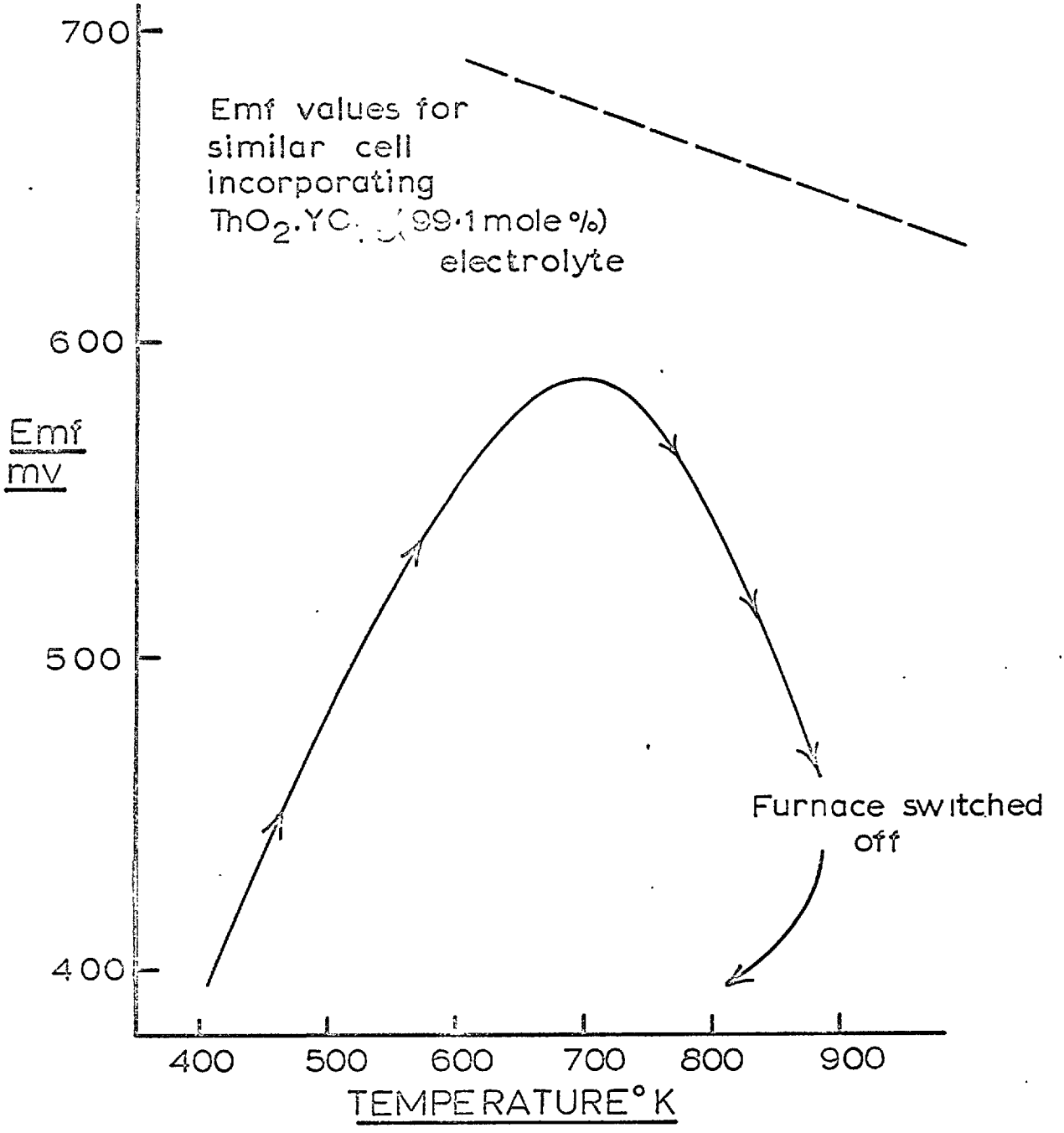


FIG.3.D.1 Emf values FOR CELL

Nb, NbO | ZrO_2 CaO (85·15 mole %) | Fe, FeO

AS A FUNCTION OF TEMPERATURE (Dynamic Conditions)

However, if the position of the two electrolytes was reversed, i.e.

Nb-NbO	$ZrO_2.CaO$ (88.15 mole%)		$ThO_2.YO_{1.5}$ (90.10 mole%)	Fe-FeO

then low, irreproducible results were again obtained.

The presence of significant electronic conduction reduces the cell voltage according to the equation,

$$E = \frac{1}{4F} \int_{\mu'_{O_2}}^{\mu''_{O_2}} t_{ion}\, d\mu_{O_2} \quad ,$$

and also provides an internal short circuit which allows oxygen ions to be transferred from the cathode to the anode even under open circuit conditions. This 'corrosion current' is presumably able to polarise the Nb-NbO electrode, and is responsible for the rapid decrease in cell voltage which is very evident in fig. 3.D.1. The simultaneous formation of a thin oxide layer, which would remain when the temperature was reduced, would also explain why the higher cell voltages could not be reproduced on cooling.

In an attempt to obtain information on the electronic transference number of the zirconia based

electrolytes at low oxygen partial pressures, emf measurements were made on the cell,

$$Nb_2O_5 \cdot NbO_2 \;\Big|\; ZrO_2.CaO(85.15\ \text{mole\%}) \;\Big|\; Fe\text{-}FeO\ ,$$

and compared to data obtained for similar cells using thoria based electrolytes (section 5.D). Reproducible results for cells incorporating the zirconia electrolyte could only be obtained in the range 750-850°C. Above these temperatures, stable voltages could not be recorded as the emf values steadily decreased with time due to transport of oxygen ions through the cell. At the lower temperatures the observed voltages were 1-3 mV smaller than the corresponding voltages obtained with the thoria based electrolytes, and it was assumed that a similar difference in the two emf values would have been recorded at 1000°C in the absence of polarisation phenomena.

If the reaction responsible for the n-type conduction in the $ZrO_2.CaO$ solid solution at low oxygen chemical potentials can be represented by the following equilibria:

$$O^{2-}(lattice) \rightleftharpoons \square^{-} + \tfrac{1}{2}O_2(gas) + 2e^{-}\ ,$$

then $\sigma_e = k_2 p_{O_2}^{-\frac{1}{4}}$, for constant anion vacancy concentration, and n in equation 3.D.3 equals 4. It follows, by substitution of the other relevant values* in the appropriate expression derived by Schmalzried (Table 3.D.1) that p_e equals 10^{-23}atm., and the corresponding lower limit for $t_{ion} > 0.99$ is $p_{O_2} = 10^{-15}$atm. For commercial zirconia electrolytes of similar composition, Schmalzried[63], has reported values of $p_e = 10^{-24}$atm. and a corresponding lower limit for t_{ion} of 10^{-16}atm. at 1000°C. These and similar data for 800°C are included in fig. 3.E.3.

An electronic transference number of approximately 1% was also obtained by Bray and Merten[61] at 1000°C, when working with cells containing ZrO_2-$YO_{1.5}$ solid solutions, and ambient oxygen partial pressures of $10^{-15} - 10^{-16}$ atm. In addition, Aronson[113] has reported that the composition of pure zirconium oxide in equilibrium with an oxygen partial pressure of 10^{-15}atm. at 1000°C is $ZrO_{1.99}$, and it is therefore not surprising that some reduction of the fluorite zirconia solid solution also occurs under similar conditions.

---

* At 1000°C,

$$E = 142\text{mV}; \quad p'_{O_2} = 10^{-17.2}\text{atm}; \quad p''_{O_2} = 10^{-14.9}\text{atm}.$$

3.D.6 Commercial solid oxide electrolyte material

Zirconia with additions of other refractory oxides such as CaO, MgO, Y_2O_3, has been available commercially for many years as "stabilised zirconia". The proportion of second oxide added in these commercial materials is usually determined by the minimum quantity required to suppress the volume change associated with the monoclinic-tetragonal transformation in pure zirconia, and in general, insufficient oxide is added to produce a single fluorite solid solution phase.

Two types of commercial stabilised zirconia refractories were occasionally used in the present investigation as electrolyte material. Reference has already been made to the stabilised zirconia tubes* used in the early experiments with separate electrode compartments, and in the oxygen meter described in section 2.E.4. Available information indicated that this material contained 4-5 wgt % (~10 mole %)CaO, and the two phase structure (fluorite solid solution crystals with zirconia

---

* "Zircoa" tubes produced by "Zirconium Corporation of America", Solon, Ohio, U.S.A.

at the grain boundaries) revealed by microscopical examination[x] was consistent with this composition. It was concluded from emf measurements on the cells,

Ni,NiO	STABILIZED ZIRCONIA TUBE	Cu,Cu_2O
Fe,FeO	STABILIZED ZIRCONIA TUBE	Ni,NiO,

that the ionic transference number of this particular commercial material was identical to that possessed by the zirconia based electrolytes fabricated from 'Specpure' chemicals.

A few commercial magnesia stabilised zirconia crucibles[xx] were also employed in the following cell,

Pt, | Ni,NiO | electrolyte | Pb,PbO | Ir | Pt

which is described in detail in the following chapter (section 4.E.1). The emf values recorded were in very good agreement (± 1 mV) with the voltages obtained for similar cells incorporating a "Specpure" electrolyte crucible (ZrO_2 solid solution containing 15 mole % CaO).

---

x Details of the microstructure of the commercial materials were supplied by E.W. Roberts, Houldsworth School of Applied Science, University of Leeds.

xx Crucibles were supplied by Degussa, Frankfurt, Germany.

The absence of significant electronic conduction in this commercial material is interesting as it possesses a complex microstructure** consisting of several phases, and the impurities present[114] also include Fe_2O_3(~0.25%) and TiO_2(~0.2%).

3.E. SUMMARY OF THE TRANSPORT PROPERTIES OF ZIRCONIA AND THORIA SOLID SOLUTIONS

3.E.1 Conductivity behaviour

Four types of conductivity behaviour, as a function of oxygen partial pressure, exhibited by solid oxides possessing a significant ionic contribution to the total conductivity, are illustrated in fig. 3.E.1.

(a) As mentioned earlier in section 1.D, a minimum in the conductivity curve is exhibited by many simple binary oxides, for example, MgO, CaO, SrO, Al_2O_3, ZrO_2, HfO_2. The preliminary results obtained for pure ThO_2(fig. 3.B.8) in the present investigation also indicate a minimum in the conductivity isotherm for this material as well.

** The zirconia fluorite solid solution containing magnesia is not stable below approximately 1300°C (Weber[115]).

(b) Ionic conduction with increasing n-type conduction at low oxygen partial pressures is shown by solid solutions based on zirconia (this work and Schmalzried[63]).

(c) Positive hole conduction followed by a range over which t_{ion} is virtually unity is shown by solid oxide solutions based on thoria(this work).

(d) No data are available for this class of material, but type (b) and (c) would in effect exhibit this pressure dependence if the range of oxygen pressures could be extended in both directions.

3.E.2. Ionic transference numbers

The ranges of oxygen partial pressure over which t_{ion} exceeds 99% at 1000°C for the oxide solutions examined in the present investigation are depicted in fig. 3.E.2. The general pattern of behaviour shown by the thoria solid solutions is similar to that proposed by Peters and Mobius[62] in that these electrolytes exhibit p-type conductivity at high oxygen partial pressures. Analyses of the emf and conductivity data, according to the method described in section 3.D.3., indicates that the oxygen partial pressures at which the p-type conductivity becomes significant are slightly dependent upon the

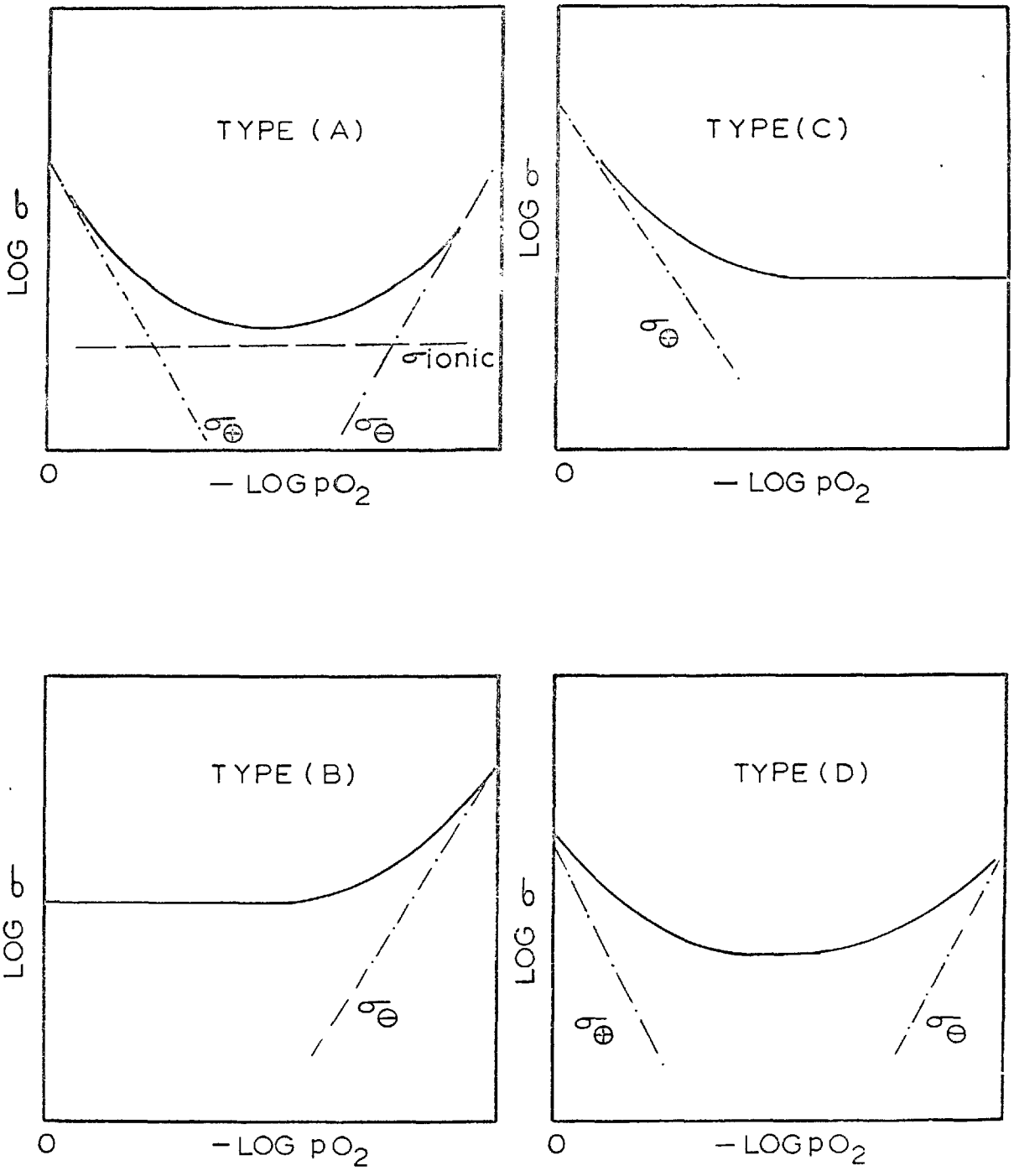


FIG. 3.E.1 TYPES OF CONDUCTIVITY BEHAVIOUR AS A FUNCTION OF OXYGEN PRESSURE

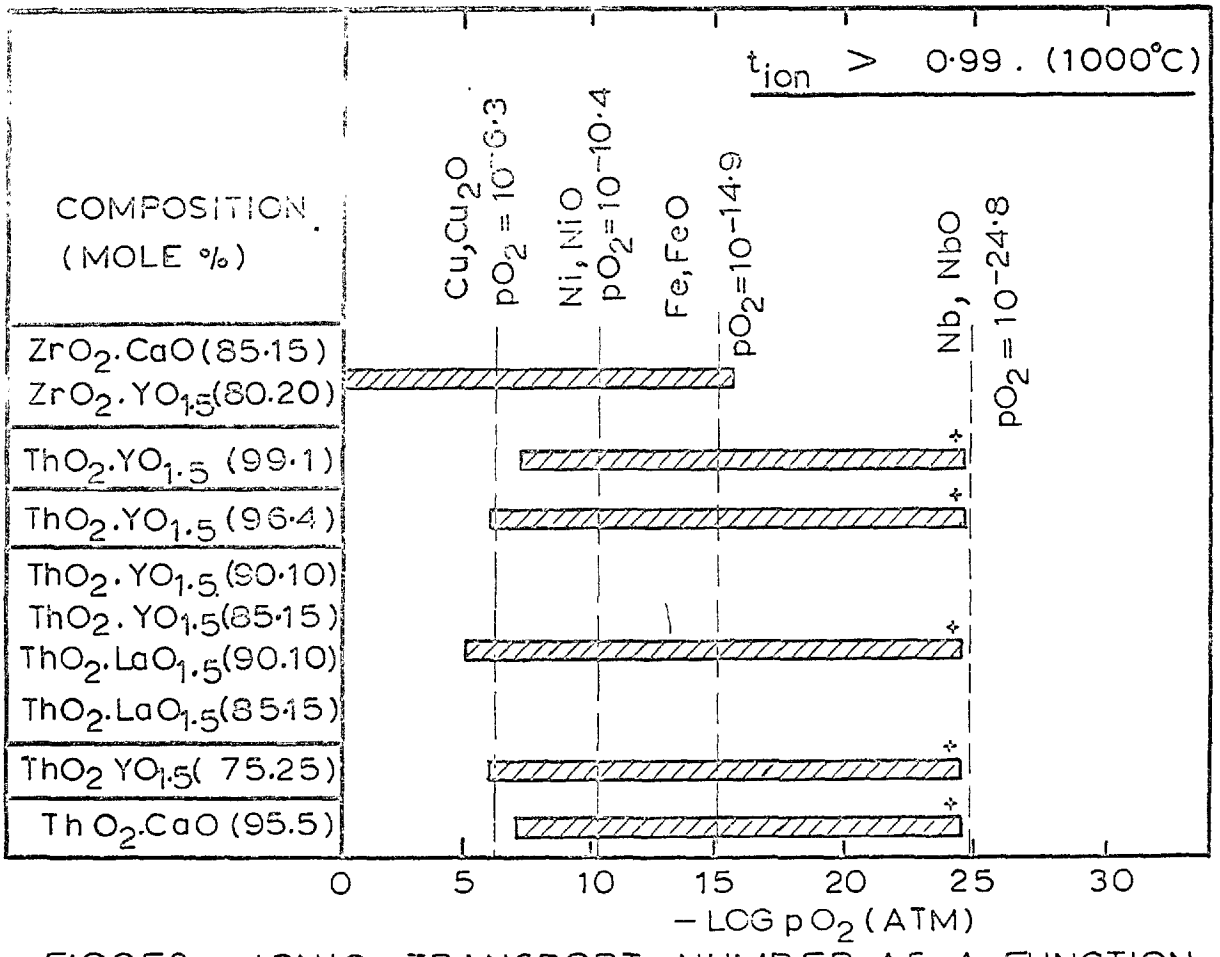


FIG.3.E2 IONIC TRANSPORT NUMBER AS A FUNCTION OF COMPOSITION AND OXYGEN PRESSURE.

* Estimated real values possibly lower

composition of the thoria solid solutions, and at 1000°C vary from 10^{-5}atm., for $ThO_2.YO_{1.5}$ solid solutions containing 10-15 mole % $YO_{1.5}$, to $10^{-7.5}$atm. at the composition $ThO_2.YO_{1.5}$(99.1 mole %). Below the appropriate oxygen partial pressures, the ionic transference numbers for the various thoria solid solutions are similar to those exhibited by the zirconia solid solutions, and it follows that $t_{ion} > 0.995$. It must be concluded, therefore, that the discrepancies,* mentioned in chapter one, between the results of Kiukkola and Wagner,[20] and Peters and Mann,[21,66] for cells containing the electrodes Fe-FeO, Co-CoO, Ni-NiO and Cu-Cu_2O, must be attributed to the different cell design, and not to the thoria based electrolyte, $ThO_2.LaO_{1.5}$ (90.10 mole %), used by Peters and Mann.

It is also important to know how the oxygen partial pressures associated with the development of significant electronic conductivity (>1%) vary with temperature. It is possible to extract information, from the results of the present work, about the temperature

---

* These discrepanices are discussed in more detail in chapter four in the appropriate sections dealing with the relevant electrode equilibria.

dependence of the p-type conduction exhibited by the thoria solid solutions (see Table 3.C.1, for example). However, such an analysis was not immediately relevant to the present research programme, and it was considered more appropriate to compare the various estimates proposed for the occurrence of significant n-type conductivity as a function of temperature and oxygen partial pressure. These relationships are depicted in fig. 3.E.3, and there is reasonable agreement at 1000°C between the curves suggested by different investigators for the zirconia solid solutions, in view of the experimental difficulties and assumptions involved.

Finally it must be emphasised that the polarisation of an electrode can be very pronounced even with small electronic contributions to the total conductivity, as exemplified by the $NbO_2.Nb_2O_5$ electrode in contact with a zirconia based electrolyte (section 3.D.5). If the presence of significant electronic conductivity is suspected, therefore, it is obviously desirable to employ a high resistance electrolyte, and relevant experiments involving the Nb-NbO electrode are described in chapter five.

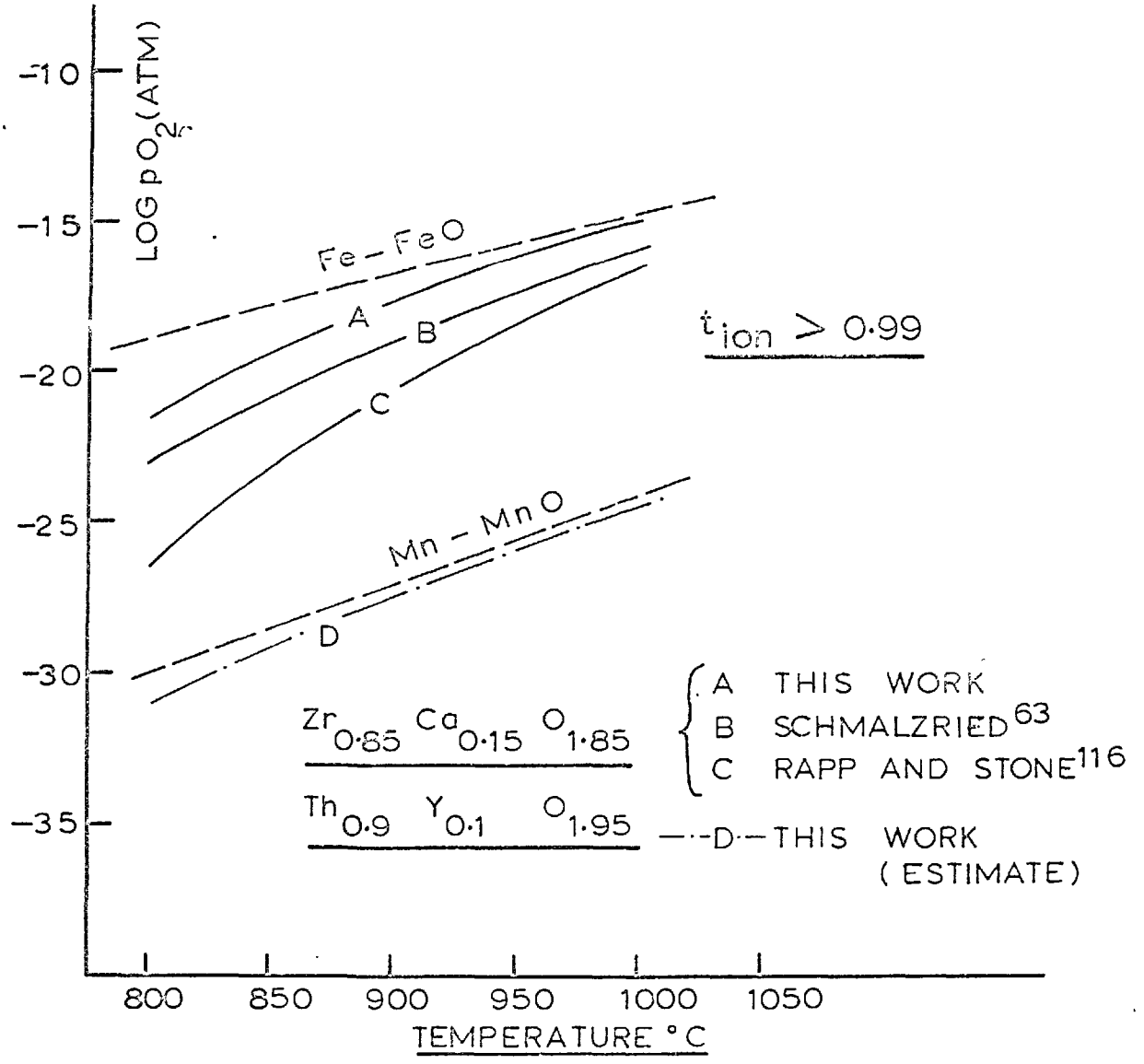


FIG.3.E.3 IONIC TRANSPORT NUMBER ($t_{ion} > 0.99$) AS A FUNCTION OF TEMPERATURE AND OXYGEN PRESSURE

CHAPTER FOUR

E.M.F. MEASUREMENTS AT HIGH OXYGEN CHEMICAL POTENTIALS

4.A. GENERAL

Oxygen chemical potentials possessing values more positive than those associated with the Fe-FeO equilibria were classified as high in the present investigation. The selection of the Fe-FeO electrode as a suitable reference material, and the observation that zirconia-based electrolytes begin to exhibit significant electronic conduction at lower oxygen chemical potentials, illustrate the convenience of this classification. Emf measurements involving the electrodes Fe-FeO, Ni-NiO, $Cu-Cu_2O$, Pb-PbO are therefore reported in this chapter, and the relevant thermodynamic data were assessed with the assistance of the following compilations: Coughlin,[65] Kubaschewski and Evans,[1] Kelley,[117] Kelley and King[118] and Elliott and Gleiser[119].

4.B. REFERENCE ELECTRODE

4.B.1. Preliminary considerations

The excellent characteristics possessed by the gasseous electrode, Pt,O_2(1 atm), were mentioned in chapter one (section 1.C.4). It appears that activation and concentration polarisation at this electrode remain insignificant even at current densities as high 10 $mA.cm^{-2}$, and it was thus an obvious choice for a reference electrode. Moreover,it follows from the relationship,

$$\mu_{O_2} - \mu^{\circ}_{O_2} = -4EF,$$

that oxygen chemical potentials (μ_{O_2}), relative to pure oxygen in its standard state ($\mu^{\circ}_{O_2}$), can be directly determined by emf measurements on galvanic cells incorporating this particular reference electrode, Pt,O_2(1 atm). However, to ensure that the gaseous oxygen does not come into contact with the other electrode, the electrolyte material must be impermeable and preferably available in the form of a closed-end tube. Although preliminary experiments (section 2.E.2) with commercial zirconia-lime electrolyte tubes were very satisfactory, it was desirable to use another reference electrode to reduce the large cell voltages (>1 volt), and to avoid the necessity of

specifying expensive, commercial, impermeable, electrolyte tubes.

It was proposed to use either Fe-FeO or Ni-NiO pellets as additional reference electrodes, and information was available about the properties of these materials from experiments conducted on the cells,

$$\text{Pt, M-MO} \;\Big|\; \begin{matrix}\text{IMPERMEABLE}\\ \text{STABILIZED}\\ \text{ZIRCONIA}\\ \text{TUBE}\end{matrix} \;\Big|\; O_2(1\ \text{atm}), \text{Pt.}$$

(M = Fe or Ni)

The equilibrium emf values at 890°C for these cells have already been reported in section 3.D.2., and in addition it was also established that both the metal-metal oxide electrodes were fully reversible at currents of 1μA. When currents of 10μA, however, were passed through the cells, for approximately 5 minutes, the Ni-NiO electrode became polarised, in contrast to the Fe-FeO electrode which still exhibited reversible behaviour under these conditions. Similar results were also obtained with the current flowing in the reverse direction. It should be noted that although polarisation effects were noted at the Ni-NiO electrode, when the flow of current was stopped equilibrium was rapidly re-established at this electrode. The results

obtained in these experiments could be attributed to differences in the electrode-kinetics of the two metal-metal oxide mixtures, and the faster electrode processes exhibited by the Fe-FeO pellet are in accordance with data[120] on the rate of oxidation of Fe and Ni.

In the present investigation, the absence of polarisation at currents up to 5μA at 1000°C (or 0.5μA at 800°C) was selected as being the minimum requirement[¤] for a reversible reference electrode. Although these values greatly exceeded the very small current (probably less than 10^{-10}amp) flowing in the external measuring circuit, cognizance had also to be taken of the possibility of current flow within the cell, due to the presence of electronic conductivity in the solid electrolyte, which has already been discussed in section 3.D.5.

It was more appropriate, therefore, to select the Fe-FeO pellet as a reference electrode, although it must be emphasised that the results of the preceding polarisation experiments apply only to Fe-FeO and Ni-NiO

¤ The appropriate current values were selected by considering the available data on the resistivity of the thoria-based electrolytes, and assuming a cell voltage of 500 mV, and an electronic transference number of 1%.

electrodes as prepared in this investigation. Changes in the metal to oxide ratio, or in the distribution of the two phases would undoubtedly influence the kinetics of the electrode processes.

Selection of the Fe-FeO mixture as a reference electrode was also supported by the available thermodynamic data for the Fe-FeO equilibria, which was assessed to be more accurate than that associated with the Ni-NiO equilibria.

The principal disadvantage associated with the Fe-FeO electrode was the contamination of the adjacent electrolyte surface due to migration of iron from the electrode. The extent of this penetration of iron obviously depended upon the duration and temperature of the experiment, and was very much more evident for zirconia-based electrolytes* than for the thoria-based electrolytes. However, no experiments failed due to complete penetration of the iron through the electrolyte, although it was invariably necessary to remove the contaminated section before using the electrolyte pellet again. In addition wustite disproportionates at 575°C, and so the electrode cannot be used below 600°C. However, these undesirable features were not of sufficient importance to outweigh the otherwise favourable properties possessed by the Fe-FeO electrode.

---

* According to Fischer[121] et al, the saturation solubility of FeO in zirconia-lime (85.15 mole %) is 2 mole% at 1000°C and 12 mole% at 1450°C.

4.B.2. Iron-wüstite equilibria

The iron-wüstite system has been studied by equilibration with both CO/CO_2 and H_2/H_2O gas mixtures. The early measurements with H_2/H_2O may be neglected as they were shown to be in error by the careful work of Emmett and Shultz[123] who demonstrated the importance of thermal diffusion in the gas mixture. The following investigations were eventually considered in the assessment of the high temperature equilibria experiments:

Schenck, Dingmann, Kirscht and Wesselkock (1929)[122]	CO/CO_2 equilibria(dynamic)
Emmett and Shultz(1930)[123]	H_2/H_2O equilibria(dynamic)
Emmett and Shultz(1933)[124]	H_2/H_2O equilibria(static)
Darken and Gurry (1945)[125]	CO/CO_2 equilibria(dynamic)

The data of other investigators, Dominy and Murphy (1931),[126] Chipman and Marshall (1940)[127] and Cirelli (1947)[128] were disregarded owing to the poor reproducibility of the published results.

The oxygen chemical potentials associated with the Fe-FeO equilibria were calculated by introducing the relevant standard free energy data for the $CO-CO_2$ and

and H_2-H_2O reactions.* The error involved by the assumption of unit activity for the iron and wüstite ($Fe_{0.95}O$)** could be neglected, and so the calculated oxygen chemical potentials could be identified with the standard free energy changes (ΔG°_T) of the equilibria:

$$1.9Fe + O_2 \rightleftharpoons 2Fe_{0.95}O$$

It was now possible to assess the high temperature thermodynamic data (ΔG°_T) by combining the various values with the relevant specific heat and entropy data as follows:

$$\Delta H^\circ_T = \Delta G^\circ_T + T\,\Delta S^\circ_T$$

$$\therefore \quad \Delta H^\circ_{298} = \Delta G^\circ_T - \Delta(H^\circ_T - H^\circ_{298}) + T\,\Delta S^\circ_T$$

$$\text{i.e.} \quad \Delta H^\circ_{298} = \Delta G^\circ_T - \Delta(H^\circ_T - H^\circ_{298}) + T[\Delta(S^\circ_T - S^\circ_{298}) + \Delta S^\circ_{298}]$$

This 'third-law treatment' gives a series of values for ΔH°_{298} which should of course be the same if both the high temperature and calorimetric data are accurate.

---

* D.D. Wagman and W.H. Evans, Natl.Bur.Standards(U.S.) Series III Compilation, 1947-1956.

** Although the composition range of the non-stoichiometric wüstite phase broadens with increasing temperature, the actual composition of the oxide in equilibrium with iron varies only very slightly with temperature and may be represented as $Fe_{0.95}O$ from 575 - 1378°C (M.P.).

The results of this treatment, using the high temperature data mentioned earlier, and the latest calorimetric values recommended by Kelley,[117,118] are presented in fig. 4.B.1. The excellent quality of the thermodynamic data is evident in that the ΔH°_{298} values only vary within very narrow limits (±120 cal) about a mean value of -127,050 cal. A value for ΔH°_{298} equal to -127,000 cal is suggested by Elliott and Gleiser, whereas Coughlin, and Kubachewski and Evans recommend values of -127,600 cal and -126,400 cal, respectively.

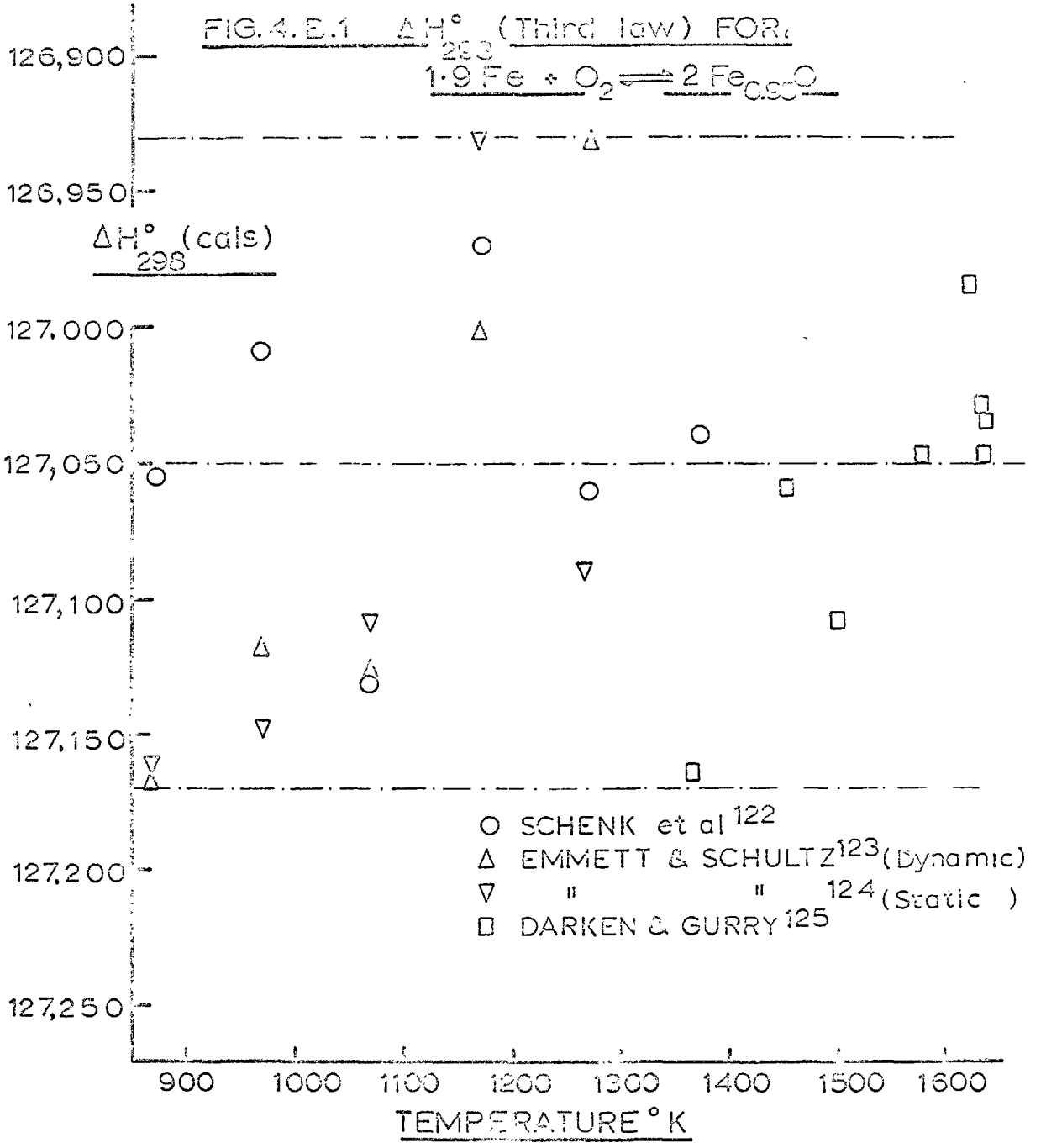
All the high temperature thermodynamic results assessed above, together with standard free energy values determined from the calorimetric data[*] were plotted on a large scale graph. Examination of the graph indicated no evident curvature, and the following linear equation[**] was derived by the method of least squares:

$$\Delta\mu_{O_2}(\text{cal.mole}^{-1}) = -126{,}470 + 31.26T \ (\pm 250 \text{ cal.}) \quad (873 - 1600^{\circ}K) \quad \ldots \text{ 4.B.1}$$

---

[*] A value of -127,000 cal. was selected for ΔH°_{298}.

[**] This equation is in very good agreement with that recently proposed by Chipman[129] (1962) for the same equilibria, i.e. $\Delta\mu_{O_2}(\text{cal.mole}^{-1}) = -126{,}400 + 31.20\,T$ (±200 cal.)


FIG. 4. E. 1 ΔH°_{298} (Third law) FOR
$1{\cdot}9\,Fe + O_2 \rightleftharpoons 2\,Fe_{0.95}O$
126,900
126,950
ΔH°_{298} (cals)
127,000
127,050
127,100
127,150
127,200
127,250
900
1000
1100
1200
1300
1400
1500
1600
TEMPERATURE °K
O SCHENK et al [122]
Δ EMMETT & SCHULTZ [123] (Dynamic)
∇ " " [124] (Static)
□ DARKEN & GURRY [125]

Darken and Gurry[125] in their classic paper also reviewed the values of oxygen chemical potential associated with the iron-ferrous oxide equilibria. Although their review did not include any calorimetric data it is interesting to record that a least squares analysis of their selected values for 1100, 1200, 1300, and 1350°C resulted in a linear equation identical to that obtained in the present assessment.

Values derived from the above linear equation are compared in Table 4.B.1 with data given in the compilations of Coughlin and Elliott and Gleiser. Also included in this table are the values derived from the experiments of Peters and Mann[67] who employed the following galvanic cell incorporating a solid oxide electrolyte:

$$\text{Pt, Fe-FeO} \;\Big|\; \text{ThO}_2\text{-YO}_{1.5}\text{(90.10 mole \%)} \;\Big|\; \text{CO+CO}_2\text{+iron oxide, Pt.}$$

These values indicate that any inaccuracies due to electronic conductivity in the solid oxide electrolytes do not exceed the errors associated with the thermodynamic data. It is not possible to attach any significance to this observation when considering the results of Peters and Mann as errors in the thermodynamic data could account for a significant part (5-30%) of the small free energy

TABLE 4.B.1

OXYGEN CHEMICAL POTENTIALS ($\Delta\mu_{O_2}$) FOR THE EQUILIBRIA

$$1.9\ Fe + O_2 \rightleftharpoons 2\ Fe_{0.95}O$$

Temp. °K	Linear Equation Derived This Investigation	Coughlin	Elliott and Gleiser	Peters[67] and Mann
	± 250 cal.	± 500 cal.	± 500 cal.	±± 300 cal.
900	-98,340	-98,800	-98,200	-98,204
1000	-95,210	-95,700	-95,100	-95,020
1100	-92,080	-92,700	-92,100	-91,856
1200	-88,960	-89,600	-88,900	-88,892
1300	-85,830	-86,400	-85,800	-85,548
1400	-82,710	-83,400	-82,800	-82,414
1500	-79,580	-80,000	-79,700	-79,340
1600	-76,450	-77,200	-76,600	----

difference measured by these workers. It was concluded in section 3.D.2, however, from measurements in the present investigation on the cell,

Pt	Fe,FeO	IMPERMEABLE STABILISED ZIRCONIA TUBE	O_2(1 atm), Pt

that the MEAN electronic transference number of the zirconia based electrolyte did not exceed 0.5% at 890°C over the relevant range of oxygen partial pressures.

4.C. NICKEL-NICKEL OXIDE EQUILIBRIA

4.C.1. Emf measurements

Preliminary emf measurements on the cell,

Fe,FeO	SOLID OXIDE ELECTROLYTE	Ni,NiO

have already been described in chapter two, and the present section, therefore, is confined to a discussion of the results obtained with cells assembled in the modified apparatus and provided with separate electrode compartments. In addition to specific experiments designed to provide information about the Ni-NiO equilibria, the above cell was also used to examine the transport

properties of thoria based electrolytes and to periodically check the apparatus, and it follows that a large amount of data was available for assessment.

The standard precautions and procedures detailed in section 2.H. were always followed, and provided the cell temperature had initially exceeded 700°C, then excellent reproducible results were always obtained over the temperature range studied, namely, 650-1100°C. All the cells examined behaved reversibly, and were successfully operated in either purified argon or vacuum. The cell performance was also independent of the large variation in conductivity possessed by the different electrolyte compositions.

Emf measurements were made at approximately 50°C intervals, and although the voltage response to changes in temperature was rapid, the measurements were continued for at least one hour to ensure that the cell had attained equilibrium. Typical results for one of the cells are detailed in Appendix VI, and a least squares analysis of similar data for another nineteen experiments gave the following linear equation;

$$E = 157.6 + 0.101\ T \quad \pm 0.86\ mV \quad . \quad . \quad . \quad . \quad . \quad . \quad . \quad 4.C.1.$$

$$[900 - 1400\ ^{\circ}K]$$

Taking into account the precision of the measurements, then the overall accuracy of the emf data is ±0.9 mV for an error in the Vibron electrometer reading of ±0.2 mV*, and a variation in the temperature measurement of ±1°C.

The excellent agreement between the results of the present work and the values obtained by other investigators is evident from Table 4.C.1.

TABLE 4.C.1.

ELECTROMOTIVE FORCE OF THE CELL

Fe, FeO / ELECTROLYTE / Ni, NiO

Temp. (°K)	This Investigation	Rapp[79]	Kiukkola[20] and Wagner
(°K)	(mV)	(mV)	(mV)
973	255.9±0.9	--	--
1073	266.0 "	266.2±0.8	266± 1
1173	276.1 "	276.4±0.9	276± 1
1273	286.2 "	286.2±0.6	286± 1
1373	296.3 "	296.4±0.5	296± 2

* For additional comments see chapter two, section 2.F.

4.C.2. Evaluation of thermochemical data

The standard free energy changes associated with the reaction,

$$NiO + 0.95\ Fe = Ni + Fe_{0.95}O ,$$

may be represented by the equation,

$$\Delta G^{\circ}_{T} = -7{,}270 - 4.66T\ (\pm 42\ \text{cal.}) \quad [900 - 1400\ ^{\circ}K] \qquad 4.C.2.$$

which was derived from the emf data (Eq. 4.C.1) of the preceding section. This equation (Eq. 4.C.2) was combined with that proposed for the iron-wüstite equilibria (Eq. 4.B.1) to give the following standard free energy expression,

$$\Delta G^{\circ}_{T} = -111{,}930 + 40.58T\ (\pm 260\ \text{cal.}) \quad [900 - 1400\ ^{\circ}K] \qquad 4.C.3.$$

for the system,

$$2\ Ni + O_2 = 2\ NiO .$$

The standard free energy changes obtained from this expression (Eq. 4.C.3) are compared with other high temperature equilibria results in Table 4.C.2., which also includes values calculated from the available calorimetric data.

TABLE 4.C.2

NICKEL - NICKEL OXIDE SYSTEM

HIGH TEMPERATURE EQUILIBRIA VALUES

Temp. °K	Present Investigation	Young and Tomlinson[130]	Calorimetric Data	Peters and Mann[66]	Fricke and Weitbrecht[131]
		[a]	[b]		
900	-75,410	-75,060	-75,460	-73,750	-76,490
1000	-71,350	-70,900	-71,340	-69,700	-72,370
1100	-67,290	-66,740	-67,260	-65,670	-68,240
1200	-63,230	-62,580	-63,180	-61,640	-64,120
1300	-59,180	-58,420	-59,120	-57,640	-59,990
1400	-55,120	-54,260	-55,080	-53,650	-55,870
Accuracy	±260cal	±600cal	±500cal	±300cal	±500cal

(a) Tomlinson and Young[130] use the following two-term equation to express their data:

$$\Delta G^{\circ}_{T} = \div 112,500 + 41.60\ T\ (\pm 600\ \text{cal})$$

(b) The calorimetric values were based on the following data:
(i) Standard heat and entropy of formation of NiO at 298°K.

ΔH°_{298} Cal.mole^{-1}	ΔS°_{298} Cal.Deg.$^{-1}$Mole^{-1}	Source
-57,300(±100)	-	Skinner[132]
-57,300(±100)	-22.42	Coughlin[65]
-57,500(±500)	-	Kubachewski and Evans[1]
-57,300(±100)	-21.92	Elliott and Gleiser[119]
-	-22.56	Kelley and King[118]

Selected values: ΔH°_{298}: -57,300(±100); ΔS°_{298}: -22.56 (±0.2)

(ii) $(H^{\circ}_{T} - H^{\circ}_{298})$ and $(S^{\circ}_{T} - S^{\circ}_{298})$: Kelley[117]

The "third law treatment" which combines the high temperature equilibria results with the calorimetric data is more informative (see fig. 4.C.1) . The values of ΔH°_{298} obtained from the results of the present investigation are virtually constant throughout the whole temperature range, and are in excellent agreement with the recommended value for the heat of formation of NiO ($-57,300 \pm 100$ cal.mole^{-1}). An additional check on the accuracy of the calorimetric data and the present emf work is provided by the point on the ΔH°_{298} plot derived from the emf measurements on the cell,

$$\text{Pt},\quad \text{Ni},\text{NiO} \;\Big|\; \begin{matrix}\text{COMMERCIAL}\\ \text{STABILIZED}\\ \text{ZIRCONIA}\\ \text{TUBE}\end{matrix} \;\Big|\; O_2(1\text{atm}),\text{Pt}$$

which were reported in section 3.D.2.

The ΔH°_{298} values derived from the data of other investigators, however, varied with temperature, and it follows that the related high temperature equilibria measurements are not so reliable. The data of Young and Tomlinson,[130] Fricke and Weitbrecht,[131] were obtained from CO/CO_2 gas equilibria experiments, and it is interesting to note that both sets of ΔH°_{298} values become

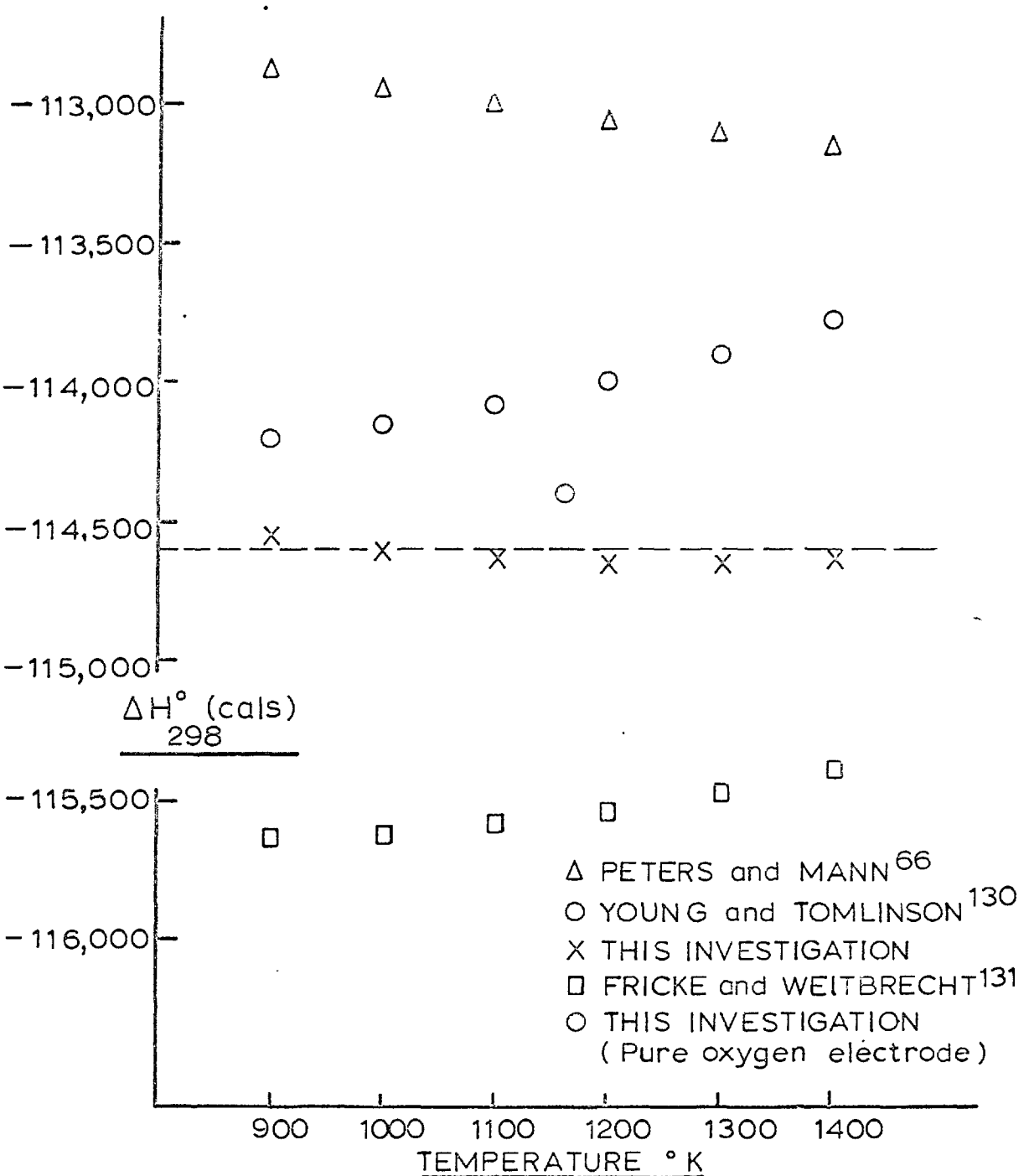


FIG. 4.C.1 ΔH°_{298} (Third law) FOR $2Ni + O_2 \rightleftharpoons 2NiO$

less negative as the temperature increases. It might be expected that the largest errors associated with this technique would occur at the lower temperatures where the gas ratios are higher (900K° : $CO/CO_2 \sim \frac{1}{200}$), yet the ΔH°_{298} values derived from the results of Young and Tomlinson appear to be more accurate at the lower temperatures. The values assigned to Peters and Mann[66] were derived from their experiments on the cell,

Pt, | Ni-NiO | $ThO_2.YO_{1.5}$(90.10 mole %) | $CO+CO_2$+ IRON OXIDE | Pt.

The experimental arrangement of this cell was such that it would be difficult to entirely eliminate the transfer of gaseous components between the two electrode compartments. The possible errors associated with this transfer process will be some function of the actual cell voltage measured by Peters and Mann, which was 0-50 mV for cells incorporating the Fe-FeO electrode (section 4.B.2), and 250-300 mV for the above cell containing the Ni-NiO electrode. This could account for the larger error ($\sim$ 1.5 kcal.) associated with their Ni-NiO data (Table 4.C.2), compared to the reasonable agreement ($\sim$ 300 cal) with the recommended values noted for the Fe-FeO equilibria (Table 4.B.1)..

The accurate and consistent data available from both the calorimetric measurements and the emf results of the present investigation, were combined by means of the sigma[*] function which is given by:

$$\Sigma = \frac{\Delta G^{\circ}_{T}}{T} + \Delta a \ln T + \frac{\Delta b}{2} T + \frac{\Delta c}{2} T^{-2} = I + \frac{\Delta H_{o}}{T} \quad \ldots\ldots \quad 4.C.4.$$

where $\Delta C_p = \Delta a + \Delta bT + \Delta c\, T^{-2}$, and $I, \Delta H_o$, represent the appropriate integration constants.

It is known that nickel exhibits a magnetic transformation (Curie pt. 633°K), and that nickel oxide undergoes two order-disorder transformations (525 and 565°K). As it is impossible to represent the specific heat data by a simple equation for a material possessing these second-order phase changes (or lamda transformations) the sigma function could only be evaluated above 650°K.

A large-scale plot of Σ against $1/T$ gave a straight line the gradient of which was equal to ΔH_o(-115,280). This figure was inserted in the expression,

$$\Sigma = I + \frac{\Delta H_{o}}{T} \quad \ldots\ldots\ldots\ldots\ldots \quad 4.C.4.$$

---

[*] The sigma function is discussed in "The Physical Chemistry of Metals by L.S. Darken and R.W. Gurry, (Publ: McGraw-Hill, New York, 1953).

and a value of I was determined for each value of Σ. The average of these values (65.781) was then used to represent the constant in Eq. 4.C.4. These calculations produced the following expression,

$$\Delta G^{\circ}_{T} = -115{,}280 + 65.781T - 7.369T \log T + 0.28 \times 10^{-3} T^{2} - 0.20 \times 10^{5} T^{-1} .$$

The accuracy of the data, however, did not justify a cumbersome 5- term expression, and a 3-term equation was derived which gave the same ΔG°_{T} values as the more complicated equation at 650, 1000, 1400°K. It is proposed, therefore, that the standard free energy changes associated with the reaction,

$$2Ni + O_2 = 2NiO,$$

are best expressed by the following equation,

$$\Delta G^{\circ}_{T} = -115{,}240 - 6.558\ T \log T + 63.57T\ (\pm 300 \text{ cals}) \quad . \quad . \quad 4.C.5.$$

[650 - 1400 °K]

which also represents the oxygen chemical potentials in equilibrium with the Ni-NiO system assuming unit activities for the condensed phases. Values obtained from the equation are listed in Table 4.C.3 which also includes the original emf data, together with values recommended in

TABLE 4.C.3.

OXYGEN CHEMICAL POTENTIALS ($\Delta\mu O_2$) FOR THE EQUILIBRIA

$$2Ni + O_2 \rightleftharpoons 2NiO$$

Temperature °K	Derived Three-Term Equation	Experimental Two-Term Equation	Elliott and Gleiser	Coughlin
	±300 cal	±260 cal	±280 cal	±280 cal
650	-85,910	(-85,550)	-86,090	-85,600
700	-83,800	(-83,520)	-84,120	-83,380
800	-79,610	(-79,470)	-79,940	-78,960
900	-75,460	-75,410	-75,880	-74,540
1000	-71,350	-71,350	-71,820	-70,160
1100	-67,250	-67,290	-67,800	-65,800
1200	-63,180	-63,230	-63,780	-61,440
1300	-59,150	-59,180	-59,780	-57,120
1400	-55,110	-55,120	-55,780	-52,820

various compilations. It is apparent from Table 4.C.3. that the high temperature data(900-1400°K) is also adequately represented by the two-term linear equation (Eq. 4.C.3), used to express the data derived from the emf measurements. At lower temperatures, however, the curvature of the 3-term equation becomes more pronounced and the linear expression is no longer valid.

4.D. COPPER-CUPROUS OXIDE

4.D.1. Emf measurements

An outstanding feature of the cell,

$$\text{Ni-NiO} \;\Big|\; \begin{matrix}\text{SOLID OXIDE}\\ \text{ELECTROLYTE}\end{matrix} \;\Big|\; \text{Cu-Cu}_2\text{O} \quad ,$$

was its reliability. The simple cell design used in the preliminary experiments (chapter two), with a stream of argon maintaining an inert atmosphere around the cell, gave excellent reproducible results (± 1 mV), and the provision of separate electrode compartments had no significant effect upon the cell performance which appeared to be relatively insensitive to minor impurities in the argon (cf. cells incorporating Ni-NiO and Fe-FeO electrodes; section 2.E.1). The cell atmosphere always consisted

of purified argon and the emf measurements, which followed the procedure detailed earlier (section 2.E), were normally confined to the temperature range 650-1000°C. At the beginning of each experiment low voltages were invariably recorded until the temperature of the cell was approximately 600°C. Thereafter the cells behaved reversibly, and in three experiments reproducible voltages were also obtained as low as 400°C, although it was essential to maintain the cell temperature constant for many hours to ensure that steady reversible voltages were being recorded. The detailed results for one of these cells are reproduced in Appendix VI.

Many electrolyte compositions (section 3.D.3) were incorporated in the cell and gave excellent results. There was also no doubt that the low voltages obtained with certain of the electrolytes[¤] could be attributed to electronic conductivity, and these results were not, therefore, included in the following assessment. The data for 21 experiments which included results from the preliminary investigations (seven runs) were incorporated on a large scale plot, and as the values exhibited no

---

¤ See Table 3.D.3.

discernible curvature, it was decided to represent the data by the following linear equation which was derived by the method of least squares,

$$E = 347.8 - 0.0695T \ (\pm 1.2 \text{ mV})^{***} \quad . \ . \ . \ . \ . \ . \ . \ . \quad 4.D.1.$$

$$[650 - 1300 \ ^{\circ}K].$$

The good agreement between the results of the present investigation and those reported by Markin and Bones [133] is evident from the adjoining Table 4.D.1.

TABLE 4.D.1.

ELECTROMOTIVE FORCE OF THE CELL

Ni, NiO | ELECTROLYTE | Cu, Cu_2O

Temperature °K	This Investigation mV	Markin and Bones [133] mV
673	301.0±1.2	301±2
773	294.0 "	293 "
873	287.1 "	286 "
973	280.1 "	278 "
1073	273.2 "	271 "
1173	266.2 "	--
1273	259.3 "	--

*** The reported error also takes into account the precision of the emf measurements (±0.2mV) and the temperature measurements (± 1°C)

Additional information about the $Cu-Cu_2O$ system was obtained by measurements on the cell,

$$Fe-FeO \;\big|\; ZrO_2.CaO \quad (85.15 \text{ mole } \%) \;\big|\; Cu-Cu_2O \;.$$

In the initial experiments no attempt was made to separate the gaseous environments of the two electrodes, and it was only possible to obtain comparable results (± 5 mV) to those reported by Kiukkola and Wagner[20] if the cell was rapidly cycled through the temperature range (650 - 1000 - 650°C) in about 3 hours. If the cell was held at a constant temperature then the emf slowly drifted downwards, and even after 24 hours a steady voltage was not observed. The introduction of separate electrode compartments overcame these difficulties and reproducible steady voltages were easily obtained in two experiments carried out in the modified apparatus. A straight line drawn through these results had the following equation,

$$E = 505.8 + 0.030\ T \quad (\pm 1.5 \text{ m V})$$

Introducing the expression (Eq. 4.C.1) derived from the cell reaction,

$$NiO + Fe \longrightarrow FeO + Ni,$$

should be represented by:

$$E = 348.2 - 0.071\ T\ (\pm 1.7\ mV)$$

This equation is almost identical to that derived from the actual measurements on this cell, viz.

$$E = 347.8 - 0.0695\ T\ (\pm 1.2\ mV) \quad \ldots\ldots \quad 4.D.1.$$

Further evidence of the accuracy of the present investigation is provided by the good agreement with the data reported by other investigators which is contained in Table 4.D.2. (p. 136).

4.D.2. Evaluation of thermochemical data

The standard free energy of formation of Cu_2O per mole of O_2 may be represented by the equation,

$$\Delta G^\circ_T = -83{,}160 - 6.55T \log T + 57.15T \quad (\pm 320\ cal.) \quad \ldots\ldots \quad 4.D.2$$
$$[650 - 1300^\circ K]$$

This equation was derived by combining the expression for the free energy changes associated with the cell reaction[x]

---

x According to Eq. 4.D.1,
$$2xE = 695.6 - 0.139T$$
i.e $\Delta G^\circ_T = -32{,}080 + 6.42T\ (\pm 110\ cal.)$ Eq. 4.D.3.

Table 4.D.2.

Electromotive force of the cell, Fe,FeO/electrolyte/Cu-Cu_2O

Temperature	This Investigation	Kiukkola[20] and Wagner	Palguev[134] and Neumin
^oK	mV	mV	mV
873	-	-	531 $\pm$ 1
973	535 $\pm$ 1.5	-	534 $\pm$ 1
1073	538 $\pm$ 1.5	532*	537 $\pm$ 1
1173	541 $\pm$ 1.5	539	540 $\pm$ 1
1273	544 $\pm$ 1.5	543	543 $\pm$ 1

* Problems encountered in the present investigation when the above electrodes were incorporated in the simple cell design have already been mentioned, and probably account for the low results reported by Wagner and Kiukkola.

$$2\ Cu_2O + 2Ni = 4Cu + 2NiO,$$

with that proposed for the standard free energy of formation of two moles of NiO (Eq. 4.C.5.).

This and other data for the free energy of formation of Cu_2O reported by Treadwell[16], Peters and Mann[66], Young

and Tomlinson[135], was examined by the 'third law' method, and the various values of ΔH^{o}_{298} are shown in Fig. 4.D.1. The ΔH^{o}_{298} values derived from the data of the present investigation are very clearly a function of temperature. There is, however, reasonable agreement with ΔH^{o}_{298} values obtained from other high temperature equilibria experiments* (Treadwell, Young and Tomlinson)** in the temperature range 1100-1300°K, which suggests that the high temperature free energy data is correct. At lower temperatures the present e.m.f. data are more reliable than the CO/CO_2 gas equilibria measurements of Young and Tomlinson which show considerable scatter below 900°C. It is also probable that the discrepancy (~800 cal.) between the results of the present investigation and those reported by Treadwell at 1073°K can

---

* The lack of agreement with the results of Peters and Mann is not surprising in view of the design of their cell which has already been criticised (Section 4.C.2.).

** The original results due to Treadwell were corrected for thermo-electric effects by Gundermann, Hauffe and Wagner[136]. Young and Tomlinson express their free energy data for Cu_2O by the equation: ΔG^{o}_{T}(per mole O_2) = -74,340 + 29.98T

(± 500 cal.) $\left[1100 - 1356^{o}K\right]$

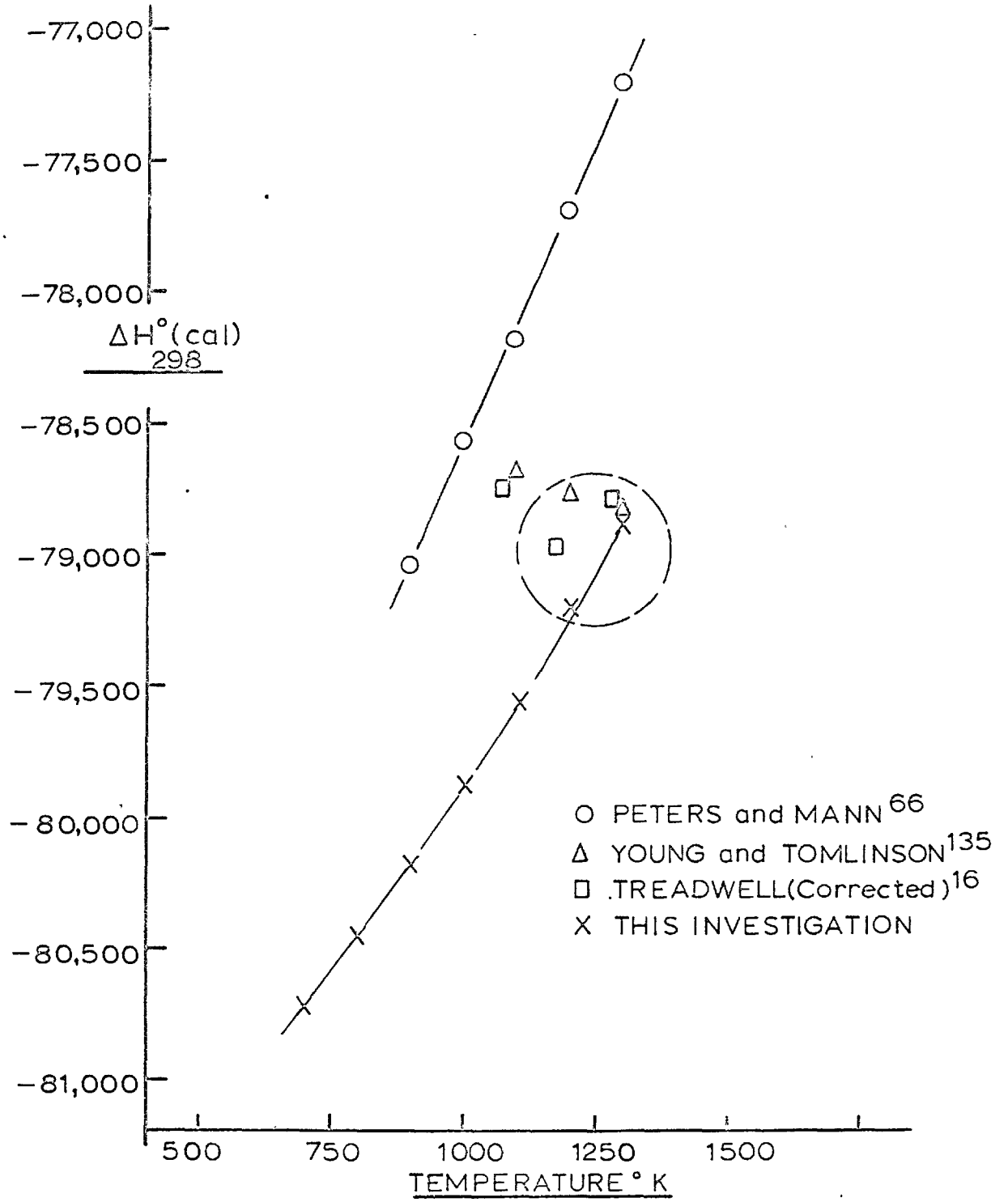


FIG. 4.D.1 ΔH°_{298} (Third law) FOR $4Cu + O_2 \rightleftharpoons 2Cu_2O$

be attributed to errors associated with the very high resistance of the auxiliary porcelain electrolyte used by the latter. As there appears to be no reason to suspect the accuracy of the present e.m.f. data which was shown to be in good agreement with similar experiments by other investigators (Markin and Bones[133], Kukkola and Wagner[20], Neumin and Polguev[134]), it must therefore be concluded that the variation in the ΔH^{o}_{298} values is due to inaccurate calorimetric data. It may also be surmised that it is the specific heat measurements on cuprous oxide most likely to be in error.

It follows that standard free energies of formation of cuprous oxide are best represented by the three term equation (Eq. 4.D.2.) derived earlier from the present e.m.f. measurements which extend over a wide range of temperatures (650-1300°K)*. Extrapolation of this equation to 298°K gives:

---

* A linear equation may also be derived as follows,
$2Ni + O_2 = 2NiO$: $\Delta G^{o}_{T} = -111,930+40.58T(\pm 260cal)$ Eq.4.C.3.
$2Cu_2O + 2Ni = 4Cu+2NiO$: $\Delta G^{o}_{T} = -32,080+6.42T(\pm 110cal)$ Eq.4.D.3.
$4Cu + O_2 = 2Cu_2O$: $\Delta G^{o}_{T} = -79,850+34.16T(\pm 280cal)$ Eq.4.D.4.
The applicability of the last equation is limited to the temperature 900-1300°K.

$$\Delta G^{\circ}_{298} = -70,960 \text{ cal.,}$$
$$\text{and } \Delta H^{\circ}_{298} = -81,700 \ (\pm 500 \text{ cal.}),$$
$$\text{when } \Delta S^{\circ}_{298} = -36.09 \text{ cal. deg}^{-1} \text{ (Kelley)}$$

This value for ΔH°_{298} derived from the high temperature e.m.f. measurements is in excellent agreement with the calorimetric value, -81,600 ($\pm$ 500 cal), determined by Balesdent[137]. The absence of any noticeable curvature in the e.m.f. data for the reaction,

$$2Cu_2O + 2Ni \rightleftharpoons 4Cu + 2NiO,$$

over a large range of temperature (650-1300°K), suggests that the ΔCp term (2.85) contained in the equation,

$$\Delta G^{\circ}_{T} = -83,160 - 6.55T \log T + 57.15T \text{ .....4.D.2.}$$

is not likely to be greatly in error at 298°K, and it is therefore proposed that the above value of ΔH°_{298} derived from the data of the present investigation is more accurate than other recommended values, for example,

Coughlin:	-80,800 $\pm$ 1,550
Kubachewski and Evans:	-80.000 $\pm$ 1,400 cal.
Elliott and Gleiser:	-83,600 $\pm$ 3000 cal.

Finally, the standard free energies of formation of cuprous oxide per mole of oxygen, calculated from equation 4.D.2., are compared in Table 4.D.3., to other values given in the various compilations.

Table 4.D.3.

Oxygen Chemical Potentials (ΔO_2) for the Equilibria

$$4\ Cu + O_2 \rightleftharpoons 2\ Cu_2O$$

Temperature °K	This Investigation ± 350 cal.	Elliot and Gleiser ± 3000 cal.	Kubachewski and Evans ± 1000 cal.	Coughlin ± 3000 cal.
650	-58,000	-59,700	-56,980	-58,000
700	-56,210	-57,800	-55,320	-56,400
800	-52,660	-54,200	-52,000	-53,000
900	-49,160	-50,400	-48,740	-49,800
1000	-45,660	-46,600	-45,520	-46,600
1100	-42,220	-43,000	-42,310	-43,600
1200	-38,780	-39,200	-39,160	-40,400

4.E. LEAD-LEAD OXIDE EQUILIBRIA

4.E.1. E.M.F. Measurements

Preliminary experiments were conducted with the cell,

$$Pt/Ni\text{-}NiO/\underset{\text{zirconia crucible}}{\text{commercial}^{*}\ \text{stabilized}}/Pb\text{-}PbO/Ir/Pt,$$

which was arranged as shown in Fig. 4.E.1. The lead and yellow lead oxide inside the electrolyte crucible made contact with an iridium probe** which had been spot welded to the iridium lid of the crucible. Electrical connections to either side of the cell consisted of platinum discs attached to platinum wires. The cell was assembled in the silica apparatus used in the first series of experiments (Section 2.E.1.), and an inert atmosphere was maintained by a stream of purified argon.

Provided the temperature of the cell had initially exceeded approximately 600°C, e.m.f. measurements over the range 400-800°C gave reproducible data ($\pm$ 1.5 mV), and this cell design was subsequently adopted by Belford and Alcock[138]

---

* The crucible was supplied by Degussa Ltd., Germany, and was partially stabilized with MgO. Further details of this material are available in Section 3.D.6.

** The results of Richardson and Webb[139] indicate that the solubility of iridium in liquid Pb and PbO is very small and can be neglected.

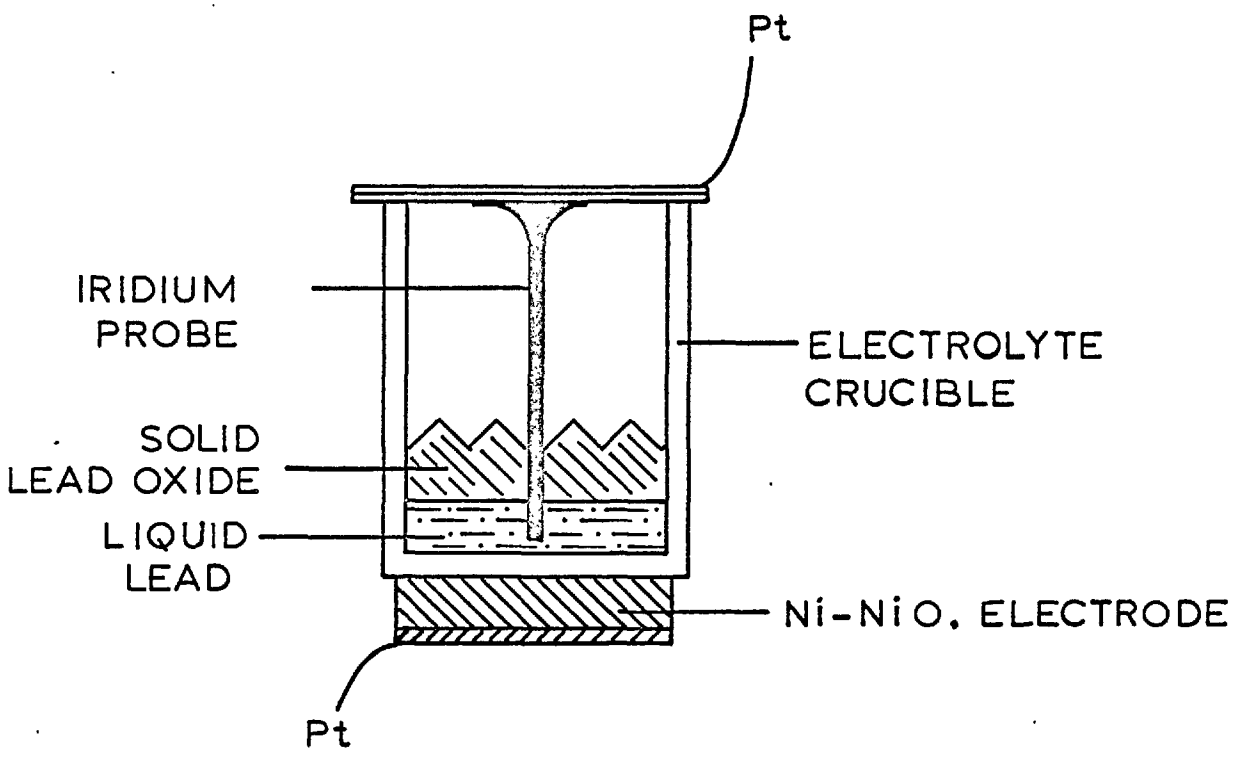


FIG. 4.E.1 CELL ASSEMBLY INVOLVING LEAD – LEAD OXIDE ELECTRODE

for their investigation into the thermodynamics and solubility of oxygen in liquid lead.

The preliminary experiments of the present ivestigation were later checked by fabricating impervious crucibles from 'Spec-pure' ZrO_2. CaO(85.15 mole %) material. Four experiments with these zirconia-calcia crucibles were carried out in the modified alumina apparatus using an identical cell assembly to that illustrated in Fig. 4.E.1. The cells were found to be reversible in the temperature range 400-700°C, and the stability of the e.m.f. values, which were measured at approximately 50°C intervals, was checked by maintaining the cells at constant temperature for several hours. Except for the lowest temperatures (400-500°C), a rapid voltage response to changes in temperature was observed. The resulting e.m.f. data could best be represented by the following linear equation,

$$E = 85.9 + 0.069\,T\ (\pm\ 1.2\ mV) \qquad \text{..... Eq.4.E.1.}$$

$$\left[673 - 973^{\circ}K\right]$$

Values derived from this expression are compared in Table 4.E.1. to the results reported by Belford and Alcock[138] for similar cells incorporating the Degussa crucibles.

Table 4.E.1.

Electromotive force of the cell,

Pt, Ni-NiO/electrolyte/Pb-PbO, Ir, Pt.

Temperature ^{o}K	This Investigation mV	Belford and Alcock mV
673	132.3 ± 1.2 mV	130.8 ± 2 mV
773	139.2 ± 1.2 mV	138.3 ± 2 mV
873	146.1 ± 1.2 mV	145.5 ± 2 mV
973	153.0 ± 1.2 mV	153.4 ± 2 mV

It is impossible to attach much significance to the slightly lower results associated with the Degussa material and it appears that the ionic transference number is virtually the same for both electrolyte materials. This interesting conclusion has already been mentioned in Section 3.D.6.

4.E.2. Evaluation of Thermochemical Data

The e.m.f. data obtained in the present investigation for the cell reaction,

$$PbO(s) + Ni(s) \longrightarrow Pb(l) + NiO(s)$$

was used to derive the following expression for the standard

free energy of formation of yellow lead oxide (per mole of oxygen),

$$\Delta G^{o}_{T} = -107{,}320 - 6.55T \log T + 69.93T \ (\pm 290 \text{ cal.}) \quad .. \text{ Eq.4.E.2.}$$

$$650\text{-}1000^{o}K$$

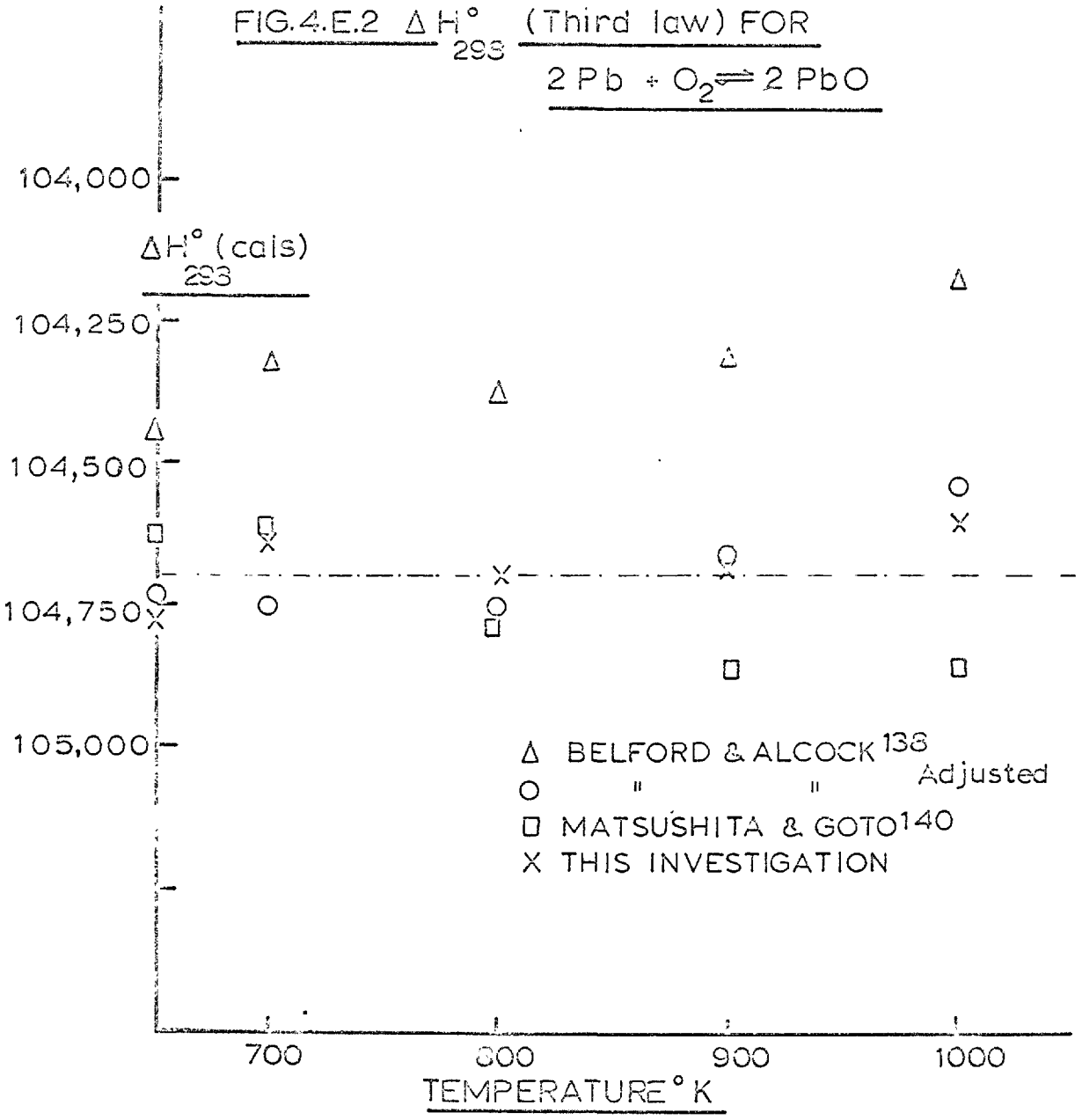
Free energies of formation determined from this expression were combined with the calorimetric data, recommended by Kelley[117, 118], and the resulting ΔH^{o}_{298} values are given in Fig. 4.E.2. as a function of temperature.

Belford and Alcock[138] derived a linear equation for the free energy of formation of lead oxide by combining their e.m.f. results with the data (700-1100°C) of Young and Tomlinson[130] for the equilibrium

$$NiO + CO \rightleftharpoons Ni + CO_2$$

The extrapolation of this data, however, to the lower temperatures involved in the e.m.f. measurements (400-700°C) introduced additional errors to those already noted in Section 4.C.2., and it was considered more appropriate to combine the original e.m.f. results of Belford and Alcock with the 3-term equation (Eq. 4.C.5.) derived in the present investigation, for the free energy of formation of NiO.

FIG. 4.E.2 ΔH°_{293} (Third law) FOR $2Pb + O_2 \rightleftharpoons 2PbO$



The corresponding ΔH°_{298} values are reproduced in Fig. 4.E.2., together with the ΔH°_{298} values associated with the linear equation.

The e.m.f. measurements of Matsushita and Goto[140] on the cell,

Pt, Ni-NiO | commercial stabilized zirconia tube | Pb-PbO, Pt

provide additional free energy data*, and the relevant ΔH°_{298} values are also included in Fig. 4.E.2.

Examination of the data presented in Fig. 4.E.2. reveals that the ΔH°_{298} values derived from the results of the present work are virtually constant (-104, 700 cal.) over the relevant temperature range, which suggests that the associated e.m.f. measurements and specific heat data are reliable. The ΔH°_{298} values assigned to Belford and Alcock (calculated from their published two-term equation) also exhibit very little variation with temperature, but are

---

* Matsushita and Goto represent their data for the equilibria

$$2Pb + O_2 \rightleftharpoons 2PbO,$$

by the linear equation,

$$\Delta G^{o}_{T} = -104,230 + 46.94T \ (\pm 200 \text{ cal.}) \quad [773 - 1159^{\circ}K]$$

some 400 cals. more positive than the values determined for the present investigation, which is to be expected from the disagreement in the relevant Ni-NiO data already noted in Section 4.C.2.

The meagre experimental information published by Matsushita and Goto makes an assessment of their e.m.f. results difficult. Although the ΔH°_{298} values obtained from the free energy equation proposed by these workers are in reasonable agreement with the ΔH°_{298} value calculated from the results of the present investigation, it must be emphasised that their free energy equation was derived by using the data compiled by Elliott and Gleiser for the reference Ni-NiO electrode. If the Ni-NiO data recommended in Section 4.C.2. is substituted, then the associated ΔH°_{298} values exhibit a dependence upon temperature, and it was therefore considered inappropriate to include the results of Matsushita and Goto in the following assessment.

It was concluded that the most accurate high temperature data for the free energy of formation of yellow lead oxide are obtained by combining the e.m.f. results of the present

investigation and those reported by Belford and Alcock, which are in excellent agreement (Table 4.E.1.), with the standard free energy values for the Ni-NiO system recommended in Section 4.C.2. The resulting ΔH^{o}_{298} value, -104,700 ± 300 cal. (see Fig. 4.E.2.), is thus considered more reliable than that favoured by Coughlin and Elliott and Gleiser (-104, 100 ± 600cal.), which is based upon extrapolated data of Spencer and Mote[141].

Finally it was considered desirable to also combine the free energy data of the present work, the corrected free energy values of Belford and Alcock, and the calorimetric data, by means of the sigma function (cf. Section 4.C.2.), and the following expression* was obtained,

$$\Delta G^{o}_{T} = -105.710 + 23.56T + 10.59T \log T - 6.22 \times 10^{-3} T^{2} - 0.20 \times 10^{5} T^{-1}$$

This cumbersome expression may be replaced by the following

---

* For the reaction, $2Pb(l) + O_2(g) \longrightarrow 2PbO(s)$
Kelley recommends the following expression for the specific heat data,

$\Delta Cp = -4.60 + 13.24 \times 10^{-3} T + 0.40 \times 10^{5} T^{-2}$ (± 0.2%)

three-term equation which gives identical ΔG°_{T} values at the three temperatures 600, 800 and 1000°K, i.e.

$$\Delta G^{\circ}_{T} = -109{,}600 - 12.87T \log T + 91.18T \quad (\pm 300 \text{ cal.}) \qquad [600\text{-}1100^{\circ}K]$$

for the reaction,

$$2Pb(l) + O_2(g) \longrightarrow 2PbO(\text{yellow, s}).$$

Data obtained from this recommended equation for the standard free energies of formation of yellow lead oxide are compared in Table 4.E.2. with the corresponding free energy values compiled by Coughlin and Elliott and Gleiser.

Table 4.E.2.

Oxygen chemical potentials for the equilibria

$$2Pb(l) + O_2(g) \rightleftharpoons 2PbO(\text{yellow, s})$$

Temperature	Experimental Data	Derived 3-term Expression	Elliott and Gleiser	Kubachewski and Evans
°K	± 290 cal	± 300 cal	±300 cal	± 3000 cal
600	-	-76,340	-76,300	-76,620
700	-71,400	-71,410	-71,500	-71,820
800	-66,580	-66,550	-66,700	-67,130
900	-61,790	-61,760	-62,000	-62,550
1000	-57,040	-57,030	-57,500	-58,000
1100	-52,300	-52,360	-52,900	-53,540

4.F. CONCLUSIONS

The preceeding analyses of the e.m.f. data for galvanic cells incorporating solid oxide electrolytes and electrodes possessing high oxygen chemical potentials, clearly establish the precision and accuracy of this technique over the relevant ranges of oxygen chemical potentials and temperatures.

In addition, there were no problems associated with electrode kinetics as all the cells were fully reversible and had a rapid voltage response to changes in temperature, features which greatly facilitated the acquisition of a large amount of useful data. Reproducibility of the cell voltages was approximately ± 1 mV which corresponds to an error of only ± 100 calories in the relevant oxygen chemical potential values. The principal uncertainties, in fact, are associated with the standard free energy values for the reference Fe-FeO electrode (± 250 cal.), and lack of precise information* about the magnitude of the electronic transference number. Available information only indicates that the MEAN electronic transference number of commercial zirconia-based electrolyte does not exceed 0.005 at high oxygen chemical potentials. It is probable that this quantity is smaller for single phase electrolytes

---

* The presence of a small electronic contribution to the total conductivity would cause an additional error in the thermochemical values recommended in the previous sections. For example, if a MEAN electronic transference number of 0.005 is assumed, then the error associated with the three-term equation (Eq. 4.C.3.) for the Ni-NiO equilibria is increased from ± 300 cal. to ± 330 cal.

(cf. Section 3.D.6.) prepared from very pure materials, and an accurate determination of the electronic transference number of such material, fabricated in the form of a closed end tube, would be most valuable, as a series of reference electrodes could then be calibrated directly against a pure oxygen electrode.

However, in spite of these minor problems, it is believed that the thermochemical data associated with this e.m.f. technique is, in general, more accurate than that obtained by comparable gas equilibration measurements*, provided certain precautions are observed.

It is desirable (see Section 4.D.1., for example) to provide separate electrode compartments to eliminate the possibility of chemical transport reactions via the gaseous

---

* Although this method produced excellent results for the Fe-FeO equilibria (Section 4.B.2.), similar data for the Ni-NiO system (Section 4.C.2.) were not so satisfactory. It is relevant to add that whereas the H_2O/H_2 and CO_2/CO ratios associated with the Fe-FeO equilibria are small (~ 1), the corresponding ratios for the Ni-NiO system are much larger (~ 100).

phase, and in addition to ensuring that reversible, stable, reproducible voltages are being recorded, the apparatus should also be periodically examined for the existence of sparious assymmetrical voltages. It is also essential that any further extension of this technique to higher temperatures (> 1100°C) should be accompanied by a careful evaluation of the electrolyte system employed.

If these procedures are followed then galvanic cells incorporating solid oxide electrolytes provide a simple reliable method for the rapid measurement of accurate high oxygen chemical potentials at elevated temperatures.

CHAPTER FIVE

OXYGEN CHEMICAL POTENTIALS IN THE NIOBIUM-OXYGEN SYSTEM

5.A. GENERAL

Oxygen dissolves interstially in the niobium metal lattice and the solubility limit increases from approximately 1 to 3 atomic per cent oxygen in the temperature range, 750-1100°C (Seybolt[142], Bryant[143], Gebhardt and Rothenbacher[144]). Under certain conditions, usually present during oxidation of the metal, it appears that niobium may dissolve more oxygen than that corresponding to the saturation value and many investigators[144, 145, 146] have claimed that various suboxides (e.g. Nb_4O, Nb_2O) can be precipitated from this supersaturated phase.

The principal oxide phases, however, in the niobium-oxygen system are NbO*, NbO_2**, Nb_2O_5***, and all these

---

* NbO possess a defective sodium chloride structure[147,148,149] and is often given the formula, $Nb_{0.75}O_{0.75}$ on account of the large numbers of atoms (one of each kind in four) missing from both the cation , and anion sublatuices.

** NbO_2 has a structure closely related to the rutile structure.

*** Nb_2O_5 exhibits polymorphism and several modifications have been reported. The high temperature modification has been indexed on the basis of a monoclinic unit cell (151,152).

oxides display some degree of non-stoichiometry. According to the X-ray data of Brauer[147], NbO and NbO_2 only exhibit small variations in composition (e.g. $NbO_{0.98-1.00}$), whereas a more extensive homogeneity range, $Nb_2O_{4.8}$ - $Nb_2O_{5.0}$ is proposed for Nb_2O_5, although two other intermediate compounds $Nb_{12}O_{29}$ and $Nb_{15}O_{37}$ have recently been reported[153, 154] in this region.

In the present investigation, oxygen chemical potentials have been measured for the equilibria, Nb-NbO, NbO-NbO_2, NbO_2-Nb_2O_5 and for five compositions within the non-stoichiometric region, $Nb_2O_{4.8}$ - $Nb_2O_{5.0}$. It was concluded from preliminary experiments on the cell,

Nb, NbO/electrolyte/Fe, FeO,

that the simple cell assembly and the zirconia-based electrolytes used by Kiukkola and Wagner[20] were inadequate for e.m.f. measurements at the very low oxygen chemical potentials associated with the Nb-NbO equilibria. These preliminary experiments and the redesigned assembly have been described earlier in Chapter Two, and discussion is confined in the present chapter to those results obtained

with the modified apparatus using thoria-based electrolytes.

5.B. Nb-NbO EQUILIBRIA

5.B.1. E.M.F. Measurements

In contrast to the e.m.f. measurements at high oxygen chemical potentials, considerable difficulties were encountered in obtaining reproducible data for cells incorporating the Nb-NbO electrode.

The initial series of experiments were conducted on the cell,

$$\text{Nb-NbO}/\text{electrolyte}/\text{Fe-FeO}$$

using either $ThO_2.YO_{1.5}$ (90.10 mole %), $ThO_2.YO_{1.5}$ (85.15 mole %) or $ThO_2.LaO_{1.5}$ (90.10 mole %) as the electrolyte material. These electrolytes were prepared by the standard procedure (Section 2.B.1.) in the form of dense translucent discs, approximately 10 mm. in diameter and 2 mm. thick. Advantage was taken of the provision in the modified apparatus for separate electrode compartments, and the cell

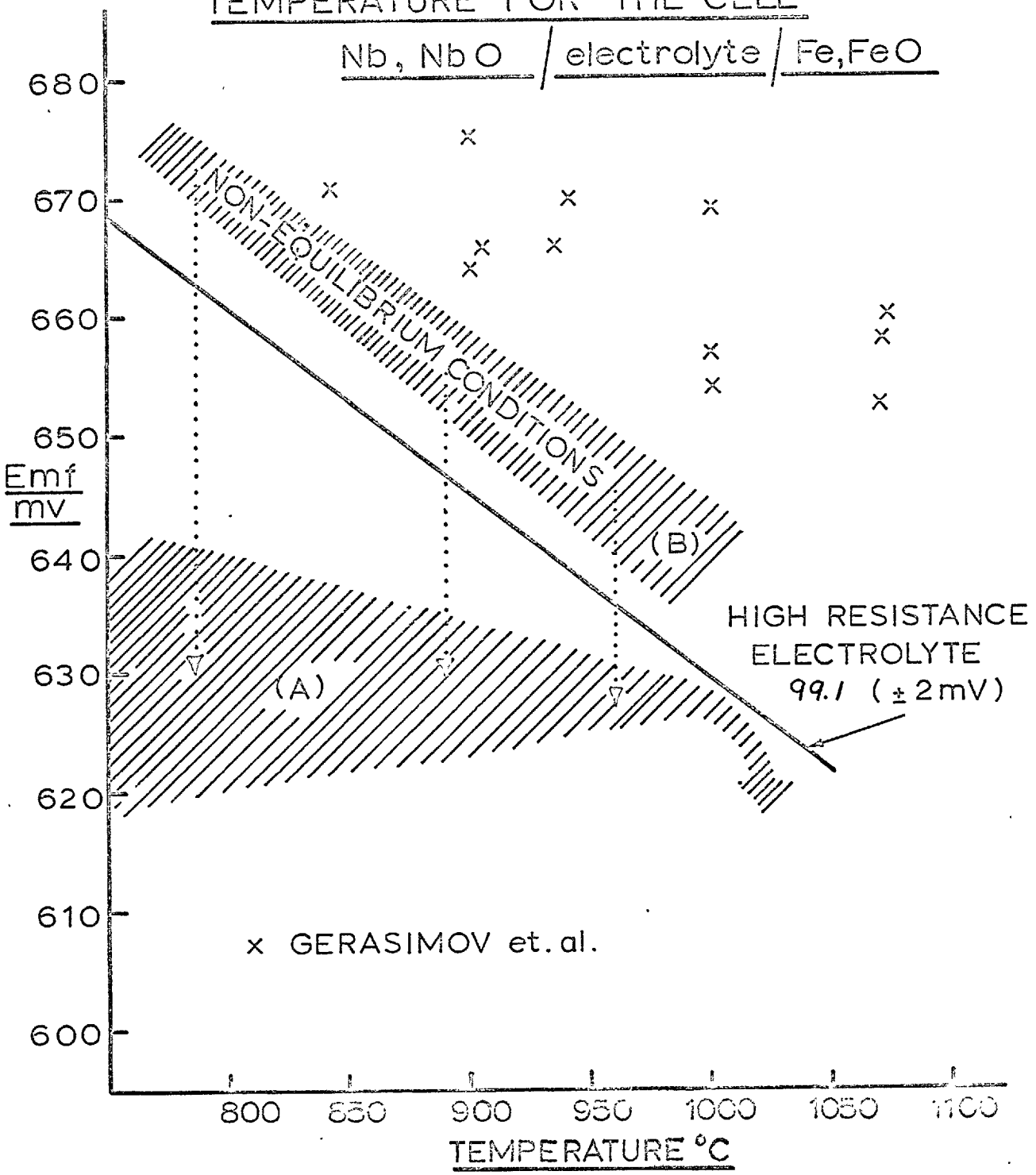
assembly illustrated in Fig. 2.E.3(d) was used, with two small (approx. 1 in. x 3 in.) strips of titanium or zirconium located above (~1 in.) and below (~2 ins.) the upper electrode (Nb-NbO). With this arrangement and using either purified argon or vacuum (1 x 10^{-5} torr.), voltages were recorded at approximately 50° intervals, in the temperature range 700-1000°C. The cell response to changes in temperature was rapid and steady voltages ($\pm$ 0.5 mV) were usually attained some 30-60 minutes after the cell had reached a selected temperature. For cell temperatures greater than 1000°C, however, the e.m.f. values slowly decreased with time (1-5 mV per hour), and it proved impossible to obtain constant voltage.

A cell was cycled throughout the temperature range at least twice and typical results are given in Appendix VI. For each experiment the reproducibility of the e.m.f. data was not very good (approximately $\pm$ 10 mV at 700°C and $\pm$ 5 mV at 1000°C), and in this respect there was no marked difference in the performance of the three electrolytes tested. Changing the cell atmosphere from vacuum to purified argon also had little effect upon the reproducibility

of the results, and all the data for this initial series of twelve experiments can be included within the area labelled (A) in Fig. 5.B.1.

The e.m.f. values for a similar cell reported by Gerasimov et al.[155] are also reproduced in Fig. 5.B.1. and can be seen to be about 30 mV higher than the initial results obtained in the present investigation. The silica apparatus used by these Russian workers was designed for vacuum operation, but contained no provision for separate electrode compartments and their cell assembly simply consisted of the three pellets, Nb-NbO electrode, $ThO_2.LaO_{1.5}$ (90.10 mole %) electrolyte, and Fe-FeO electrode, pressed together between spring loaded platinum or nickel contacts. A similar arrangement was tried in the present investigation with varying results. Only two of the seven experiments performed gave results comparable to those obtained in the initial series of experiments (i.e. e.m.f. values in the area labelled (A): Fig. 5.B.1.), and even though these values appeared reasonably steady over a period of 1-2 hours, maintaining the cell temperature constant for longer periods invariably produced a gradual decrease

FIG. 5.B.1 Emf DEPENDANCE UPON TEMPERATURE FOR THE CELL



in the cell voltage (1-5 mV per hour). The proportion of metal in the Nb-NbO electrode was also increased to 75 mole %, but this change was not attended by any significant improvement in the behaviour of the cell.

It was observed during these experiments that if the cell was rapidly cycled (100-150° per hour) through the temperature range, then the voltages recorded under these dynamic conditions (Area (B) in Fig. 5.B.1.) were only slightly lower than those reported by Gerasimov et al.[155]. However, as soon as the cell temperature was maintained at a constant value then the voltage steadily decreased. This procedure was repeated using the separate electrode compartment arrangement, and again under dynamic conditions higher voltages were obtained which steadily decreased to lower values (Area (A) in Fig. 5.B.1.) when the cell was maintained at a constant temperature. Unfortunately Gerasimov and his associates do not comment upon the stability of their e.m.f. values, and although the reproducibility of their results is reported as ± 8 mV it is not evident from their published data that the voltages recorded by these workers were either stable or reversible. It certainly appeared from the relevant experiments in the

present investigation that the higher values obtained by Gerasimov et al. were measured under some non-equilibrium conditions*, and should not, therefore, be included in an evaluation of the associated thermochemical data.

In a further series of experiments, electrolytes of the following composition, ThO_2.CaO (90.10 mole %), $ThO_2.YO_{1.5}$ (96.4 mole %) and $ThO_2.YO_{1.5}$ (99.1 mole %) were each incorporated into a cell which was assembled with separate electrode compartments. Operating the apparatus in vacuum it was observed that although the cells containing the electrolytes ThO_2.CaO (90.10 mole %) and $ThO_2.YO_{1.5}$ (96.4 mole %) again gave results within the area labelled (A) (Fig. 5.B.1.), higher voltages were recorded for cells incorporating the elctrolyte $ThO_2.YO_{1.5}$ (99.1). These higher voltages are represented by the line marked "99.1" in Figure 5.B.1. and the results of a typical experiment are detailed in Appendix VI. An outstanding

---

* It may also be significant that Gerasimov and his associates annealed their Nb-NbO electrodes at 1700°C. In the present investigation the electrodes were prepared at 1400°C (Section 21B.2.), and then annealed for at least 48 hours at 1000°C.

feature of these voltages was their reproducibility ($\pm$ 1.5 mV over the whole temperature range). Moreover, the response of this cell to changes in temperature was such that these reproducible e.m.f. values were usually attained after about one hour except at the lower temperatures (700-800°C), when the associated voltage changes were somewhat sluggish and equilibrium voltages were only recorded after 2-3 hours. Thereafter the voltages remained steady for at least 24 hours.

To investigate if the relatively high resistance possessed by the 99.1 $ThO_2.YO_{1.5}$ electrolyte (Section 3.B.3.) was responsible for these higher reproducible voltages, a specially designed high resistance electrolyte was fabricated of similar composition to one of the electrolytes, $ThO_2.YO_{1.5}$ (90.10 mole %), used in the first series of experiments. A thin walled crucible was first prepared, and the sides of this crucible were then almost completely cut away with a diamond saw until only two thin 'legs' remained. This special electrolyte shape was then incorporated into a cell as illustrated in Fig. 5.B.2.

The e.m.f. values obtained with this cell arrangement

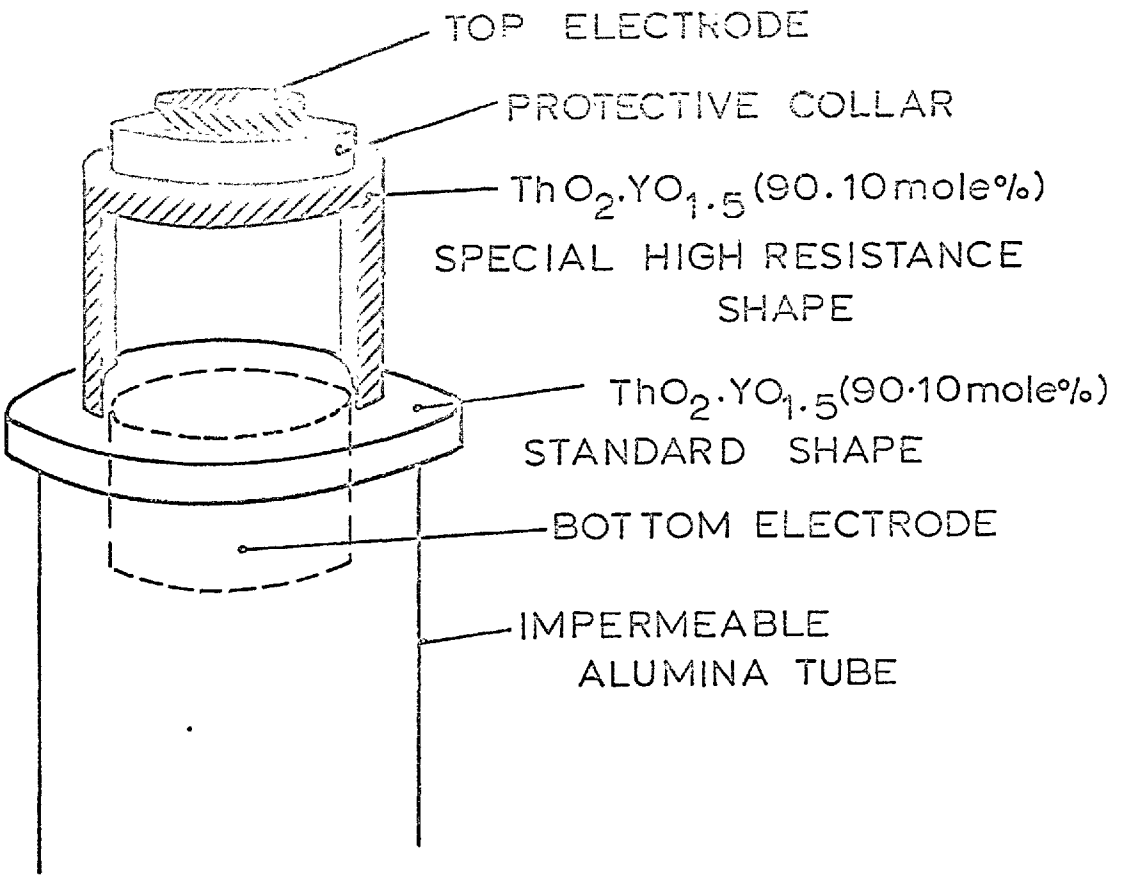


FIG.5.B.2 CELL ARRANGEMENT INCORPORATING HIGH RESISTANCE ELECTROLYTE

were in excellent agreement ($\pm$ 2 mV) with those reported for the 99.1 $ThO_2.YO_{1.5}$ electrolyte.

Six experiments were performed with high resistance electrolytes and the associated cell voltages are best expressed by the linear equation,

$$E = 827.4 - 0.1555T \quad (\pm 2.5 \text{ mV})^* \quad \ldots\ldots\ldots \text{Eq. 5.B.1.}$$

$$\left[1023 - 1323^\circ K\right]$$

from which the following e.m.f. values may be calculated.

Table 5.B.1.

Electromotive force of the cell, Nb, NbO/electrolyte/Fe, FeO		
Temperature		E.M.F.
$^\circ K$	$^\circ C$	mV
1023	750	668.3
1073	800	660.6
1173	900	645.0
1273	1000	629.5
1323	1050	621.7

* The precision of the e.m.f. temperature measurements was $\pm$ 0.2 mV and $\pm$ 1°, respectively.

Additional confirmation of the above results was provided by combining e.m.f. measurements on the cells,

$$Nb\text{-}NbO/ThO_2.YO_{1.5}(99.1 \text{ mole } \%)/Ni\text{-}NiO \text{ (two experiments)},$$

$$Nb\text{-}NbO/ThO_2.YO_{1.5}(90.10 \text{ mole } \%)/Ni\text{-}NiO \text{ (one experiment)},$$
(High resistance shape)

with the relevant e.m.f. data already reported (Section 4.C.1.) for the cell reaction,

$$NiO + 0.95Fe \longrightarrow Fe_{0.95}O + Ni$$

The voltages derived in this way were in good agreement ($\pm$ 3 mV) with the values listed in Table 5.B.1.

5.B.2. Discussion of e.m.f. data

The e.m.f. of a truly reversible galvanic cell should not be affected by changes in the resistance of the electrolyte. It follows, therefore, from the observations reported in the previous section that one or both the electrodes in the cell,

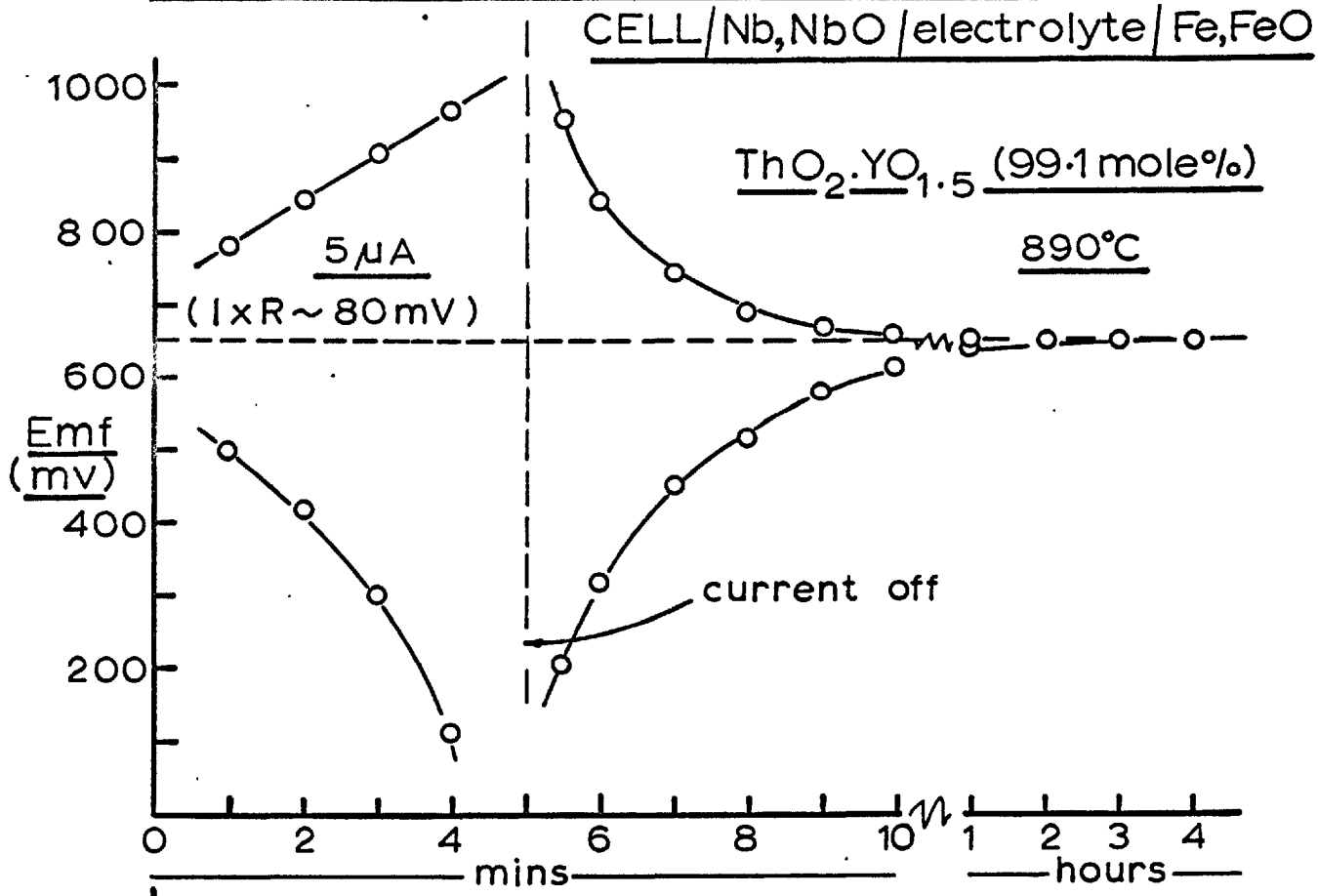
$$Nb\text{-}NbO/electrolyte/Fe\text{-}FeO,$$

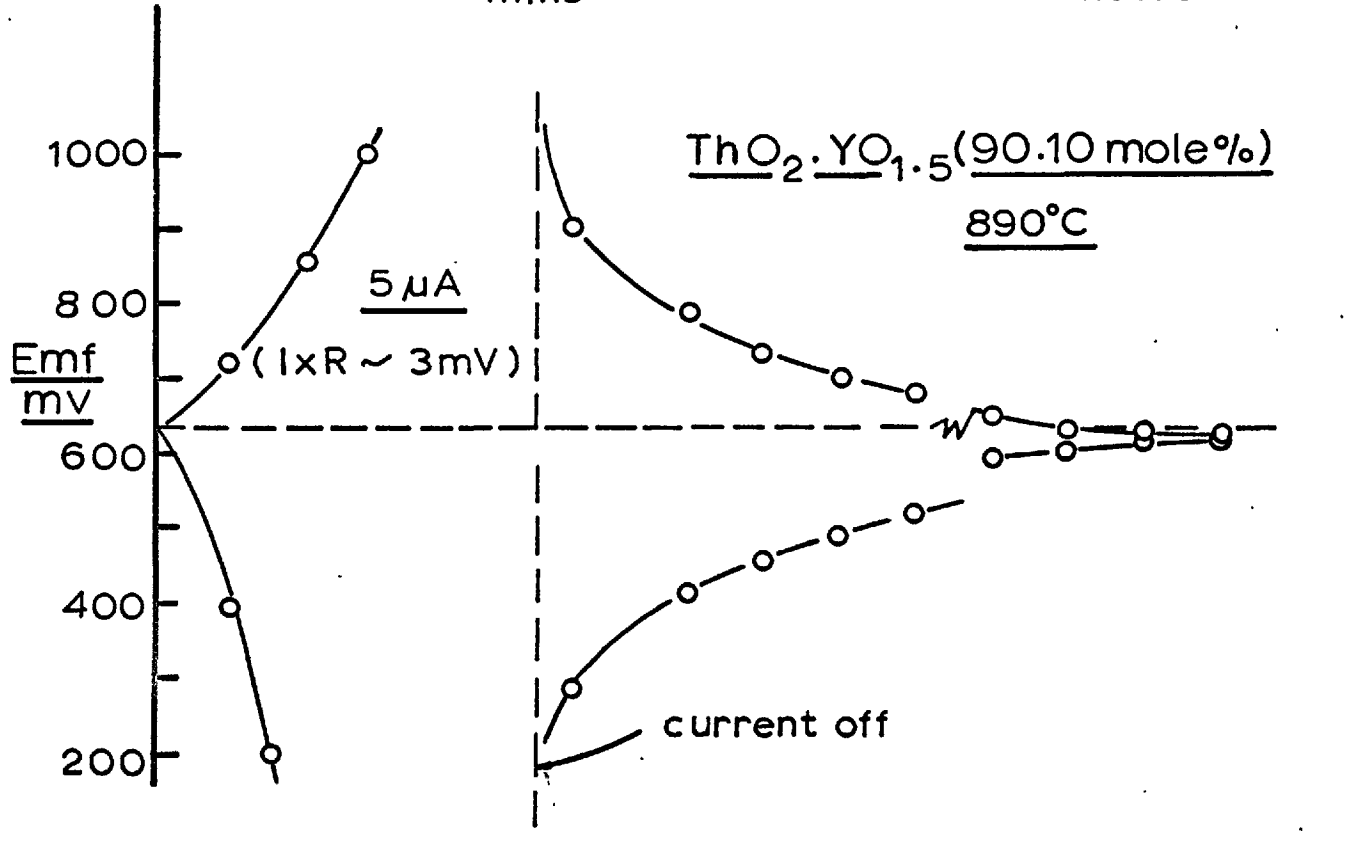
can become polarised under the relevant experimental

conditions. This conclusion was supported by the results of the routine reversibility tests which required the e.m.f. to be unaffected by the passage of a small current (1μA) in either direction. The divergence from reversible behaviour is illustrated in Fig. 5.B.3. for cells incorporating low and high resistance electrolytes. Although both cells became polarised during the passage of the current, the polarisation was less marked in the case of the cell containing the high resistance electrolyte. Moreover the final voltage eventually obtained for this type of cell was always identical ($\pm$ 1 mV) to the initial e.m.f., whereas cells containing low resistance electrolytes never attained the voltage originally recorded prior to the polarisation experiment, even after several hours had elapsed. The behaviour of the Fe-FeO electrode was considered earlier (Section 4.B.1.), and it was concluded that this electrode was fully reversible, at least up to currents of 10μA at 890°C. It would appear, therefore, the Nb-NbO electrode is probably responsible for the lack of reversibility exhibited by certain of these cells.

The importance of the electrolyte resistance is immediately apparent if it is assumed that the thoria-based

FIG.2.B.3 POLARISATION EXPERIMENTS ON CELL/Nb,NbO/electrolyte/Fe,FeO





electrolytes possess a small but finite electronic conductivity, equal, for example, to 0.5% of the total ionic conductivity. This level of electronic conductivity would certainly be undetected by any of the methods currently available for measuring electronic transference numbers, and Table 5.B.2. indicates the magnitude of the resultant internal 'short-circuiting' current for cells containing low and high resistance electrolytes.

Table 5.B.2.

Comparison of hypothetical electronic currents.

Electrolyte Composition Mole %	Resistance OHMS		Electronic Current* Micro-amps	
	800°C	1000°C	800°C	1000°C
$ThO_2.YO_{1.5}$(90.10)	1540	245	2	13
$ThO_2.YO_{1.5}$(99.1)	159,600	12,640	0.02	0.3

* Calculated for a cell voltage of 650 mV and an electronic transference number of 0.005.

The Nb-NbO electrode is obviously more able to cope with the smaller internal currents associated with the higher

resistance electrolytes, and it follows that the correct equilibrium potential is more likely to be maintained under these conditions.

Many reasons can be advanced for the relatively poor performance of the Nb-NbO electrode. It is possible, for example, that the magnitude of the internal 'short-circuiting' currents envisaged in Table 5.B.2. should be increased. This would certainly be the case if the thoria-based electrolytes were becoming slightly reduced at the low oxygen chemical potentials associated with the Nb-NbO equilibria, and in the absence of any reliable data to the contrary, this possibility must certainly be considered.

Oxygen from the surrounding atmosphere can also interfere with the Nb-NbO equilibria as was very evident in the preliminary experiments (Section 2.E.2.). All these later experiments, however, were conducted with zirconium or titanium metal 'getters' present, and in addition, the Nb-NbO electrodes were always surrounded by protective collars of the same composition. Under these conditions, therefore, it appears that interaction between the Nb-NbO pellet and its gaseous environment would have little effect

upon the equilibria at the electrode-electrolyte interface.

At present it is only possible to speculate about the process which determines whether the Nb-NbO electrode is reversible or not. It is not known whether this process is diffusion controlled or associated with a specific chemical reaction, and it is considered inappropriate, therefore, to include any further comments about the behaviour of this particular electrode in the absence of any information about the relevant electrode kinetics.

Low oxygen chemical potentials have also recently been measured by Markin et al. in the systems UO_{2+x}[77] and PuO_{2-x}[78] using solid oxide electrolyte galvanic cells. These workers employed Ni-NiO or Fe-FeO reference electrodes with $ThO_2.YO_{1.5}$ (85.15 mole %) electrolytes in conjunction with an impermeable stabilized zirconia tube as devised in the present investigation (Section 2.E.2.). Reproducible voltages ($\pm$ 2 mV) were claimed for values of μO_2 (1000°C) as low as -105 Kcals. in the UO_{2+x} system and -155 Kcals. in

the PuO_{2-x} system (cf. Nb-NbO equilibria $\Delta\mu O_2$ (1000°C) = -145 Kcal.). The solid state coulometric titrations performed with cells incorporating the UO_{2+x} electrodes suggests that these cells were reversible. It is not stated, however, whether cells incorporating the PuO_{2-x} electrode also behave reversibly, although concordant emf values ($\pm$ 2 mV) were obtained for both the reference electrodes, Ni-NiO, Fe-FeO, provided the oxygen chemical potentials ($\Delta\mu O_2$ (1000°C)) were higher than -143 Kcal. Below this value the two sets of data were not in agreement and it is possible that the electrodes became progressively more polarised as the oxygen chemical potential was lowered. It is tempting to suggest that these observations, and the results obtained in the present investigation for the Nb-NbO equilibria, indicate a lower limit for accurate oxygen chemical potential measurements, using galvanic cells with thoria-based solid electrolytes, of approximately -145 Kcal. at 1000°C. Whether this apparent lower limit is determined by reduction of the thoria-based electrolytes or some special feature of the electrode processes is even more a matter for speculation.

Whatever interpretation is placed upon the results of

Markin and his associates, their experiments illustrate once again the importance of clearly establishing that reversible e.m.f.'s are being measured. The present investigation also demonstrates the value of measuring cell voltages as a function of electrolyte resistance particularly under conditions (e.g. very low oxygen chemical potentials) where the transport properties of the oxide electrolyte material are not well defined.

5.B.3. Assessment of thermochemical data

The experiments of Gerasimov et al.[155] are the only other attempt, so far reported, to measure oxygen chemical potentials in equilibrium with the Nb-NbO system. It was suggested earlier (Section 5.B.1.) that these e.m.f. measurements are probably in error and do not represent steady reversible voltages. The results of the present investigation obtained with the high resistance electrolytes are therefore preferred and the principal uncertainty with these e.m.f. data is associated with the lack of information about the transport properties of the thoria-based electrolytes at very low oxygen chemical potentials. Fortunately oxygen chemical potentials for the Mn-MnO equilibria

($\Delta\mu O_{2(1000^{\circ}C)}$ = -139,500 Kcal.) have recently been determined by Zador[156] using the same apparatus employed in the present investigation. The data were obtained by e.m.f. measurements on the cell,

$$Mn\text{-}MnO/electrolyte/Fe\text{-}FeO,$$

for a variety of electrolyte compositions including $ThO_2.YO_{1.5}$ (90.10 mole %) and $ThO_2.YO_{1.5}$ (99.1 mole %). It was concluded from the excellent agreement* found between the experimental values of oxygen chemical potentials and those calculated from the latest calorimetric data[117, 118], that the electronic component of the total conductivity was less than 1% for the thoria-based electrolytes over the relevant range of oxygen chemical potentials. Even if the electrolytes were becoming slightly non-stoichiometric in contact with the Nb-NbO electrode ($\Delta\mu O_{2\ (1000^{\circ}C)}$ = -145,000 Kcal.), a significant increase in the electronic conductivity

---

* A significant electronic conductivity would tend to make the experimental Mn-MnO oxygen chemical potentials more POSITIVE than those calculated from the calorimetric data. The experimental e.m.f. values, however, were consistently more NEGATIVE (~200 cal.).

is very improbable for a change of only 5 Kcals. and a MEAN electronic transference number of 0.01 was therefore assumed for the present investigation. It follows that the oxygen chemical potentials associated with the Nb-NbO equilibria are given by the expression*,

$$\Delta\mu_{O_2} = -202{,}810 + 45.60T \ (\pm\ 700 \text{ cal.}) \quad \ldots\ldots\ldots \text{Eq. 5.B.3.}$$

$$[1023 - 1323^{\circ}K]$$

Provided the errors** introduced by equating the activities of Nb and NbO to unity can be neglected, then the above equation also represents the standard free

---

* $Nb + Fe_{0.95}O \longrightarrow Nb + 0.95Fe$: $\Delta G^{\circ} = -38{,}170 + 7.17T$ (Eq. 5.B.1.)

$0.95Fe + \frac{1}{2}O_2 \longrightarrow Fe_{0.95}O$: $\Delta G^{\circ} = -63.235 + 15.63T$ (Eq. 4.B.)

$Nb + \frac{1}{2}O_2 \longrightarrow NbO$: $\Delta G^{\circ} = -101{,}405 + 22.80T$ (Eq. 5.B.2.)

** For example, if the activity of Nb equals 0.95 at $1000^{\circ}C$ then the corresponding error would only be 260 cal.

energy change for the reaction,

$$2Nb + O_2 \longrightarrow 2NbO$$

Although Gerasimov[155] et al. refer to specific heat values for NbO and NbO_2 it was impossible to obtain these data, and in the absence of any other reliable specific heat measurements for these oxides no attempt was made to calculate the associated ΔH°_{298} values.

5.C. NbO-NbO_2 EQUILIBRIA

5.C.1. E.M.F. Measurements

The following cells were used to obtain data on the NbO-NbO_2 equilibria:

$NbO, NbO_2 / ThO_2.YO_{1.5}(90.10) / Fe, FeO$ (two expts.), I

$NbO, NbO_2 / ThO_2.YO_{1.5}(99.1) / Fe, FeO$ (one expt.), II

$NbO, NbO_2 / ThO_2.YO_{1.5}(99.1) / Ni, NiO$ (one expt.), III

$NbO, NbO_2 / ThO_2.YO_{1.5}(90.10) / Ni, NiO$ (one expt.), IV

$NbO, NbO_2 / ThO_2.YO_{1.5}(90.10) / NbO_2, Nb_2O_{5-x}$ (two expts.), V

$Nb, NbO / ThO_2.YO_{1.5}(99.1) / NbO, NbO_2$ (three expts.), VI

To provide a basis for comparing the data, the recorded voltages were adjusted*, where appropriate, so that all the e.m.f. values eventually referred to the standard Fe-FeO electrode. These e.m.f. values are incorporated in Fig. 5.C.1., and it is evident that the data obtained from all the cells are self consistent ($\pm$ 3 mV) in the temperature range 900-1100°C. Below 900°C, however, the results show a considerable scatter.

---

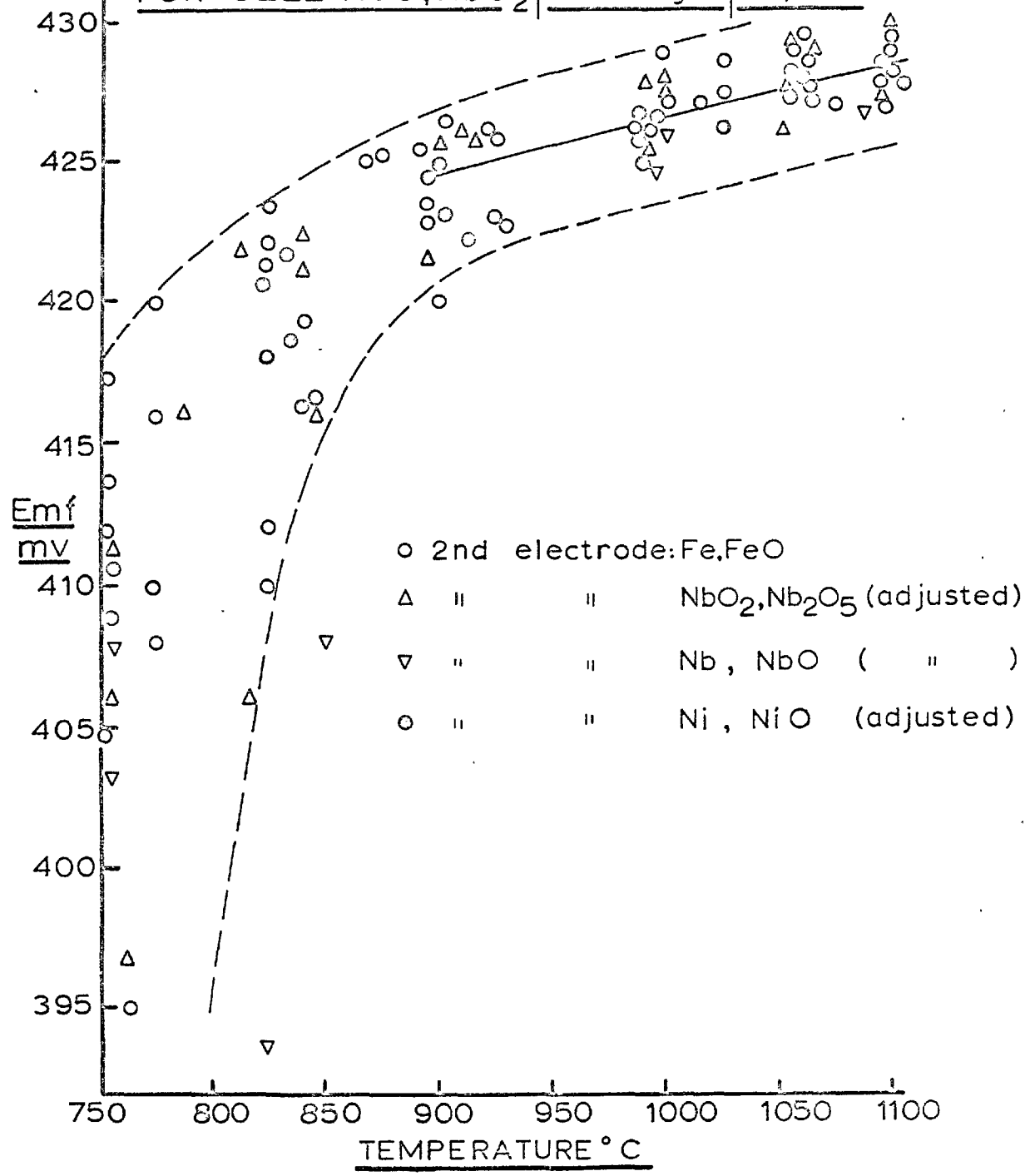
* i.e. by using the available e.m.f. data for the reactions,

$NiO + 0.95Fe \longrightarrow Fe_{0.95}O + Ni$ (Eq. 4.C.)

$Fe_{0.95}O + 2NbO_2 \longrightarrow 0.95Fe + Nb_2O_5$ (Eq. 5.D.1.)

$Fe_{0.95}O + Nb \longrightarrow 0.95Fe + NbO$ (Eq. 5.B.1.)

FIG.5.C1 Emf DEPENDANCE UPON TEMPERATURE FOR CELL NbO, NbO_2 | electrolyte | Fe, FeO.



The response of all the cells examined to changes in temperature was very sluggish*, and it was considered necessary to maintain the cells at the various selected temperatures for at least 3-5 hours to ensure that steady voltages were being recorded. The behaviour of the cells during the reversibility tests also reflected the slow electrode kinetics. Large overvoltages (~1 volt) were observed during the passage of the current (1μA), and the cells only regained their original voltage after 6-24 hours at the higher temperatures (> 900°C). At lower temperatures the cells behaved irreversibly, and data below 900°C were disregarded.

It is not known whether the poor performance of cells incorporating the $NbO-NbO_2$ electrode is a characteristic property of the relevant electrode processes, or can be

---

* It was extremely difficult to obtain reproducible data for cell VI, $Nb,NbO/ThO_2.YO_{1.5}(99.1)/NbO,NbO_2$, Reversible voltages could only be recorded after the cell had been maintained initially at 1000°C for approximately two days, and even then it was only possible to obtain meaningful data in the temperature range 950-1050°C.

attributed to the actual physical structure of the NbO-NbO_2 pellets. Although the standard procedure (Section 2.B.2.) for preparing the electrodes was varied (higher sintering temperatures, longer annealing times, changes in the NbO: NbO_2 ratio), the pellets always appeared poorly sintered, and it was possible to remove particles of the constituent oxides by rubbing a finger across the surface of the pellet.

Hoch[157] and his associates have carried out experiments with the cell,

$$Nb,NbO/ZrO_2.CaO\ (80.20\ mole\ \%)/NbO,NbO_2,$$

The values reported by these workers are very different from data obtained in the present investigation on cell VI. This lack of agreement, however, is not surprising as the zirconia-based electrolyte used by Hoch et al. must have possessed considerable electronic conductivity in contact with the Nb-NbO and NbO-NbO_2 electrodes (see Section 5.D.5.), and it suggested that spurious voltages from the R.F.

induction coil used to heat their cell assembly probably contributed to the erroneous e.m.f. values recorded by these investigators.

The absence of any marked dependence of the emf values reproduced in Fig. 5.C.1. upon temperature, and the limited temperature range (900-1100°C) over which the data was considered to be accurate, made it difficult to select an equation which best represented the emf values. As the cell which actually incorporated the Fe-FeO reference electrode was judged to give the best performance in terms of voltage response to changes in temperature and reversibility experiments, more weight was given to the results associated with this cell, and the following linear equation,

$$E = 401.0 + 0.02\ T\ (\pm\ 3\ mV) \qquad \text{..... Eq. 5.C.1.}$$

$$\left[1173\text{-}1373^{\circ}K\right]$$

was considered to be the most appropriate to express the emf data for the cell reaction,

$$NbO + Fe_{0.95}O \longrightarrow 0.95Fe + NbO_2.$$

5.C.2. Thermochemical data

According to the present investigation the oxygen chemical potentials associated with the $NbO-NbO_2$ equilibria are given by the expression,

$$\Delta\mu_{O_2} = -163{,}470 + 29.42\ T\ (\pm\ 370\ \text{cal.}) \qquad \ldots\ldots\ \text{Eq. 5.C.2.}$$

$$[1173\text{-}1373^{\circ}K]$$

which was obtained by combining the data from Eq. 5.C.1. with the equation (Eq. 4.B.1.) derived for the Fe-FeO equilibria.

The only other relevant high temperature equilibria measurements have been made by Gerasimov et al.[155] who studied the reaction,

$$NbO_2 + H_2 \longrightarrow NbO + H_2O,$$

over the temperature range 1400-1550°C. The relevant oxygen chemical potentials were calculated by combining the free energy equation reported by these workers,

$$\Delta G = 29{,}490 - 6.10\ T,$$

with the appropriate data for the standard free energy of formation of water vapour, and the values so derived are plotted in Fig. 5.C.2., together with the data obtained in the present investigation. Although both sets of data were acquired over very different ranges of temperature, it does appear that the oxygen chemical potentials associated with the results of Gerasimov and his associates are much higher, and the entropy term much larger, than would be expected by extrapolation of the results of the present work. This discrepancy could be due to uncertainties associated with the measurement of large ($\sim$200) H_2/H_2O gas ratios at very high temperatures, such as thermal diffusion, and porosity of the refractory tubes. These experimental difficulties could produce erroneous data in that oxygen chemical potentials, higher than the true equilibrium values, would be recorded.

Finally, if the equation (Eq. 5.C.2.) for the reaction,

$$2NbO + O_2 \longrightarrow 2NbO_2$$

is combined with the expression (Eq. 5.B.3.) for the standard free energy of formation of NbO obtained in the present

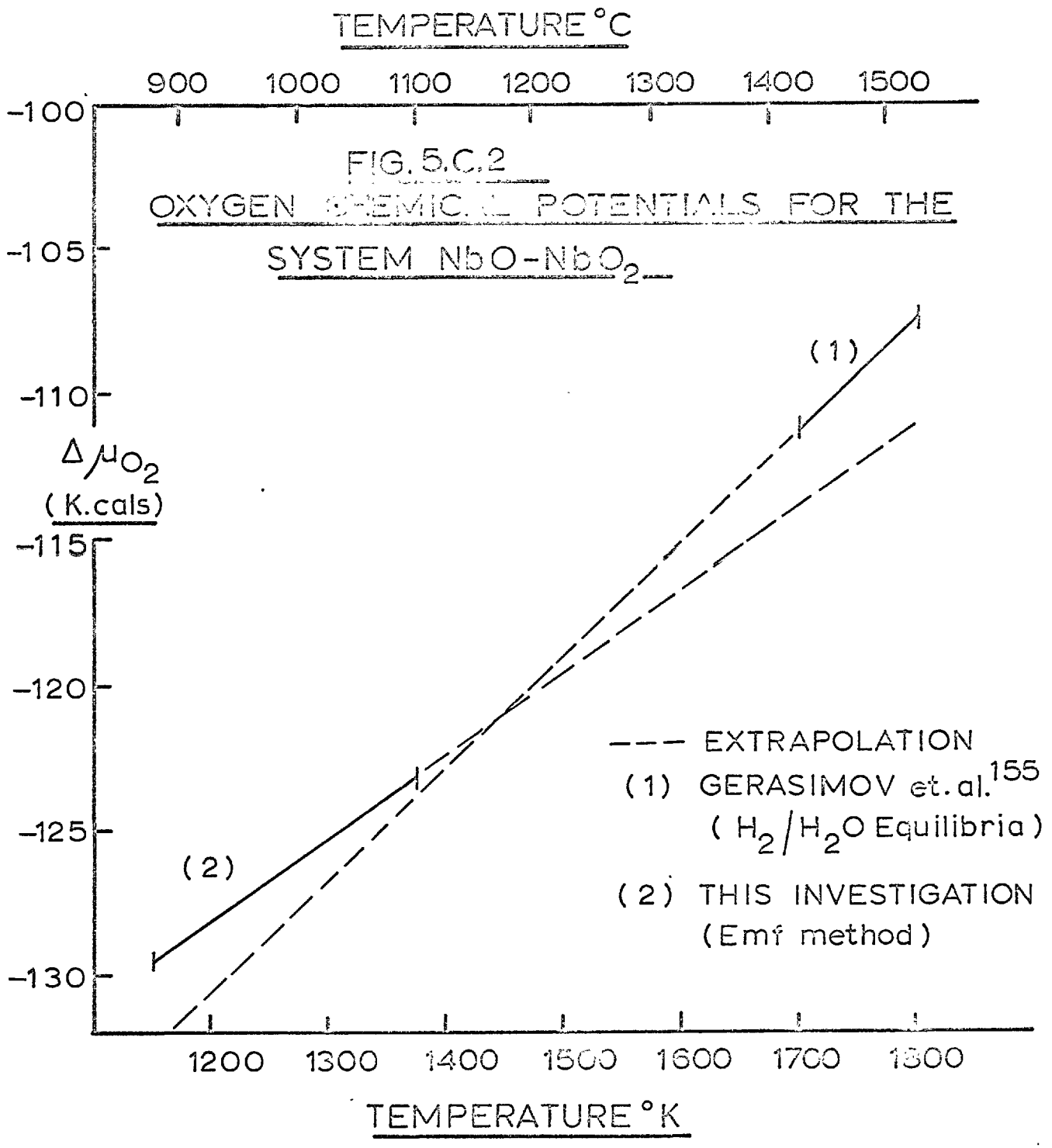


FIG. 5.C.2

OXYGEN CHEMICAL POTENTIALS FOR THE SYSTEM $NbO-NbO_2$

investigation, then the standard free energy changes associated with the reaction,

$$Nb + O_2 \longrightarrow NbO_2$$

are given by:

$$\Delta G^{\circ}_T = -181,140 + 37.51\ T\ (\pm\ 400\ cal.) \quad \ldots\ldots \quad Eq.5.C.3.$$

$$\left[1173\text{-}1373^{\circ}K\right]$$

assuming, of course, that the activities of NbO and NbO_2 can be equated to unity in equation 5.C.2.

5.D. NbO_2-Nb_2O_{5-x} EQUILIBRIA

5.D.1. EMF Measurements

No problems were encountered with the cell,

$$NbO_2, Nb_2O_{5-x} / \text{electrolyte} / Fe, FeO,$$

which gave steady, reversible, reproducible ($\pm$ 1 mV) voltages over the temperature range 700-1100°C. The cell response to changes in temperature was rapid, and the results obtained

from three experiments with the above cell were confirmed by additional experiments in which the Fe-FeO reference electrode was replaced by Ni-NiO (two experiments) and $NbO-NbO_2$ (two experiments*). The electrolytes** incorporated in the cells were either $ThO_2.YO_{1.5}$ (99.1 mole %) or $ThO_2.YO_{1.5}$ (90.10 mole %) and identical voltages ($\pm$ 1 mV) were recorded for both electrolyte compositions.

The data obtained in this series of seven experiments were plotted on a large-scale graph by referring all the emf values to a standard Fe-FeO reference electrode, and the equation of the best straight line drawn through the points is given by,

$$\Delta E = 281.8 - 0.1067\ T\ (\pm\ 1.2\ mV) \quad \ldots\ldots\ldots \quad Eq.\ 5.D.11$$

$$\left[973\text{-}1373^{\circ}K\right]$$

---

* Only emf measurements above 900°C were considered for this cell.

** The results obtained with similar cells incorporating zirconia-based electrolytes have already been discussed (Section 3.D.5.), and presented as evidence for the occurence of electronic conductivity in these electrolytes.

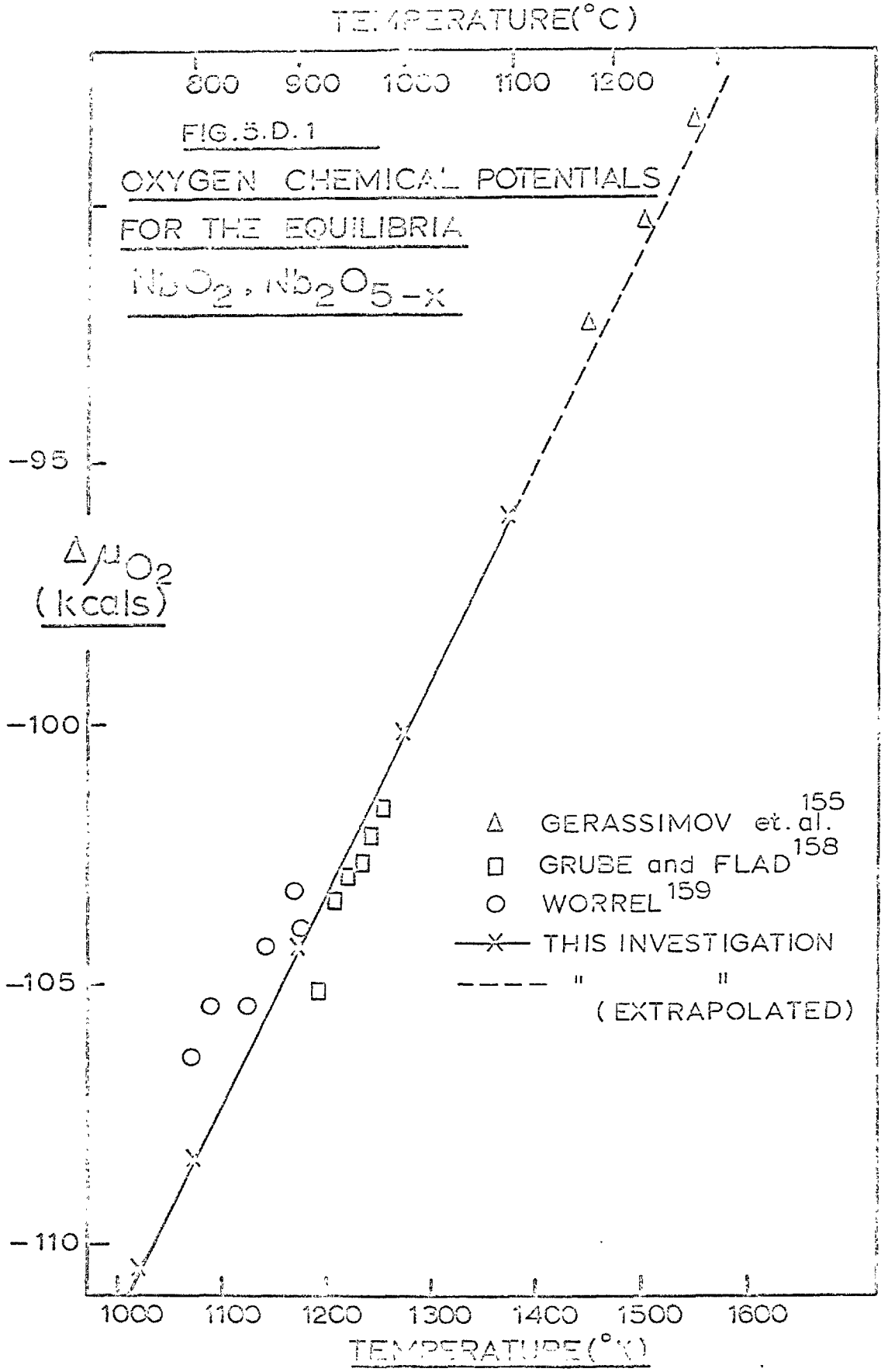
5.D.2. Comparison of thermochemical data

The partial molar free energies of oxygen, derived from the emf results of the present investigation, for the NbO_2-Nb_2O_{5-x} system can be expressed by the following equation,

$$\Delta\bar{G}_{O_2} = -152{,}470 + 41.10\ T\ (\pm\ 290\ \text{cal.}) \quad \ldots\ldots\ldots \text{Eq. 5.D.2.}$$

$$\left[973\text{-}1373^{\circ}K\right]$$

The straight line represented by this equation is shown in the adjoining Fig. 5.D.1., together with data reported by Gerasimov et al.[155] (H_2O/H_2 equilibria), Grube and Flad[158] (H_2/H_2O equilibria), and Worrel[159] (C/CO equilibria) for the same system. The line derived from the emf results of the present investigation is in good agreement ($\sim$500 cal.) with the values recorded by Grube and Flad in the temperature range 925-975°C, and the extrapolated line is also consistent ($\sim$500 cal.) with the data of Gerasimov et al. obtained at higher temperatures (1175-1375°C). It is proposed, therefore, that equation 5.D.2. need not be modified as it represents the most accurate data available over a wide range of temperatures (700-1100°C)


TEMPERATURE(°C)
800
900
1000
1100
1200
FIG.5.D.1
OXYGEN CHEMICAL POTENTIALS
FOR THE EQUILIBRIA
NbO_2, Nb_2O_{5-x}
−95
$\Delta\mu_{O_2}$
(kcals)
−100
−105
−110
GERASSIMOV et. al. 155
GRUBE and FLAD 158
WORREL 159
THIS INVESTIGATION
" "
(EXTRAPOLATED)
1000
1100
1200
1300
1400
1500
1600
TEMPERATURE(°K)

Further discussion of the NbO_2-Nb_2O_{5-x} system is postponed until the composition of Nb_2O_{5-x} in equilibrium with NbO_2 has been considered in the following sections.

5.E. NON-STOICHIOMETRIC Nb_2O_{5-x}

5.E.1. EMF Measurements

Electrodes were prepared from the five compositions listed in the following Table 5.E.1.

Table 5.E.1.

Electrode Compositions

	Nb_2O_{5-x}	x	Nb_2O_5	NbO_2
			Mole %	
a	$Nb_2O_{4.823}$	0.177	70	30
b	$Nb_2O_{4.857}$	0.143	75	25
c	$Nb_2O_{4.889}$	0.111	80	20
d	$Nb_2O_{4.918}$	0.082	85	15
e	$Nb_2O_{4.946}$	0.054	90	10

The standard procedure, summarised in Section 2.B.2., was followed for the preparation of the electrodes in that compacts of the appropriate quantities of Spec-pure niobium and niobium pentoxide powder were placed in thoria crucibles and heated in vacuum for 24 hours at 1200°C, and then annealed for a 48 hour period at 1000°C. The pellets were subsequently ground, re-pressed, and then annealed for a further 24 hours at 1000°C. At the completion of this treatment the electric power to the vacuum furnace was switched off which ensured that the pellets were rapidly cooled, at least to approximately 300°C.

X-ray diffraction photographs indicated that four (b, c, d, e) of the electrode compositions consisted of only one phase with a structure similar to that of stoichiometric αNb_2O_5. The X-ray photographs of the fifth composition ($Nb_2O_{4.823}$) contained additional lines which did not, however, correspond to the diffraction pattern for the lower oxide NbO_2.

Three separate batches of each composition were prepared and one electrode from each batch was incorporated into the cell,

$$Nb_2O_{5-x}/ThO_2.YO_{1.5}\ (90.10\ \text{mole}\ \%)/Fe,FeO$$

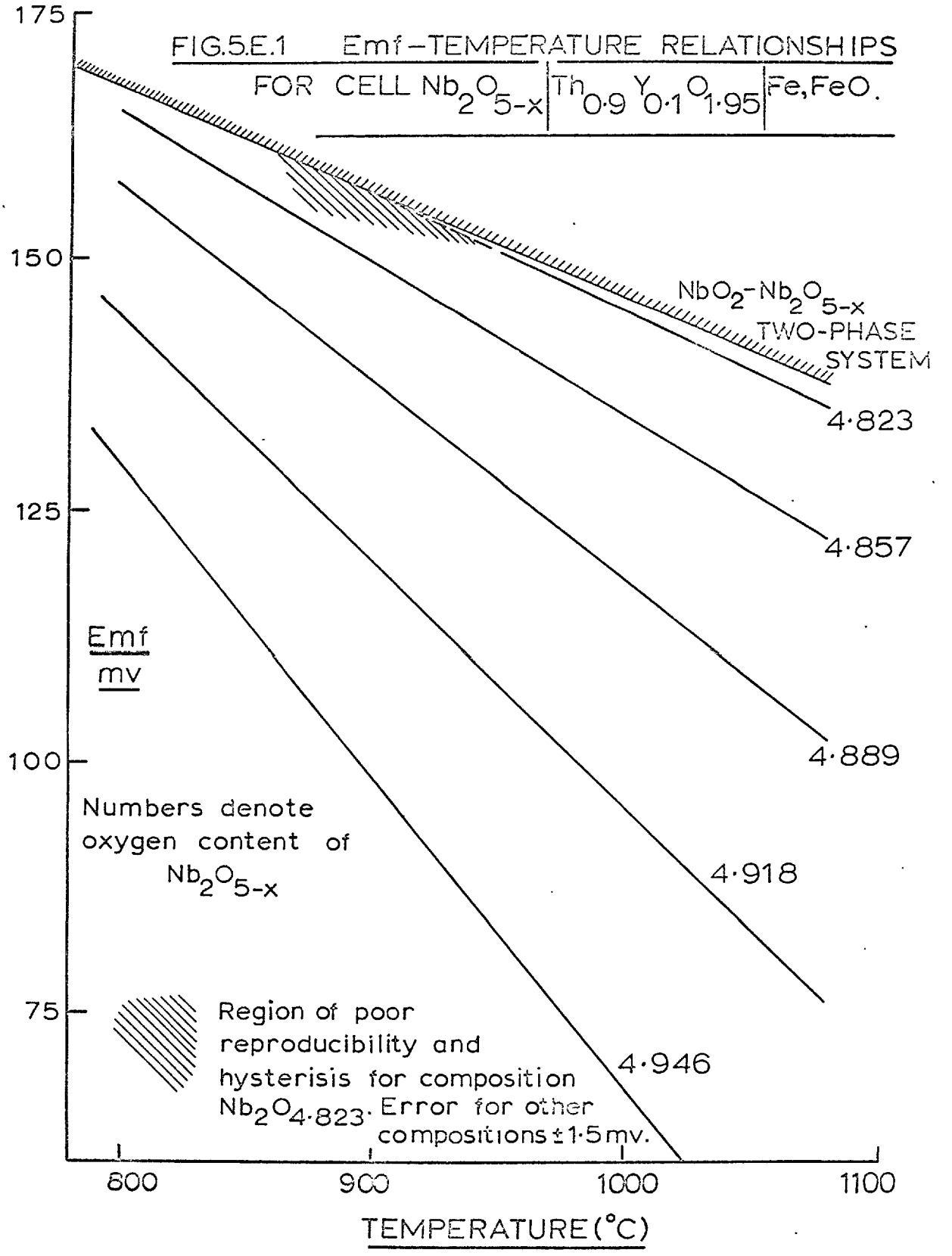
For each composition it was observed that pellets from the three different batches produced similar emf values (± 2 mV), which indicated that the method of preparation gave reproducible compositions*, although the precise composition was not verified by chemical analysis. The excellent reproducibility of these voltages, which were also shown to be reversible, was, however, limited to temperatures above approximately 800°C for the four compositions, b, c, d, e. Below this temperature there was a greater variation (± 5 mV at 700°C) in the emf values recorded, and so the following linear equations, reproduced in Fig. 5.E.1., only represent the data obtained in the temperature range 800-1100°C,

$$E(Nb_2O_{4.857}) = 328.6 - 0.1525\ T \quad (\pm 2\ \text{mV}) \quad \ldots\ldots \text{5.E.1.}$$

$$E(Nb_2O_{4.889}) = 370.4 - 0.1983\ T \quad (\pm 2\ \text{mV}) \quad \ldots\ldots \text{5.E.2.}$$

---

* To confirm that the original components (Nb and Nb_2O_5) had completely reacted and to ensure that the composition of the pellets was not being affected by the vacuum treatment, one of the batches of composition 'e' ($Nb_2O_{4.946}$) was annealed for a week at 1000°C. The emf values subsequently recorded were similar (± 2 mV) to those obtained with electrodes taken from the other two batches prepared by the standard procedure.


FIG.5.E.1 Emf–TEMPERATURE RELATIONSHIPS
FOR CELL Nb_2O_{5-x} | $Th_{0.9}Y_{0.1}O_{1.95}$ | Fe,FeO.
175
150
125
100
75
Emf
mv
NbO_2–Nb_2O_{5-x}
TWO-PHASE
SYSTEM
4·823
4·857
4·889
4·918
4·946
Numbers denote
oxygen content of
Nb_2O_{5-x}
Region of poor
reproducibility and
hysterisis for composition
$Nb_2O_{4.823}$. Error for other
compositions ±1·5mv.
800
900
1000
1100
TEMPERATURE (°C)

$$E(Nb_2O_{4.918}) = 408.2 - 0.2456\ T \quad (\pm 2\ mV) \ldots\ldots \text{5.E.3.}$$

$$E(Nb_2O_{4.946}) = 465.4 - 0.3125\ T \quad (\pm 2.5\ mV) \ldots \text{5.E.4.}$$

More variable results were obtained with cells incorporating composition 'a' ($Nb_2O_{4.823}$). Emf values were always in good agreement ($\pm$ 2 mV), and reversible, in the range 1000-1100°C, and also between 1000°C and 900°C when the voltages were recorded for decreasing temperatures. Below 900°C, however, there was considerable scatter in the results which is depicted by the shaded area in the adjoining Fig. 5.E.1. The cell was not reversible in this region, and reproducible values could not be recorded again until the cell temperature had exceeded 1000°C for several hours. It is reasonable to conclude with reference to Fig. 5.E.1. that the phase NbO_2 is being precipitated around 900°C, and the apparently sluggish kinetics associated with this process made it impossible to record reproducible equilibrium voltages. The following equation for the emf values associated with the electrode composition $Nb_2O_{4.823}$, is therefore only applicable to the temperature range, 900-1100°C,

$$E = 294.2 - 0.1173\ T \quad (\pm 2\ mV) \ldots\ldots \text{5.E.5.}$$

5.E.2. Discussion of thermochemical data

The emf values for the five non-stoichiometric compositions reported in the previous section, were converted* into the following expressions for the relevant oxygen partial molar free energies of solution,

$$\Delta\bar{G}_{O_2}(Nb_2O_{4.823}) = -153{,}610 + 42.08\ T\ (\pm\ 310\ \text{cal.}) \quad [1173\text{-}1373^{\circ}K]$$

$$\Delta\bar{G}_{O_2}(Nb_2O_{4.857}) = -156{,}790 + 45.32\ T\ (\pm\ 310\ \text{cal.}) \quad [1073\text{-}1373^{\circ}K]$$

$$\Delta\bar{G}_{O_2}(Nb_2O_{4.889}) = -160{,}650 + 49.56\ T\ (\pm\ 310\ \text{cal.}) \quad [1073\text{-}1373^{\circ}K]$$

$$\Delta\bar{G}_{O_2}(Nb_2O_{4.918}) = -164{,}130 + 53.92\ T\ (\pm\ 310\ \text{cal.}) \quad [1073\text{-}1373^{\circ}K]$$

$$\Delta\bar{G}_{O_2}(Nb_2O_{4.946}) = -169{,}410 + 60.10\ T\ (\pm\ 340\ \text{cal.}) \quad [1073\text{-}1373^{\circ}K]$$

---

* e.g., for the composition $Nb_2O_{4.889}$,

$Fe_{0.95}O + 1/x\ Nb_2O_{4.889} \quad 0.95Fe + 1/x\ Nb_2O_{4.889+x}$ $(x\to 0)$

$\Delta\bar{G} = -17{,}090 + 9.15\ T$ (Eq. 5.E.2.)

$0.95Fe + \tfrac{1}{2}O_2 \quad Fe_{0.95}O$: $\Delta\bar{G} = -63{,}235 + 15.63\ T$ (Eq.4.B.1.)

$\therefore\ 1/xNb_2O_{4.889} + \tfrac{1}{2}O_2 \quad 1/xNb_2O_{4.889+x}$: $\Delta\bar{G} = -80{,}325 + 24.78\ T$

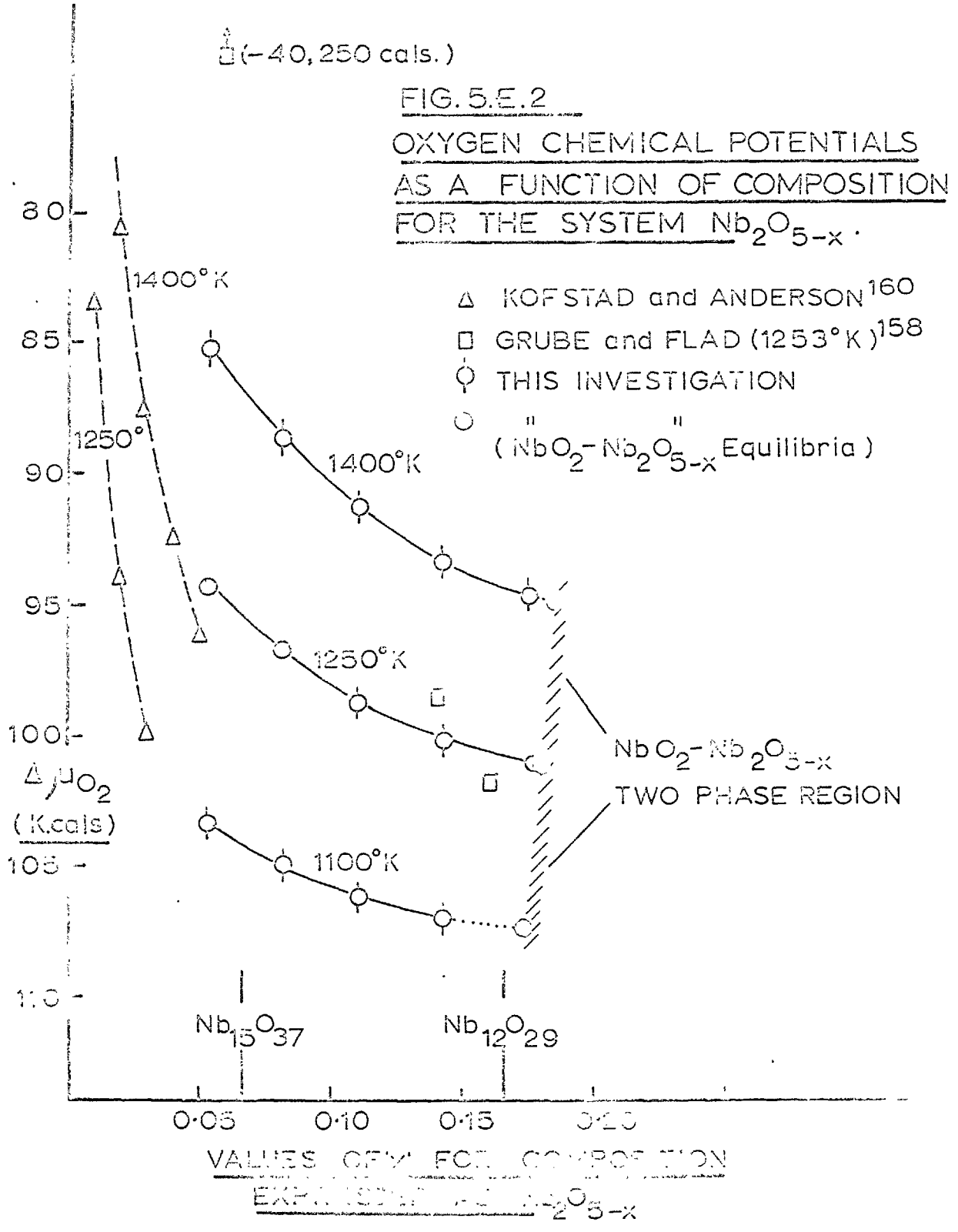


FIG. 5.E.2

OXYGEN CHEMICAL POTENTIALS AS A FUNCTION OF COMPOSITION FOR THE SYSTEM Nb_2O_{5-x}.

These oxygen chemical potentials are plotted as a function of composition for the three temperatures 1100, 1250, 1400°K, in Fig. 5.E.2. As there are no evident discontinuities, the isotherms are drawn as smooth curves which may be extrapolated to provide an estimate of the composition of the Nb_2O_{5-x} phase in equilibrium with NbO, as the oxygen chemical potentials associated with this equilibria have already been established (Section 5.D.2.). This limiting composition is indicated in Fig. 5.E.2. and varies from approximately $Nb_2O_{4.827}$ at 1100°K to $Nb_2O_{4.815}$ at 1400°K.

The oxygen partial molar free energies of solution (Fig. 5.E.2.) measured by Grube and Flad[158] (H_2/H_2O equilibria) at 1253°K become less negative with decreasing defect concentration much more rapidly than the values obtained in the present investigation at 1250°K. There is, however, reasonable agreement with the present data at large deviations from stoichiometry. The results reported by Kofstad and Anderson[160] are also included in Fig. 5.E.2., and although the composition range examined by these workers did not extend to the larger deviations from stoichiometry studied in the present investigation, it is evident that both sets

of data are inconsistent*. This discrepancy might be due to the experimental difficulties mentioned by Kofstad and Anderson in a description of the gravimetric technique which was used to measure the changes in composition.

The present electrochemical experiments provide no evidence for the occurrence of discrete intermediate phases in non-stoichiometric Nb_2O_5 as the oxygen partial molar free energies of solution appear to be a continuous function of composition. It was concluded, however, by Norin and Magneli[153], and Gruehn and Schafer[154], from X-ray examinations of reduced Nb_2O_5, that two separate compounds exist within the composition range investigated in the present study (see Fig. 5.E.2.). Although the crystal structures have not yet been published it has been proposed that these compounds are members of an homologous series of oxides, with the general formula $M_{3n}O_{8n-3}$, and are also isomorphous with a series of mixed oxides reported by Wadsley[161] in the

---

* The good agreement with the results of Grube and Flad noted by Kofstad and Anderson is erroneous, as the values used by the latter workers for the relevant Nb_2O_{5-x} compositions are incorrect.

$Nb_2O_5 - TiO_2$ system. The formulae of these related oxide phases is shown in the following Table 5.E.1., and the compositions of the relevant oxides are also included in Fig. 5.E.2.

Table 5.E.1.

Intermediate Oxide Compositions.

n	$M_{3n}O_{8n-3}$	(Ti^4, Nb^5) Ox	(Nb^4, Nb^5) Ox
3	M_9O_{21}	$Ti_3Nb_6O_{21}$	$NbO_{2.333}$ (?)
4	$M_{12}O_{29}$	$Ti_2Nb_{10}O_{29}$	$NbO_{2.417}$
5	$M_{15}O_{37}$	$TiNb_{14}O_{37}$ (?)	$NbO_{2.467}$
6	$M_{18}O_{45}$	-	$NbO_{2.500}$

(?) indicates that compounds have not so far been prepared or reported.

Homologous sequences of intermediate compounds are known to exist at low temperatures in many other systems originally reported as homogenous non-stoichiometric phases, as exemplified by the series of homologous oxides of molybdenum, (M_nO_{3n-1}), tungsten (M_nO_{3n-1}), titanium

(Ti_nO_{2n-1}), and vanadium (V_nO_{2n-1}), discovered by Magneli and his associates[162, 163]. Other sequences of intermediate phases have also been established for the oxides cerium[164], praseodynium[165] and terbium[166]. It appears, however, from the high temperature studies of Bevan and Kordis (Ce-O)[167], Brauer and Gingerich (Ce-O)[109], Bevan, Hyde and Eyring (Pr-O)[110], that the phase-boundaries of these intermediate compounds broaden and eventually disappear to produce a single phase possessing an extensive range of non-stoichiometry. Analogous behaviour may be exhibited by the intermediate niobium oxides, $Nb_{12}O_{29}$, $Nb_{15}O_{37}$, which would explain why these phases were not detected at the higher temperatures (>800°C) involved in the present investigation*.

An unequivocal decision about the defect structure of

---

* Schafer has recently identified SIX phases in the composition range Nb_2O_4-Nb_2O_5 and reports that the associated compounds are stable up to 1300°C[168]. It is possible, therefore, that the oxygen partial molar free energies of solution of the five compositions examined in the present investigation do not fall on a smooth curve as assumed in Fig. 5.E.2., but are separated by narrow, univariant two-phase regions. This uncertainty would be resolved by making additional emf measurements with compositions spaced much closer together.

non-stoichiometric αNb_2O_5 is not possible with the data at present available, although an oxygen vacancy model is usually preferred to a structure involving interstial niobium ions (cf. non-stoichiometric TiO_2). Kofstad and Anderson[160], for example, interpreted their gravimetric results on αNb_2O_5 in terms of non-interacting doubly-ionized oxygen vacancies, and claimed that the concentration of these vacancies was proportional to $p_{O_2}^{-\frac{1}{6}}$ as required by the Schottky-Wagner approximation*. This treatment leads to a constant value for the oxygen partial molar enthalpy of solution, whereas the values derived in the present investigation (Fig. 5.E.3.) are obviously a function of the defect concentration. It is unlikely, however, that the Schottky-Wagner theoretical model, which is strictly valid for very dilute systems, is applicable at

---

* The relevant equilibria may be represented as follows:

$$O^{2-}_{lattice} \quad \tfrac{1}{2}O_2(g) + \square_{_} + 2e^-$$

and $[e^-] = 2[\square_{_}]$ $\quad \therefore \quad K = 4[\square_{_}]^3 \times p_{O_2}^{\frac{1}{2}}$

i.e. $[\square_{_}] \propto p_{O_2}^{-\frac{1}{6}}$

It should be noted, however, that the measurements of Greener et al.[172], and the more recent investigation of Kofstad[173], indicate that the electrical conductivity of almost stoichiometric Nb_2O_5 is proportional to $p_{O_2}^{-\frac{1}{4}}$.

FIG.5.E.3 PARTIAL MOLAR HEATS OF SOLUTION OF OXYGEN IN SELECTED ANION DEFICIENT COMPOUNDS

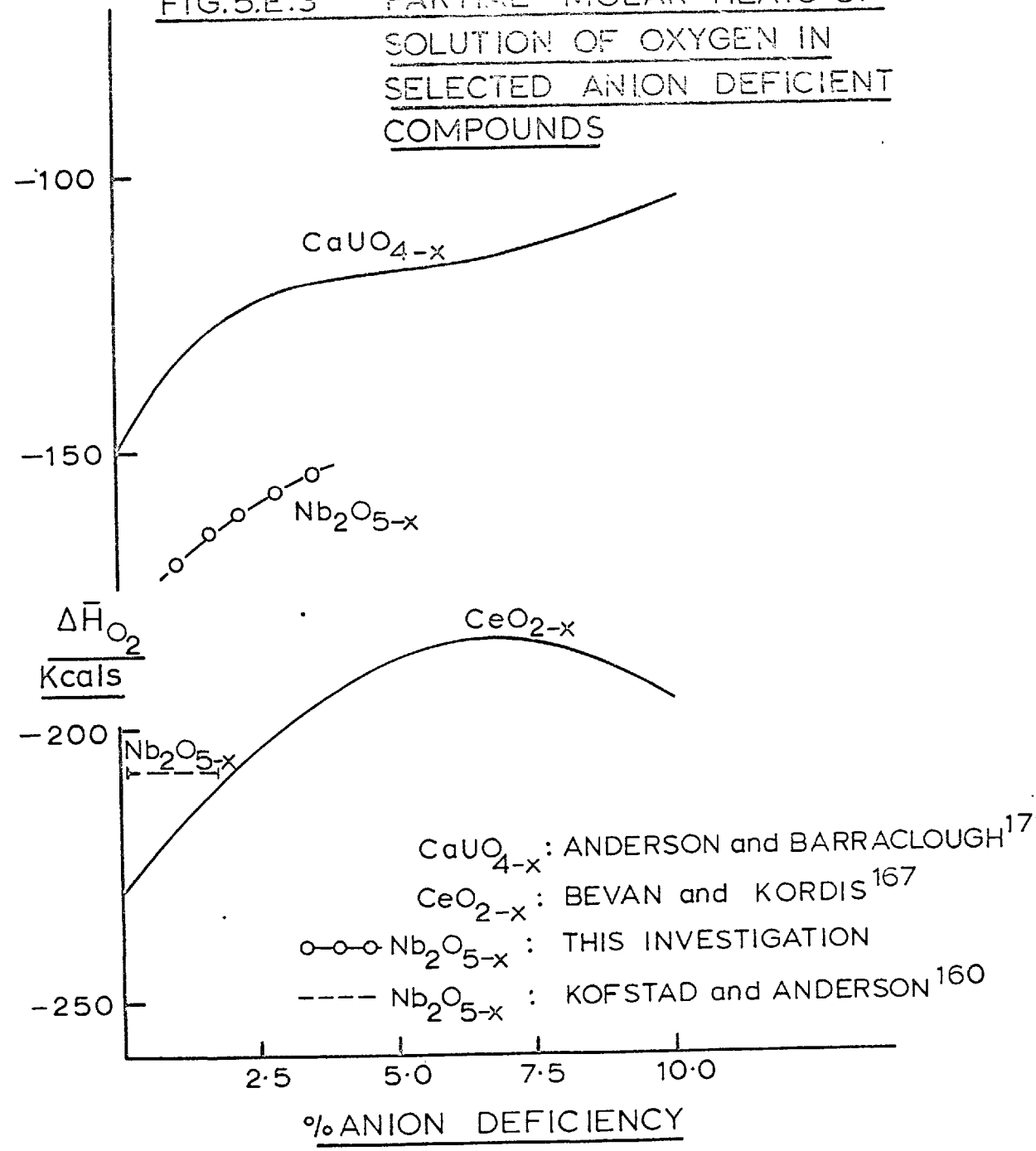
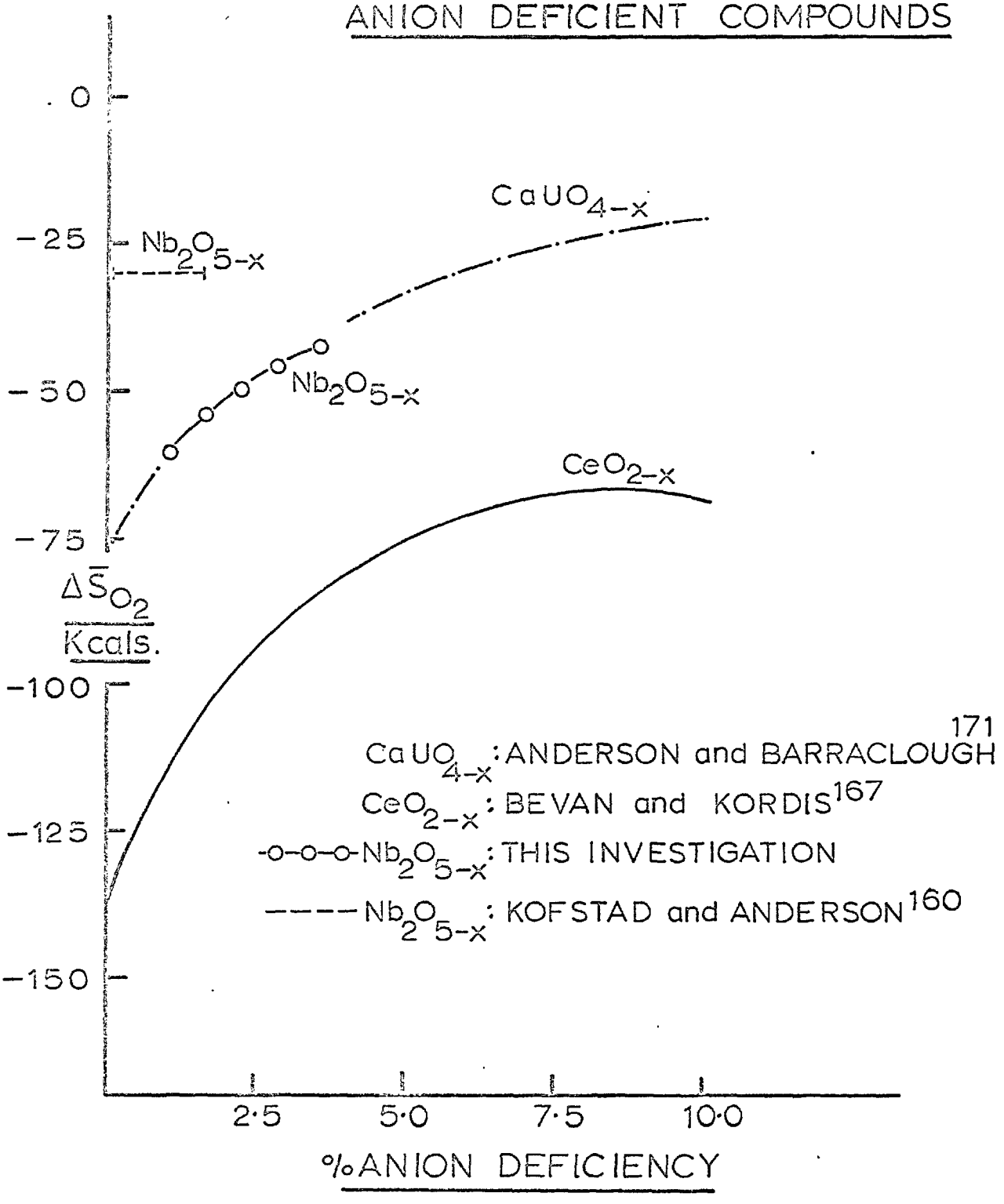


FIG.5.E.4 PARTIAL MOLAR ENTROPIES OF OXYGEN IN SELECTED ANION DEFICIENT COMPOUNDS



the defect concentrations ($Nb_2O_{4.920}$-$Nb_2O_{4.995}$) investigated by Kofstad and Anderson, and the apparent confirmation of the predicted relationship between defect concentration and oxygen partial pressure is probably fortuitous as no allowance is made for interaction or association of defects. If interactions between defects on adjacent sites are considered as in the theoretical models of Anderson[169] and Rees[170], then the partial molar enthalpies of oxygen should depend upon the concentration of defects (x) and the nearest-neighbour interaction energy (En) according to a relationship of the type,

$$\Delta\bar{H}_{O_2} \simeq Es - x\,En,$$

where Es is the energy (per mole O_2) associated with the transfer of gaseous oxygen molecules to anion sites in the crystal lattice. An almost linear dependence upon defect concentration is shown by the partial molar enthalpies obtained in the present investigation (Fig. 5.E.3.)*. A simple linear equation, however, would probably be inadequate to express the variation of this thermodynamic quantity over a more extensive range of composition, as similar data*, reproduced in Fig. 5.E.3., for other anion

* Relevant values of oxygen partial molar entropies of solution are also compared in Fig. 5.E.4.

deficient oxide systems, CeO_{2-x}[167], $CaUO_{4-x}$[171], indicate that the partial molar enthalpy values change more rapidly as the stoichiometric composition is approached. It is possible to further improve the theoretical model by taking into consideration association of defects as demonstrated by Anderson and Barraclough for the $CaUO_{4-x}$ system. Before attempting a similar analysis of the Nb_2O_{5-x} phase it is desirable to acquire more extensive data than is available from the present preliminary study of this system, and it is suggested that the additional measurements be made with galvanic cells incorporating solid oxide electrolytes as the data associated with this technique should be more accurate and precise than that obtained by alternative methods.

5.F. THERMOCHEMICAL DATA FOR STOICHIOMETRIC Nb_2O_5

Oxygen partial molar free energies of solution as a function of composition for the non-stoichiometric Nb_2O_{5-x} phase are available from the previous section, and these values can be combined with the relevant data for the NbO_2-Nb_2O_{5-x} equilibria (Section 5.E.2., Eq. 5.E. .) to provide information about the free energy of formation of

stoichiometric Nb_2O_5.

For the reaction,

$$2NbO_2 + \tfrac{1}{2}O_2 \longrightarrow Nb_2O_5,$$

$$\Delta G = 2x \int_{2.0}^{2.5} \Delta\bar{G}\,(\tfrac{1}{2}O_2).dn,$$

and it follows that if $\Delta\bar{G}\,(\tfrac{1}{2}O_2)$* is plotted against n (where n is the composition expressed as NbOy, i.e. $\frac{No}{N_{Nb}}$) then the integral free energy ΔG may be obtained by determining the area under the curve. If ΔG is therefore determined at two temperatures (e.g. 1173 and 1373°K), then an equation for the relevant standard free energy change as a function of temperature can be derived. Appropriate values at

---

* Although the oxygen partial molar free energies of solution were only determined over a limited composition range in the present investigation, it was assumed that Nb_2O_5 is exactly stoichiometric at an oxygen partial pressure of 1 atm. The shape of the above curve is such that the error introduced by this assumption is probably negligible.

1173 and 1373°K are -51,290 and -46,790 cal., respectively, and it follows for the reaction,

$$2NbO_2 + \tfrac{1}{2}O_2 \longrightarrow Nb_2O_5$$

that,

$$\Delta G^\circ = -77,660 + 22.49T \qquad \ldots\ldots\ldots \text{Eq. 5.F.1.}$$

If this equation is combined with the expression derived earlier for the standard free energy of formation of NbO_2 (Eq. 5.C.3.), then for the reaction,

$$2Nb + \tfrac{5}{2}O_2 \longrightarrow Nb_2O_5,$$

$$\Delta G^\circ = -443,940 + 97.51T \qquad \ldots\ldots\ldots \text{Eq. 5.F.2.}$$

Values derived from this equation are compared with calorimetric data* at 1000 and 1300°K in the adjoining Table 5.F.1.

---

* Values recommended by Kelley[117, 118] were used for the quantities $(H^\circ_T - H^\circ_{298})$, $(S^\circ_T - S^\circ_{298})$ and S°_{298}, together with the H°_{298} value listed by Skinner[132].

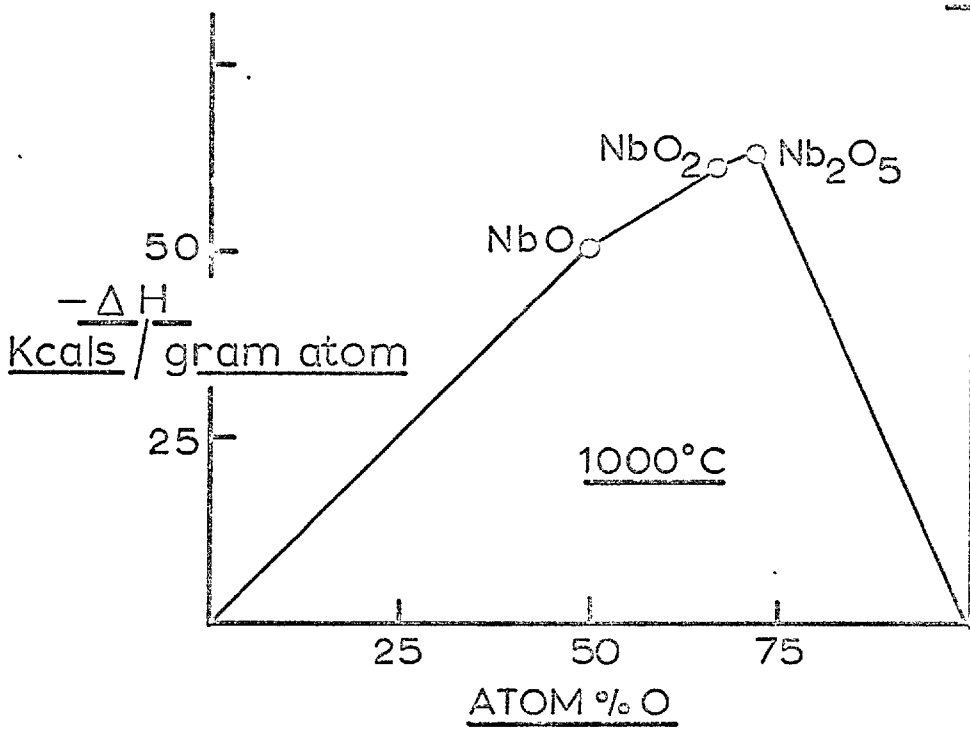
Table 5.F.1.

Temperature ^{o}K	Thermodynamic Quantity	This Investigation	Calorimetric
1000	ΔG^{o} (cal. mole^{-1})	-346,430	-349,920
	ΔH^{o} (cal. mole^{-1})	-443,940	-450,500
	ΔS^{o} (cal./mole^{-1} deg^{-1})	- 97.51	-100.58
1300	ΔG^{o} (cal. mole^{-1})	-317,260	-320,030
	ΔH^{o} (cal. mole^{-1})	-443,940	-448,270
	ΔS^{o} (cal./mole^{-1} deg^{-1})	- 97.51	- 98.65

It can be seen that there is reasonable agreement between the two sets of data, particularly in view of the simplifying assumptions made in the present investigation about the activities of NbO and NbO_2, which were always taken as equal to unity.

Finally, the integral free energies and enthalpies of formation at 1273^{o}K (1000^{o}C) of NbO, NbO_2, Nb_2O_5 are summarised in Fig. 5.F.1. per gm-atom of oxide, and in Fig. 5.F.2. per gm-atom of niobium.

FIG.5.F.1 INTEGRAL HEATS AND FREE ENERGIES OF FORMATION (per gram atom of oxide)



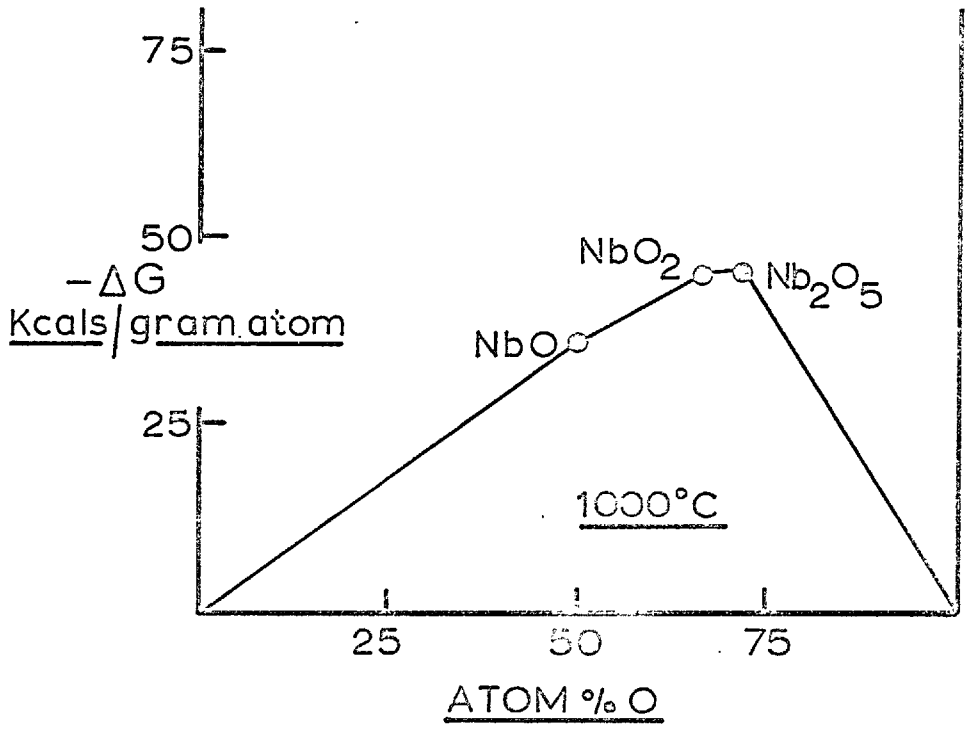
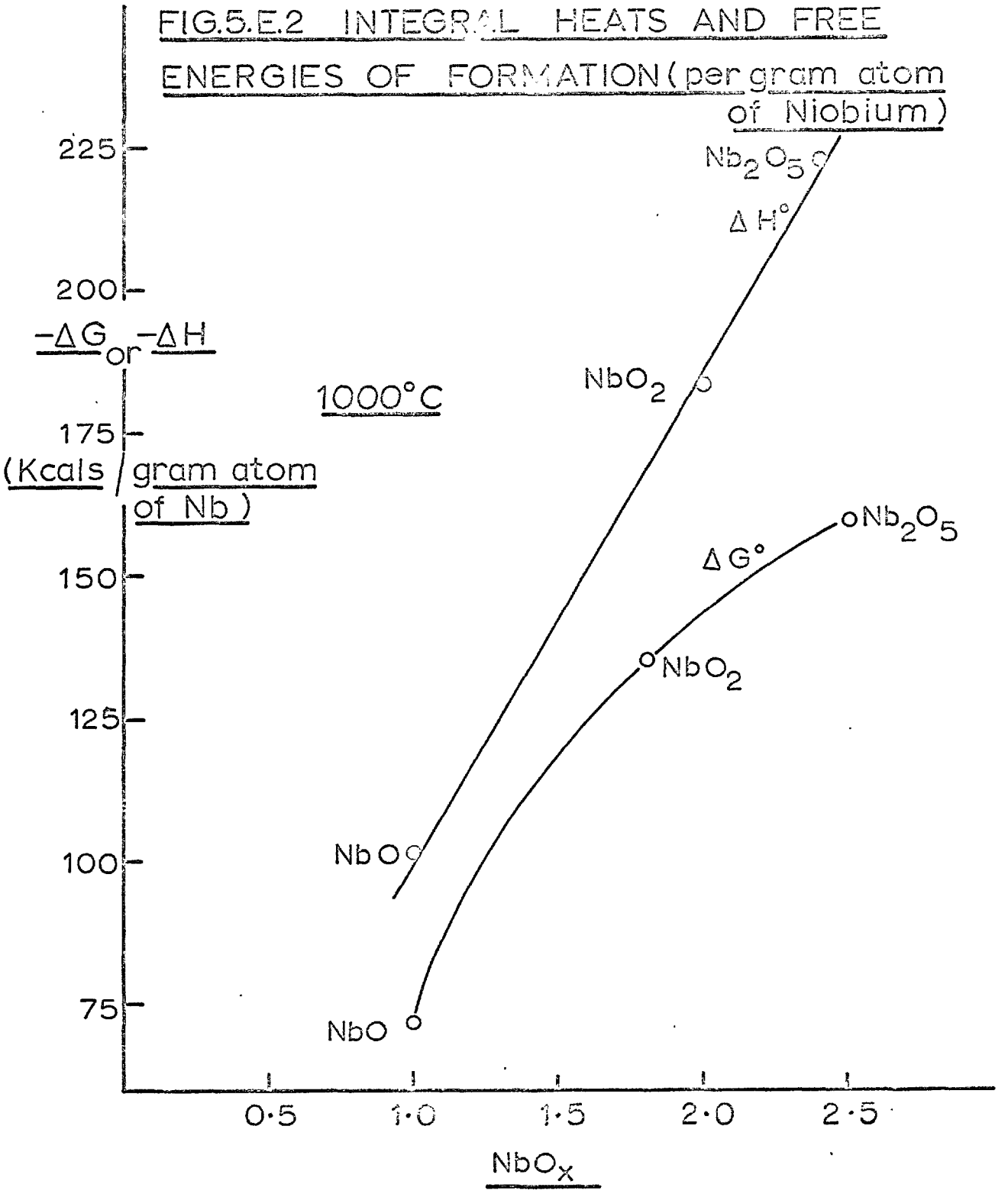


FIG.5.E.2 INTEGRAL HEATS AND FREE ENERGIES OF FORMATION (per gram atom of Niobium)



5.G. CONCLUSIONS

The present investigation has demonstrated that galvanic cells incorporating solid oxide electrolytes can be successfully used to measure oxygen chemical potentials outside the range of conventional gas equilibration techniques. However, in spite of the potentialities of the emf method only a few similar studies at low oxygen chemical potentials have so far been reported, which also illustrate the precautions to be observed if reliable, reproducible, data are to be obtained. It is impossible, for example, to assess the results of Hoch and his associates[157,174] as their zirconia-based electrolytes must have possessed considerable electronic conductivity under the prevailing experimental conditions, and reference has already been made to certain of the measurements associated with Gerasimov, Kusnetsov and Rezukhina[25, 80, 81, 155, 175]. The cell arrangement used by these workers did not include any provision for separate electrode compartments, and whilst this may not be absolutely essential, it does greatly facilitate the acquisition of reliable reproducible data, and its omission may account for certain of the low voltages recorded by Yakovleva and Ariyah[176] in a preliminary emf study of the Ti-O system.

Many of the experimental problems are due to the high affinity for oxygen possessed by these low oxygen chemical potential electrodes, and it is obviously desirable to incorporate any feature in the cell design which promotes local equilibrium at the electrode/electrolyte interface. Modifications which were found necessary in the present investigation included the use of 'getters', separate electrode compartments, protective electrode collars, high resistance electrolytes, and it is suggested that if these features

are embodied in the cell design, and providing the oxygen chemical potentials are not too low [$\Delta\mu O_2$ (1000°C) $\geq$ -145 Kcal.] , then the reproducibility of the experimental values is generally very good ($\pm$ 200 cal.). Once again the principal uncertainty is due to lack of precise information about the magnitude of the electronic conductivity. It appears, however, that the electronic component does not exceed 1% over the range of oxygen chemical potentials studied, and may well be considerably lower.

In addition to measuring thermochemical data, similar cells incorporating solid oxide electrolytes have obvious commercial applications for determining the oxygen content of both gaseous and condensed phases (e.g. liquid metals). Application of this technique, however, to higher temperatures and lower chemical potentials may well require the development of alternative solid oxide electrolyte systems, and it is most important, therefore, that further studies be made of the electrolytic transport properties of this class of materials. Additional studies should also include investigations of the relevant electrode kinetics so that the electrochemistry of galvanic cells incorporating solid oxide electrolytes can be made more amenable to a satisfactory theoretical interpretation.

ACKNOWLEDGMENTS

I wish to thank Professor F. D. Richardson for his interest, and for providing the opportunity which enabled the present investigation to be undertaken. I also wish to express my thanks to Dr. C. B. Alcock for his advice and general supervision of the research work, and the many useful discussions with Dr. J. W. Tomlinson are also gratefully acknowledged.

Thanks are due as well to the workshop and laboratory staff of the Nuffield Research Group, and also to Imperial Chemical Industries Ltd., for financing the purchase of certain items of equipment.

June 1965.

REFERENCES

1. O. Kubaschewski and E. Ll. Evans: "Metallurgical Thermochemistry", (3rd edition, Pergamon Press, London 1958).
2. F. D. Richardson and C. B. Alcock: "Physico-chemical Measurements at High Temperatures", edit. by J. O'M. Bockris, J. L. White J. D. Mackenzie, Chap. 6, pp. 135-170, (Butterworths, London, 1959).
3. J. Chipman, J. F. Elliott, B. L. Averbach: N.P.L. Symposium No 9, "The Physical Chemistry of Metallic Solutions and Intermetallic Compounds", Paper 1B, Vol 1, (H.M.S.O., London 1959).
4. N. P. Allen, O. Kubaschewski, O. von Goldbeck, J. Electrochem. Soc., 1951, 98, 417-424.
5. O. Kubaschewski and W. A. Dench, J. Inst. Metals, 1953-4, 82, 87-91.
6. O. Kubaschewski and W. A. Dench, ibid., 1955-6, 84, 440-444.
7. A. Veinbachs, M. D. Silver and K. L. Komarek, Proc. I.A.E.A. Symposium, "Thermodynamics of Nuclear Materials", pp. 749-774, (I.A.E.A. Vienna, 1962).
8. M. D. Silver, P. A. Farrar and K. L. Komarek, Trans. A.I.M.E., 1963, 227, 876-884.

9. F. D. Richardson and J. H. E. Jeffes, J. Iron Steel Inst., 1948, 160, 261-270.

10. W. D. Treadwell and L. Terebesi, Helv. Chim. Acta., 1933, 16, 922-939.

11. W. D. Treadwell, A. Amman and Th. Zurrer, Helv. Chim. Acta., 1936, 19, 1255-1270.

12. P. Hersch, Instrument Practice, 1957, 11, 817-823 and 937-941.

13. J. A. Christiansen and M. Pourbaix, Compt. Rend. Conf. Union Intern. Chim. Pure et Appl. (I.U.P.A.C.), 17th Conf., Stockholm, p. 83, (1953).

14. D. J. G. Ives, "Reference Electrodes", edit. D. J. G. Ives and G. J. Janz, Chap. 7, (Academic Press, London 1961).

15. F. Haber and A. Moser, Z. Elektrochem., 1905, 11, 593-609.

16. W. D. Treadwell, Z. Elektrochem., 1916, 22, 414.

17. B. A. Rose, G. J. Davis, H. J. T. Ellingham, Disc. Faraday Soc., 1948, No. 4, 154-162.

18. H. Flood, T. Foreland and K. Motzfeldt, Acta. Chem. Scand., 1952, 6, 257-269.

19. K. Kiukkola and C. Wagner, J. Electrochem. Soc., 1957, 104, 308-316.

20. K. Kiukkola and C. Wagner, ibid., 1957, 104, 379-387.

22. S. Aronson and J. Belle, J. Chem. Phys., 1958, 29, 151-158.

23. K. Kiukkola, Acta Chem. Scand., 1962, 16, 327-345.

24. T. L. Markin, L. E. J. Roberts and A. Walter, Proc. I.A.E.A. Symposium, "Thermodynamics of Nuclear Materials", pp. 693-711, (I.A.E.A., Vienna 1962).

25. T. N. Rezukhina, V. A. Levitskii and N. M. Kazimirova, Russ. J. Phys. Chem. (English Trans.), 1961, 35, 1305-1306.

26. R. Rapp, and F. Maak, Acta Met., 1962, 10, 63-69.

27. J. Frenkel, Z. Physik, 1926, 35, 652- .

28. W. Schottky, Z. Physik. Chem., 1935, B29, 335- .

29. W. Schottky and C. Wagner, Z. Physik. Chem., 1930, B11, 163.

30. A. B. Lidiard, Handbuch der Physik, Vol 20, pp. 246-349, (Springer-Verlag, Berlin, 1957).

31. C. Wert, Phys. Rev., 1950, 79, 601-605.

32. F. Kerkhoff, Z. Physik, 1951, 130, 449-456.

33. R. W. Dreyfus and A. S. Nowick, Phys. Rev., 1962, 126, 1367-77.

34. F. G. Fumi and M. P. Tosi, Disc. Faraday Soc., 1957, No 23, 92-98.

35. C. Wagner, Proc. 7th meeting C.I.T.C.E., pp. 361-376, (Butterworths Scientific Publ., London 1957).

36. K. Compaan and Y. Haven, Trans. Faraday Soc., 1956, 52, 786-801.

ibid. , 1958, 54, 1498-1508.

37. A. B. Lidiard, Proc. 4th Intern. Conf. on Reactivity of Solids, pp. 52-56, (Elsevier, Amsterdam 1961).

38. R. J. Friauf, J. Appl. Phys., 1962, 33S, 494-505.

39. L. W. Barr and A. D. Le Claire, Proc. Brit. Ceram. Soc., 1964, No 1, 109-128.

40. J. O'M. Bockris, "Modern Aspects of Electrochemistry", Vol 1, pp. 180-276, (Butterworths, London 1954).

41. A. D. Neuimin, S. V. Karpachev and S. F. Pal'guev, Doklady. Akad. Nauk., S.S.S.R., 1961, 141, 402-404.

42. S. V. Karpachev, A. T. Filyayev and S. F. Pal'guev, Electrochim. Acta, 1964, 9, 1681-1685.

43. J. Weissbart and R. Ruka, J. Electrochem. Soc., 1962, 109, 723-726.

44. M. L. Kronenberg, (Private communication), Union Carbide Corp., Parma 30, Ohio, U.S.A.

45. H. Schmalzried, Z. Phys. Chem, N.F., 1963, 38, 87-102.

46. H. Schmalzried, J. Chem. Phys., 1960, 33, 940.

47. S. P. Mitoff, J. Chem. Phys., 1962, 36, 1383-1389.

48. S. F. Pal'guev and A. D. Neumin, Soviet Phys. Solid State (English Trans.), 1962, 4, 629-632.

49. J. Rudolph, Z. Naturforsch., 1959, 14A, 727-737.

50. W. D. Kingery and J. Pappis, J. Am. Ceram. Soc., 1961, 44, 459-464.

51. R. W. Vest, N. M. Tallon and W. C. Tripp, J. Am. Ceram. Soc., 1964, 47, 635-640.

52. P. Kofstad and D. J. Ruzicka, J. Electrochem. Soc., 1963, 110, 181-184.

53. O. Esin, N. Gavrilov and P. Lepinskikh, Doklady, Akad. Nauk. S.S.S.R., 1953, 88, 713.

54. M. Ohtani and K. Sanbongi, Tetsu-to-Hagane, 1963, 49, 22-29.

55. W. Nernst, Z. Elektrochem., 1900, 6, 41-43.

56. C. Wagner, Naturwiss., 1943, 31, 265-68.

57. F. Hund, Z. Physik. Chem., 1952, 199, 142-51.

58. W. D. Kingery, J. Pappis, M. E. Doty, and D. C. Hill, J. Am. Ceram. Soc., 1959, 42, 393-98.

59. W. H. Rhodes and R. E. Carter, presented at the American Ceramic Society Meeting, April 1962, Abstract in Bull. Am. Ceram. Soc., 1962, 41, 283.

60. H. H. Mobius, H. Witzmann and D. Gerlach, Z. Chem., 1964, 4, 154-5.

61. D. T. Bray and U. Merten, J. Electrochem. Soc., 1964, 111, 447-452.

62. H. Peters and H. H. Mobius, Z. Physik. Chem. (Leipzig), 1958, 209, 298-309.

63. H. Schmalzried, Z. Elektrochem., 1962, 66, 572-76.

64. H. H. Mobius, Z. Chem., 1964, 4, 81-94.

65. J. P. Coughlin, U.S. Bureau of Mines Bull. No 542 (1954).

66. H. Peters and G. Mann, Naturwiss., 1958, 45, 209-210.

67. H. Peters and G. Mann, Z. Elektrochem., 1959, 63, 244-248.

68. P. Best and E. Proudfoot, Ind. Chem., 1957, 33, 448-451.

69. W. D. Kingery, "Ceramic Fabrication Processes", (Technology Press of M.I.T. and Wiley, New York, 1958).

70. T. W. Penrice, Powder Metallurgy 1958, No 1/2, 79-84.

71. J. B. Nelson and D. P. Riley, Proc. Phys. Soc., (London) 1945, 57, 160-177.

72. G. M. Fryer and J. P. Roberts, Trans. Brit. Ceram. Soc., 1963, 62, 537-548.

73. A. Brown and A. Chitty, J. Nuclear Energy (B), 1960, 1, 145.

74. R. Benz and H. Schmalzried, Z. Phys. Chem (N.F.), 1961, 29, 77-82.

75. H. Schmalzried, Z. Phys. Chem. (N.F.), 1960, 25, 178-192.

76. M. Coll-Palagos and C. R. Masson, Trans. Faraday Soc., 1961, 57, 1621-1626.

77. T. L. Markin and R. J. Bones, Report R.4178 (26pp. 1962), A.E.R.E., Harwell, Berks, U.K.

78. T. L. Markin and R. J. Bones, Report R.4608 (19pp; 1964), A.E.R.E., Harwell, Berks, U.K.

79. R. A. Rapp, Trans. A.I.M.E., 1963, 227, 371-374.

80. T. N. Rezukhina, V. I. Lawrent'ev, V. A. Levitskii and F. A. Kuznetsov, Russ. J. Phys. Chem., (English Trans.), 1961, 35, 671-672.

81. T. N. Rezukhina, V. A. Levitskii and P. Ozhegov, Russ. J. Phys. Chem. (English Trans.), 1963, 37, 358-59.

82. J. Weissbart and R. Ruka, Rev. Sci. Instruments, 1961, 32, 593-595.

83. H. Palevsky, R. Greenshik and R. K. Swank, Rev. Sci., Inst., 1947, 18, 298-314.

84. B. T. M. Willis, Proc. Roy. Soc. A, 1963, 274, 134-144.

85. F. Hund and R. Mezger, Z. Physik. Chem; 1952, 201, 268-277.

86. F. Hund and W. Durrwachter, Z. Anorg. Allgem. Chem., 1951, 265, 67-72.

87. G. Brauer and H. Gradinger, Z. Anorg. Allgem. Chem., 1954, 276, 209-226.

88. L. Pauling, "The Nature of the Chemical Bond", 3rd edn. (Oxford Univ. London 1960).

89. L. H. Ahrens, Geochim. Cosmochim. Acta. 1952, 2, 155-169.

90. C. E. Curtis and J. R. Johnson, J. Am. Ceram, Soc., 1957, 40, 63-68.

91. H. H. Mobius, H. Witzmann and W. Witte, Z. Chem., 1964, 4, 152-154.

92. D. W. Strickler and W. G. Carlson, J. Am. Ceram. Soc., 1964, 47, 122-127.

93. J. Dixon, L. La Grange, U. Merten, C. Miller and J. Porter, J. Electrochem. Soc., 1963, 110, 276-280.

94. E. C. Subbarao and P. H. Sutter, Report No 63-929-268-P2, (13 pp. 1963), Westinghouse Research Laboratories, Pittsburgh, Pennsylvania, U.S.A.

95. C. Kawashima, S. Saito and O. Fukunaga, J. Ceram. Assoc. Japan, 1963, 71, 49-54.

96. N. J. Bridger, W. A. Denne, T. L. Markin and M. H. Rand, Report R.4329 (5 pp. 1963), A.E.R.E. Harwell, Berks, U.K.

97. Z. S. Volchenkova and S. F. Pal'guev, Trans. Inst. Electrochem. (English Trans.), 1961, No 1, 104-106.

98. R. E. Carter and W. L. Roth, Report No 63-RL-3479M (27 pp. 1963), General Electric Co., Research Labs., Schenectady, New York, U.S.A.

99. J. S. Anderson, "I.U.P.A.C. Symposium on High Temperature Technology", (Butterworths, London 1964).

100. H. A. Johansen and J. G. Cleary, J. Electrochem, Soc., 1964, 111, 100-103.

101. T. Y. Tien and E. C. Subbarao, J. Chem. Phys., 1963, 39, 1041-47.

102. J. B. Wachtman, Phys. Rev., 1963, 131, 517-527.

103. L. Himmel, C. E. Birchenall and R. F. Mehl, Trans. A.I.M.E., 1953, 197, 827.

104. R. H. Condit and C. E. Birchenall, Report No AFOSR-TN-60-245(1960), Armed Services Technical Information Agency (ASTIA), Arlington 12, Virginia, U.S.A.

105. E. F. Bertaut, Acta Cryst., 1953, 6, 557-561.

106. W. C. Hagel, (Private communication), General Electric Co., Research Laboratories, Schenectady, New York, U.S.A.

107. E. C. Subbarao and P. H. Sutter, J. Phys. Chem. Solids, 1964, 25, 148-150.

108. R. Collongues, M. Perezy Jorba and J. Lefevre, Bull. Soc. Chim. France, 1961, p.70.

109. G. Brauer and K. A. Gingerich, J. Inorg. Nucl. Chem., 1960, 16, 87-99.

110. D. J. M. Bevan, B. G. Hyde and L. Eyring, To be published in Proc. Roy. Soc. (Lond.).

111. D. W. Strickler and W. G. Carlson, Abstract in Bull. Amer. Ceram. Soc., 1964, 43, 351.

112. Y. Haven, Proc. Brit. Ceram. Soc., 1964, No 1, 93-108.

113. S. Aronson, J. Electrochem. Soc., 1961, 108, 312-316.

114. D. Hayes, E. W. Roberts and J. P. Roberts, "Science of Ceramics", Vol 2 p. 343 (Academic Press, London 1965).

115. B. C. Weber, J. Garrett, F. A. Mauer, M. A. Schwartz, J. Am. Ceram. Soc., 1956, 39, 197-206.

116. R. A. Rapp and C. Stone (Private communication), Metallurgy Department, Ohio State University, Columbus, Ohio, U.S.A.

117. K. K. Kelley, U.S. Bureau of Mines Bull. No 584 (1960).

118. K. K. Kelley and E. G. King, U.S. Bureau of Mines Bull. No 592 (1961).

119. J. F. Elliott and M. Gleiser, "Thermochemistry for Steelmaking", Vol 1 (Addison-Wesley, Mass. U.S.A., 1960).

120. O. Kubaschewski and B. E. Hopkins, "Oxidation of Metals and Alloys", 2nd edn. (Butterworths Sci. Publ., London, 1962).

121. W. A. Fischer and A. Hoffman, Acta Eisenhuttenw. 1957, 28, 771-76.

122. R. Schenck, Th. Dingmann, P. H. Kirscht and H. Wesselcock, Z. Anorg. Allgem. Chem., 1929, 182, 97-117.

123. P. H. Emmett and J. F. Schultz, J. Am. Chem. Soc., 1930, 52, 4268-85.

124. P. H. Emmett and J. F. Schultz, J. Am. Chem. Soc., 1933, 55, 1576-89.

125. L. S. Darken and R. W. Gurry, J. Am. Chem. Soc., 1945, 67, 1398-1412.

126. W. D. Jominy and D. W. Murphy, Ind. Eng. Chem., 1931, 23, 384-387.

127. J. Chipman and S. Marshall, J. Am. Chem. Soc., 1940, 62, 299-305.

128. V. Cirelli, Gazzeta Chimica Italiana, 1947, 76, 331-336.

129. J. Chipman, Pure and App. Chem., 1962, 5, 361.

130. D. Young and J. W. Tomlinson (Private communication), Metallurgy Dept., Imperial College, London.

131. R. Fricke and G. Weitbrecht, Z. Elektrochem., 1942, 48, 87-110.

132. H. A. Skinner, Pure and Appl. Chem., 1964, 8, 113-130.

133. T. L. Markin and R. J. Bones, Report R.4042 (22 pp. 1962), A.E.R.E. Harwell, Berks. U.K.

134. S. F. Pal'guev and A. D. Neumin, Trans. Inst. Electrochem. (English Trans.), 1961, No 1, 90-96.

135. D. Young and J. W. Tomlinson , (Private communciation), Metallurgy Dept., Imperial College, London.

136. J. Gundermann, K. Hauffe and C. Wagner, Z. Physik, Chem. B, 1937, 37, 148.

137. C. Balesdent, Comp. Rend., 1955, 240, 1884.

138. C. B. Alcock and T. N. Belford, Trans. Faraday Soc., 1964, 60, 822-835.

139. F. D. Richardson and G. Webb, Trans. Inst. Min. Met., 1954-5, 64, 529.

140. Y. Matsushita and K. Goto, (Private communication), Dept. of Metallurgical Engineering, University of Tokyo, Japan.

141. H. M. Spencer and J. H. Mote, J. Amer. Chem. Soc., 1932, 54, 4618-4624.

142. A. U. Seybolt, J. Metals, 1954, 6, 774-776.

143. R. T. Bryant, J. Less. Comm. Metals, 1962, 4, 62-68.

144. E. Gebhardt and R. Rothenbacher, Z. Metallkde., 1963, 54, 443-448 and 623-630.

145. G. Brauer, H. Muller and G. Kuhner, J. Less Common Metals, 1962, 4, 533-546.

146. N. Norman, P. Kofstad, O. J. Krudtaa, J. Less Common Metals, 1962, 4, 124-137.

147. G. Brauer, Z. Anorg. Allgem. Chem., 1941, 248, 1-31.

148. G. Anderson and A. Magneli, Acta Chem. Scand., 1957, 11, 1065-1066.

149. H. Krebs, Acta Cryst., 1956, 9, 95-108.

150. A. Magneli, G. Anderson and G. Sundkvist, Acta Chem. Scand., 1955, 9 1402.

151. H. J. Goldschmidt, J. Inst. Met., 1959, 87, 235-239.

152. A. Magneli and S. Lagergren, A.S.T.M. Index Card 5-0379.

153. R. Norin and A. Magneli, Naturwiss., 1960, 47, 354-5.

154. R. Gruehn and H. Schafer, Naturwiss., 1963, 50, 642-43.

155. V. I. Lavrent'ev, Y. I. Gerasimov, T. N. Rezukhina, Doklady Akad. Nauk, S.S.S.R., 1961, 136, 1372-75.

156. S. Zador (Private communication), Metallurgy Dept., Imperial College, London.

157. M. Hoch, A. S. Iyer and J. Nelken, J. Phys. Chem. Solids, 1962, 23, 1463-71.

158. G. Grube and M. Flad, KWI Metallforschung, Stuttgart, 1945.

159. W. L. Worrell, J. Phys. Chem., 1964, 68, 952-953.

160. P. Kofstad and P. B. Anderson, J. Phys. Chem. Solids, 1961, 21, 280-286.

161. A. D. Wadsley, Acta Cryst., 1961, 14, 660-670.

162. A. Magneli, Acta Cryst., 1953, 6, 495.

163. S. Anderson, B. Collen, U. Kuylenstierna, A. Magneli, Acta Chem. Scand., 1957, 11, 1641.

164. D. J. M. Bevan, J. Inorg. Nucl. Chem., 1955, 1, 49-59.

165. C. I. Sieglaff and L. Eyring, J. Am. Chem. Soc., 1957, 79, 3024-3026.

166. E. D. Guth and L. Eyring, J. Am. Chem. Soc., 1954, 76, 5242-5244.

167. D. J. M. Bevan and J. Kordis, J. Inorg. Nucl. Chem. 1964, 26, 1509-1523.

168. H. Schafer (Private communication), Inorganic Chemistry Department, University of Munster, Westphalia, Germany.

169. J. S. Anderson, Proc. Roy. Soc. (London) 1946, A185, 69-89.

170. A. L. G. Rees, Trans Faraday Soc., 1954, 50, 335-342.

171. J. S. Anderson and C. G. Barraclough, Trans. Faraday Soc., 1963, 59, 1572-1579.

172. E. H. Greener, D. H. Whitmore and M. E. Fine, J. Chem Phys. 1961, 34, 1017-1023.

173. P. Kofstad, J. Phys. Chem. Solids, 1962, 23, 1571-1578.

174. M. Hoch and D. Ramakrishnan, J. Phys. Chem. Solids, 1964, 25, 869-872.

175. F. A. Kusnetsov, V. I. Belyi and T. N. Rezukhina, Doklady Akad. Nauk, S.S.S.R., 139, 1405, 1961.

176. M. S. Yakovleva and S. M. Ariya, Russ. J. Phys. Chem., (English translation), 1963, 37, 880-881.

APPENDIX I

Expression for the diffusion potential in a solid electrolyte

The following derivation is based upon the method used by Wagner* in his theoretical treatment of the parabolic growth rate of a metal oxide film during oxidation.

Independent migration of each type of particle is assumed, and the final expression is strictly confined to small concentrations of lattice defects and to small deviations from the ideal stoichiometric ratio.

The rate of migration will be determined by both the chemical potential gradient and the electrical potential gradient. If μ_i is the chemical potential of N particles (i.e. one mole), the force acting on the average upon a particle in the x-direction is:

$$-\frac{1}{N}\frac{\partial \mu_i}{\partial x}$$

If B_i is the mobility of particles of species i, that is, the velocity obtained under the action of unit

---

* C. Wagner, Z. Phys. Chem., B21, 25, 1933.

force, then the velocity of these particles due to the gradient of chemical potential will be:

$$v_i = -\frac{B_i}{N} \cdot \frac{\partial \mu_i}{\partial x}$$

The corresponding expression for the action of the electrical potential ϕ on a particle having a charge $z_i e$, will be:

$$v_i = -B_i z_i e \cdot \frac{\partial \phi}{\partial x}$$

$\therefore$ When the two forces are acting together:

$$v_i = -B_i \left(\frac{1}{N} \cdot \frac{\partial \mu_i}{\partial x} + z_i . e . \frac{\partial \phi}{\partial x} \right)$$

If C_i is the concentration in moles. cm^{-3}, then the rate of transport (flux J_i) of any constituent i in moles per unit time in the x-direction is given by:

$$J_i = v_i C_i = -B_i C_i \left(\frac{1}{N} \cdot \frac{\partial \mu_i}{\partial x} + z_i . e . \frac{\partial \phi}{\partial x} \right) \quad \text{.....A.I.a.}$$

The flux is related to the respective partial current density by:

$$I_i = z_i . \mathcal{F} . N . J_i = z_i . F . J_i$$

$$\therefore \quad I_i = -B_i C_i z_i F \left(\frac{1}{N} \frac{\partial \mu_i}{\partial x} + z_i . e . \frac{\partial \phi}{\partial x} \right) \quad \text{.....A.I.b.}$$

When there is no gradient of composition ($\frac{\partial \mu_i}{\partial x} = 0$) then:

$$I_i = -C_i B_i z_i^2 e F \frac{\partial \phi}{\partial x} = -\sigma_i \frac{\partial \phi}{\partial x}$$

where σ_i is the partial electrical conductivity of constituent i.

If the total conductivity is represented by σ, then the transference number of the species i is defined by:

$$t_i^* = \frac{\sigma_i}{\sigma}$$

and $C_i B_i = \frac{t_i \sigma}{z_i^2 e F}$ and equation A. I .b. may be re-written:

$$I_i = -\frac{t_i \sigma}{z_i e}\left(\frac{1}{N} \cdot \frac{\partial \mu_i}{\partial x} + z_i . e . \frac{\partial \phi}{\partial x}\right)$$

$$= -\sigma\left(\frac{1}{F} \cdot \frac{t_i}{z_i} \cdot \frac{\partial \mu_i}{\partial x} + t_i \cdot \frac{\partial \phi}{\partial x}\right) \quad \text{.....A.I.c.}$$

It follows that when chemical potential gradients are imposed across a solid, for example the metal compound MX, the constituent ions and electrons ($M^{z\overset{+}{m}}$, $X^{z\bar{x}}$, e^-) will commence to migrate, and the individual partial currents ($IM^{z\overset{+}{m}}$, $IX^{z\bar{x}}$, Ie^-) within the solid may be expressed by equation A. I .c. The different mobilities of the various charged species will produce a charge separation, which, under steady state conditions, will lead to the rapid establishment of a constant electrical potential (the diffusion potential) within the solid. Further, in the

* The relationship between experimentally determined transference numbers and those defined as above, are discussed in Appendix IV.

absence of any external electrical circuit, there can be no resultant total current, and therefore the sum of the internal partial currents must be zero.

Therefore: $IM^{z_m^+} + IX^{z_x^-} + Ie^- = 0$

But $IM^{z^+m} = -\mathcal{C}\left(\frac{1}{F}\cdot\frac{tM^{z_m^+}}{zM}\cdot\frac{\partial\mu_M^{z_m^+}}{\partial x} + tM^{z_m^+}\cdot\frac{\partial\phi}{\partial x}\right)$

and $IX^{z_x^-} = -\mathcal{C}\left(\frac{1}{F}\cdot\frac{tX^{z_x^-}}{zX}\cdot\frac{\partial\mu_X^{z_x^-}}{\partial x} + tX^{z_x^-}\cdot\frac{\partial\phi}{\partial x}\right)$

and $Ie = -\mathcal{C}\left(\frac{1}{F}\cdot\frac{te}{ze}\cdot\frac{\partial\mu e}{\partial x} + te\cdot\frac{\partial\phi}{\partial x}\right)$

$\therefore (tM^{z_m^+} + tX^{z_x^-} + te)\frac{\phi}{x} = -\frac{1}{F}\left(\frac{tM^{z_m^+}}{zM}\frac{\partial\mu_M^{z_m^+}}{\partial x} + \text{etc.}\right)$

$tM^{z_m^+} + tX^{z_x^-} + te = 1$

$\therefore \Delta\phi = -\frac{1}{F}\left(\int_I^{II}\frac{tM^{z_m^+}}{zM}\cdot d\mu M^{z_m^+} + \int_I^{II}\frac{tX^{z_x^-}}{zX}\cdot d\mu X^{z_x^-} + \int_I^{II}\frac{te}{ze}\cdot d\mu e\right)$

which may be expressed in the general form:

Diffusion potential $= \Delta\phi = -\frac{1}{F}\int_I^{II}\sum_i\frac{ti}{zi}\cdot d\mu i.$

In this expression the charge carried by a particular species also determines whether zi is positive or negative.

APPENDIX II

Derivation of EMF for cells involving solid electrolytes

The electrochemical potentials of charged particles have values depending upon the electrical state of the appropriate phase as well as on its chemical composition. Accordingly the electrochemical potential of a charged particle may be conceptually divided into two terms as follows:

$$\tilde{\mu}^{\alpha}_{i} = \mu_{i} + z_{i} F \phi^{\alpha}$$

where $\tilde{\mu}^{\alpha}_{i}$ is the electrochemical potential of the charged component i in phase α, μ_{i} is its chemical potential in the same phase, $z_{i} F$ is its charge per mole with appropriate sign, and ϕ^{α} is the inner electrical potential of the phase α. It should be emphasized, however, that any division of the electrochemical potential into a chemical part and an electrical part is in general arbitrary and without physical significance.

It follows* that the electromotive force of a

---

* For example see,
E. A. Guggenheim, 'Thermodynamics', 4th edn., North-Holland Press, Amsterdam, 1959.
D. J. G. Ives and G. J. Janz, 'Reference Electrodes', Academic Press, London, 1961.

galvanic cell can only be thermodynamically defined by measuring the emf between two phases having the same chemical composition but different electrical potentials. Invariably a metallic phase (Cu, Ag, Pt, etc.) is employed so that no space charge can be sustained, thus ensuring that the bulk material has the same overall electrical potential.

To facilitate the theoretical analysis of cells involving solid electrolytes it is convenient to regard the measured emf as the sum of the potential differences existing between the various phases in contact. Consider, for example, the following:

M	solid electrolyte		M
ϕ'	ϕ^{α}	ϕ^{β}	ϕ''

In this cell, the two chemically identical metal electrodes have the electric potentials ϕ' and ϕ'' respectively, and the corresponding potentials within the electrolyte phase are designated ϕ^{α} and ϕ^{β} .

By definition, the electromotive force (E) of the cell is given by:

$$E = \phi'' - \phi' = \frac{1}{F}\left(\bar{\mu}_e^{M'} - \bar{\mu}_e^{M''}\right)$$

But $\phi'' - \phi' = (\phi^{\alpha} - \phi') + (\phi^{\beta} - \phi^{\alpha}) + (\phi'' - \phi^{\beta})$

At both the metal/electrolyte interfaces, the electrochemical potentials of the electrons in the adjoining phases must be equal when local equilibrium has been established,

i.e. $\bar{\mu}_e^{M'} = \bar{\mu}_e^{\alpha}$ and $\bar{\mu}_e^{M''} = \bar{\mu}_e^{\beta}$

$\therefore \quad \mu_e^{M'} - F\phi' = \mu_e^{\alpha} - F\phi^{\alpha}$

$\therefore \quad \phi^{\alpha} - \phi' = \frac{1}{F}(\mu_e^{\alpha} - \mu_e^{M'})$

and similarly,

$$\phi'' - \phi^{\beta} = \frac{1}{F}(\mu_e^{M''} - \mu_e^{\beta})$$

The metal electrodes, M' and M'', have the same chemical composition, and it follows that: $\mu_e^{M'} = \mu_e^{M''}$,

$\therefore \quad (\phi^{\alpha} - \phi') + (\phi'' - \phi^{\beta}) = \frac{1}{F}(\mu_e^{\alpha} - \mu_e^{\beta})$

and $E = \frac{1}{F}(\mu_e^{\alpha} - \mu_e^{\beta}) + (\phi^{\beta} - \phi^{\alpha})$ .....A.II.a.

To illustrate the application of the above expression, the following typical cell is considered in which the auxiliary electrolyte consists of a solid solution of the oxides ZrO_2 and CaO.

$$\bar{Pt}/Fe,FeO/ZrO_2 + CaO/Ni,NiO/\dot{Pt}$$

At elevated temperatures, diffusion will certainly occur, and the cell is more correctly represented as:

$$\begin{array}{ccccccc} \bar{Pt},Fe & | & FeO(a=1) \\ & | & ZrO_2+CaO & \vdots & \vdots & | & \dot{Ni},Pt \\ \phi' \quad \phi^{Fe} & | & \phi^{\alpha} & \vdots & \vdots & | & \phi^{Ni} \quad \phi'' \end{array} \qquad \begin{array}{c} NiO(a=1) \\ ZrO_2+CaO \\ \phi^{\omega} \end{array}$$

It is assumed that the solid solutions adjoining each electrode meet in an intermediate boundary zone in which the composition varies continuously from one extreme to the other. This zone may be considered as being located between the two dashed lines in the above cell.

$$E = \phi'' - \phi' = (\phi^{Fe} - \phi') + (\phi^{\alpha} - \phi^{Fe}) + (\phi^{\beta} - \phi^{\alpha}) +$$

$$+ (\phi^{Ni} - \phi^{\beta}) + (\phi'' - \phi^{Ni}) = (\phi^{\alpha} - \phi') + (\phi^{\beta} - \phi^{\alpha}) + (\phi'' - \phi^{\beta})$$

At equilibrium, the electrochemical potentials of the electrons in the Pt, Fe and adjoining electrolyte phase

must be equal, and therefore equation A.II.a. is valid, i.e.

$$E = \frac{1}{F}(\mu_e^{\alpha} - \mu_e^{\beta}) + (\phi^{\beta} - \phi^{\alpha}) \quad \text{.....A.II.a.}$$

Alternative expressions for the two terms in this equation may be derived as follows.

If the electrode Fe/FeO, is reversible to oxygen ions, then the local thermodynamic equilibrium may be expressed by:

$$2Fe + 2O^{2-} \rightleftharpoons 2FeO + 4e$$

i.e. $2\mu_{Fe}^{(\alpha)} + 2\bar{\mu}_{O^{2-}}^{(\alpha)} = 2\mu_{FeO}^{(\alpha)} + 4\bar{\mu}_e^{(\alpha)}$

Now $2\bar{\mu}_{O2-}^{(\alpha)} = 2\mu_{O^{2-}}^{(\alpha)} - 4F\phi^{(\alpha)}$

and $4\bar{\mu}_e^{(\alpha)} = 4\mu_e^{(\alpha)} - 4F\phi^{(\alpha)}$

∴ The electrochemical potentials of the oxygen ions and electrons can be replaced by their respective chemical potentials.

Rearranging:

$$4\mu_e^{(\alpha)} = 2\mu_{Fe}^{(\alpha)} - 2\mu_{FeO}^{(\alpha)} + 2\mu_{O^{2-}}^{(\alpha)}$$

But $2\mu_{FeO} - 2\mu_{Fe} = \mu_{O_2}^{(\alpha)}$,

where $\mu_{O2}^{(\alpha)}$ is the chemical potential of oxygen established

by the Fe-FeO equilibria,

$$\therefore \quad 4\mu_e^{(\alpha)} = -\mu_{O_2}^{(\alpha)} + 2\mu_{O^{2-}}^{(\alpha)}$$

Similarly at the R.H.S. electrode:

$$4\mu_e^{(\beta)} = -\mu_{O_2}^{(\beta)} + 2\mu_{O_2}^{(\beta)},$$

where $\mu_{O_2}^{(\beta)}$ is the chemical potential of oxygen established by the Ni-NiO equilibria,

$$\therefore \frac{1}{F}\left(\mu_e^{\alpha} - \mu_e^{\beta}\right) = \frac{1}{4F}\left(\int d\mu_{O_2} - 2\int d\mu_{O^{2-}}\right).$$

The second term in equation A.II .a., $(\phi^{\beta} - \phi^{\alpha})$, is the diffusion potential within the electrolyte and is due to the different mobilities of the various constituent ions and electrons. An equation for the diffusion potential has been derived in Appendix I, and for the cell under consideration:

$$\Delta\phi = \phi^{\beta} - \phi^{\alpha}$$

$$= -\frac{1}{F}\left[\int_{\alpha}^{\beta}\frac{t_{Zr^{4+}}}{4}\,d\mu_{Zr^{4+}} + \int_{\alpha}^{\beta}\frac{t_{Ca^{2+}}}{2}\,d\mu_{Ca^{2+}} + \int_{\alpha}^{\beta}\frac{t_{Ni^{2+}}}{2}\,d\mu_{Ni^{2+}}\right.$$
$$\left.+\int_{\alpha}^{\beta}\frac{t_{Fe^{2+}}}{2}\,d\mu_{Fe^{2+}} = \int_{\alpha}^{\beta}\frac{t_{O^{2-}}}{2}\,d\mu_{O^{2-}} - \int_{\alpha}^{\beta} t_e\,d\mu_e\right]$$

Experimental data, which is discussed in Section 1.D. indicates that $tO^{2-} \gg tZr^{4+}$, tCa^{2+}, tFe^{2+}, tNi^{2+}, for the solid electrolyte (ZrO_2 + CaO), and therefore the expression for the diffusion potential reduces to:

$$\phi^{\beta} - \phi^{\alpha} = -\frac{1}{F}\left[-\int_{\alpha}^{\beta}\frac{t_{O}^{2-}}{}\,d\mu_{O}^{2-} - \int_{\alpha}^{\beta} te\; d\mu e\right]$$

The total electromotive force (E) for the cell under consideration is now given by:

$$E = \frac{1}{F}(\mu_e^{\alpha} - \mu_e^{\beta}) + (\phi^{\beta} - \phi^{\alpha})$$

$$= \frac{1}{4F}\left[\int_{\alpha}^{\beta} d\mu_{O_2} - 2\int_{\alpha}^{\beta} d\mu_{O}^{2-}\right] + \frac{1}{F}\left[\int_{\alpha}^{\beta}\frac{t_{O}^{2-}}{2}\,d\mu_{O}^{2-} + \int_{\alpha}^{\beta} te.d\mu e\right]$$

As stated above, t_{Zr}^{4+}, t_{Ca}^{2+}, t_{Fe}^{2+}, t_{Ni}^{2+} may be neglected,

$$\therefore \quad te + t_{O}^{2-} = 1$$

Rearranging:

$$E = \frac{1}{4F}\int_{\alpha}^{\beta} d\mu_{O_2} - \frac{te}{4F}\left[\int_{\alpha}^{\beta} 2d\mu_{O}^{2-} - \int_{\alpha}^{\beta} 4d\mu e\right]$$

Now $O_2 + 4e = 2O^{2-}$

$\therefore \quad \mu_{O_2} = 2\mu_{O^{2-}} - 4\mu_e$

and $\int_\alpha^\beta d\mu_{O_2} = \int_\alpha^\beta 2d\mu_{O^{2-}} - \int_\alpha^\beta 4\, d\mu_e$

$\therefore \quad E = \frac{1}{4F}\int_\alpha^\beta d\mu_{O_2} - \frac{te}{4F}\int_\alpha^\beta d\mu_{O_2}$

$$= \frac{1}{4F}\int_\alpha^\beta t_{O^{2-}} \cdot d\mu_{O_2} = \frac{1}{4F}\int_{\mu_{O_2}^{(\alpha)}}^{\mu_{O_2}^{(\beta)}} t_{O^{2-}} \cdot d\mu_{O_2}$$

(Equation A.II.b.)

Further, if the electronic transport number is also negligible then:

$$E = \frac{1}{4F}\left(\mu_{O_2}^{(\beta)} - \mu_{O_2}^{(\alpha)}\right) = \frac{RT}{4F} \ln \frac{p_{O_2}^{(\beta)}}{p_{O_2}^{(\alpha)}}$$

and the expression, $G = -nEF$, is thus applicable.

Because none of the ions present Zr^{4+}, Ca^{2+}, Fe^{2+}, Ni^{2+}, has a mobility in the solid electrolyte $ZrO_2 + CaO$ comparable to that of the oxygen ions, then there can be no transfer of one of the oxide components between

different activity levels in the electrolyte. It should be emphasised, therefore, that the emf of the cell is given by equation A.II.b., regardless of the solubility of Fe and Ni in the solid electrolyte.

Similarly, for any oxygen concentration cell the following general expression can also be derived,

$$E = \frac{1}{4F} \int_{\mu_{O_2}'}^{\mu_{O_2}''} t_{ion} \cdot d\mu_{O_2},$$

where t ion is the ionic transference number of the electrolyte.

APPENDIX III

Transference numbers in solid electrolytes

The problem of defining transference numbers in a solid electrolyte, as compared to aqueous electrolytes, arises from the absence of an inert solvent reference frame against which to compare the relative velocities of the ions. This difficulty has been discussed by Bray and Merten* who have shown that the apparent transference numbers determined by different experimental techniques are not identical.

Due to the relative motion of the entire crystal lattice, the expression for the flow of charged species (cf. Appendix I, equation A.I.a.) is more correctly written as the sum of two terms, one representing the diffusion of the species in the crystal lattice, and the other the motion of the lattice as a whole, viz.

$$J_i = - C_i B_i \left(\frac{1}{N} \frac{\partial \mu_i}{\partial x} + z_i . e. \frac{\partial \phi}{\partial x} \right) + C_i \vec{v}$$

where $\vec{v}$ is the velocity of the lattice in the x-direction with respect to a reference frame.

---

* D. T. Bray and V. Merten, J. Electrochem. Soc., 1964, 111, 447-452.

When there is no gradient of composition ($\frac{\partial \mu_i}{\partial x} = 0$), the partial current densities may be written as:

$$I_i = -\sigma_i \frac{\partial \phi}{\partial x} + C_i . Z_i . e . \vec{v}$$

where the partial conductivity $\sigma_i = Z_i^2 eFB_i C_i$.
The total current is

$$I = \sum I_i = -\sum \sigma_i \frac{\partial \phi}{\partial x} + \vec{v} \sum C_i . Z_i . e = -\sigma \frac{\partial \phi}{\partial x}$$

The term $\vec{v} \sum C_i . Z_i . e.$ must be zero to maintain charge neutrality throughout the crystal.

A 'true' transference number may now be defined as:

$$t_i = \frac{\sigma_i}{\sigma}$$

It can be seen that a knowledge of $\vec{v}$ is required for the determination of the partial conductivities, σ_i's, although the total conductivity is independent of this quantity. Experimentally the partial current densities (IM, IX, Ie) of a metal compound MX, may be measured in a reference frame for which IM = 0 (i.e. the cations are assumed immobile), then

$$\vec{v} = \left(\frac{\sigma_M}{C_M z_M e}\right) \frac{\partial \phi}{\partial x}$$

and the apparent anionic conductivity σ_{X} (a.l) is given by:

$$\sigma_{X(a.l)} = \sigma_{X} - \sigma_{M}\left(\frac{c_{X} z_{X} e}{c_{M} z_{M} e}\right)$$

$$\text{and } t_{X(a.l)} = \frac{\sigma_{X(a.l)}}{\sigma}$$

Clearly if $\sigma_{X} \gg \sigma_{M}$, then $t_{X(a.l)} = t_{X}$ (true).

Fortunately, in the electrolytes used in the present investigation the mobility of the anions is many orders of magnitude greater than that of the cations, and accordingly the transference numbers used in the expression for the diffusion potential can be identified with the transference numbers determined experimentally by conductivity measurements.

APPENDIX IV

Preparation of Thoria Solid Solutions.

In addition to the straight forward evaporation of the mixed nitrate solutions described in Chapter two, experiments involving co-precipitation of hydroxide and oxalates were also carried out.

For the hydroxide method a reverse precipitation technique was tried in which the hot nitrate solution was added to an excess quantity of ammonia solution ($\sim 50^{\circ}C$). After cooling to $20^{\circ}C$, the solution was filtered, and the precipitate dried prior to the heat treatments. Although this technique appeared satisfactory for 'Analar' grade materials, with 'Spec-pure' chemicals, approximately 3-5 wt. % of the oxide material was always present in the filtrate, even though the procedure was varied in an attempt to overcome this problem. As the sintered pellets ($2000^{\circ}C$) prepared from hydroxide precipitated material were less dense that those prepared from 'nitrate powder', and contained large closed pores, no further development of the hydroxide method was attempted.

The oxalate method was more successful. A solution

of oxalic acid or ammonium oxalate was added to the mixed nitrate solution, and experiments were conducted to determine the optimum conditions of pH and temperature. In the prodedure eventually adopted only about 1 wt. % of the oxide material was present in the filtrate. However, it was found difficult to avoid segregation of the thorium and yttrium oxalates during filtration of the solution, and unless the material was carefully ground and mixed during the preliminary heat treatments, then the sintered pellets prepared from this material consisted of two phases, even after firing at 2000°C for 3 hours. Although the density of the sintered pellets prepared from oxalate precipitated material was comparable to that obtained for pellets fabricated from powder produced by the straightforward evaporation of the mixed nitrate solutions, it was considered that the oxalate technique was in no way superior to the nitrate method which was to become the standard procedure in the present investigation.

APPENDIX V

Analyses of Spec-Pure Chemicals

The following spectrographic analyses were supplied by Johnson Matthey and Co., Ltd.,

Thorium Nitrate

Silicon	5 ppm
Magnesium	<1 ppm

Other elements were either not present or below the limits of detection.

Yttrium Oxide

Si	10 ppm
Al	3 ppm
Fe	3 ppm
Ca	3 ppm
Mg	1 ppm
Cu	<1 ppm
rare earths	
Yb_2O_3	0.002%
Gd_2O_3	<0.01%

Tb_4O_7	<0.01%
Dy_2O_3	<0.005%
Nd_2O_3	<0.003%

Other elements were either not present or below the limits of detection.

Lanthanum Oxide

Ca	5 ppm
Si	4 ppm
Pb	3 ppm
rare earths	
Pr_6O_{11}	0.004%

Other elements were either not present or below the limits of detection.

Calcium Carbonate

Mg	10 ppm
Sr	4 ppm
Ba	1 ppm
Si	1 ppm
Na	1 ppm

Other elements were either not present or below the limits of detection.

APPENDIX VI

TYPICAL EMF MEASUREMENTS

A. $Fe, FeO / ThO_2.YO_{1.5}$ (90.10 mole %) / Ni, NiO

Experiment: Run 72

Apparatus: Separate Electrode Compartments cathode earthed.

Atmosphere: Vacuum.

TIME	TEMP(°C)	EMF(mV)
27.11.62.		
10.30	890	273.6(P)
10.45	893	274.6(P)
10.55	893.5	274.8(P)
11.10	893	274,9(P)
11.30	894	274.8(P)
11.35	892	(250)24.5(E)
12.45	1000	286.5(P)
13.55	1002	286.7(P)
14.15	1002	286.6(P)
15.00	1083	295.0(P)
15.15	1090	295.5(P)
15.30	1092	295.6(P)
15.40	1093	295.6(P)
15.55	1092	295.7(P)
16.20	1038	290.5(P)
16.45	1033	290.1(P)
17.05	1035	290.0(P)
17.30	1036	290.1(P)
18.30	895	286.1(P)
18.40	896	285.9(P)
18.55	897	286.0
28.11.62.		
9.40	710	(250)6.2(E)
1 μA passed for 5 mins.		
9.50	711	(250)7.4(E)
10.05	710	(250)6.9(E)
10.15	710	(250)6.8(E)
1 μA passed for 5 mins.		
10.25	711	(250)5.7(E)

TIME	TEMP(°C)	EMF(mV)
10.50	710	(250)6.4(E)
12.00	794	(250)15.7(E)
12.10	793	265.5(P)
12.30	795	265.6(P)
13.40	844	270.2(P)
14.05	845	270.3(P)
14.40	890	275.0(P)
14.55	892	275.5(P)
15.20	893	275.6(P)
16.05	952	281.9(P)
16.20	954	282.0(P)
16.30	953	282.0(P)
17.10	998	285.6(P)
17.30	1001	285.7(P)
17.50	1000	285.6(P)
18.45	898	275.5(P)
19.05	901	275.7(P)
29.11.62.		
10.20	756_{off}	(250)11.1(E)

P - Potentiometer

E - Electrometer

B. Ni, NiO/$ZrO_2.YO_{1.5}$(80.20 mole %)/Cu, Cu_2O

Experiment: Run 29

Apparatus: Electrodes in same compartment
Cathode earthed,

Atmosphere: Single stream of purified
argon (50 mls/min)

TIME	TEMP(°C)	EMF(mV)
10.5.60		
11.50	788	273.6(P)
12.25	792	273.8(P)
13.50	793	273.9(P)
Argon flow-rate increased to 75mls/min		
14.05	791	273.2(P)
14.15	790	273.0(P)
14.35	791	273.2(P)
Argon flow-rate decreased to 25 mls/min		
14.50	792	273.8(P)
15.10	794	273.6(P)
Argon flow rate adjusted to 50 mls/min		
15.45	793	273.6(P)

TIME	TEMP(°C)	EMF(mV)
11.5.60		
9.45	544	(270)20.8(E)
11.20	840	269.8(P)
11.45	845	270.4(P)
12.05	846	270.2(P)
12.30	947	263.3(P)
13.40	949	263.3(P)
14.30	885	266.3(P)
14.45	887	266.4(P)
14.55	888	266.3(P)
15.40	845	269.2(P)
15.50	843	269.3(P)
16.05	844	269.4(P)

TIME	TEMP(°C)	EMF(mV)
17.00	703	278.9(P)
17.45	700	279.2(P)
17.50	701	(270)9.5(E)
18.00	698	279.3
18.30	699	279.4
12.5.60		
10.40	538	(270)21.2(E)
1μA (~3 mins)		
10.50	537	(270)>30(E)
11.10	537	(270)25.3(E)
12.05	538	(270)22.6(E)
14.05	536	(270)22.3(E)
1μA (~3 mins)		
14.25	537	(270)<0(E)
15.10	538	(270)9.4(E)
15.40	536	(270)15.7(E)
16.15	538	(270)18.9(E)
17.05	537	(270)20.7(E)
18.10	417	(270)26.0(E)
18.30	412	(270)26.8(E)
19.05	410	(270)27.5(E)
19.40	409	(270)27.8(E)
13.5.60.		
10.10	406	(270)29.2(E)
10.30	407	(270)29.4(E)
11.55	538	(270)23.8(E)
12.30	542	(270)22.7(E)
13.50	543	(270)22.1(E)
14.15	542	(270)22.0(E)
15.05	543	(270)21.9(E)
16.25	698	280.7(P)
16.45	700	280.5(P)
17.00	701	280.3(P)
17.50	842	270.9(P)
18.15	844	270.6(P)
18.35	845	270.5(P)
19.10	941	264.2(P)
19.35	944	263.8(P)
19.45	945	263.8(P)
14.5.60.		
10.20	443	(270)27.3(E)
12.05	444 off	(270)27.6(E)

C. Nb,NbO/$ThO_2.YO_{1.5}$(99.1 mole %)/Fe,FeO

Experiment: Run 105

Apparatus: Separate Electrode Compartments

Cathode earthed.

Atmosphere: Vacuum

TIME	TEMP(°C)	EMF(mV)
3.6.63.		
12.00	945	631(P)
12.30	949	634.8(P)
13.50	951	635.5(P)
14.25	950	636.2(P)
15.00	948	636.5(P)
5μA passed for 5 mins		
15.10	950	648.6(P)
15.35	949	638.7(P)
15.45	950	638.5(P)
16.10	950	638.2(P)
16.30	949	638.4(P)
5μA passed for 5 mins		
16.40	950	586(P)
17.00	948	625(P)
17.30	949	632.3(P)
18.00	948	634.7(P)
18.35	950	635.8(P)
19.05	950	636.2(P)
19.40	951	636.2(P)
4.6.63.		
9.20	762	(600)65.5(E)
9.45	764	(600)65.0(E)
11.20	843	(600)55.5(E)
11.45	845	(600)55.0(E)
12.00	847	655.5(P)
12.30	846	655.0(P)

TIME	TEMP(°C)	EMF(mV)
13.55	943	640.5(P)
14.20	946	639.8(P)
14.45	945	639.5(P)
15.20	946	640.0(P)
16.15	1043	623.5(P)
16.40	1048	623.1(P)
17.05	1050	622.5(P)
17.25	1051	621.8(P)
17.45	1050	622.3(P)
18.30	1005	626.5(P)
19.05	998	627.8(P)
19.25	997	628.2(P)
19.45	999	628.4(P)
20.10	997	628.2(P)
5.6.63.		
10.10	788	(600)62.0(E)
10.30	789	(600)62.5(E)
10.55	895	648.0(P)
11.25	902	646.8(P)
11.45	901	646.5(P)

TIME	TEMP(°C)	EMF(mV)
12.15	903	645.5(P)
12.40	902	645.8(P)
14.10	995	631.5(P)
14.35	997	630.1(P)
15.05	998	630.0(P)
Anode earthed		
15.15	999	628.7(P)
Restored original connections i.e. (cathode earthed)		
15.30	998	629.5
16.25	1044	623.0(P)
17.05	1048	622.2(P)
17.30	1047	621.8(P)
18.10	1048	622.3(P)
19.05	953	634.5(P)
19.30	951	635.5(P)
19.55	952	635.8(P)
9.45	755	(600)66.0(E)
10.15	756_{off}	(600)65.0(E)

D. Nb, NbO/$ThO_2.YO_{1.5}$(90.10 mole %)/Fe, FeO

Experiment: Run 76

Apparatus: Separate Electrode compartments

Cathode earthed.

Atmosphere: Vacuum

TIME	TEMP(°C)	EMF(mV)
18.12.62.		
10.20	885	615.0(P)
12.05	892	624.3(P)
12.30	895	625.2(P)
13.35	897	625.5(P)
14.05	896	625.0(P)
5μA passed for 5 mins		
14.10	895	705(P)
14.20	896	650(P)
14.30	897	645(P)
14.50	895	640(P)
15.10	895	636(P)
15.30	896	632(P)
16.00	895	628(P)
16.35	895	6260(P)
17.05	896	624.0(P)
17.25	897	623.0(P)
18.30	896	623.5(P)

TIME	TEMP(°C)	EMF(mV)
5μA passed for 5 mins		
18.50	897	587(P)
19.00	898	612(P)
20.15	897	616(P)
21.05	898	617(P)
22.10	898	617.5(P)
23.00	897	616.5(P)
19.12.62.		
9.55	740	(600)45(E)
11.10	742	(600)43.5(E)
12.15	887	634.2(P)
12.40	892	633.0(P)
13.55	893	633.5(P)
15.10	1035	618.3(P)
15.30	1038	615.4(P)
16.05	1039	611.6(P)
17.00	1040	607.3(P)

TIME	TEMP(°C)	EMF(mV)
18.00	903	612.4(P)
19.15	895	615.3(P)
19.45	894	616.3(P)
20.05	895	615.5(P)
Passed 10μA for 30 mins		
in an attempt to reduce		
anode surface.		
Left overnight to equilibriate		

TIME	TEMP(°C)	EMF(mV)
20.12.62.		
11.10	806	(600)31.5(E)
12.15	888	622(P)
12.45	897	621.6(P)
13.40	899	621.0(P)
14.25	985	620.3(P)
14.45	991	618.5(P)
15.00	992	617.4(P)
15.25	993	612.2(P)
16.05	992_{off}	610.0(P)